Improvements to the [^{13}C]MTG breath test for measuring fat digestion

Christine Slater BSc (Hons), MPhil, RNutr

Thesis submitted for the Degree of Doctor of Philosophy

University of Glasgow
Division of Developmental Medicine

March 2004

The work described in this thesis is dedicated to my father

John Gladstone Holliday

29 September 1926 –12 December 1973

Acknowledgements

The original idea that formed the hypothesis tested in the work presented in this thesis was conceived by my husband, Dr Tom Preston (Scottish Universities Environmental Research Centre (SUERC), East Kilbride). I am indebted to him for advice and support throughout. The thesis would not have been completed without the encouragement and constructive advice of my supervisor, Professor Lawrence Weaver (Division of Developmental Medicine).

I would like to thank Professor Dave Halliday & Dr Joel Bradley (Cambridge Isotopes Laboratory Inc., Andover, MA, USA) for donating the [^{13}C] and [^{2}H]MTG used in these studies, Dr Simon Ling & Dr Neil Gibson (Consultants, Royal Hospital for Sick Children, Glasgow) for assistance in recruiting children with cystic fibrosis, Dr Sergio Amarri (former EU Clinical Research Fellow, Department of Human Nutrition, University of Glasgow and MRC Dunn Nutrition Unit, Cambridge, now Department of Pediatrics, University of Modena, Italy) for access to some of the data from his fellowship, and Dr Victor Zammit (Hannah Research Institute, Ayr) for helpful discussion of fatty acid metabolism and my advisor of studies, Dr Kay Dodson (Bell College, Hamilton) for support and encouragement throughout.

I acknowledge the assistance of Paul Gorman (research technician, SUERC), who calibrated our CO_2 reference gas against secondary references traceable to the international standards, Karen Cooper (summer student, SUERC), who gave technical assistance with *in vitro* experiments, Usman Rehman (B.Sc. (Med.Sci.) project student) for assistance in collecting postprandial thermogenesis and heart rate calibration data in adult subjects and John Lindsay (B.Sc. (Med.Sci.) project student) for assistance in collecting breath samples from some children with cystic fibrosis.

Grateful thanks to my colleagues: Diane Jackson, Colette Montgomery, Emma-Jane Gault, Louise Kelly, Gordon MacKay, Douglas Morrison, Martin McMillan, Jean Hyslop and Myra Fergusson for helpful distraction/discussion and moral support over the years.

Finally, I would like to thank all the subjects and their families who took part in this study: my colleagues, who acted as adult control subjects; the healthy children, who gave up two Saturdays to blow into breath sampling tubes for ten hours, and the children with cystic fibrosis, who took time off school to help with this research.

List of Contents

List of Figures

List of Tables

List of Publications

Work from this thesis has been presented at the following meetings of learned societies:

1. SIMSUG (Stable Isotope Mass Spectrometry Users Group), January1999, Exeter. Breath tests on the move. Poster.
2. SIGN (Stable Isotopes in Gastroenterology and Nutrition), June 1999, Glasgow. What is the appropriate $V\!CO_2$ term for ^{13}C breath tests in free-living subjects? Oral presentation.
3. The Nutrition Society Summer Meeting, July 1999, Glasgow. What is the appropriate $V\!CO_2$ term for ^{13}C breath tests in free-living subjects? *Proceedings of the Nutrition Society,* **59** (OCA), 15A. Poster.
4. SIMSUG, January 2000, Glasgow. Stable isotopes and the International System of Units. *Rapid Communications in Mass Spectrometry* **15**(15), 1270-1273. Poster.
5. The Nutrition Society Summer Meeting, July 2000, Coleraine. Calibration of a heart rate monitor to estimate CO_2 production rate for ^{13}C breath tests. *Proceedings of the Nutrition Society,* **60** (OCA), 8A. Poster.
6. ESPEN (European Society for Parenteral and Enteral Nutrition), September 2001, Munich. Validation of the ^{13}C-mixed triacylglycerol breath test using a ^{2}H-labelled tracer. *Clinical Nutrition,* **20** (Suppl.3), 39-40. Poster.
7. SIGN, January 2002 Leuven. Calibration of a heart rate monitor to estimate $V\!CO_2$ during the mixed triacylglycerol breath test. Oral presentation.
8. The Nutrition Society Scottish Section Meeting, March 2002, Edinburgh. A shelf-stable, palatable test meal suitable for use with hydrophilic and lipophilic tracers in ^{13}C breath tests. *Proceedings of the Nutrition Society,* **61** OCB, 66A. Poster.
9. The Nutrition Society Scottish Section Meeting, March 2003, Glasgow. Use of calibrated heart rate monitors to estimate $V\!CO_2$ during the ^{13}C-mixed triacyglycerol breath test. *Proceedings of the Nutrition Society,* **62** OCA/B, 9A. Oral presentation.
10. FENS (Federation of European Nutrition Societies) Congress October 2003, Rome. Comparison of [^{2}H]MTG, [^{2}H]octanoate and [^{2}H]acetate metabolism in healthy adults. *Annals of Nutrition and Metabolism,* **49**, 492. Poster.
11. SIGN/EUROSTARCH Workshop October 2003, Rome. The [^{2}H]MTG test for intraluminal fat digestion. Oral presentation.

List of Abbreviations

α-KG	α-ketoglutarate
BMR	Basal metabolic rate
CF	Cystic fibrosis
CF-IRMS	Continuous flow isotope ratio mass spectrometry
CoA	Coenzyme A
CPT	Carnitine palmitoyl transferase
FABP	Fatty acid binding protein
FATP	Fatty acid transport protein
GC/MS	Gas chromatography-mass spectrometry
HR	Heart rate
IRMS	Isotope ratio mass spectrometer or isotope ratio mass spectrometry
MAG	Monoacylglycerol
MTG	Mixed triglyceride or mixed triacylglycerol
NEFA	Non-esterified fatty acid
OAA	Oxaloacetate
PAL	Physical activity level
PDR	Percentage dose recovered
cPDR	Cumulative percentage dose recovered
PERT	Pancreatic enzyme replacement therapy
PI	Pancreatic insufficient
PS	Pancreatic sufficient
ppm	Parts per million
RHR	Resting heart rate
RMR	Resting metabolic rate
RNA	Ribonucleic acid
RQ	Respiratory quotient ($\dot{V}CO_2/\dot{V}O_2$)
TAG	Triacylglycerol
TBW	Total body water
TCA cycle	Tricarboxylic acid cycle
TEE	Total daily energy expenditure
TG-ROC	Two graph-receiver operator characteristics
$\dot{V}CO_2$	Carbon dioxide production rate
$\dot{V}O_2$	Oxygen consumption rate

Summary

Background

There is a need for a robust, non-invasive clinical test to assess fat digestion, especially in children with cystic fibrosis. Labelling of substrates with ^{13}C enables investigation of their digestion, absorption and subsequent metabolism. The mixed triacylglcerol (MTG) ^{13}C-breath test is an indirect measure of fat digestion, and therefore exocrine pancreatic function. Cystic fibrosis is the commonest cause of pancreatic insufficiency in children. ^{13}C-breath tests are particularly attractive for use in children because they are non-invasive, and pose no radiation hazard.

MTG is a synthetic triacylglycerol (1,3 distearyl 2-[1-^{13}C] octanoyl-glycerol). Pancreatic lipases preferentially hydrolyse triacylglycerol at the *sn*-1 and -3 positions, releasing ^{13}C-labelled octanoate which is rapidly absorbed and oxidised with the generation of $^{13}CO_2$. Quantitation of tracer excretion requires knowledge of the volume of distribution of the ^{13}C-labelled tracer as well as quantity of ingested dose and ^{13}C abundance in breath CO_2. In ^{13}C-breath tests, labelled CO_2 originating from oxidation of the tracer is diluted by endogenously produced CO_2 from metabolic processes. Therefore knowledge of CO_2 production rate ($\dot{V}CO_2$) is required. A resting value based on basal metabolic rate is often assumed, but if subjects are not at rest and in the postprandial state throughout the test, this will be an underestimate of the true CO_2 production rate and therefore underestimate the quantity of tracer excreted.

The MTG breath test has not been widely adopted because it lacks discrimination due to its poor specificity. The hypothesis tested in this study is that the poor specificity of the [^{13}C]MTG breath test is due to lack of knowledge of the true carbon dioxide production rate during the test.

Subjects and Methods

A series of interrelated studies were undertaken to test this hypothesis.

Eight healthy adults, ten healthy children and seven children with cystic fibrosis were the subjects of these interrelated studies. Use of calibrated heart rate monitors to estimate $\dot{V}CO_2$ from heart rate continuously during ^{13}C-breath tests was investigated. Use of a

generic calibration, applied to subjects of all ages and size was explored by normalising measured VCO_2 to various body parameters including surface area, weight^n and height^n.

[^{13}C]MTG breath tests were performed on all subjects. The percentage dose recovered in each breath sample was calculated using predicted or measured values of resting VCO_2 and non-resting VCO_2 estimated from heart rate. Cumulative excretion of ^{13}C in breath CO_2 (cPDR) was calculated using the trapezoidal rule. The physical activity level (PAL) during the test was determined by dividing cPDR calculated using non-resting VCO_2 by cPDR calculated using resting VCO_2.

[1-^{13}C]acetate breath tests were performed on all of the adults and twelve of the children (nine healthy controls and three children with cystic fibrosis). Use of an acetate correction to account for ^{13}C retained in the body during the [^{13}C]MTG test was also explored.

Two healthy adults took part in studies using [^{13}C]MTG and its labelled metabolites, to assess the effect of factors including rest, exercise, fasting and feeding on the recovery of $^{13}CO_2$ in breath, and simultaneous use of a tracers, which do not enter the body's CO_2 pool, deuterium (^{2}H) labelled MTG, octanoate and acetate.

Results and Discussion

Calibration of heart rate monitors to estimate VCO_2 during ^{13}C breath tests

The most accurate and precise method of estimating VCO_2 from heart rate was use of a sigmoid model on smoothed heart rate data. Use of a generic calibration, to avoid the need for individual calibration, introduced unacceptably large errors.

The [^{13}C]MTG test: VCO_2 estimated from heart rate

The reference range (mean ± 2SD) of cPDR in the breath of pancreatic sufficient subjects (n = 19) in 6 h following ingestion of [^{13}C]MTG was 24 to 58 %, when VCO_2 was estimated continuously from heart rate. The cut-off point determined using Two Graph-Receiver Operator Characteristics on data from 25 subjects was 25 %, with sensitivity, specificity, positive and negative predictive values all = 1.0. For comparison, the reference range calculated using a constant value of VCO_2 of 5 mmol.min^{-1}.m^{-2} was 18 to 43 % and using a constant value of measured resting VCO_2 was 17 to 40 %. In both cases the cut-off point was 20 % with sensitivity and specificity = 0.86, giving an equivocal range of 17 to 20 %. The positive predictive value was 0.71 and the negative predictive value was 0.94, which is similar to previous studies. Use of individually calibrated heart rate monitors to

estimate VCO_2 during the [^{13}C]MTG test improved the positive predictive value of the test from 0.71 using resting VCO_2 to 1.0 using non-resting VCO_2 estimated from heart rate.

The mean PAL in tests that were performed under clinical conditions was 1.3. This factor was applied to the cumulative recovery in six hours (PDR_{6h}) during the [^{13}C]MTG breath test data from children with cystic fibrosis (n = 45), who took part in a previous study. The results were compared with the reference range established in this study with no loss of specificity. This approach could be adopted in future [^{13}C]MTG tests undertaken under clinical conditions, thus avoiding the need for individual heart rate calibration.

The [^{13}C]MTG test with an acetate correction

Use of acetate correction factors is not recommended as it requires two breath tests on separate occasions, and the assumptions that any deviations from basal VCO_2 are the same on each occasion and both tracers are metabolised in an identical manner may not be valid. Use of [^{2}H]labelled substrates revealed that acetate and MTG are not metabolised in the same manner by the body. Less ^{2}H was recovered in body water following ingestion of [$^2H_3$]acetate (87 & 91 %) than [^{2}H]MTG (93 & 98 %) or [$^2H_{15}$]octanoate (94 & 101 %), suggesting that a greater proportion of [$^2H_3$]acetate may be sequestered, most probably during lipogenesis.

The [^{2}H]MTG test

The [^{2}H]MTG test may provide a simpler, more robust non-invasive test of fat digestion.

Conclusions

Use of non-resting VCO_2 improved the discrimination of the [^{13}C]MTG breath test by increasing the positive predictive value of the test. Calculation of recovery of ^{13}C during the [^{13}C]MTG breath test, using resting VCO_2 with a PAL of 1.3, together with the reference range from pancreatic sufficient subjects measured in this study, could provide a useful clinical test of fat digestion in children with cystic fibrosis. Problems associated with lack of knowledge of the true CO_2 production rate during the [^{13}C]MTG could be avoided by using [^{2}H]MTG, if supplies of this novel stable isotope labelled tracer were available.

Author's Declaration

I declare that the work contained in this thesis is original. The recruitment of participants, collection and analysis of samples, and the analysis and presentation of data were undertaken entirely by the author, unless otherwise stated. This thesis was supervised by Professor Lawrence T. Weaver, Division of Developmental Medicine.

Christine Slater

Chapter 1 Introduction

1.1 Background

There is a well-recognised need for a non-invasive method of measuring fat digestion especially in children with cystic fibrosis, who have impaired exocrine pancreatic function. Cystic fibrosis is the most common inherited disease in the UK, affecting over 7500 babies, children and young adults (data from the Cystic Fibrosis Trust). The incidence of the disease is 1 in 2000 live births and 135 children attend the cystic fibrosis clinic at the Royal Hospital for Sick Children, Yorkhill NHS Trust, Glasgow. Clinically, cystic fibrosis is characterized by recurrent pulmonary infections, pancreatic insufficiency with maldigestion and malabsorption and excessive losses of electrolytes in sweat caused by abnormal function of an epithelial chloride channel called the cystic fibrosis transmembrane conductance regulator (CFTR).

This inherent defect in anion transport by epithelial cells of exocrine glands results in reduction of Cl^-, Na^+, K^+ and HCO_3^- levels in secretions. Fluid secretion is also reduced, but is normal when adjusted for Cl^- and HCO_3^- levels, suggesting that this is secondary to the reduction in these ions. Since the Cl^-/HCO_3^- ratio is unchanged in cystic fibrosis, it is likely that the secretion of both these ions is abnormal. The finding that HCO_3^- passes readily through the ORDIC (outwardly rectifying, depolarisation-induced Cl^-) channel (and other Cl^- channels) suggests that the same defect may be responsible for both abnormalities (Alton & Smith, 2000). In the pancreas, the consequence of this is viscous secretions, which result in blockage of the pancreatic ducts reducing the amount of pancreatic enzymes reaching the small intestine (Shepherd *et al.* 1991; Couper *et al.* 2002). Only 1-2 % of residual pancreatic capacity for secreting enzyme is required to prevent maldigestion (Gaskin *et al.* 1984). This allows patients to be classified as either pancreatic insufficient (PI) with less than 2 % of normal activity, or pancreatic sufficient (PS) with 2-100 % of normal activity (Couper *et al.* 2002). Patients with PI secrete insufficient pancreatic lipolytic enzymes (e.g. lipase, colipase) or proteolytic enzymes (e.g. trypsin, chymotrypsin) and bicarbonate for normal fat and protein digestion and absorption. In patients with PS, the pancreas is affected, but they have sufficient exocrine pancreatic function to permit normal nutrient digestion and absorption.

In children, cystic fibrosis is the commonest cause of exocrine pancreatic insufficiency. Between 10 and 15 % of children with cystic fibrosis are PS. They have milder disease expression, slower progression of lung disease, better nutritional status and a higher survival rate than PI patients (Wilson & Pencharz, 1998). When diagnosis of cystic fibrosis has been established, PI is often inferred by clinical signs and symptoms such as, frequent, malodorous, greasy stools, the presence of meconium ileus, or distal intestinal obstruction syndrome (Borowitz, Baker & Stallings, 2002). In about 85 % of children with cystic fibrosis, PI is present from neonatal life. Some patients, whose tests initially indicate that they are PS become PI. The Consensus Report on Nutrition for Pediatric Patients with Cystic Fibrosis advises that PS patients should be re-evaluated annually for conversion to PI (Borowitz *et al.* 2002).

Treatment of PI in children with cystic fibrosis is based on oral replacement with pancreatic enzymes, usually porcine enzyme extracts. Adults with PI due to chronic pancreatitis or pancreatic cancer may also require pancreatic enzyme replacement therapy (PERT). Pancreatic enzymes are rapidly degraded by stomach acid and pepsin and function best in an alkaline environment. Enteric-coated microspheres have been shown to increase delivery of enzymes to the duodenum and distal small bowel. This results in improved utility, but there have been problems with miscibility of the microspheres with food and sub-optimal dissolution of the spheres in the relatively acid environment caused by inefficient alkalinisation of the duodenal contents in children with cystic fibrosis due to deficient bicarbonate production (Couper *et al.* 2002). Proton pump inhibitors, H_2 antagonists and misoprostil have all been used to either reduce stomach acid or to render the duodenum contents more alkaline and hence improve enzyme utility. Lipase doses above 25,000 units of lipase/kg/d have been associated with fibrosing colonopathy (Smyth *et al.* 1994, 1995), which may result in intestinal obstruction secondary to colonic stricture, failure to thrive and abdominal pain (Schwarzenberg *et al.* 1995, Smyth, 1996). For this reason, it is recommended that lipase dose does not exceed 10,000 units/kg/d.

The aim of PERT is to achieve normal or near-normal fat and protein digestion. From this should follow normal nutrition, growth and development, and a normal or near-normal stooling pattern (Davidson, 2000). Despite prescription of adequate enzyme dosage, 10 % or more of children with cystic fibrosis may continue to have significant fat malabsorption, abdominal complaints or poor growth (Littlewood, 1996). A pancreatic function test is required for conversion to PI and also to optimise PERT to ensure adequate nutrition, while avoiding the complications associated high doses of PERT. There are three specific

times when special attention should be focussed on growth and nutritional status. These are in the first twelve months after diagnosis of cystic fibrosis, birth to twelve months of age for infants diagnosed prenatally or at birth, and the peripubertal growth period, which occurs between about nine and sixteen years in girls and about twelve to eighteen years of age in boys (Borowitz *et al.* 2002).

The ideal pancreatic function test should be inexpensive, easily performed, repeatable and reliable (Couper *et al.* 2002). It should be specific for pancreatic disease and able to define the exact level of pancreatic function in subjects with PI in whom partial impairment of exocrine function is present, but nutrient assimilation is unaffected. There should be no interference from pancreatic enzyme supplements. None of the currently available tests meets all these criteria.

The classical 72-hour fat balance technique is widely used and is a measure of the difference between dietary fat intake and stool output (Van de Kamer, Huinick & Weyers, 1949), but does not discriminate between PI and other causes of steatorrhea (foul smelling, fatty stools), e.g. untreated coeliac disease, Crohn's disease and small intestinal bacterial overgrowth. It does not take endogenous lipids into account, nor does it discriminate between fat maldigestion and malabsorption.

The definitive test for exocrine pancreatic function is duodenal intubation with secretin-pancreozymin stimulation (Wong, Turtle & Davidson, 1982), but the test is invasive, uncomfortable, expensive and difficult to perform. However, it remains the only test capable of measuring functional reserve. Non-specific evidence of pancreatic insufficiency is provided by demonstration of unsplit fat globules on stool smear (by microscopy), by increased 3-day faecal fat excretion, or by evidence of fat-soluble vitamin deficiency (Davidson, 2000). Other currently available tests of exocrine pancreatic function include: serum immunoreactive trypsinogen, the pancreolauryl test, BT-PABA (N-benzoyl-L-tyrosyl-*p*-aminobenzoic acid) or PABA test, faecal elastase-1 and faecal chymotrypsin (Borowitz *et al.* 2002, Boeck *et al.* 2001). The last two have the advantage of requiring a single stool sample and are relatively inexpensive to assay, but do not establish the adequacy of enzyme replacement. The faecal elastase test has been shown to be more sensitive and specific than the faecal chymotrypsin test, is not affected by concurrent administration of PERT (Löser *et al.* 1998, Brydon *et al.* 2004). Both tests could be used simultaneously to verify therapeutic fulfilment (Martinez-Costa, 2002).

The ^{13}C-mixed triacylglycerol (MTG) breath test is non-invasive, safe and avoids the need for stool sampling, which is greatly appreciated by patients, their parents and laboratory staff. It has been used to assess the need for (PERT) in children with cystic fibrosis and to assess the ideal dose (Amarri *et al.*1997; de Boeck *et al.* 1998). It has not been widely adopted because it lacks discrimination due to its poor specificity, resulting in too many false positive results caused by low recovery of ^{13}C in the breath of healthy subjects, and requires breath sampling for five to six hours in order to discriminate between PI and disorders of motility e.g. delayed gastric emptying. Disorders of motility have been shown to be present in children with cystic fibrosis (Davidson, 2000) and could result in the late appearance of labelled CO_2 in the breath of a child with PS, although the amount of tracer recovered in breath (area under the curve of rate of appearance versus time) might be the same as a healthy child.

MTG is a synthetic triacylglycerol (1,3 distearyl 2-[1-^{13}C] octanoyl-glycerol). Pancreatic lipases preferentially hydrolyse triacylglycerol at the *sn*-1 and -3 positions, releasing ^{13}C-labelled octanoate which is rapidly absorbed and oxidised with the generation of $^{13}CO_2$. Quantitation of tracer excretion requires knowledge of the volume of distribution of the ^{13}C-labelled tracer as well as quantity of ingested dose and ^{13}C abundance in breath CO_2. In ^{13}C-breath tests, labelled CO_2 originating from oxidation of the tracer is diluted by endogenously produced CO_2 from metabolic processes. Therefore knowledge of CO_2 production rate ($\dot{V}CO_2$) is required. A resting value based on basal metabolic rate is often assumed, but if subjects are not at rest and in the postprandial state throughout the test, this will be an underestimate of the true CO_2 production rate and therefore underestimate the quantity of tracer excreted.

The [^{13}C]MTG breath test is an indirect measure of fat digestion, as medium-chain fatty acids are absorbed without the aid of bile salts once the long-chain fatty acids have been hydrolysed by pancreatic lipase. Hence, it is a test of maldigestion (defective enzymatic degradation to absorbable products) independently from malabsorption (insufficient product solubilization caused by bile salt deficiency or diminished absorption resulting from damaged intestinal mucosa), and therefore an indication of exocrine pancreatic function.

Cost issues

The full economic cost of tests is difficult to calculate. Labour costs are often excluded and are highly variable. The full economic cost of MTG test for a 50 kg child (10 mg/kg MTG) is approximately £100, including tracer, salary, laboratory consumables, mass spectrometer maintenance and depreciation, PC consumables and indirect costs at 100% of salary. The cost of the [^{13}C]MTG amounts to half the total (£50), but if market demand were bigger, the price would fall. Analysis by spectroscopic methods may be cheaper, but the current instruments are not as sensitive as isotope ratio mass spectrometry and therefore a larger dose would be required. The price quoted above does not include the time of the clinical staff taking the breath samples, which will vary depending on whether an auxiliary nurse, trained nurse or research fellow is involved. The latter is relatively expensive because they would need to devote the whole six-hour sampling time to this activity, whereas a member of the nursing staff could perform other activities between breath samples.

The Yorkhill NHS Trust has not calculated the full economic cost of the tests it performs, but an internet search revealed two hospital laboratories with price lists for their assays. The cost of a human pancreatic faecal elastase-1 assay at the City Hospital Birmingham is £25. The same test costs NZ$112 (approx £41) at the Canterbury Health Laboratories in Christchurch, New Zealand. The New Zealand Laboratory also quoted prices for faecal fat analysis (NZ$150, approx £55), faecal chymotrypsin (NZ$50, approx £20) and analysis of pancreatic enzymes in duodenal juice (NZ$100, approx £36). The latter does not include the time of the gastroenterologist and support staff necessary to obtain the sample of duodenal juice.

The MTG breath test is currently more expensive than its main competitor, the faecal elastase-1 test, as a test of exocrine pancreatic function. Neither test directly measures residual pancreatic function. Both tests are non-invasive and can be used to assess the conversion from PS to PI, but in addition, the MTG test can be used to assess the adequacy of PERT.

The MTG breath test avoids the need for stool sampling, but the discrimination of the test must be improved if it is to be adopted into clinical practice and before any economy of scale can be realised.

1.2 Dietary lipids

1.2.1 Introduction

Lipids are present in the diet in many forms. They can be overtly present as in salad oils, butter and margarines, or they can be concealed in cooked and processed foods such as biscuits, cakes and confectionery. They comprise about 40% of the energy value of the average UK diet (British Nutrition Foundation, 1992). Children with cystic fibrosis are advised to consume a high fat diet (35-40 % energy as fat), contrary to the recommendation for the general population (<35 % energy as fat, Department of Health, 1991), as fat is more energy dense than protein and carbohydrate (Borowitz *et al.* 2002).

To a chemist, the term lipid (from the Greek *lipos,* meaning 'fat') refers to any naturally occurring, nonpolar substance that is nearly or totally insoluble in water, but is soluble in nonpolar solvents (Bohinski, 1983). To a nutritionist, lipids are the component of the diet composed mainly of storage fats of mammals and fish, and the seed oils of plants (British Nutrition Foundation, 1992). The lipid in most foods is a mixture of triacylglycerols (previously referred to as triglycerides), phospholipids, sterols and related compounds. Triacylglycerols are the major component (92-96 %) in Western diets (Carey & Hernell, 1992). Figures quoted in nutritional tables refer to total fat and not just to the triacylglycerols (Holland *et al.* 1991).

1.2.2 Structure and nomenclature of fatty acids

A fatty acid is an aliphatic carboxylic acid with from 2 to 24 carbon atoms. The hydrocarbon chain terminates with a carboxyl (-COOH) group at one end and a methyl ($-CH_3$) group at the other. Short chain fatty acids, or volatile fatty acids, have between two and six carbon atoms. Medium chain fatty acids have between 6 and 12 carbon atoms, and long chain fatty acids have between 14 and 24 carbon atoms. Most animal and plant derived fatty acids have an even number of carbon atoms in the hydrocarbon chain, although odd-numbered fatty acids can be synthesised by bacteria in the colon of monogastric animals or in the rumen of ruminants. Fatty acids are ionised at physiological pH and are often referred to according to their carboxylate form e.g. acetate, octanoate, palmitate (Stryer, 1988).

When each of the carbon atoms, except the two terminal ones, is bonded to two hydrogen atoms, the acid is said to be saturated, since all of the bonding capacity of the carbon is saturated with hydrogen. When each of two adjacent carbon atoms is bonded to only one hydrogen, there is a double bond between the pair of carbons and the fatty acid is said to be unsaturated. If the chain contains only one double bond, it is a monounsaturated fatty acid (MUFA) and if the chain contains more than one double bond, it is a polyunsaturated fatty acid (PUFA). Saturated fatty acids are given systematic names, according to the rules of International Union of Pure and Applied Chemistry (IUPAC), that denote the number of carbon atoms (Table 1.1) e.g. the 18-carbon, straight chain saturated fatty acid is octadecanoic acid. The presence of a double bond is indicated by the change of the suffix from -anoic to -enoic. An 18-carbon acid with one double bond is octadecenoic acid, and with two double bonds is octadecadienoic acid.

A system of common names, widely used by nutritionists, has grown up beside that of the official chemical nomenclature. Octadecanoic acid is also known as stearic acid. The most widespread form of octadecenoic acid is known as oleic acid and the most common form of octadecadienoic acid is known as linoleic acid. Some very long chain fatty acids (e.g. eicosapentenoic acid, EPA and docosahexenoic acid, DHA) do not have trivial names, but are usually referred to by the abbreviated form of the systemic name. A useful shorthand nomenclature consists of two numbers separated by a colon. The number before the colon signifies the carbon chain length, and the number after the colon signifies the number of double bonds. Thus, stearic acid is 18:0, oleic acid is 18:1 and linoleic acid is 18:2.

The position of double bonds in the hydrocarbon chain of a fatty acid is denoted by a prefix indicating the number of the first of the pair of carbon atoms, which form the double bond. Carbon 1 is the carboxyl carbon atom. Thus, the systematic name for oleic acid is *cis*-9-octadecanoic acid and linoleic acid is *cis*-9,12-octadecanoic acid.

Table 1.1 Nomenclature of medium and long chain fatty acids

	Common name/ abbreviation	Systematic Name- numbers are position of double bonds from carboxyl end
8:0	caprylic	octanoic
10:0	capric	decanoic
12:0	lauric	dodecanoic
14:0	myristic	tetradecanoic
16:0	palmitic	hexadecanoic
16:1 n-7	palmitoleic	cis-9-hexadecenoic
18:0	stearic	octadecanoic
18:1 n-9	oleic	cis-9-octadecenoic
18:1 n-9	elaidic	trans-9-octadecanoic
18:2 n-6	linoleic	cis, cis-9,12-octadecadienoic
18:3 n-3	alpha-linolenic	all-cis-9,12,15-octadecatrienoic
18:3 n-6	gamma-linolenic	all-cis-6,9,12-octadecatrienoic
20:0	arachidic	eicosanoic
20:1 n-9	gadoleic	cis-11-eicosaenoic
20:4 n-6	arachidonic	all-cis-5,8,11,14-eicosatetraenoic
20:5 n-3	EPA	all-cis-5,8,11,14,17-eicosapentenoic
22:0	behenic	docosanoic
22:1 n-9	erucic	cis-13-docosaenoic
22:6 n-3	DHA	all-cis-4,7,10,13,16,19-docosahexenoic

When a fatty acid is elongated, two carbon atoms are added at the carboxyl end of the chain, and therefore the numbering of the double bonds in the systematic name changes each time the chain is lengthened.

An alternative notation, often used in metabolic studies, numbers the carbon atoms from the methyl terminal carbon atom rather than from the carboxyl end. Under this system, the shorthand notation for oleic acid is 18:1 n-9 and that for linoleic acid is 18:2 n-6. Arachidonic acid is 20:4 n-6 and gamma linolenic acid is 18:3 n-6, and it is easier to see that the former has been formed from the latter by the addition of two carbon atoms and one double bond.

Some older publications use a system of notation based on the Greek alphabet (Stryer, 1988).

$$\underset{\omega}{H_3C} - (CH_2)_n - \underset{\beta}{\overset{3}{CH_2}} - \underset{\alpha}{\overset{2}{CH_2}} - \overset{1}{COOH}$$

Carbon atoms 2 and 3 are often referred to as α (alpha) and β (beta), respectively. The terminal methyl carbon is the ω (omega) carbon. The position of a double bond is represented by the symbol Δ (Delta) followed by a superscript number e.g. $\Delta^{9,12}$. Under this system $C_{x:y}\ \Delta^z$ is the general formula for an unsaturated fatty acid (Bohinski, 1983), and linoleic acid is $(C_{18:2})\Delta^{9,12}$ or *cis, cis*-$\Delta^{9,12}$-octadecadienoic acid. If the position of the double bond is denoted by counting from the terminal methyl group, the ω notation is used e.g. arachidonic acid is an ω-6 fatty acid and alpha linolenic acid is an ω-3 fatty acid (Marinetti, 1990).

1.2.3 Triacylglycerols

Triacylglycerol (TAG) molecules are composed of three fatty acids esterified to a glycerol moiety. In most natural oils and fats, the three constituent fatty acids are not randomly distributed (Table 1.2).

Table 1.2 Characteristic positioning of fatty acids in triacylglycerol and phosphoglyceride molecules

	Cows' milk fat	Human milk fat	Animal depot fat	Phosphoglycerides
sn-1	Random	Unsaturated	Saturated	Saturated
sn-2	Random	Saturated	Unsaturated and short chain	Unsaturated
sn-3	Short chain		Random	Phosphate group

British Nutrition Foundation (1992)

There is a tendency for specific fatty acids to be located at particular positions on the three glycerol carbons. These are given stereospecific numbers, *sn*-1, *sn*-2 and *sn*-3. In nature, the more unsaturated fatty acids tend to be found at the *sn*-2 position. In human milk, the *sn*-2 position tends to be occupied by palmitic acid (16:0), and unsaturated fatty acids are found in the *sn*-1 position. These specific distributions are important both in terms of the physico-chemical properties of lipids and their metabolic activities.

1.2.4 Phosphoglycerides

In mammals, the lipids involved in membrane structures are mainly phosphoglycerides and unesterified cholesterol. Phosphoglycerides belong to the more general class of phosphorous containing lipids, the phospholipids, which also includes sphingomyelins and cerebrosides, found mainly in nervous tissue.

Phospholipids have important properties in membranes and foods because of their amphipathic properties i.e. they possess both hydrophilic and hydrophobic moieties. In contrast, hydrophobic fats, without polar groups, such as triacylglycerols are often called neutral, apolar or non-polar lipids.

1.2.5 Food fats

Fat makes an important contribution to the texture and palatability of foods and plays an important role in providing energy, especially in the diets of young children. Food fats usually contain small amounts of other fat-soluble substances, including flavour components and vitamins. The amount of energy obtained from common fats is about the same, despite the different functions of the fatty acid constituents. It is estimated that at least 15% of dietary energy should be provided by fat to facilitate the absorption of the fat-soluble vitamins A, D, E and K. However, the indispensable role of fat in the diet is to provide the essential fatty acids, linoleic and α-linolenic acid and their derivatives, because the body cannot synthesise these from other constituents in the diet (Sanders, 1994).

Lipid in human diets is derived mainly from the storage fats of mammals, birds, fish, and the seed oils of plants (British Nutrition Foundation, 1992). The fatty acid profile depends on the source of the oil; animal fats have a higher percentage of saturated fatty acids (16:0 and 18:0), than plants sources, such as soyabean, sunflower and maize, which contain higher concentrations of polyunsaturated fatty acids (18:2 and 18:3) than animal sources. Oleic acid (18:1) is a common fatty acid from both plant and animal sources. Fish oils are distinguished from mammalian and avian sources by the relatively high concentration of fatty acids with 20 or more carbon atoms and are normally rich in polyunsaturated fatty acids of the n-3 family.

1.3 Lipid digestion, absorption and metabolism

1.3.1 Background

Approximately 92-96 % of the fat in a typical Western diet is long chain triacylglycerol and the rest is composed of phospholipids, free and esterified cholesterol, fat-soluble vitamins and other lipid-soluble components. These lipids are mixed with endogenous lipids originating from bile, desquamated cells and dead bacteria. Faecal fat is therefore a mixture of dietary, biliary, cellular and bacterial sources. In healthy subjects fat uptake is very efficient and faecal fat is only ~2.5 % of the intake (Hernell, 2001).

1.3.2 Introduction to digestion and absorption

Digestion is the chemical breakdown of food by enzymes secreted in the mouth, stomach and the exocrine cells of the pancreas (Johnson, 1997). Although some digestion of dietary macronutrients takes place in the stomach, the final breakdown occurs in the small intestine (Figure 1.1). Luminal digestion is due to enzymes secreted by the salivary glands, stomach and pancreas. Absorption is the movement of the products of digestion from the intestinal lumen into the blood. Only digestion and absorption of lipids will be discussed here. Dietary fat must be made accessible to the enzymes, which break it down. This achieved by emulsification – the formation of microscopic droplets in which the ratio of surface area (where enzymes can act) to volume is very large. Thus, both physico-chemical changes and enzymatic processes must be considered in the digestion and absorption of lipids.

The process of digestion and preparation for absorption begins before food enters the mouth. The cephalic phase represents the brain's anticipation of food through the sight, smell or thought of food. This is reinforced by the taste of food in the mouth. Cephalic stimulation of the flow of saliva occurs through activation of the parasympathetic nervous supply to the salivary glands (Frayn, 1996). Stimulation of gastric juice secretion also occurs. Lingual lipase is also secreted into the mouth from glands behind the tongue and soft palate. It is not thought to produce much hydrolysis of lipids in adults, but may have an important role in neonates, as a large proportion of the energy in milk is in the form of triacylglycerol. Its pH optimum is low (~5), and it may produce some lipid hydrolysis in the stomach. The most important processes that occur in the mouth are the mechanical breakdown of food and its hydration with saliva.

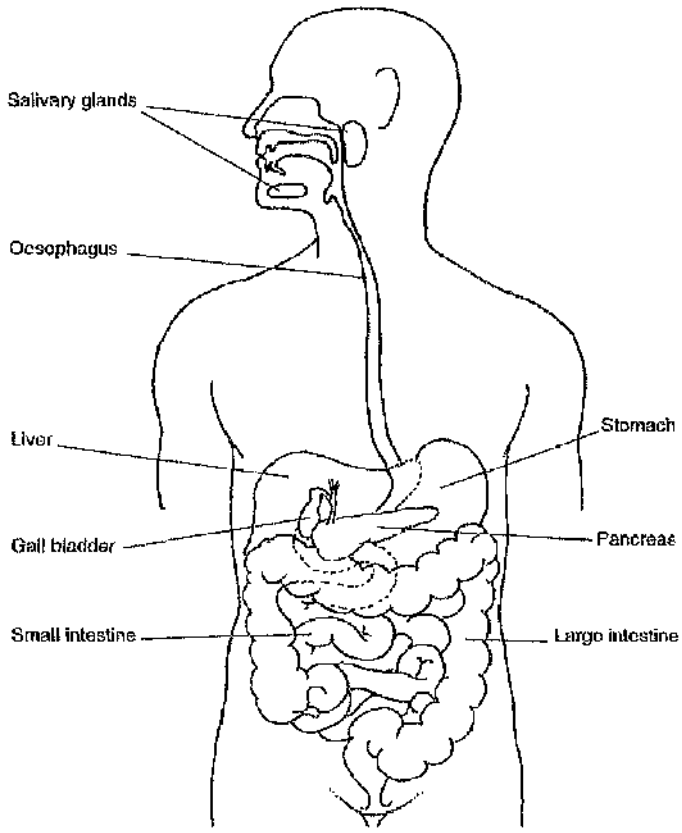

Figure 1.1 Diagram of the gastrointestinal tract

After swallowing, the chewed food is propelled rapidly through the oesophagus into the stomach, where it is physically broken up further and mixed with the stomach's digestive juices. Food is pounded into a creamy mixture known as chyme by the rhythmical contractions of the lower part of the stomach. Entry to the duodenum is regulated by the pyloric sphincter, which opens at regular intervals - about twice each minute. The pyloric sphincter only opens partially, so large particles are retained for further pummelling. Except for short-chain fatty acids, there is no absorption of fat from the stomach (Johnson, 1997).

1.3.3 Small intestinal digestion

The first part of the small intestine is the duodenum. Two important organs discharge into it. The gall bladder, the storage reservoir for bile salts produced in the liver, discharges its contents via the common bile duct. The exocrine part of the pancreas releases its secretions through the pancreatic duct. The common bile duct joins the pancreatic duct

and both discharge into the duodenum (Frayn, 1996). Thus bile salts and pancreatic enzymes are liberated together into the small intestine.

1.3.3.1 The pancreas

The pancreas contains both exocrine and endocrine tissues. The exocrine function of the pancreas is to discharge digestive juices into the small intestine. The endocrine function consists of the production and secretion of hormones (most importantly insulin and glucagon) into the bloodstream. The vast majority of cells in the pancreas are exocrine.

Pancreatic exocrine secretion is an alkaline digestive juice composed of bicarbonate, water and enzymes such as amylase, trypsinogen and lipase. Three phases of pancreatic exocrine stimulation can be identified. The cephalic stage is initiated by the sight, smell or thought of food, and increases bicarbonate and enzyme output by a neural mechanism via the vagus nerve. The gastric phase starts when food distends the stomach and the hormone, gastrin is secreted. The most significant phase is the intestinal phase. This is mediated by the secretion of the hormones, secretin and cholecystokinin (CCK). Both of these hormones are secreted by specific endocrine cells in the intestinal epithelium of the duodenum and jejunum, with low concentrations found elsewhere in the gut. Secretin stimulates the output of fluid and bicarbonate by the pancreas and is released in response to gastric acid entering the duodenum. CCK secretion is initiated by the presence of fatty acids and amino acids in the proximal small intestine and stimulates pancreatic enzyme production (Woodward & Colagiovanni, 1998), but also slows gastric motility and emptying when fat is in the small intestine (Johnson, 1997).

1.3.3.2 Micelle formation and triacylglycerol digestion

Lipid digestion and absorption depend upon emulsification of triacylglycerol and formation of micelles. The main emulsifying agents are the bile salts. Bile salts are derivatives of cholesterol, which are synthesised in the liver and secreted in bile in the form of covalent conjugates. The major bile salts are sodium glycocholate – a conjugate of cholic acid and glycine, and sodium taurocholate – a conjugate of cholic acid and taurine. Bile salts are amphipathic molecules with a predominantly non-polar ring structure and a highly polar acidic group. As lipid digestion proceeds, further amphipathic molecules are formed, which may help emulsification. These include monoacylglycerols and phospholipids. Micelles form an oil-in-water emulsion by the non-polar tails of the

amphipathic molecules stabilising small groups of non-polar molecules, predominantly triacylglycerol. The polar end faces outwards to the aqueous environment of the intestinal contents. A net repulsive action of the outward facing polar groups also tends to split the lipid droplets further, resulting in a finer and finer emulsion. These emulsified particles are typically 1 μm in diameter. It is in this form that most of the hydrolysis of triacylglycerols proceeds (Frayn, 1996).

Pancreatic lipase (EC 3.1.1.3) is a family of lipases that act on the ester links in the 1 and 3 positions in an acylglycerol, but not the 2-position. Thus fatty acids are liberated and 2-monoacylglycerol remains. Pancreatic lipase has optimum activity at pH 8 and remains active down to pH 3. Although bile salts inhibit its activity, this is prevented under physiological circumstances by the combination of lipase with colipase, which is secreted by the pancreas as procolipase in a 1:1 ratio with lipase. Procolipase is activated by trypsin. Lipase-colipase complexes are scarce within the duodenum during fasting, but the presence of fat stimulates their secretion in large quantities. Colipase can replace bile salts at the oil-water interface. Once colipase is attached to the fat droplet, lipase binds to a specific site on the colipase molecule in a 1:1 ratio and consequently carries out its catalytic function, hydrolysing fatty acids from the 1 and 3 positions of a triacylglycerol. There is very little hydrolysis of the ester bond at position 2 and very little isomerization to 1(3)-monoacylglycerol, presumably because of rapid uptake of the monoacylglycerol into epithelial cells (Gurr, Harwood & Frayn, 2002).

Both fatty acids and monoacylglycerols have amphipathic properties. The monoacylglycerol is an effective emulsifying agent and aids in the action of bile salts. Gradually, much smaller groups of molecules are formed – the mixed micelles. Mixed micelles contain bile salts and other molecules, particularly fatty acids and monoacyglycerols and are typically 4-6 nm in diameter. They are so small that they can diffuse easily through the unstirred aqueous layer overlying the enterocytes (Figure 1.2) and thus bring the products of triacylglycerol hydrolysis, i.e. non-esterified fatty acids and monoacyglycerols, to the surface of the absorptive cells.

1.3.4 Lipid absorption

The brush border membrane is separated from the bulk solution of the intestinal lumen by the unstirred aqueous layer. Non-esterified fatty acids and monoacylglycerols are poorly soluble in water and therefore move slowly across this barrier. Since uptake depends on

the number of molecules in contact with the enterocyte membrane, their absorption is diffusion limited. In contrast, mixed micelles are water soluble, diffuse readily through the unstirred layer and increase the concentration of fatty acids and monoacylglycerols at the membrane by 100- to 1000-fold. Short- and medium-chain fatty acids are not dependent on micelles for uptake because of their higher solubility in and diffusion through the unstirred aqueous layer (Johnson, 1997).

Solutes moving across the enterocyte from the intestinal lumen to the blood must traverse an unstirred layer of fluid, a glycocalyx covering the microvilli, the apical cell membrane, the cytoplasm of the cell, the basal or lateral cell membrane, the basement membrane, and finally the wall of the capillary or lymph vessel (Figure 1.2). Microvilli are morphological modifications of the cell membrane and comprise the brush border.

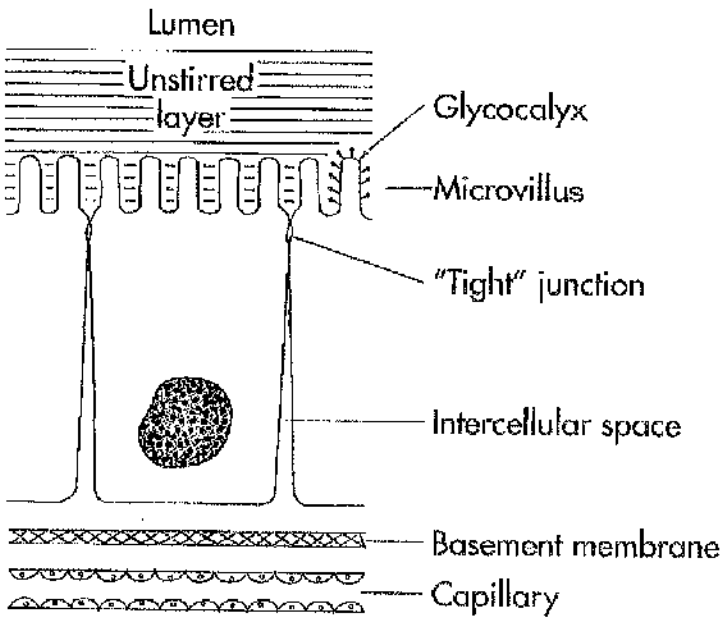

after Johnson (1997)

Figure 1.2 Schematic diagram of the mucosal barrier

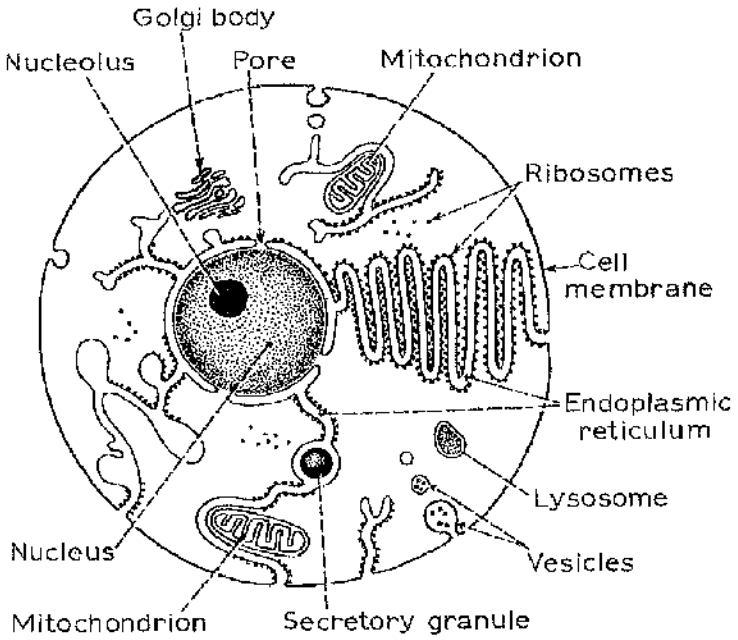

after Bell, Emslie-Smith & Paterson (1976)

Figure 1.3 Schematic diagram of a typical animal cell

1.3.4.1 Absorption of long-chain fatty acids

It was thought that uptake of monoacylglycerols and fatty acids by the intestinal epithelial cells (enterocytes) occurred by simple diffusion, but there is evidence of protein-mediated transport processes (Frayn, 1996). It is possible that both protein-mediated and diffusional mechanisms contribute to the *in vivo* movement of fatty acids (Frohnert & Bernlohr, 2000). Several candidate proteins have been identified: the first was plasma membrane fatty acid binding protein (PABPpm), which was isolated from rat liver plasma (or cell) membranes. PABPpm is expressed on the plasma membrane of liver, adipose tissue, cardiac muscle intestinal and vascular epithelium as well as internal membranes (Frohnert & Bernlohr, 2000). PABPpm is not related structurally to the family of intracellular fatty acid binding proteins (Gurr *et al.* 2002). Fatty acid transport protein (FATP) is also found in the liver. It is an integral membrane protein found in the plasma membrane and internal membranes. It is highly expressed in adipose tissue, skeletal muscle and heart, but is also expressed at lower levels in liver, brain, kidney and lung (Frohnert & Bernlohr, 2000).

Once inside the cell, fatty acids must be 'activated' before taking part in metabolic reactions. The active form is usually the thiolester of the fatty acid with the complex nucleotide, coenzyme A (CoA) or the small protein known as acyl carrier protein (ACP).

Both these molecules contain a thiolester, which renders the acyl chains water soluble (Gurr *et al.* 2002). The formation of acyl-CoAs is catalysed by acyl-CoA synthetases. The acyl-CoA synthetases differ from each other with respect to their subcellular location and their specificity for fatty acids of different chain lengths. Their overlapping chain length specificities and tissue distributions mean that most fatty acids in the range 2-22C can be activated, although at different rates. Originally, it was thought that short-, medium- and long-chain isoforms were often present, but molecular biology techniques have revealed many more.

Within the enterocyte, long-chain fatty acids and monoacylglycerols are re-esterified to form new triacylglycerol molecules. This occurs mainly by the monoacylglycerol esterification pathway, which begins with monoacylglycerol, unlike most other tissues in which the formation of triacylglycerols occurs by the phosphatidic acid pathway, which begins with glycerol-3-phosphate. The monoacylglycerol esterification pathway involves the synthesis of triacylglycerols from 2-monoacylglycerols and coenzyme A (CoA)-activated fatty acids. The enzymes involved in this pathway are associated with the smooth endoplasmic reticulum (Figure 1.3 and Section 1.3.5.2). Certain fatty acids are used in preference to others, and this occurs despite similar rates of absorption by enterocytes and similar rates of enzymatic Co-A activation and acylglycerol esterification. These observations have been explained by the presence of intracellular FABP's, which have affinities for fatty acids of different chain lengths and varying degrees of saturation, and which may play a role as carriers and for intracellular storage.

Absorbed fatty acids bind strongly to the apical membrane of enterocytes. Solubilization is brought about when the fatty acids bind specifically with receptors on FABP's. This facilitates the transfer of the non-esterified fatty acids from the apical membrane, through the cytosol to the smooth endoplasmic reticulum, where esterification to diacylglycerols and triacylglycerols takes place (Johnson, 1997).

Triacylglycerols form lipoprotein particles, chylomicrons, with phospholipids and proteins, particularly apolipoprotein B. Chylomicrons are typically 100 nm - 1 μm in diameter and are the largest of the lipoprotein particles present in blood. Synthesis of both triacylglycerol and apolipoprotein B occurs in the endoplasmic reticulum, where they form complexes with phospholipids. This complex is transported to the Golgi apparatus (or Golgi body), where the protein is glycosylated. Newly formed chylomicrons are secreted by exocytosis into the interstitial space, traverse the basement membrane, and enter the

gaps between the endothelial cells, which comprise the lacteals. From there they flow slowly into more major branches of the lymphatic system, up the thoracic duct and thence into the circulation. Chylomicrons are too large to enter the pores of capillary blood vessels.

The process described above is summarised in Figure 1.4, but only applies to long-chain (C_{16} or more) fatty acids. Short- and medium-chain fatty acids are present in the diet in dairy products, but most dietary fatty acids are long-chain and enter the bloodstream as chylomicron-triacylglycerol. This route of absorption means that dietary triacylglycerols, unlike other nutrients, bypass the liver on their entry into the circulation. Most of the triacylglycerol is removed from chylomicrons in tissues outside the liver, particularly adipose tissue and to a lesser extent skeletal muscle and heart (Frayn, 1996).

Non-esterified fatty acids are liberated from adipose tissue in the post-absorptive state i.e. when all of the last meal has been absorbed from the intestinal tract, but not much thereafter. In humans, this is usually represented by the state after an overnight fast before breakfast is consumed. After an overnight fast, the concentration of non-esterified fatty acids in plasma is around 0.5 mM, and the total triacylglycerol concentration is around 1 mM. The chylomicron triacylglycerol concentration will be very low, usually less than 0.05 mM. Lipid fuels are an important energy source at this time. The turnover of non-esterified fatty acids involves their liberation from adipose tissue and uptake by a number of tissues, predominantly skeletal muscle and liver.

1.3.4.2 Absorption of short- and medium-chain fatty acids

Short- and medium-chain fatty acids show less affinity for the enterocyte cell membrane, are water-soluble and are not bound to specific proteins. They are not esterified within enterocytes because the specific medium-chain acyl-CoA synthetase (EC 6.2.1.2) required for their activation is not present (Frayn, 1996). Therefore, they enter the capillary plasma directly in the form of non-esterified fatty acids and are transported into portal blood without involvement of chylomicrons. Short- and medium-chain fatty acids are carried from the small intestine to the liver via the portal vein, weakly bound to albumin. Their uptake by the liver reaches from 80 to 100 % of the portal flux. The remaining fraction is discharged into the bloodstream and is available to peripheral tissues (Guillot *et al.* 1993).

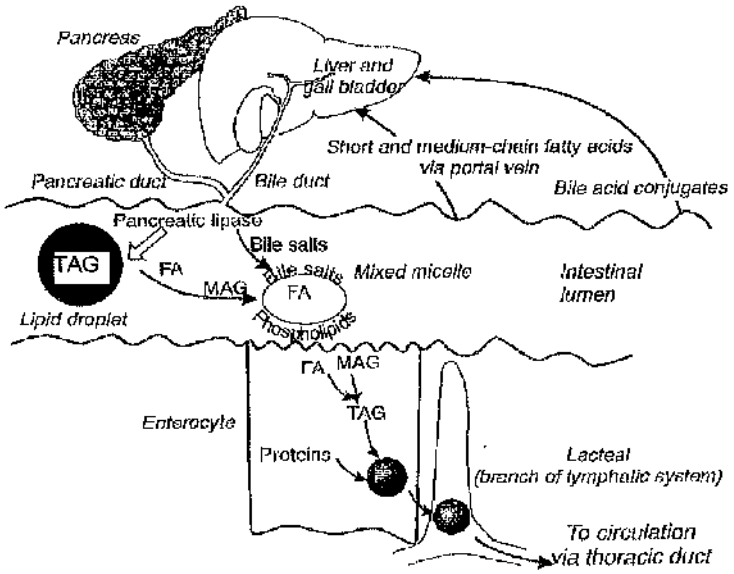

after Gurr *et al.* (2002)

Figure 1.4 Digestion and absorption of dietary triacylglycerol in the small intestine

Lipid droplets entering the small intestine from the stomach are subjected to the action of pancreatic lipase, which hydrolyses triacylglycerol (TAG) to produce monoacylglycerols (MAG) and fatty acids (FA). These are emulsified with bile salts (from the gall bladder) to produce a micellar suspension (the mixed micelles) from which components are absorbed across the epithelial cell (enterocyte) membranes. Short- and medium-chain fatty acids pass through into the portal vein, and are carried to the liver. Bile salts are reabsorbed in the lower part of the small intestine. Within the enterocyte TAG is reformed from MAG and FA, and packaged into chylomicrons (the largest of the lipoprotein particles). Chylomicrons are secreted into small branches of the lymphatic system, the lacteals and eventually enter the circulation via the thoracic duct.

1.3.5 Lipid metabolism in the liver

1.3.5.1 Structure and function of the liver

The portal vein is short (7-8 cm in length) and is formed by the union of veins from different parts of the intestinal tract, including the stomach. These veins carry water-soluble substances absorbed from the intestinal tract to the liver, and thereafter via the hepatic veins to the heart.

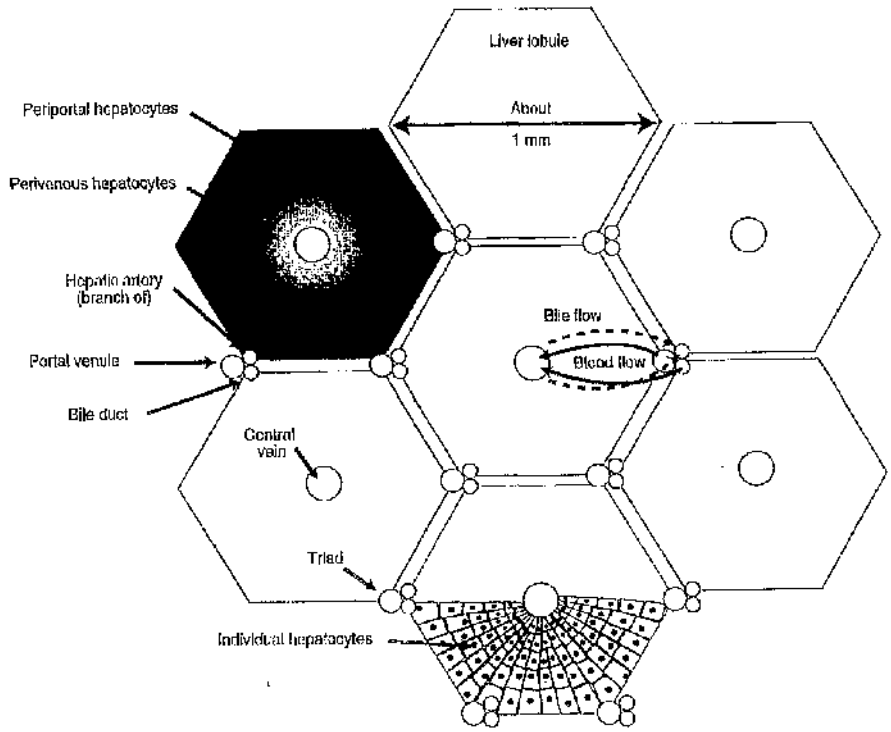

after Frayn (1996)

Figure 1.5 Arrangement of hepatocytes

The major part of the liver (80 % by volume) is composed of hepatocytes. These are arranged as hexagonal units or lobules (Figure 1.5). At the corner of the hexagon is a triad of three blood vessels, which are tiny branches of the portal vein, hepatic artery and bile duct. In the centre of the lobule is branch of the hepatic vein, which carries blood away. The hepatocytes radiate outwards from the central vein. Blood flows from the triads towards the central vein in small passages between the hepatocytes, the sinusoids. Sinusoids are the equivalent of the capillaries found in other tissues and are lined with flat endothelial cells, as are all capillaries. The blood in the sinusoids is in intimate contact with the hepatocytes.

The precise arrangement of hepatocytes within the liver is closely related to the function of the cells. This is known as the metabolic zonation of hepatic metabolism. The periportal hepatocytes on the outside of each lobule are exposed to blood that has recently arrived at the liver in the hepatic portal vein and hepatic artery. Thus these cells are well oxygenated and supplied with substrates, and oxidative metabolism predominates. The synthesis of glucose (gluconeogenesis) occurs mainly in these cells, whereas the cells nearer the centre of each lobule (perivenous hepatocytes) are more involved in glycolysis and ketone body production. This arrangement is very flexible, and each individual cell can perform either function depending upon its location in the lobule and the prevailing physiological circumstances (Frayn, 1996).

1.3.5.2 Hepatocyte structure and function

The internal structure of a typical hepatocyte is comparable to that shown in Figure 1.3. The cell membrane or plasma membrane serves as the interface between the interior of the cell and its external environment. Cell membranes are composed of a phospholipid bilayer, which is differentially permeable i.e. permits water molecules to pass through, but is a barrier to the easy passage of ions such as Na^+, K^+, Cl^-. The phospholipid bilayer has associated proteins, some of which are much more intimately associated with the lipids than others. The proteins that are less closely allied to lipids tend to be quite hydrophilic glycoproteins and are known as extrinsic proteins. They occur on both the outer and inner surface of the membrane. The extrinsic proteins probably do not penetrate into the phospholipid bilayer of the membrane. Other proteins penetrate into and, in some cases, all the way through the lipid bilayer. These are intrinsic proteins such as transport proteins. The cell membrane is not symmetrical. The extrinsic proteins associated with the outer surface of the membrane are usually different from those associated with the inner surface (Kimball, 1978).

The nucleus is responsible for replication. Several kinds of RNA molecules are synthesised in the nucleolus. Some of this RNA is used in the assembly of ribosomes. Ribosomes are essential for protein synthesis in the cell. The term cytoplasm is traditionally used to describe everything within the cell except the nucleus. Electron microscopy reveals the extraordinary complexity of structures within the cytoplasm. These clearly defined structures are called organelles. Cytosol is the fluid in which the organelles are suspended. It is an aqueous solution of small molecules, ions and proteins. A number of important enzymes are found in the cytosol, including some of those involved in *de*

novo lipogenesis (Section 1.3.5.3), but most of the functions of the cytoplasm are the functions of the organelles located in it.

Mitochondria are spherical or rod shaped bodies that range in size from 0.2 μm to 5 μm. Muscle mitochondria are typically sausage-shaped and several micrometers long, whereas liver mitochondria are more nearly spherical, 1-2 μm diameter. Hepatocytes, as metabolically very active cells, may have over a thousand mitochondria.

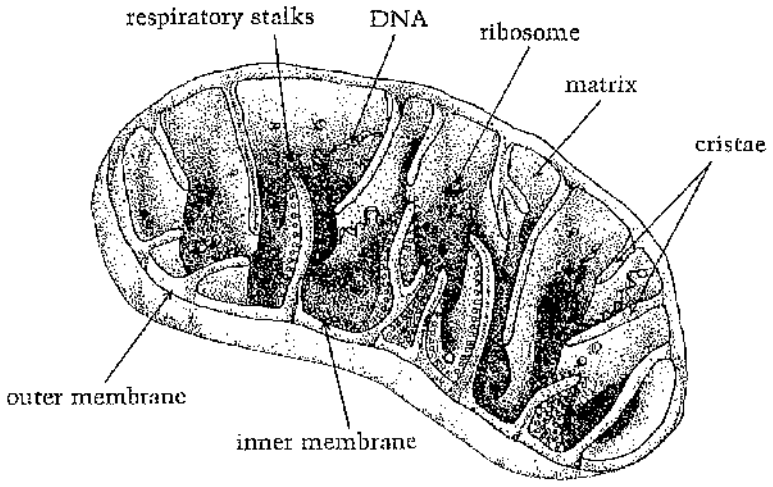

after Bohinski (1983)

Figure 1.6 Schematic drawing of a mitochondrion

Each mitochondrion is bounded by a double membrane (Figure 1.6). The outer membrane provides a smooth, uninterrupted boundary to the mitochondrion. The inner membrane is repeatedly extended into folds that project into the inner space of the mitochondrion. These inner folds are called cristae. The membranes of the mitochondria are similar to those of the cell membrane. They contain phospholipid and protein. Some of the protein is extrinsic, but much of it is intrinsic i.e. embedded in the lipid bilayer. Mitochondria contain the enzymes that carry out the oxidation of sugars, amino acids and fatty acids from the diet, and are the site of cellular respiration via the TCA (tricarboxylic acid) cycle.

Ribosomes are amongst the smallest structures suspended in the cytoplasm (~20 nm). They are the site at which protein synthesis takes place. Some of the proteins are simply added to the cytosol and perform their function there; others are packaged in some type of

membrane-bound organelle and are ultimately secreted from the cell. The ribosomes that secrete these proteins are attached to the membranes of the endoplasmic reticulum.

The endoplasmic reticulum is an elaborate system of membranes within the cell, which are probably interconnected with each other. The membranes have a lipid-protein structure similar to that of other membranes in the cell. Each membrane of the endoplasmic reticulum has one surface that faces the cytosol and one that faces the interior of the cavity. Evenly spaced ribosomes adhere to the cytosol-facing surface of the reticulum membranes. Ribosome-studded endoplasmic reticulum is known as rough endoplasmic reticulum. Proteins and polypeptides synthesised by the ribosomes are deposited in the interior space of the reticulum. As this happens further processing of the polypeptide takes place, such as the formation of disulphide bonds between cysteine residues or glycosylation. The proteins synthesised by the rough endoplasmic reticulum are thus packed within a membrane. They may remain to be used within the cell or they may be secreted from the cell. Endoplasmic reticulum is also found without adhering ribosomes. This is called smooth endoplasmic reticulum and is involved in the synthesis of fats, phospholipids and steroids. It may be the source of the membranes that make up the Golgi apparatus.

The Golgi apparatus (or Golgi body) consists of a stack of flat membrane-bounded sacs. Proteins synthesised by the rough endoplasmic reticulum are transferred to the Golgi apparatus. Here additional carbohydrate may be added. Proteins accumulate within the sacs of the Golgi apparatus until they are stuffed with protein. These protein-filled sacs may migrate to the surface of the cell and discharge their contents to the outside. Others may be retained within the cell as lysosomes.

Lysosomes are roughly spherical structures bounded by a single membrane and filled with hydrolytic enzymes that digest polysaccharides, lipids, phospholipids, nucleic acids and proteins. They are prevented from digesting the other components of the cell by confinement within the lysosome. Lysosomes play an important role in the death of cells. When a cell is injured or dies, its lysosomes aid in its disintegration. This clears it away so that a healthy cell can replace the damaged one.

Peroxisomes are about the size of lysosomes and are bounded by a single membrane. They are filled with catalase, which catalyses the breakdown of hydrogen peroxide (H_2O_2), a potentially dangerous product of cell metabolism produced during peroxisomal β-oxidation of fatty acids.

1.3.5.3 Fatty acid metabolism in the liver

Summary

The main pathways of fatty acid metabolism in the liver, and their hormonal regulation are shown in Figure 1.7. The liver, like many other tissues, may take up non-esterified fatty acids from the plasma. These occur due to leakage from the peripheral tissues after lipoprotein lipase action, or after hydrolysis of adipose tissue triacylglycerol, or within remnant lipoproteins as triacylglycerol or cholesteryl esters. Short- and medium-chain fatty acids are carried directly to the liver via the hepatic portal vein. Fatty acids have two major fates within the liver: oxidation or acylglycerol formation (triacylglycerol and phospholipids).

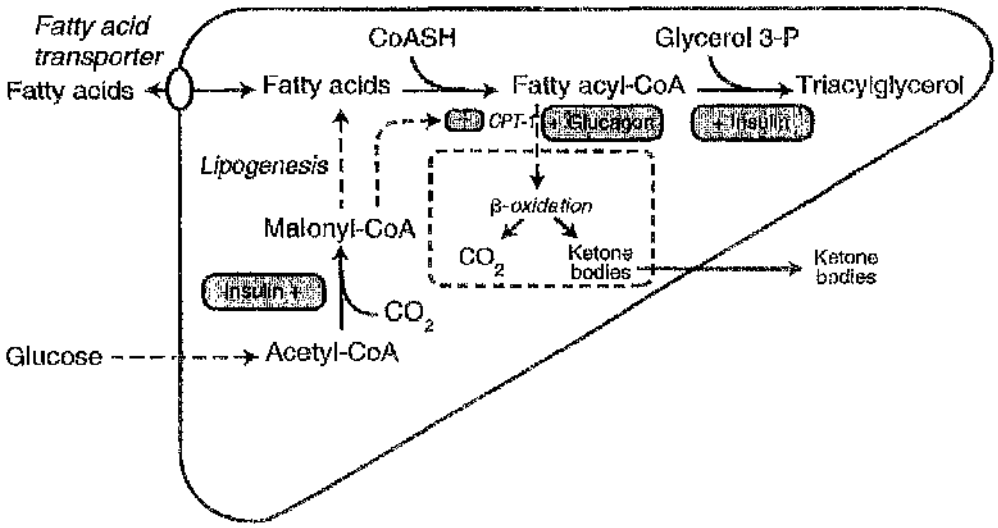

after Frayn (1996)

Figure 1.7 Fatty acid metabolism in the liver

The liver may oxidise fatty acids by the mitochondrial β-oxidation pathway to produce energy for its metabolic activities. Gluconeogenesis, an energy requiring process, appears to be fuelled by oxidation of fatty acids (Frayn, 1996). During the oxidation of fatty acids in the liver, the ketone bodies acetoacetate and 3-hydroxybutyrate are produced and exported into the circulation to provide energy rich substrates to the periphery. Ketones can substitute for glucose in muscle and brain at times of reduced dietary intake. The rate of ketogenesis in the liver is determined by the rate of fatty acid oxidation, which in turn is

determined by the availability of fatty acids and the balance between their two fates in the liver. The alternative fate of fatty acids taken up by the liver is esterification to form triacylglycerol, which is stored within hepatocytes. Hepatic triacylglycerol can be mobilised to be incorporated into very-low-density lipoprotein (VLDL) and secreted from the liver into the bloodstream. Accumulation of triacylglycerol can occur when the supply of fatty acids to the liver exceeds the rate of oxidation and VLDL-triacylglycerol secretion in certain pathological conditions. Insulin and glucagon control the balance between fatty acid oxidation and esterification in the liver.

Long-chain fatty acid metabolism in the liver

Long chain fatty acids cross the hepatocyte membrane by a carrier mediated process (Frayn, 1996). Inside the hepatocyte they are transported through the cytosol by binding to specific fatty acid-binding proteins. Further metabolism of long-chain fatty acids is dependent upon their activation by forming thioesters with coenzyme-A (CoASH). Acyl-CoA synthetase (EC 6.2.1.3) activates fatty acids containing from six to 20 carbon atoms and occurs on the outer mitochondrial membrane, in endoplasmic reticulum and peroxisomes (Gurr *et al.* 2002). In animals, it is thought that mitochondrial and peroxisomal acyl-CoA synthetases are used for fatty acid oxidation, whilst the endoplasmic reticulum enzyme is used for lipid biosynthesis.

$$\text{CoASH} + \text{R-COOH} \rightarrow \text{R-CO.SCoA} + \text{H}_2\text{O} \qquad (1.1)$$

Coenzyme A + fatty acid → thioester (acyl-SCoA) + water

The enzymes participating in the degradation of the acyl group (by β-oxidation) are located in mitochondria and peroxisomes. This compartmentalisation requires the passage of acyl-SCoA from the cytoplasm into the organelle. However, the inner mitochondrial membrane is impermeable to CoA, therefore fatty acyl-CoAs formed in the cytosol cannot enter the mitochondria directly for oxidation. This barrier is overcome by the participation of carnitine, which serves as an acyl-group carrier. Esterification of the fatty acid with carnitine is catalysed by carnitine O-palmitoyltransferase-1 (CPT-1, CPT-I or CPTo, EC 2.3.1.21), that is found on the outer mitochondrial membrane. This enzyme is able to transfer a variety of fatty acyl groups from coenzyme A to carnitine. There is a specific carrier to transport fatty acyl-carnitine across the outer membrane. In order to achieve effective transport of acyl-SCoA, carnitine palmitoyltransferase activity is also present on the inner surface of inner mitochondrial membrane (Figure 1.8).

The properties of the enzymes in the two locations are different and the 'outer' enzyme is known as carnitine palmitoyltransferase-1 (CPT-1) and the 'inner' enzyme is known as carnitine palmitoyltransferase-2 (CPT-2, CPT-II or CPTi). These two proteins are the products of different genes (Zammit, 1999a). CPT-1 generates acyl-carnitine (from acyl-SCoA), which is transported across the inner membrane, after which CPT-2 regenerates acyl-SCoA and free carnitine. The latter is transported out of the mitochondrion by the same carrier that transports acyl carnitine in. In fact, the entry of acyl-carnitine is obligatorily linked to the exit of carnitine.

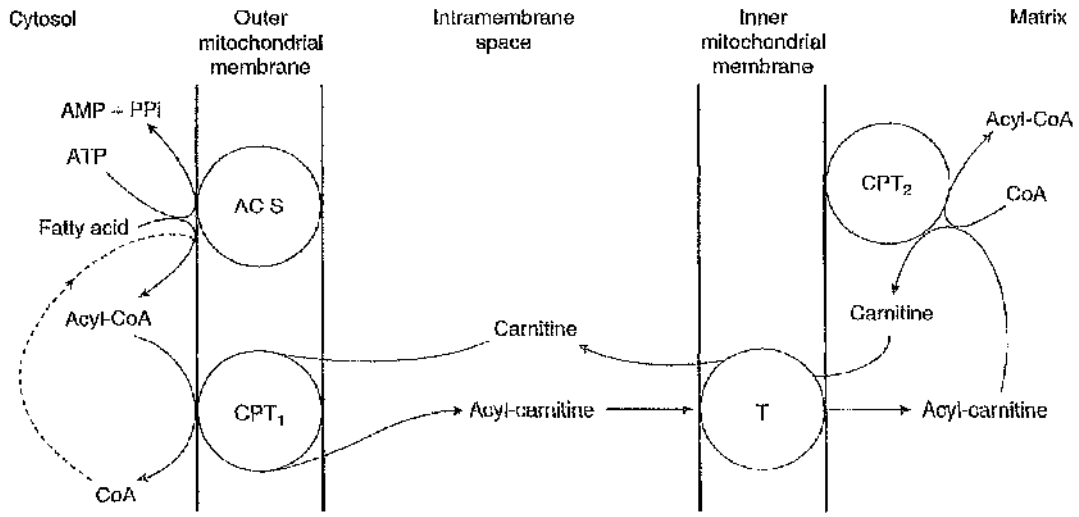

after Gurr *et al.* (2002)

Figure 1.8 Movement of acyl residues into mitochondria via carnitine

ACS = acyl-CoA synthetase; T = translocase; CPT = carnitine palmitoyltransferase

CPT-1 is inhibited by malonyl-CoA (McGarry & Foster, 1980), an intermediate in the pathway of hepatic *de novo* lipogenesis (Figure 1.13). Glucagon increases fatty acid oxidation, by lowering malonyl-CoA concentrations. By contrast, in 'fed' conditions, when insulin is elevated, malonyl-CoA levels will be high and fatty acid oxidation will be inhibited. Fatty acids will tend to be esterified to form triacylglycerol. This process also appears to be stimulated by insulin, although the exact locus of control is not clear (Frayn, 1996). Hence in the fed state, the liver tends to divert a higher proportion of fatty acid metabolism towards acylglycerol synthesis, rather than oxidation.

Peroxisomes and the endoplasmic reticulum also have CPTs, which are identical to CPT-1 and are also severely inhibited by malonyl-CoA. The collective term for all of these

transferases is CPTo, so termed because of the overt or cytosol-facing active site (Zammit, 1999a,b).

Medium- and short-chain fatty acid metabolism in the liver

Medium- and short-chain fatty acids are highly ionised at physiological pH and therefore soluble in aqueous biological fluids. Their small size and water solubility enables them to cross the cell membrane by facilitated diffusion, which is also know as passive diffusion or passive transport. This is made possible by membrane proteins that provide a pathway for specific solutes through the lipid bilayer. These membrane proteins are known as transporters or permeases (Nelson & Cox, 2000). Transporters are not enzymes in the usual sense; their 'substrates' are moved from one compartment to another, but are not chemically altered. Transporters span the lipid bilayer at least one and usually several times, forming a transmembrane channel lined with hydrophilic amino acid side chains. The channel provides an alternative route for a specific substrate to move across the lipid bilayer without having to dissolve in the bilayer. The result is an increase in the rate of transmembrane passage of the substrate, of orders of magnitude. The rate of uptake is proportional to the difference in the concentrations inside and outside the cell.

In all tissues, mitochondria are the main oxidative site of medium-chain fatty acids. Although activation of medium-chain fatty acids can occur in the cytoplasm (Zammit, 1984), it takes place mostly in the mitochondrial matrix, where a medium-chain acyl-CoA synthetase has been found. Medium-chain acyl-CoA synthetase (EC 6.2.1.2*) activates fatty acids containing from four to twelve carbon atoms. Although carnitine O-octanoyltransferase (EC 2.3.1.137) is found in liver mitochondria, octanoate oxidation is not limited by mitochondrial transport (Groot & Hulsmann, 1973) and carnitine O-octanoyltransferase is not inhibited by malonyl-CoA to the same extent as carnitine O-palmitoyltransferase-1 under either fasting or fed conditions (Saggerson & Carpenter, 1981). The oxidation rate of medium-chain fatty acids is faster than that of long-chain fatty acids. Medium-chain fatty acids are extensively oxidised by the liver regardless of the physiological state of the subject (Bach, Ingenbleek & Frey, 1996).

*Enzyme classification number according to the recommendations of the International Union of Biochemistry and Molecular Biology (IUBMB) - a system introduced to avoid confusion caused by some enzymes having several common names. The database can be searched at http://www.chem.qmul.ac.uk/iubmb/enzyme.

1.3.5.4 Beta-oxidation

The mitochondrial β-oxidation pathway is quantitatively the most important route of fatty acid oxidation. The mechanism was originally proposed by Knoop in 1904 (Stenesh, 1999, Gurr *et al.* 2002). The process consists of four steps (Figure 1.9): dehydrogenation, addition of water to the resulting double bond, oxidation of the β-hydroxyacyl-CoA to a ketone, and thiolytic cleavage by coenzyme A, which results in the cleavage of two carbons at a time from the acyl chain. The 2C product, acetyl-CoA, may then enter the TCA cycle (Section 1.3.5.5) and the acyl-CoA (two carbons shorter) is recycled. The enzymatic stages of mammalian mitochondrial β-oxidation were elucidated 30-40 years ago, but molecular biology techniques have revealed many more isoforms than was previously assumed. Eaton, Bartlett & Pourfarzam (1996) reviewed the enzymological and organisational aspects of mitochondrial β-oxidation together with its intrinsic control.

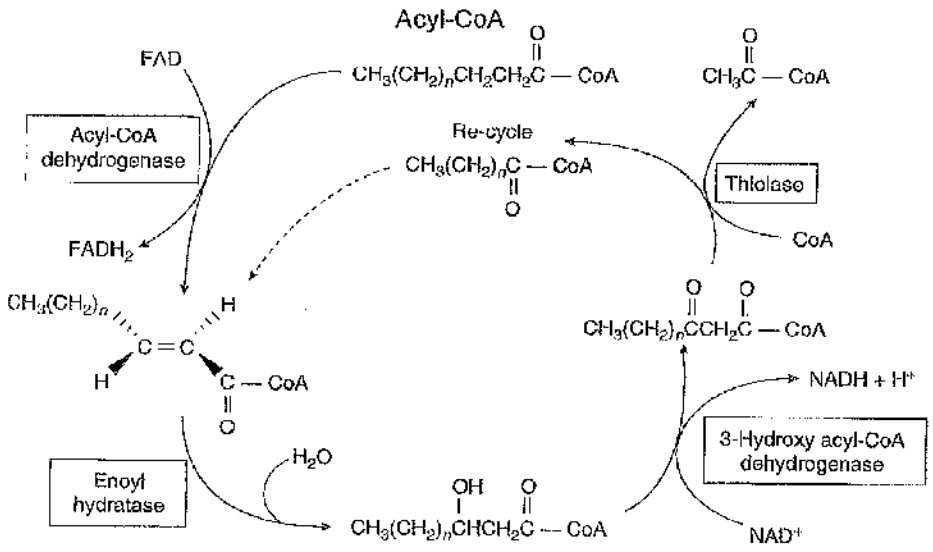

after Gurr *et al.* (2002)

Figure 1.9 Mitochondrial β-oxidation pathway

Each of the four enzymes involved (acyl-CoA dehydrogenase, EC 1.3.2.2; enoyl hydratase, EC 4.2.1.17; L-3-hydroxyacyl-CoA dehydrogenase, EC 1.1.1.35; acyl-CoA:acetyl-CoAS acyltransferase, EC 2.3.1.16, a thiolase) are present as isoforms that have varying chain-length specificities. Three of the enzymes (enoyl hydratase, 3-hydroxyacyl-CoA dehydrogenase (EC 1.1.1.211) and thiolase) have their long-chain isoforms present on the inner mitochondrial membrane. All the other isoforms of the enzymes are soluble in the mitochondrial matrix. There is evidence of metabolite channelling between individual

enzymes. This improves the efficiency of β-oxidation and prevents intermediates building up, which could be inhibitory or lead to a greater requirement for scarce CoA (Eaton *et al.* 1996). As a generalisation, it is thought that long-chain acids are oxidised by the membrane located enzymes while medium-chain substrates use the matrix enzymes (Liang *et al.* 2001).

Acetyl-CoA from mitochondrial β-oxidation of fatty acids is the substrate for two competing reactions: with oxaloacetate to form citrate in the TCA cycle (Figure 1.10) and with acetoacetyl-CoA to form ketone bodies (ketogenesis). Which reaction predominates depends partly on the rate of β-oxidation and partly on the availability of oxaloacetate. The proportion of acetyl groups entering the TCA cycle relative to ketogenesis is sometimes referred to as the 'acetyl ratio'. Availability of fatty acids and the rate of utilisation of β-oxidation products control the overall rate of β-oxidation.

An active β-oxidation pathway is present in peroxisomes as well as mitochondria. This pathway is particularly important in the liver and kidneys. In fact, in the liver it seems that mitochondria and peroxisomes collaborate in overall fatty acid oxidation (Gurr *et al.* 2002). Very long-chain fatty acyl-CoA is oxidised to medium-chain products in peroxisomes. The medium-chain fatty acids are then transported to mitochondria for complete β-oxidation or to the endoplasmic reticulum, where they may form glycerolipids. The final fate depends on the identity of the acyl chain (Sprecher *et al.* 1995).

Peroxisomal β-oxidation has been estimated to contribute up to 30 % (Frayn, 1996) or 50 % (Gurr *et al.* 2002) of the total rate of hepatic fatty acid oxidation. A high fat diet, such as that recommended to children with cystic fibrosis, increases the rate of peroxisomal β-oxidation. Thus, although medium-chain fatty acids comprise only a small portion of dietary fatty acids, they are not unusual substrates for mitochondrial β-oxidation in the liver as they are produced during intermediary metabolism in this tissue.

1.3.6 Acetate metabolism in the liver

1.3.6.1 The tricarboxylic acid (TCA) cycle

The tricarboxylic acid (TCA) cycle is also known as the citric acid cycle or the Krebs cycle, after the metabolic studies of Hans Krebs, who won the Nobel Prize in 1953 for elucidating the reaction sequence (Figure1.10). The TCA cycle is a hub in metabolism

integrating the metabolic flow of carbon among the main classes of biomolecules, with degradative pathways leading in and anabolic pathways leading out. It is closely regulated in coordination with other pathways.

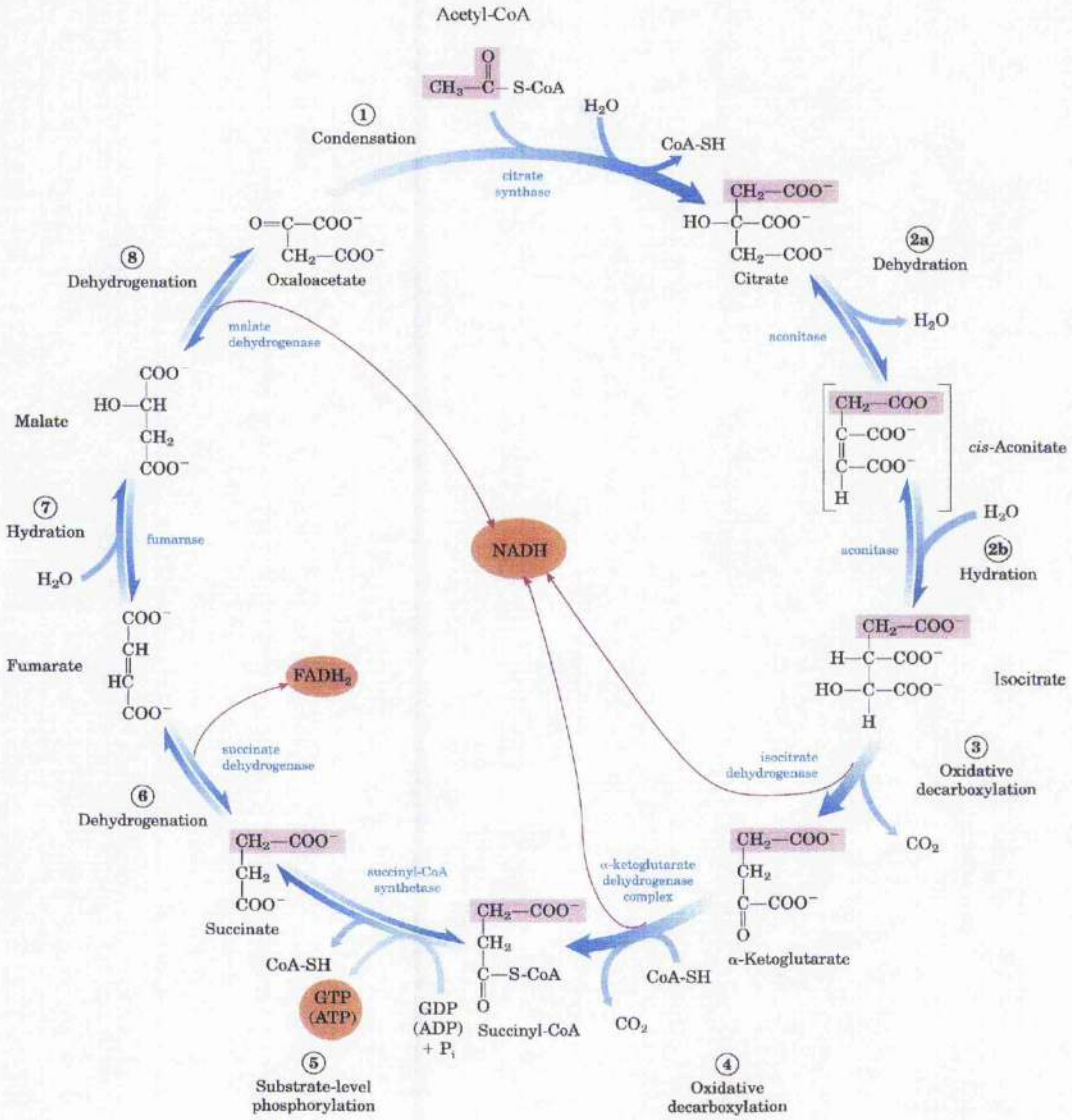

after Nelson & Cox (2000)

Figure 1.10 Reactions of the TCA Cycle

The carbon atoms shaded in pink are those derived from the acetate of acetyl-CoA in the first turn of the cycle; these are not the carbons released as CO_2 in the first turn. In fumarate, the two-carbon group derived from acetate can no longer be identified, because succinate and fumarate are symmetrical molecules, C-1 and C-2 are indistinguishable from C-4 and C-3. Steps (1), (3) and (4) are irreversible in the cell; all other steps are reversible.

Acetyl-CoA from mitochondrial β-oxidation of fatty acids (or oxidation of glucose and some amino acids) donates its acetyl group to the four-carbon compound oxaloacetate (OAA) to form the six-carbon citrate. Citrate is then transformed into isocitrate, also a six-carbon molecule, which is dehydrogenated with loss of CO_2 to yield the five-carbon α-ketoglutarate (α-KG). Alpha-KG undergoes loss of CO_2 and ultimately yields the four-carbon compound succinate. Succinate is then enzymatically converted in three steps into the four-carbon oxaloacetate, with which the cycle began. OAA is then ready to react with another molecule of acetyl-CoA. In each turn of the cycle, one acetyl group (2 carbons) enters as acetyl-CoA and two molecules of CO_2 leave. One molecule of OAA is used to form citrate, but after a series of reactions, the OAA is regenerated. No net removal of OAA occurs and OAA is present in cells at very low concentrations.

The TCA cycle is an amphibolic pathway, i.e. one that serves in both catabolic and anabolic processes. Besides its role in the oxidative catabolism of carbohydrates, fatty acids and amino acids, the cycle provides precursors for many biosynthetic pathways (Figure 1.11). For example, α-KG and OAA can serve as precursors of the amino acids, glutamate and aspartate by transamination. Through aspartate and glutamate, the carbons of OAA and α-KG are then used to build other amino acids as well as purine and pyrimidine nucleotides. OAA is converted to glucose in gluconeogenesis. Succinyl-CoA is a central intermediate in the synthesis of the porphyrin ring of haem groups, which serve as oxygen carriers in haemoglobin and myoglobin (Nelson & Cox, 2000). Quantitatively, synthesis of aspartate and glutamate from OAA and α-KG are the most important. The mitochondrial membrane is impermeable to OAA and α-KG, therefore these intermediates are removed in the form of their precursors-malate and isocitrate, respectively (Figure 1.10), which can be transported across the membrane. The action of dehydrogenase enzymes produces OAA and α-KG in the cytosol.

As intermediates of the TCA cycle are removed to serve as biosynthetic precursors, they are replenished by anaplerotic reactions (Figure 1.11). Under normal circumstances, the reactions by which cycle intermediates are siphoned off into other pathways and those by which they are replenished are in dynamic equilibrium. Thus, concentrations of the TCA cycle intermediates remain almost constant. The most important anaplerotic reaction in mammalian liver is the reversible carboxylation of pyruvate by CO_2 to form OAA. When the TCA cycle is deficient in OAA or any other intermediates, pyruvate is carboxylated to produce more OAA.

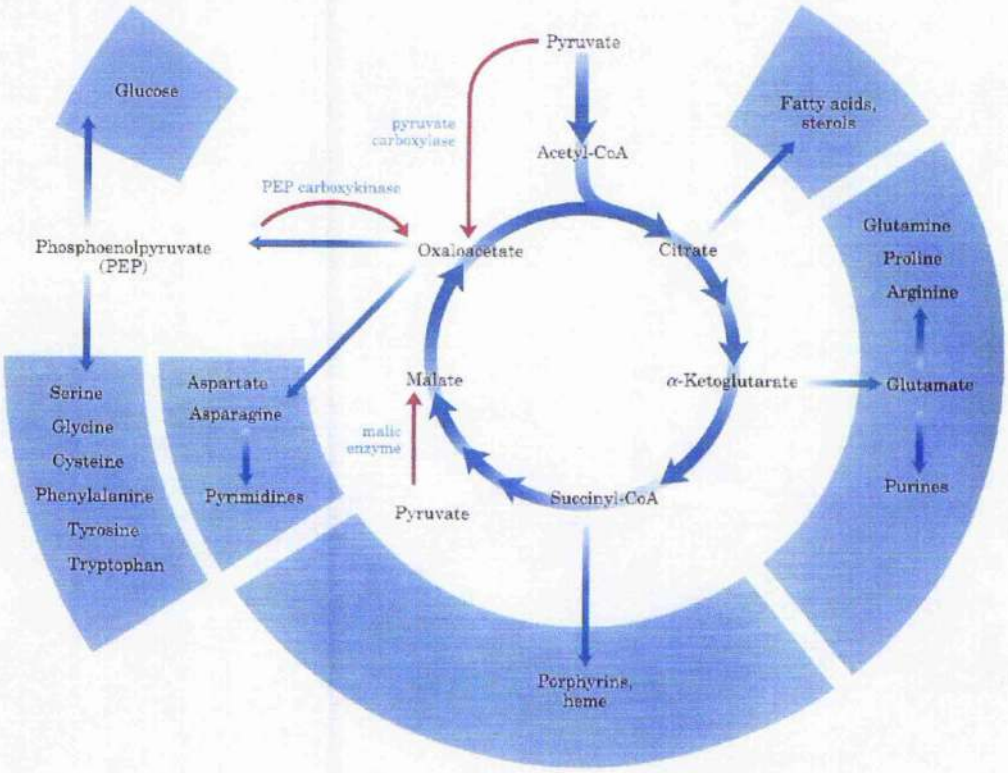

after Nelson & Cox (2000)

Figure 1.11 Role of the TCA cycle in anabolism

Intermediates of the TCA cycle are drawn off in many biosynthetic pathways. Shown in red are anaplerotic reactions that replenish depleted cycle intermediates.

The flow of carbon atoms into and through the TCA cycle is under strict regulation at two levels: the conversion of pyruvate to acetyl-CoA and the entry of acetyl-CoA into the cycle. Following a mixed meal, glucose is transported into the liver and phosphorylated to form glucose-6-phosphate, which can be metabolised to pyruvate via glycolysis in hepatocytes. Pyruvate is converted to acetyl-CoA, but acetyl-CoA is produced by the oxidation of fatty acids and certain amino acids, as well as from pyruvate, therefore availability of intermediates from these pathways is also important in the regulation of pyruvate oxidation and of the TCA cycle.

1.3.6.2 Fatty acid biosynthesis

In humans, fatty acid biosynthesis consists of *de novo* synthesis, where a small precursor molecule (usually acetyl-CoA) is gradually lengthened by 2C units to give rise to 16C and 18C products. This can be followed by various modifications of which elongation and desaturation are the most important.

The starting point of *de novo* lipogenesis may be glucose or amino acids, which can form pyruvate or acetyl-CoA, or acetyl-CoA from β-oxidation of fatty acids. The pathway occurs in the cytosol of both hepatocytes and adipocytes, but acetyl-CoA is mainly generated in mitochondria. Under conditions favouring fatty acid biosynthesis, pyruvate is transported into mitochondria, where pyruvate dehydrogenase is activated (Figure 1.13) and acetyl-CoA is produced. Acetyl-CoA is also produced during β-oxidation of fatty acids (Figure 1.9). Acetyl-CoA is combined with oxaloacetate to produce citrate, which leaves the mitochondria via a tricarboxylate anion carrier. In the cytosol, acetyl-CoA is produced by ATP:citrate lyase (Gurr *et al.* 2002).

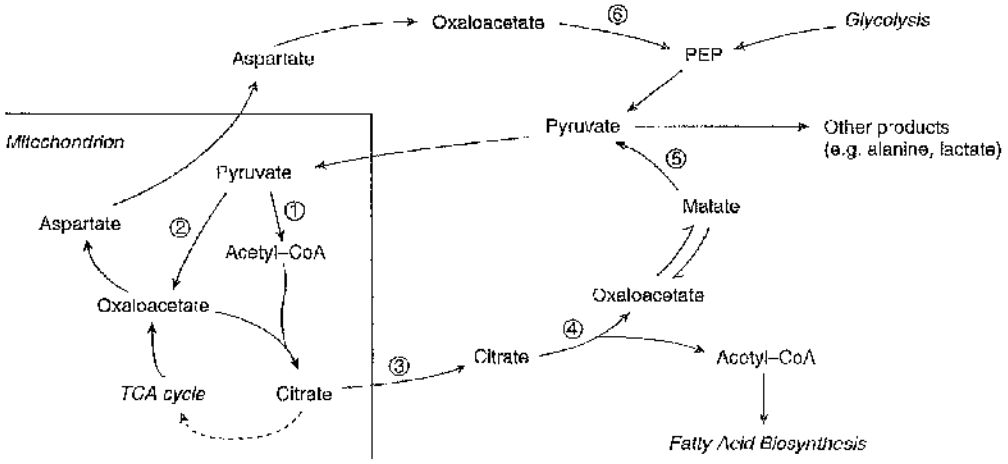

after Gurr *et al.* (2002)

Figure 1.12 Acetyl-CoA generation for *de novo* fatty acid biosynthesis

1: pyruvate dehydrogenase; 2: pyruvate carboxylase; 3: tricarboxylate anion carrier; 4: ATP:citrate lyase; 5: malic enzyme; 6: PEP carboxykinase

The process of *de novo* synthesis to produce long-chain fatty acids involves two enzymes, acetyl-CoA carboxylase (ACC) and fatty acid synthase (FAS). Both of these are complex and catalyse multiple reactions (Figure 1.13). The intermediates at all steps of the reaction are attached to a protein known as acyl carrier protein (ACP).

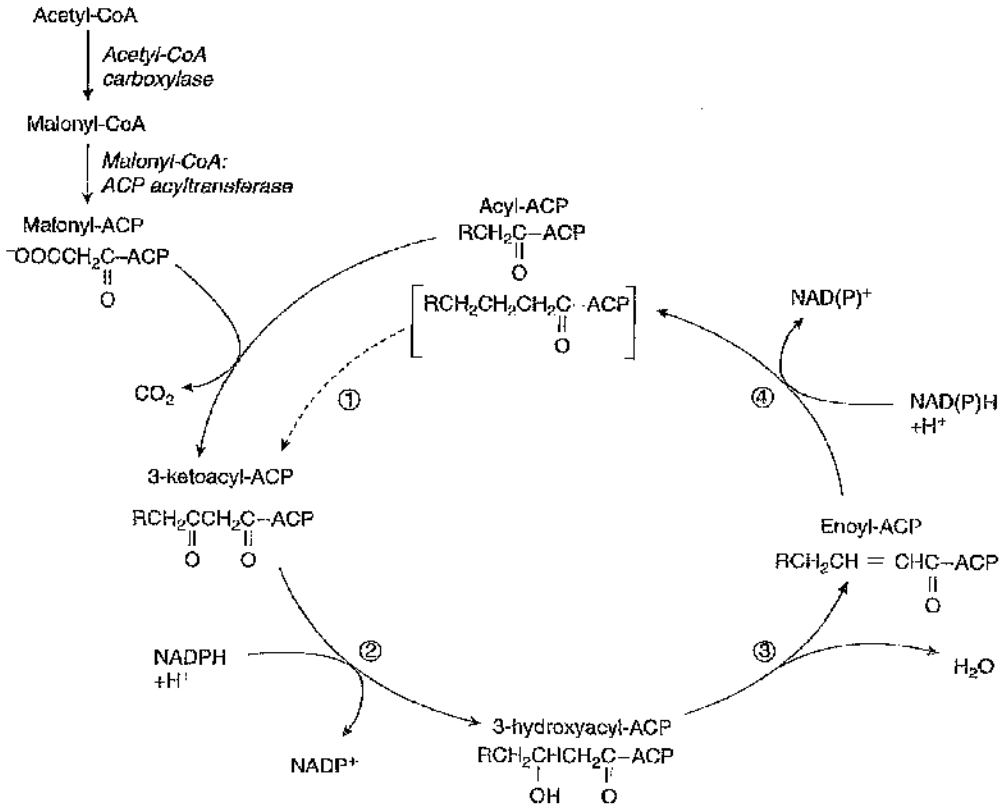

after Gurr *et al.* (2002)

Figure 1.13 Pathway of *de novo* lipogenesis

The repeat cycle of reactions for the addition of two carbons by fatty acid synthase. Reactions of the cycle: (1) condensation (3-ketoacyl-ACP synthase); (2) reduction (3-ketoacyl-ACP reductase); (3) dehydration (3-hydroxyacyl-ACP dehydrase; (4) reduction (enoyl-ACP reductase).

1.3.7 Transport of CO_2 to the lungs

CO_2 released from respiring tissues, such as the liver and skeletal muscle, into blood plasma enters erythrocytes via the chloride-bicarbonate exchanger. Within the erythrocyte, it is converted into bicarbonate (HCO_3^-) by carbonic anhydrase (EC 4.2.1.1). The HCO_3^- re-enters the plasma for transport to the lungs. HCO_3^- is much more soluble in blood plasma than CO_2, and thus the capacity of the blood to carry CO_2 from the tissues to the lungs is increased. In the lungs, HCO_3^- re-enters the erythrocyte and is converted to CO_2, which is eventually released into the lung space and exhaled. This shuttle requires very rapid movement of HCO_3^- across the erythrocyte membrane (Nelson & Cox, 2000).

The chloride-bicarbonate exchanger, also called the anion exchange protein, increases the permeability of the erythrocyte membrane to HCO_3^- by a factor of more than a million. It is an intrinsic protein that mediates the simultaneous movement of two anions; for each HCO_3^- ion that moves in one direction, one Cl^- ion moves in the opposite direction (Figure 1.14). The coupling of Cl^- and HCO_3^- is obligatory; in the absence of chloride, bicarbonate transport stops.

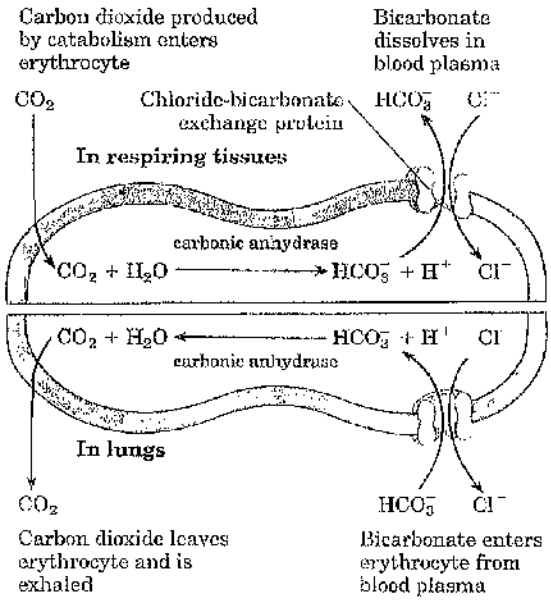

after Nelson & Cox (2000)

Figure 1.14 Chloride-bicarbonate exchanger of the erythroctye membrane

1.4 ^{13}C breath tests

1.4.1 Introduction to ^{13}C breath tests

Breath tests are based on the idea that the sampling of exhaled breath can provide information about biochemical, physiological or pathological processes within the body. ^{13}C-breath tests have become useful non-invasive tools to measure gastrointestinal functions and to monitor pharmacological and nutritional interventions (Young & Ajami, 1999). Labelling of nutritional substrates with ^{13}C enables investigation of their digestion, absorption and subsequent metabolism. The labelled compound is taken by mouth, usually as part of a test meal. Thereafter it is digested, absorbed, it or its products oxidised and the label appears in breath carbon dioxide (CO_2). Typically, a substrate is chosen such that the rate-limiting step in its metabolism to CO_2 is the process to be measured. CO_2 is the end product of the oxidation of carbohydrate, fat and protein. The CO_2 in breath reflects alveolar CO_2, which is in equilibrium with circulating bicarbonate (Section 1.3.7). ^{13}C-breath tests are particularly attractive for use in children and pregnant women, in whom the use of radioactive tracers is prohibited.

Breath is composed of a mixture of exhaled air and a mixture of the products of metabolism. Air is composed nitrogen (79 %), oxygen (21 %), argon (1 %), carbon dioxide (0.035 %) and water vapour. The products of metabolism are mainly water vapour, carbon dioxide (~5 % of breath), traces of hydrogen, hydrocarbons including methane, nitric oxide, ketones, ammonia and other gases at concentrations of parts per million (ppm). Hydrogen and methane are not generated by mammalian biochemical pathways and their presence in the breath is an indication of bacterial metabolic activity, most often in the large bowel, but sometimes in the small bowel or elsewhere. Hydrogen breath tests have been used to measure oro-caecal transit rate and small intestinal bacterial overgrowth (Bond & Levitt, 1975; Barr *et al.* 1978; King & Toskes, 1979; Jorge, Wexner & Ehrenpreis, 1994).

When a ^{13}C-labelled substrate is ingested, it is subject to a number of physiological processes, each of which can be considered potentially rate limiting. Taken by mouth the substrate is exposed to salivary enzymes, gastric acid and enzymes, is emptied from the stomach, and may be digested in the small intestine under the influence of pancreatic enzymes. Substrate that escapes digestion in the small intestine may reach the colon where it may be metabolised by bacterial enzymes. It, or its products of digestion, is absorbed

and may or may not be incorporated in the synthesis of a new substrate, transported directly or by a carrier molecule to the liver via the portal circulation, where all or a proportion may undergo metabolism, culminating in oxidation with the generation of CO_2.

Decline in cost of isotopically labelled compounds, the development of more user-friendly analytical instrumentation, and the avoidance of radioactive hazards, have made ^{13}C-breath tests increasingly attractive tools in biomedical research and clinical diagnosis. The urea breath test to detect the presence of *Helicobacter pylori* in the stomach is now a well established test for both diagnostic and research purposes (e.g. Graham *et al.* 1987; Graham & Klein, 1991; Weaver *et al.* 1993; Thomas, 1998; Weaver, 1998; Savarino, Vigneri & Celle, 1999; Slater, Preston & Weaver, 2004). It can be viewed as an example of an ideal breath test: a single rate-limiting step (the presence or absence of urea-secreting bacteria in the stomach) determines the rate of recovery of $^{13}CO_2$ in the breath after ingestion of ^{13}C-labelled urea. Many other breath tests have been developed to study organ function including gastric emptying rate, liver function, pancreas exocrine function, intestinal integrity; to study digestion, absorption or metabolism of carbohydrates, fat or protein; and to detect bacterial colonisation in the stomach or small intestine (Stellaard & Geypens, 1998).

The labelled CO_2 is diluted many-fold by the much larger volume of CO_2 produced in the body by other metabolic processes, leading to very small enrichments over the background level. There have been several reviews of the use of ^{13}C breath tests e.g. Schoeller *et al.* (1977); Barr *et al.* (1978); Klein & Klein (1985); Klein (1991); Amarri & Weaver (1995); Rating & Langhans (1997); Weaver, Manson & Amarri (1997); Klein & Helge (1998); Perri & Andriulli (1998).

1.4.2 Determining the value of a diagnostic test

1.4.2.1 Sensitivity and specificity

Diagnostic tests are designed to aid the clinician in determining whether or not a patient has a particular condition or disordered organ function, i.e. whether they are disease positive or disease negative. The effectiveness of a test can be determined by how well it identifies those with the condition (disease positives) and excludes those without the condition (disease negatives). The indices usually used to do this are sensitivity and specificity (Bland, 1995).

$$\text{Sensitivity} = \frac{\text{Number who are both disease positive and test positive}}{\text{Number who are disease positive}} \quad (1.2)$$

$$\text{Specificity} = \frac{\text{Number who are both disease negative and test negative}}{\text{Number who are disease negative}} \quad (1.3)$$

The sensitivity is the proportion of people with the disease, who test positive, and specificity is the proportion of people without the disease who test negative.

1.4.2.2 Positive and negative predictive values

The positive predictive value and negative predictive value of a test can also be estimated. The positive predictive value is the probability that a subject who is test positive will also be a true positive i.e. has the disease and has been correctly classified. The negative predictive value is the probability that a person who is test negative will be a true negative i.e. does not have the disease and is correctly classified (Bland, 1995). These depend on the prevalence of the condition (p_{prev}) as well as the sensitivity (p_{sens}) and specificity (p_{spec}). The probability of being disease positive and test positive is (p_{prev} x p_{sens}), and the probability of being disease negative and test positive is (1- p_{prev}) x (1-p_{spec}), so the probability of being test positive is (p_{prev} x p_{sens}) + ((1- p_{prev}) x (1-p_{spec})). The positive predictive value is:

$$PPV = \frac{(p_{prev} \cdot p_{sens})}{(p_{prev} \cdot p_{sens}) + ((1 - p_{prev})(1 - p_{spec}))} \quad (1.4)$$

Similarly, the negative predictive value is:

$$NPV = \frac{((1 - p_{prev})p_{spec})}{((1 - p_{prev})p_{spec}) + ((p_{prev})(1 - p_{sens}))} \quad (1.5)$$

1.4.2.3 Normal range or reference interval

Diagnostic tests for a particular condition require knowledge of the normal range of whatever is measured in healthy individuals from the same local population for comparison. To avoid confusion between the "normal distribution" as used in statistics and "normal range" as used in medicine, the term "reference interval" is finding increasing favour. If the variable is normally distributed, the reference interval is the mean ± 1.96 standard deviations. This will include 95 % of the observations, with 2.5 % lying outside the reference range at each extreme.

If the reference data are not normally distributed, it is possible to estimate percentiles without any assumptions about the distribution (Bland, 1997). The data must be sorted in rank order, and the 2.5 and 97.5 centiles calculated. If there are n observations, then the point below which 2.5 % of the observations lie, the i-th observation, is 0.025 x (n+1), and the point above which 97.5 % of the observations lie is 0.975 x (n+1). The interval between is the 95 % reference interval.

1.4.2.4 Determining the cut-off point

When the results of a test are based on a continuous variable, the sensitivity and specificity can be altered by changing the cut-off point. If high values indicate the disease positive state then raising the cut-off point will mean fewer cases, so the sensitivity will be decreased. However, there will be fewer false positives, so the specificity will be increased. Two graph-receiver operator characteristics (TG-ROC) is a mathematical method of determining the appropriate cut-off, where both the sensitivity and specificity are maximised (Greiner, 1995). TG-ROC is a plot of the test sensitivity (Se) and specificity (Sp) against the threshold (cut-off) value assuming the latter to be an independent variable. A cut-off (d0) that realises equal test parameters (Se = Sp = θ_0, theta-zero) can be obtained at the intersection point of the two graphs at the chosen level of accuracy (95 % or 90 %). Since the value for θ_0 is below the chosen accuracy level, two cut-off values are selected that represent the bounds of an intermediate range (IR) that can be considered as the equivocal range for the clinical interpretation of test results (Greiner, Sohr & Göbel, 1995). The proportion of the measurement range (MR) that gives unambiguous test results is the valid range proportion (VRP). VRP = (MR - IR) / MR. VRP and θ_0 can be used to compare tests since they do not depend upon the selection of a single cut-off point. In the ideal test both equal unity.

1.4.3 Basic principles of stable isotope methodology

^{13}C is the minor stable isotope of carbon. Isotopes of an element have the same atomic number (the number of protons in the nucleus) but different atomic mass (the sum of the number of protons and the number of neutrons). For instance, ^{12}C has 6 protons and 6 neutrons in the nucleus; ^{13}C has 6 protons and 7 neutrons; ^{14}C has 6 protons and 8 neutrons. The 6 protons in the nucleus are balanced electrostatically by 6 electrons, and all isotopes of carbon take part in the same chemical reactions within the body. ^{14}C is the radioisotope of carbon and decays to ^{14}N (7 protons and 7 neutrons) with the loss of a beta particle. The use of ^{14}C in clinical studies has diminished in recent years because of concerns about safety and disposal.

^{12}C and ^{13}C are stable isotopes and are present in all organic materials. ^{13}C forms 1.1% of all the carbon atoms naturally present in the environment. This is the natural abundance of ^{13}C. Enrichment is the term used to describe abundance of a sample above a baseline level. In metabolic tracer studies the term "stable isotope" is often synonymous with a non-radioactive isotope that is less abundant than the most abundant naturally occurring isotope, for example ^{13}C. The isotope of greatest abundance (^{12}C) is sometimes referred to as the major isotope, and that of lower abundance as the minor isotope. In fact both ^{12}C and ^{13}C are stable isotopes of carbon.

Stable isotope labelled tracers are compounds in which one or more of the naturally occurring, major isotopes of its atoms have been replaced by the minor (heavy) stable isotope of the atom. The compound is said to be labelled with the minor stable isotope. The unlabelled endogenous compound is known as the tracee. It is incorrect to refer to a labelled compound as a stable isotope, because this term refers to atoms rather than molecules.

It is possible to synthesise "highly enriched" compounds in which 99 % of the atoms in a particular position on the molecule are in the form of the heavy isotope of that atom, e.g. 99 atom % [^{13}C]-urea, where 99 % of the carbons are ^{13}C, rather than ^{12}C. Such highly enriched tracers can be "diluted" with unlabelled material to achieve enrichments of any percentage above natural abundance.

1.4.4 Measuring stable isotope abundance

1.4.4.1 Measuring ^{13}C abundance in breath, stool and labelled substrates

The ^{13}C abundance in breath CO_2 is most commonly measured using gas isotope ratio mass spectrometry (IRMS). There are two kinds if IRMS commonly available: dual inlet IRMS and continuous-flow IRMS. Dual inlet IRMS is a very accurate method, but many fewer samples can be prepared and analysed in a day compared to continuous flow techniques (Preston and McMillan, 1988). Samples for analysis by IRMS must be in the form of a pure gas and hence breath CO_2 must be separated from N_2 and O_2. IRMS are low resolution mass spectrometers for analysis of simple gases. They measure up to three ions simultaneously e.g. 44/45/46 for CO_2 analysis, but can measure very small differences in isotope ratios (of the order of 0.0001 atom % or 1 ppm). Spectroscopic methods including those based on laser diode arrays are coming onto the market. They potentially provide instant results at the bedside, but the current instruments are not as sensitive as IRMS.

The simplest CF-IRMS instruments are those dedicated to the analysis of $^{13}CO_2$ in breath samples. They are composed of an autosampler for gas sampling vials (e.g. 10 ml Exetainer Breath Sampling Vials, Labco, Welwyn Garden City, UK), water trap, isothermal GC oven (to separate CO_2 from N_2 and O_2) and capillary for introduction of the sample into the IRMS. Analysis of the abundance of ^{13}C in solid samples e.g. labelled substrates (Harding *et al.* 1994; Boirie *et al.* 1995; Evenepoel *et al.* 1997; Morrison *et al.* 2001; Edwards *et al.* 2002) requires combustion of the solid to produce CO_2, N_2 and water. Combustion-IRMS differs from the breath test instrument in having oxidation and reduction furnaces prior to the water trap and an autosampler for solid samples. This technique can also be used to measure tracer excreted in stool in studies of lipid metabolism (Murphy *et al.* 1998; Slater *et al.* 1998; Slater *et al.* 2002), and tracer excreted in urine in gastrointestinal motility studies (Morrison, Dodson & Preston, 1999).

The IRMS should be calibrated against internationally agreed standards to take into account day-to-day fluctuations and to standardise measurements between laboratories. In practice each laboratory will have a secondary standard (reference gas), which should be traceable to the international standard. For analysis of breath ^{13}C abundance, a suitable reference gas contains 3-5 % CO_2, with the balance being nitrogen.

Compound specific analysis of highly enriched ^{13}C-labelled tracer excreted in stool can be made by gas chromatography-mass spectrometry (GC/MS) (Slater *et al.* 1998; Slater *et al.* 2002), and low enrichments in plasma, urine or tissue samples can be measured using GC-combustion-IRMS (Preston & Slater, 1994). There are few internationally traceable standards for compound specific isotope analysis therefore each laboratory must make its own gravimetric standards using carefully weighed mixtures of labelled and unlabelled material (Slater *et al.* 1998).

1.4.4.2 Measuring ^{18}O and ^{2}H abundance in body fluids

The abundance of ^{18}O and ^{2}H in body fluids such as plasma, saliva and urine can be measured by continuous flow IRMS techniques by sampling the head-space after equilibration of the sample with a reference gas in an Exetainer (McMillan, Preston & Taggart, 1989; Posser *et al.* 1991; Scrimgeour *et al.* 1993). The abundance of ^{18}O is usually measured as $CO^{18}O$, and can be therefore be measured on the same instrument as breath $^{13}CO_2$ abundance. It is technically more challenging to measure deuterium enrichment by continuous flow methods, but several instruments are now commercially available for this purpose. The first was described by Prosser & Scrimgeour (1995).

1.4.5 Units of stable isotope abundance and enrichment

Most IRMS software calculates isotopic abundance in terms of delta notation (δ; in units of $^{o}/_{oo}$, per mil), which is a convention used in geochemistry, since most of the original IRMS instruments were developed in isotope geochemistry laboratories, to measure natural abundance variations. Delta is defined as the relative difference in parts per thousand between the sample isotope ratio and the isotope ratio of the international standard. The international standard for ^{13}C was Pee Dee Belemnite (PDB), a limestone standard. The $^{13}C/^{12}C$ isotope ratio of PDB is 0.0112372.

$$\text{e.g.} \quad \delta^{13}C_{PDB} = \left(\frac{R_S - R_{PDB}}{R_{PDB}}\right) \times 1000 = \left(\left(\frac{R_S}{R_{PDB}}\right) - 1\right) \times 1000 \qquad (1.6)$$

where R_S is the $^{13}C/^{12}C$ ratio in the sample and R_{PDB} is the ratio in the standard.

The supply of PDB was exhausted in the mid 1990's and Standard Mean Ocean Water (SMOW), the international standard for stable hydrogen and oxygen isotopes, but did not have a unique definition. Therefore, the Commission on Atomic Weights and Isotopic

Abundances of the International Union of Pure and Applied Chemistry recommended that the use of PDB and SMOW be discontinued and that isotope abundances of hydrogen-, carbon-, and oxygen-bearing materials be reported relative to the reference water VSMOW (Vienna standard mean ocean water) and to VPDB (Vienna Pee Dee Belemnite), defined by adopting a $\delta^{13}C$ value of +1.95 per mil (‰) for NBS 19 carbonate relative to VPDB (Coplen 1995). Relative $^{2}H/^{1}H$ values ($\delta^{2}H$) and $^{18}O/^{16}O$ ($\delta^{18}O$) should be expressed per mil (‰) relative to VSMOW water (0 ‰) on a scale normalized such that SLAP (standard light Antarctic precipitation) has a $\delta^{2}H$ value of –428 ‰ and a $\delta^{18}O$ value of –55.5 ‰ (Coplen, 1996).

Units of atom per cent (atom %) are preferred for tracer studies. Atom % is a measure of absolute isotope concentration, rather than the relative ratio delta (δ) notation and has its basis in SI units (Slater, Preston & Weaver, 2001a). Atom % (AP) is the atom fraction expressed as a percentage.

$$\text{atom \% } ^{13}C = \frac{[^{13}C]}{[^{12}C]+[^{13}C]} \times 100 \tag{1.7}$$

Small abundances can be expressed in units of parts per million (ppm) (Klein & Klein, 1982).

$$\text{ppm} = \text{atom \%} \times 10^{4} \tag{1.8}$$

In practice, IRMS measures ratios of molecular species, rather than isotopes and the ^{13}C abundance of CO_2 is usually determined by measuring the ion intensities at *m/z* 44 and 45. The ion beam at *m/z* 45 contains a small contribution from $[^{17}O]CO$. In practice, this is removed using the 'Craig correction' (Craig, 1957) when calculating ^{13}C units using the IRMS software.

To convert $\delta^{13}C_{PDB}$ to atom % ^{13}C,

$$AP^{13}C = \frac{100}{\dfrac{1}{\left(\dfrac{\delta}{1000}+1\right)R_{PDB}}+1} \tag{1.9}$$

where δ = measured $\delta^{13}C_{PDB}$ and R_{PDB} is the isotope ratio of PDB = 0.0112372.

Similar equations can be used to convert δ^2H_{VSMOW} to atom % ^2H and $\delta^{18}O_{VSMOW}$ to atom % ^{18}O using the isotope ratios shown in Table 1.3.

Enrichment is the abundance of a sample above a baseline level and is expressed in units of atom % excess (APE).

$$APE = (\text{atom \%})_E - (\text{atom \%})_B \quad (1.10)$$

where, $(\text{atom \%})_E$ is the measured abundance of the enriched sample and $(\text{atom \%})_B$ is the measured abundance of the baseline sample.

Low enrichments can be quoted in parts per million excess (ppm excess = APE x 10^4).

Sometimes enrichment is expressed as delta over baseline (DOB or $\Delta^{13}C_{PDB}$). This is defined as the difference between the basal ^{13}C abundance of breath CO_2 ($\delta^{13}C_{PDB}$) before administration of labelled substrate and the ^{13}C abundance of breath CO_2 at a certain time point after administration.

$$DOB = \delta_{post\text{-}dose} - \delta_{baseline} \quad (1.11)$$

Table 1.3 Isotope ratios of international standards

Standard		Isotope ratio
Vienna Standard Mean Ocean Water (VSMOW)	$^2H/^1H$	0.00015576
Vienna Standard Mean Ocean Water (VSMOW)	$^{18}O/^{16}O$	0.00200520
Standard Light Antarctic Precipitation (SLAP)	$^2H/^1H$	0.00008909
Standard Light Antarctic Precipitation (SLAP)	$^{18}O/^{16}O$	0.00189391
Vienna Pee Dee Belemnite (VPDB)	$^{13}C/^{12}C$	0.0112372
Vienna Pee Dee Belemnite (VPDB)	$^{18}O/^{16}O$	0.0020671
Atmospheric Nitrogen	$^{15}N/^{14}N$	0.0036765
Canyon Diablo Troilite meteorite	$^{34}S/^{32}S$	0.0450045

after De Bievre & Barnes (1985)

1.4.6 Procedure for a typical breath test

1.4.6.1 Breath sampling methods

The labelled compound is taken by mouth, often as part of a test meal. Breath samples are collected before ingestion of the labelled compound and at intervals thereafter. A simple way to collect breath samples is by blowing through a straw into a glass vial (e.g. Exetainer, 10 ml gas sampling vial, Labco, High Wycombe, UK). The cap, containing a septum, is replaced immediately thereafter. For younger children and babies a "bag and mask" can be used (Weaver *et al.* 1993), constructed from an anaesthetic mask attached to a gas tight bag via a one-way valve. These are commercially available from QuinTron (Milwaukee, Wisconsin, USA), or can be made in-house using an Ambu Transparent Face Mask attached to an Ambu Paedi Valve (Ambu, Brondby, Denmark; www.ambu.com) and a 600 ml gas sampling bag (Laerdal Medical, Orpington, UK; www.laerdal.com), which has been fitted with a 3-way Luer tap to facilitate gas transfer. The child breathes into the mask and exhaled breath is collected in the bag, the breath sample is transferred to an evacuated vial using a syringe, and the abundance of ^{13}C is measured by IRMS.

1.4.6.2 Control of background ^{13}C abundance

The amount of ^{13}C in breath CO_2 is expressed as enrichment above the background abundance of $^{13}CO_2$. It is important to have low and constant background ^{13}C abundance, especially if the end point of interest is quantitation of cumulative excretion of label from the tracer. It is therefore important that the test meal is composed of ingredients of low ^{13}C abundance. The ^{13}C abundance of the test meal can be calculated from food composition tables, and the natural abundance of each individual component (Morrison *et al.* 2000). Foods eaten before and during ^{13}C breath tests should be of low ^{13}C abundance so that they and the test meal will have minimal effect on basal breath $^{13}CO_2$ enrichment. It is possible to achieve baseline variations of approximately ±7 ppm ^{13}C (0.6 per mil) on a ^{13}C controlled diet, compared with variations of ±30 ppm ^{13}C (2.7 per mil) on an uncontrolled diet (Jones *et al.* 1985; Garlick *et al.* 1987; Morrison, 2000).

In terms of their ^{13}C abundance, there are two major classes of plants, which are consumed as part of the diet of humans. They can be distinguished on the basis of isotope fractionation during photosynthesis. C_3 plants incorporate CO_2 from the atmosphere by

carboxylation of ribulose bisphosphate (RuBP) via the enzyme RuBP carboxylase, producing a 3-carbon product, phosphoglycerate (O'Leary, 1981; Boutton, 1991). The average $\delta^{13}C$ VPDB value of C_3 plants is –27 ‰ C_4 plants reduce CO_2 to aspartic or malic acid, both 4-carbon compounds, via the enzyme phosphoenolpyruvate (PEP) carboxylase. This enzyme does not discriminate against ^{13}C as much as RuBP carboxylase, so that C_4 plants have relatively high ^{13}C content (average –13 $\delta^{13}C_{VPDB}$). C_3 and C_4 plant species thus have distinct $\delta^{13}C_{VPDB}$ values and differ from each other by approximately 14 ‰ (~160 ppm ^{13}C). Most terrestrial plant species are C_3, including the staple food plants, wheat, rice, potatoes and sugar beet, but tropical and subtropical grasslands consist almost exclusively of C_4 species, including important food crops such as maize and sugar cane.

Photosynthesis in the marine environment occurs mainly via the C_3 pathway. However, $\delta^{13}C_{VPDB}$ values of phytoplankton are substantially higher than terrestrial plants, averaging –22 ‰. This is related to the use of bicarbonate as a carbon source for photosynthesis, which has substantially higher ^{13}C content than atmospheric CO_2 (Boutton, 1991). Fish, which consume the plankton have an even higher $\delta^{13}C_{VPDB}$ value closer to –17 ‰. For this reason, fish should also be excluded from the diet in the days preceding ^{13}C breath tests.

The European diet is composed mainly of foods derived from C_3 plants, but it is necessary to avoid foods containing maize, maize products, sugar cane, pineapple and seafood for several days before the test day, in order to minimise the background ^{13}C enrichment.

The natural abundance of food is not the only factor that can affect basal $^{13}CO_2$ variation. Physical activity is another factor that should be considered when planning ^{13}C breath tests. Increased energy expenditure may generate unwanted changes in the ^{13}C abundance of breath CO_2, owing to changes in the relative proportion of fat and carbohydrate oxidised, which can cause breath $^{13}CO_2$ enrichment to fluctuate (Jacobson *et al.* 1970). Fat stores are more depleted in ^{13}C than the body's carbohydrate stores due to fractionation occurring during biosynthesis in both plant and animal tissues. Hence changes in the ratio of fat to carbohydrate oxidised will influence the isotopic ratio of ^{13}C:^{12}C in breath CO_2 (Schoeller *et al.* 1977; Schoeller *et al.* 1984). For these reasons, it is recommended that food intake should be controlled for three days prior to test, the diet should be strictly controlled during the test, and physical activity should be restricted.

1.4.6.3 Factors concerning the dose of labelled material

Many ^{13}C-breath tests are performed using synthesised tracers with 99 atom % ^{13}C at a particular position on the tracer molecule. This will be diluted by several orders of magnitude in the test meal and in the body. It is, therefore, important to give sufficient labelled material to allow detection of significant elevation above the background abundance of 1.1 atom % or 11,000 ppm ^{13}C. Ideally the maximum enrichment of breath CO_2 should be ~100 ppm excess ^{13}C. Labelled tracers are expensive and not always available in large quantities, and economic considerations therefore often determine the dose given and the number of subjects studied. In any case, the amount of material ingested should be weighed accurately and account taken of losses during preparation, or incomplete consumption, of the test meal.

1.4.7 Expression of breath test results

The results of ^{13}C breath tests can be expressed in one of four ways. In the simplest diagnostic test, the ^{13}C urea breath test (UBT), they are reported to the clinician as being positive or negative, based simply on the analysis of ^{13}C enrichment in breath CO_2, usually at 30 min post dose (e.g. Rowland *et al.* 1997; Thomas *et al.* 1999; Kato *et al.* 2002; Slater *et al.* 2004). The next category of test, such as in GI motility studies, reports results in units of time. In the case of gastric emptying, gastric emptying half time and lag time may be expressed (e.g. Ghoos *et al.* 1993; Maes *et al.* 1994; Wyse *et al.* 2001a,b; Bluck *et al.* 2002). Although rarely used for diagnosis, it is easy to imagine that the result from an individual subject's test could be reported as being 'fast, normal or slow' when compared with the range of results of a standard test from a healthy population. The third type of test, such as liver function or exocrine pancreatic function, express results as the quantity of dose recovered in breath (commonly, percentage dose recovered or PDR) (e.g. Parker *et al.* 1994, 1997a,b; Amarri *et al.* 1997; Manson *et al* 1999; Ling *et al.* 2000; Slater *et al.* 2002). A diagnostic form of such a test could report a standardised test on an individual as being 'high, normal or low' when compared with the reference range of results from a healthy population. Finally, in substrate oxidation studies results are expressed as the absolute quantity of substrate oxidised in a given time (e.g. Sidossis *et al.* 1995a; Mittendorfer *et al.* 1998; Bowtell *et al.* 2000).

PDR is calculated from CO_2 production rate ($\dot{V}CO_2$) and breath CO_2 enrichment.

$$\text{PDR h}^{-1} = \frac{\dot{V}CO_2 \text{ (mmol.h}^{-1}\text{)} \times \text{Breath } CO_2 \text{ enrichment (ppm } ^{13}\text{C excess)} \times 100}{\text{Tracer amount (mmol)} \times \text{Tracer enrichment (atom \% excess} \times 10^4\text{)}} \quad (1.12)$$

The sum of the PDR from each sample in a test is the cumulative per cent dose recovered (cPDR).

When PDR is the desired outcome, it is necessary to have a measurement of $\dot{V}CO_2$ or to use a predicted value (Shreeve, Cerasi & Luft, 1970; Schofield 1985). This will be discussed further in Section 1.5.

1.4.8 The mixed triacylglycerol breath test

The mixed triacylglycerol breath test, commonly known as the mixed triglyceride (MTG) breath test, was developed by Ghoos *et al.* (Ghoos *et al.* 1981; Vantrappen *et al.* 1989) as an indirect measure of intraluminal fat digestion in adults with impaired pancreatic function. The substrate is a synthetic triacylglycerol (1,3 distearyl 2-[1-^{13}C]octanoyl-glycerol) composed of two long-chain saturated fatty acids (18:0, stearic acid) at the *sn*-1 and -3 positions, and a ^{13}C-labelled medium-chain fatty acid (8:0, octanoic acid) at the *sn*-2 position (Figure 1.16).

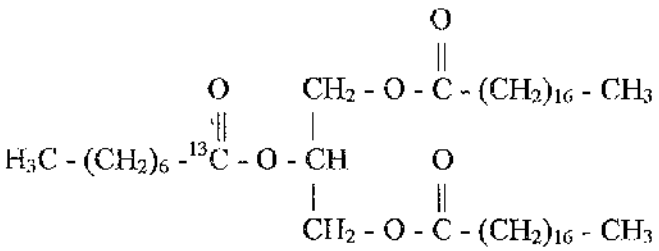

Figure 1.16 Structure of [^{13}C]mixed triacylglycerol (MTG)

Pancreatic lipases preferentially hydrolyse mixed triacylglycerol at the *sn*-1 and -3 positions, leaving 2-[1-^{13}C]octanoyl-glycerol. Hydrolysis of medium-chain 2-monoacyl glycerol is rapid and complete (Desnuelle & Savery, 1963), releasing [1-^{13}C]octanoate. The enhanced water solubility of octanoate, its diminished affinity for acyl-CoA synthetase compared to long-chain fatty acids, and lack of medium-chain acyl-CoA synthetase for its activation in enterocytes, results in rapid absorption via the portal vein. The increased blood flow relative to lymph also contributes to more rapid entry of medium-chain fatty

acids into the circulatory system (Odle, 1997). As a consequence, the liver is the first organ reached by octanoic acid, whereas long-chain fatty acids enter systemic circulation via chylomicrons in the thoracic duct and may perfuse other tissues prior to the liver (Figure 1.4).

In the liver, octanoate may be incorporated into long-chain fatty acids (Carnielli *et al.* 1994; Pakula *et al.* 1997), but the major metabolic fate is oxidation. The ^{13}C-label is removed by β-oxidation in the mitochondria resulting in [1-^{13}C]acetyl-CoA, which reacts with oxaloacetate and enters the TCA cycle (Section1.3.6.1). Some ^{13}C leaves the TCA cycle as $^{13}CO_2$, which equilibrates with the bicarbonate pool before being excreted in breath as labelled CO_2 or urine as labelled bicarbonate, or it can enter the urea cycle and be excreted in urine as labelled urea. Some ^{13}C enters anaplerotic reactions (Figure 1.11) and products so formed re-enter the TCA cycle and these carbons may become sequestered in shared carbon skeletons (e.g. oxaloacetate ⇒ aspartate, α-ketoglutarate ⇒ glutamate). The rate-limiting step in the digestion, absorption and oxidation of MTG in children with cystic fibrosis is hydrolysis of the long-chain fatty acids by pancreatic lipase, and the [^{13}C]MTG breath test is an indirect measure of intraluminal fat digestion and hence exocrine pancreatic function.

Digestion and absorption of lipids by children with cystic fibrosis has been studied using [^{13}C]tripalmitin (Murphy *et al.* 1998) and [^{13}C]triolein (Wutzke *et al.* 1999). The MTG test is a test of lipid digestion, and indirectly of exocrine pancreatic function, whereas the [^{13}C]tripalmitin/triolein tests are tests of both digestion and absorption.

In adults, the [^{13}C]MTG breath test gives an excellent correlation between lipase output in the duodenum and 6-h cumulative $^{13}CO_2$ excretion in breath (Ghoos *et al.* 1981; Vantrappen *et al.* 1989), where low lipase output and low recovery of ^{13}C in breath indicate poor exocrine pancreatic function. As a test of exocrine pancreatic function, the MTG test was found to have a sensitivity of 0.89, specificity of 0.81, positive predictive value of 0.63 and negative predictive value of 0.95 (Perri & Andriulli, 1998), compared to duodenal lipase output. It has been shown to be a specific test of intraluminal digestion and to be independent of factors affecting absorption, such as small bowel disease (Vantrappen *et al.* 1989; Amarri *et al.* 1997) and coeliac disease (Amarri *et al.* 1997; Perri *et al.* 1998). In children with cystic fibrosis, the presence of concurrent liver disease has been shown not to affect the amount of ^{13}C excreted in breath (Ling *et al.* 2000).

The [^{13}C]MTG test has been largely confined to research projects (e.g. Kalivianakis *et al.* 1997, 2000; Swart *et al.* 1997; Löser *et al.* 1998; Perri *et al.* 1998; Wutzke *et al.* 1999) due to its poor positive predictive value and the need to collect breath samples for six hours. However, it has been used to assess the adequacy of pancreatic enzyme replacement therapy in children with cystic fibrosis (Amarri *et al.* 1997; de Boeck *et al.* 1998), to study the development of fat digestion in infancy (Manson *et al.* 1999) and the effect of liver disease on intraluminal fat digestion in children with cystic fibrosis (Ling *et al.* 2000). In pancreatic sufficient subjects 15-44 % of the ^{13}C label is excreted in breath CO_2 (Amarri *et al.* 1997; van Dijk-van Aalst *et al.* 2001). In healthy children and children with cystic fibrosis, who were taking their normal pancreatic enzyme replacement therapy, only about 1 % of the tracer was recovered in stool (Slater *et al.* 2002). The remainder must be retained in the body. It can therefore be concluded that variability in breath cPDR, other than due to MTG digestion, is due to postabsorptive rather than predigestive factors.

The final oxidation product of [^{13}C]MTG is $^{13}CO_2$. Most of the labelled CO_2 is excreted in breath, but some is excreted in urine either as [^{13}C]bicarbonate or [^{13}C]urea, fixed via the urea cycle, and in faeces. The remainder is retained within the body. Labelled CO_2 originating from oxidation of [^{13}C]MTG is greatly diluted by endogenously produced CO_2 from metabolic processes. Therefore, to estimate PDR, knowledge of CO_2 production rate ($\dot{V}CO_2$) is required. A resting value based on basal metabolic rate is often assumed, but if subjects are not lying quietly on a bed and in the postabsorptive state throughout the test, this will be an underestimate of the true CO_2 production rate. Factors affecting CO_2 production rate are discussed further in Section 1.5.

There are two methods of approaching the problem of lack of knowledge of CO_2 production rate. $\dot{V}CO_2$ can either be measured continuously during the test or an empirically derived correction can be used, which eliminates the need for its measurement by compensating for tracer sequestered in the body.

1.4.9 Sequestration of ^{13}C within the body

Bicarbonate and acetate correction factors are used in studies of substrate oxidation, where a tracer is infused into a vein and blood and breath samples are taken at intervals to determine the rate of oxidation of the tracer. There is a need to correct the calculated oxidation rate, to take account of the proportion of labelled CO_2 that does not appear as breath CO_2, but is temporarily sequestered into other metabolites, usually via the TCA

cycle. The bicarbonate correction factor accounts for label entering the bicarbonate pool (mainly bone and intracellular reserves e.g. skeletal muscle) and therefore not excreted in breath during the test (e.g. Irving *et al.* 1983, 1984, 1985; Kien, 1989; Armon *et al.* 1990). Alternatively an acetate correction factor can be used when this is more appropriate i.e. in studies of lipid and carbohydrate metabolism (Sidossis *et al.* 1995a,b). The acetate correction factor accounts for label fixation that might occur at any step between the entrance of acetyl-CoA into the TCA cycle (Section 1.3.6.1) until recovery of label in breath CO_2.

Changes in metabolic rate induced by feeding, physical activity or hormonal changes affect both correction factors (Van Hall, 1999). It may be necessary to use bicarbonate or acetate correction factors with the calculated PDR from ^{13}C breath tests, if the aim is to account for all of the ingested tracer (Slater, Preston & Weaver, 2001b), in which case it will be necessary to perform two breath tests on separate days.

1.5 Measurement of CO_2 production rate

1.5.1 Background

As shown by Equation 1.12, any error in the $\dot{V}CO_2$ term results in a proportional error in the calculated PDR. The enrichment of breath CO_2 and of the tracer can be analysed accurately and precisely (CV 0.5%) by continuous-flow isotope ratio mass spectrometry (Prosser *et al.* 1991). The amount of tracer taken can be determined accurately by weighing on a 5-figure balance, and by rinsing vessels and consuming the contents to ensure that all the tracer is consumed. $\dot{V}CO_2$ can be measured at rest with less, but acceptable precision (CV 2.6%) using a ventilated hood indirect calorimeter (Ventham & Reilly, 1999). However, resting $\dot{V}CO2$ is not the appropriate value to use unless subjects are sitting still and fasting during the entire breath test procedure. This is particularly unlikely with children, and in tests lasting for up to 24 hours (Morrison *et al.* 1998; Edwards, Zavoshy & Preston, 1998; Morrison *et al.* 2003b). Many researchers have not measured $\dot{V}CO_2$, but have simply used a predicted value of 5 $mmol.min^{-1}.m^{-2}$ (Shreeve *et al*, 1970). Body surface area (m^2) can be predicted from height (cm) and weight (kg) using the Haycock equation in both adults and children (Haycock, Schwartz & Wisotsky, 1978). Basal metabolic rate can also be predicted from the subject's height and weight using the Schofield equations (Schofield, 1985).

Physical activity is not the only factor that can affect $\dot{V}CO_2$ during a breath test. Amarri *et al.* (1998) have shown that resting $\dot{V}CO_2$ is higher in children with cystic fibrosis than in healthy children. CO_2 production rate is also increased following food intake, including consumption of the test meal as well as subsequent meals. This is due to the thermic effect of the food eaten or "diet-induced thermogenesis", and is approximately 10 % of total daily energy expenditure.

The factors discussed so far all lead to an increase in $\dot{V}CO_2$ and therefore an underestimation of PDR. However, if subjects fall asleep during the study, their metabolic rate will fall below their resting metabolic rate, and for this period use of resting $\dot{V}CO_2$ will result in an overestimation of PDR. There is, therefore, a need to find a way of continuously monitoring CO_2 production rate during the entire breath test, in order that the correct $\dot{V}CO_2$ value for the particular circumstances of the test can be used to calculate the percent dose recovered in each breath sample.

1.5.2 Components of daily energy expenditure

Total daily energy expenditure (TEE) is composed of three major components: basal metabolic rate (BMR), the thermic effect of food or diet-induced thermogenesis (DIT), and the energy required for physical activity (PA). The latter is highly variable between individuals.

$$TEE = BMR + DIT + PA \qquad (1.13)$$

Basal metabolism is the energy required to sustain the basic essential metabolic processes involved in keeping the body alive and healthy and, where appropriate, growing at an appropriate rate (van Raaij, 2002). The energy required to sustain basal metabolism is usually expressed as basal metabolic rate (BMR). BMR is defined as the energy expenditure of a healthy subject lying at rest, in a thermally neutral environment, at least 12 h postprandially (Harris & Benedict, 1919). In most individuals BMR is the largest component of TEE, amounting to 50-70 % TEE (FAO/WHO/UNU, 1985).

BMR is measured under precisely defined conditions. It is measured while the subjects are lying in bed or on a couch, immediately after awakening, in a state of physical and emotional relaxation, and in a thermoneutral environment. They should have fasted for the 12-14 h immediately before the measurement, and heavy physical exercise should be

avoided on the day before the measurement (van Raaij, 2002). Subjects should also be free from disease and not suffer from fever. If any of the conditions for BMR are not met, the energy expenditure of the subject should be termed resting metabolic rate (RMR).

The BMR of a subject is influenced by many factors including body size, body composition, age, gender, and nutritional and physiological state. Body size and composition are major determinants of BMR, since adipose tissue has a lower metabolic rate than the tissues, with core tissues such as viscera having a higher oxygen demand at rest than peripheral tissues, such as skeletal muscle. These tissues compromise the lean body mass, (LBM). In lean male adult subjects, LBM accounts for approximately 75 % body weight and fat mass accounts for approximately 18 % body weight (ICRP 23, 1975). In obese adults and children, fat mass can rise to ~40 % body weight (Slater & Preston, 2002). Therefore BMR is usually expressed per kg body weight or preferably per kg lean body mass. This eliminates the effect of body size and therefore differences between males and females. The lower resting energy expenditure observed in women than in men is partly explained by the fact that women are usually smaller than men, and partly by the fact that a woman of the same weight as a man has more body fat and less muscle. As muscle is more metabolically active than adipose tissue, men have a relatively high BMR. Nevertheless, BMR per kg body weight declines with increasing age, so that small children have a relatively high BMR, compared to adults.

1.5.3 Resting energy expenditure

BMR and RMR can either be predicted or measured.

1.5.3.1 Predicting basal metabolic rate and resting energy expenditure

There have been several proposals of equations to predict BMR including Harris & Benedict (1919), FAO/WHO/UNU (1985), Schofield (1985), Maffeis *et al.* (1993). The Schofield (1985) equations are the most widely used and are recommended by the UK Panel on Dietary Reference Values of the Committee on Medical Aspects of Food Policy (Department of Health, 1991). Schofield (1985) proposes two sets of equations to estimate basal metabolic rate from weight alone or from weight and height. The latter are superior in children (Kaplan *et al.* 1995; Rodriguez *et al.* 2000) and probably in patients with wasting diseases. $\dot{V}CO_2$ can be estimated from BMR by assuming a respiratory quotient ($\dot{V}CO_2/\dot{V}O_2$) of 0.85 (IDECG, 1990). Resting $\dot{V}CO_2$ is elevated in certain diseases

compared with healthy control subjects e.g. children with cystic fibrosis (Amarri *et al.* 1998; Castro *et al.* 2002) and patients with pancreatic cancer (Wigmore *et al.* 1995; Barber *et al.* 1999). In such cases it is important to measure $\dot{V}CO_2$, rather than use the prediction equations.

1.5.3.2 Measuring basal metabolic rate and resting energy expenditure

RMR is usually measured using a ventilated hood indirect calorimeter, although portable respirometers and whole body calorimeters are sometimes used. Indirect calorimetry is based on measuring respiratory gas exchange i.e. whole body consumption of oxygen ($\dot{V}O_2$) and production of carbon dioxide ($\dot{V}CO_2$) during the oxidation of various fuels. In a ventilated hood system, the subject lies under a perspex hood, which is made air-tight around the neck or shoulders using a canopy. A stream of air is drawn through the hood using a pump. This mixes with expired air and the concentration of O_2 and CO_2 is measured using on-stream analysers. The rate of energy expenditure is calculated from the volume of air flowing through the hood and the difference in concentration of O_2 and CO_2 between the out-flowing and in-flowing air. This is described in more detail in Section 2.2.2.2.

Principles of indirect calorimetry

Humans consume macronutrients (carbohydrate, fat and protein) in the food they eat. These are absorbed, oxidised and eventually leave the body as CO_2, H_2O and urea. The macronutrients are almost completely oxidised, except for the formation of urea from protein. The body produces heat and energy for external work from the oxidation of macronutrients. It is irrelevant that the process of oxidation within the body may not be direct e.g. glucose may form glycogen, then lactate, then be recycled as glucose before being oxidised, or it may be converted to fat before oxidation. The net heat production will be the same as if the oxidation had occurred directly (Frayn, 1996).

Glucose from starch, sugars and glucogenic amino acids is the most commonly metabolised fuel in the body. A glucogenic amino acid is any amino acid, which is catabolised to pyruvate or a TCA cycle intermediate. Alanine is quantitatively the most important (Newsholme & Leech, 1985). The equation for complete oxidation of glucose is:

$$C_6H_{12}O_6 + 6O_2 \rightarrow 6CO_2 + 6H_2O + \text{heat} \qquad (1.14)$$

The ratio of CO_2 production to O_2 consumption, the respiratory quotient (RQ) for this reaction is 6/6 = 1.00.

1 mol glucose (180 g) + (6 x 22.4) L O_2 → (6 x 22.4) L CO_2 + (6 x 18 g) water + 2780 kJ

$$1 \text{ L oxygen} = 2780 \div (6 \times 22.4) \text{ kJ} = 20.7 \text{ kJ} \quad (1.15)$$

If a subject is metabolising only carbohydrate, then for every litre of oxygen used in respiration, 20.7 kJ of heat (energy) is produced and therefore energy expenditure can be measured from the oxygen utilisation (Raaij, 2002).

If the body is using fat as an energy source, whether from the diet or stored adipose tissue, the equation is more complex because triacylglycerol molecules are larger and can be composed of a range of fatty acids. A typical fatty acid molecule e.g. palmitic acid ($C_{16}H_{34}O_2$) contains a lower proportion of oxygen than glucose. Therefore, fat metabolism requires more oxygen than the metabolism of glucose because oxygen is used for the oxidation of hydrogen to water as well as carbon to CO_2.

A typical triacylglycerol is palmitoyl, stearoyl, oleoly-glycerol, $C_{55}H_{106}O_6$.

$$2C_{55}H_{106}O_6 + 157O_2 \rightarrow 110CO_2 + 106H_2O + \text{heat} \quad (1.16)$$

The RQ for this reaction is 110/157 or 0.70.

The RQ for oxidation of one mole of a standard protein is 0.83 from,

$$C_{100}H_{159}N_{32}O_{32}S_{0.7} + 104O_2 \rightarrow 86.6CO_2 + 50.6H_2O + \text{other products} + \text{heat} \quad (1.17)$$

The other products are assumed to be urea (11.7 mol), ammonia (1.3 mol), creatinine (0.43 mol) and sulphuric acid (0.7 mol). The RQ for this reaction is 86.6/104 or 0.83 (Frayn, 1996).

Elia (1990) gives a detailed discussion of the energy equivalence of different fuels in terms of the heat liberated for each litre of oxygen consumed and carbon dioxide produced. The heat produced per litre of oxygen consumed is almost constant, but energy equivalence of CO_2 varies to a much greater extent (Table 1.4), and therefore the RQ depends on the mixture of fuels being oxidised.

Table 1.4 Energy equivalent of O_2 & CO_2 and RQ of macronutrients & alcohol

		Energy equivalent ($kJ.L^{-1}$)	
	RQ	O_2	CO_2
Fat	0.710	19.60	27.46
Protein*	0.835	19.48	23.33
Carbohydrate**	1.000	21.12	21.12
Alcohol	0.677	20.33	30.49

From Livesey & Elia (1988). *End products assumed to be urea, ammonia and creatinine in the nitrogenous ration 90:5:5. **Glucose polysaccharide

The measurement of oxygen consumption alone allows the calculation of energy expenditure to a reasonable accuracy, but the estimate can be improved by also measuring CO_2 production and urinary nitrogen excretion. Most ventilated hood indirect calorimeters measure both oxygen consumption and CO_2 production and energy expenditure (EE) is related to oxygen consumption ($\dot{V}O_2$) and carbon dioxide production ($\dot{V}CO_2$) by the modified Weir equation (Weir, 1949) without directly measuring urinary nitrogen excretion.

$$EE\ (kcal) = 1.44(3.9\dot{V}O_2 + 1.1\dot{V}CO_2) \quad (1.18)$$

where,

EE = Energy Expenditure (kcal/24h, 1 kcal = 4.18 kJ)

$\dot{V}O_2$ = O_2 consumption ($ml.min^{-1}$ at STPD)

$\dot{V}CO_2$ = CO_2 production ($ml.min^{-1}$ at STPD)

In the context of ^{13}C breath tests, the measurement of CO_2 production is the required output, but factors that lead to an increase in energy expenditure, such as postprandial thermogenesis and physical activity also lead to an increase in CO_2 production.

RQ and FQ

The energy content of a person's diet can be calculated from macronutrient content of the diet. The food quotient (FQ) is the calculated CO_2 produced divided by the O_2 consumed during oxidation of foods (Black *et al.* 1986). Under conditions of perfect nutrient balance the FQ must equal the RQ. The equation for calculating the FQ of a diet or meal is shown in full in section 2.4.2. The FQ of the average British or 'western' type diet composed of

11 % energy from protein, 38 % energy from fat, 6 % energy from alcohol and the remaining 45 % energy from carbohydrate is 0.85 (Elia, 1990).

1.5.4 Postprandial or diet-induced thermogenesis

Diet-induced thermogenesis (DIT) is the stimulation of metabolism that occurs for 3-6 h after a meal and represents the energy cost of digestive activity including gastric emptying, intestinal motility, digestion, absorption, metabolism and storage of nutrients within the body. Weststrate (1993) showed that DIT could be measured in 3 h following a mixed meal of 1.3-2.6 MJ. Approximately 85 % of the total observed thermic effect (over 3.5 h) was observed in the first 2 h of the postprandial period. The magnitude of DIT over 24 h is about 10 % of the total daily energy expenditure. DIT was originally called 'the specific dynamic effect of food' because the stimulation of energy expenditure depends upon the composition of the meal. DIT is also called postprandial thermogenesis (PPT) and the thermic effect of food (TEF).

1.5.5 Physical activity level (PAL)

The 1985 FAO/WHO/UNU expert committee on energy and protein requirements expressed the energy needs of adults as multiples of BMR (FAO/WHO/UNU,1985). The ratio of TEE to BMR later became known as physical activity level or PAL (James, Ferro-Luzzi & Waterlow, 1988).

$$PAL = TEE/BMR \qquad (1.19)$$

The PAL ratio is a convenient way to control for age, gender, weight and body composition, and to express the energy needs of a wide range of people in shorthand form (Black *et al.* 1996). Annex 5 of the 1985 FAO/WHO/UNU report, gives the gross energy expenditure of specified activities, expressed in terms of BMR multiplied by a "metabolic constant". Examples for adult males are: sleeping 1.0, sitting quietly 1.2, standing quietly 1.4, walking slowly 2.8, playing cards 1.4. The term physical activity ratio (PAR) is now used for this metabolic constant (Department of Health, 1991). PAR can be used to estimate the contribution of a particular activity to TEE by multiplying the time spent on a particular activity by the energy cost of that activity. The weighted sum of PAR over a 24 hour period equates to PAL. The PAL of sedentary adults undertaking non-active pursuits in their leisure time and light occupational activity is 1.4 (Department of Health, 1991).

Recently, the term MET for the "metabolic constant" has found increasing favour. One MET is the ratio of the metabolic rate associated with a particular activity to resting metabolic rate (Ainsworth *et al.* 1992, 2000). MET's are not exactly equivalent to PAR e.g. the MET associated with sleeping is 0.9, sitting quietly 1.0, standing quietly 1.2 and sitting playing cards, playing board games 1.5, but MET's are finding increasing use as data are available for more activities.

BMR is rarely measured prior to ^{13}C-breath tests, although resting metabolic rate (RMR) is sometimes measured 3-4 h following the test meal (Amarri *et al.* 1997, 1998). Most studies use a predicted value of BMR. In any case energy expenditure during a breath test is above BMR, even in compliant subjects, because they are usually sitting, not fasting and are mentally alert, because they are concentrating on the protocol. During the course of a 6-10 h breath test, metabolic rate will vary depending on nutritional status as well as activity. The appropriate value of $\dot{V}CO_2$ should be used to calculate PDR in each breath sample, rather than assuming a constant rate throughout.

1.5.6 Use of heart-rate monitors to measure total energy expenditure

1.5.6.1 Introduction

Heart rate monitors have been used to measure TEE in individuals of all ages and offer potential to estimate of $\dot{V}CO_2$ over periods of several hours. The doubly labelled water method can accurately measure TEE over a period of several days (IDECG, 1990), but is not suitable for the time course of a typical ^{13}C breath test, which lasts for several hours rather than several days. The doubly labelled water method averages EE during the measurement period and cannot detect patterns of activity. Accelerometers and other motion sensors have been widely used to monitor physical activity (e.g. Meijer *et al.* 1989; Pambianco, Wing & Robertson, 1990; Sallis *et al.* 1990; Freedson, 1991; Bouten *et al.* 1994; Janz, 1994; Melanson & Freedson, 1995; Welk & Corbin, 1995; Eston, Rowlands & Ingldew, 1998; Johnson, Russ & Goran, 1998; Trost *et al.* 1998; Ekelund *et al.* 2002; Jackson *et al.* 2003; Reilly *et al.* 2004), but do not take account of infection, inflammation, diet-induced thermogenesis and other factors which might increase $\dot{V}CO_2$ independently of increased physical activity. Activity questionnaires (Harro, 1997; Bernstein *et al.* 1998; Kriemler *et al.* 1999) do not give detailed enough information to detect changes in $\dot{V}CO_2$ over short time periods. Heart rate monitors provide minute-by-minute data, which potentially enables estimation of $\dot{V}CO_2$ at the time of each breath sample.

1.5.6.2 Heart rate monitors

Booyens & Hervey (1960) explored the possibility of using pulse rate as a means of measuring metabolic rate in man over 40 years ago. They noted that observations of the correlation between changes in heat production and changes in pulse rate had been reported by Benedict as early as 1907, and a relationship between changes in pulse rate and oxygen consumption was observed by Lindhard (1913) and Murlin & Greer (1914). Henderson & Prince (1914) were the first to show that in any one individual, one relationship between pulse rate and oxygen consumption existed during rest and very light activity, while there was an abrupt transition to a second relationship when activity was increased during exercise. The relationship during exercise was found to be consistent and linear, though it broke down at high levels of exertion. Booyens & Hervey themselves measured metabolic rate in two female and four male subjects (Booyens & Hervey, 1960). The relationship between pulse rate and metabolic rate was established lying, sitting and standing and at three rates of work on a bicycle ergometer.

By 1969, it was possible to measure heart rate and oxygen consumption simultaneously, and Bradfield, Huntzicker & Fruehan (1969) compared this technique with the respirometer-diary technique of Durnin and co-workers (Garry *et al.* 1955; Durnin, Blake & Brockway, 1957; Durnin & Brockway, 1959; Durnin *et al.* 1961a, 1961b) in a group of 24 young men. Christensen *et al.* (1983) used Bradfield's method (Bradfield *et al.* 1969) to estimate EE from heart rate and oxygen consumption data in patients with metabolic disorders (obesity, untreated thyrotoxicosis and anorexia nervosa). He found considerable intrasubject variability when measurements were made on the same subject under identical conditions on consecutive days. Generally the correlation coefficients of the regression lines were high, but fairly large differences between the slopes and intercepts of the duplicate lines resulted in large discrepancies between duplicate estimates. Christensen, therefore concluded that the method had limited applicability in subjects with low levels of activity, because heart rate is influenced by factors which do not affect $\dot{V}O_2$.

Uncalibrated heart-rate monitors have been used to study the pattern of physical activity in 6-7 y old children (Gilliam *et al.* 1981). Treiber *et al.* (1989) showed that heart rate monitors give an accurate record of heart rate in children (aged 4-10 y), when compared to electrocardiographic (ECG) telemetry in the laboratory. Activities, such a throwing a tennis ball, batting a tennis ball and playing on a climbing frame were included in the study. These are activities which are commonly performed by children, but which might

result in poor reception by the receiver or disconnection of the transmitter. They concluded that heart rate monitors are a practical and inexpensive means of accurately assessing heart rate in children under field conditions. This was confirmed by Durant *et al.* (1993).

Calibrated heart rate monitors have been used in studies of TEE in free-living populations of adults including Livingstone *et al.* (1990), Davidson *et al.* (1997), Morio *et al.* (1997), Wareham *et al.* (1997). Heart rate monitoring has also been used in studies of activity in pre-school children (Bar-Or *et al.* 1996; Pate *et al.* 1996), primary school children and adolescents (Emons *et al.* 1992; Janz *et al.* 1992; Livingstone *et al.* 1992; Treuth, Adolph & Butte, 1998; Ribeyre *et al.* 2000a, Vermorel *et al.* 2002), and pregnant women (Heini *et al.* 1991). These studies have relied on individual calibration of the heart rate monitor either using indirect calorimetry or analysis of oxygen in exhaled breath.

1.5.6.3 Calibration methods

All published studies have relied on individual calibration to establish a relationship between heart rate and oxygen consumption or EE. Methods of calibrating heart rate against EE, $\dot{V}O_2$ or $\dot{V}CO_2$ need to take into account the fact that there is a different linear relationship at resting levels than at levels of activity above resting (Figure 1.15). Calibration procedures therefore must include measurements where the subjects are lying quietly, sitting quietly and standing still as well as at levels of increasing activity, usually either on a bicycle ergometer or a treadmill.

The most widely used calibration method in studies of energy expenditure is that of Spurr *et al.* (1988), which used a two-component linear model. Measurements were made after several minutes equilibration time in each position (lying, sitting on a chair, standing and sitting on a bicycle ergometer). The mean of all the inactive measurements was used as the resting metabolic rate, RMR, which is ~5 MJ d^{-1} in the example shown in Figure 1.15. The subjects then began cycling on the ergometer at 50 cycles min^{-1} with no resistance. Every 3 min the resistance was elevated until the subject's heart rate increased to approximately 150 beats min^{-1}. Measurements of $\dot{V}O_2$ were made during the last minute of each 3 min cycling period.

Spurr *et al.* (1988) defined a critical heart rate, above which the slope and intercept of the linear calibration curve obtained on the exercise bicycle was used to determine $\dot{V}O_2$, and below which the resting rate was used. The critical value was calculated by adding 10 to

the flex heart rate, which was determined empirically by taking the average of the highest resting heart rate and the lowest during exercise on the bicycle. The flex point in the example shown in Figure 1.15 is approximately 90 beats per min. Therefore, the critical value is 100 beats per min. Below a heart rate of 100 beats per min a constant relationship (RMR) is assumed, and above 100 beats per min the linear calibration curve is used. EE calculated from heart rate data was -20 to +15 % of that determined in the whole body calorimeter (mean -2.4 %). The inter-individual coefficient of variation (CV) was 9.6 %. Ceesay *et al.* (1989) used a modification of Spurr's method to validate the heart rate method against whole-body indirect calorimetry in 20 healthy adult subjects. They found that on average the heart rate method underestimated TEE by only 1.2 %. The difference between the two methods was not significant.

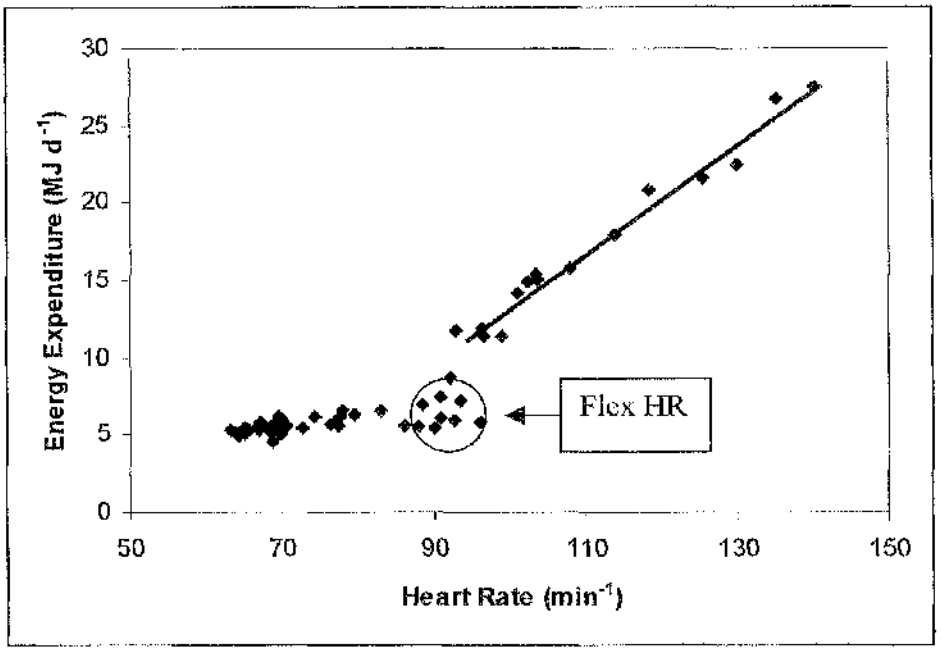

Figure 1.15 Relationship between heart rate and energy expenditure

A variation of the linear-flex method was used by Livingstone (1992) who used a treadmill to calibrate heart rate and $\dot{V}O_2$ in children aged 7 to 15 y. TEE calculated from heart rate data was compared to that determined by the doubly labelled water method (Coward, 1988; IDECG, 1990). During the calibration procedure, heart rate and $\dot{V}O_2$ were measured simultaneously at three resting levels (supine, sitting quietly, standing quietly) and two levels of work on a treadmill. A preliminary equilibration period of 3 min was allowed for each activity, followed by a 3 min sampling period. The calibration point for each activity was computed as the mean for the 3 min sampling period of heart rate and $\dot{V}O_2$. As before,

RMR was determined as the mean $\dot{V}O_2$ of the resting activities, and the flex point was defined as mean of the highest heart rate for the resting activities and the lowest heart rate from the treadmill. Unlike Spurr *et al.* (1988), Livingstone did not add 10 to the flex heart rate to determine the critical point. In this case the critical point was equal to the flex point.

Determination of a flex point can be avoided by the use of non-linear models. Schulz, Westerterp & Breuck (1989) and Davidson *et al.* (1997) used a 2nd order polynomial with reasonable success, and 3rd order polynomials have been used by Bitar *et al.* (1996); Mario *et al.* (1997); Ribeyre *et al.* (2000a); Beghin *et al.* (2002); Rodriguez *et al.* (2002) and Vermorel *et al.* (2002). A disadvantage of 2nd and 3rd order polynomials is that at low heart rates, such as when sleeping, they tend to overestimate energy expenditure, unless a flex point is introduced at the minimum of the model. This problem is avoided by the use of an appropriate exponential model. As long ago as 1979, Dauncey and James (1979) assessed the heart-rate method for determining energy expenditure over 24 h periods on subjects carrying out near-normal activities in a whole-body calorimeter. In this study, simultaneous measurements of heart rate and heat production were made with the subjects lying, sitting, standing quietly and while cycling at four levels of work on a bicycle ergometer. Dauncey and James compared several linear regression methods of their non-resting data with a logistic fit of all their calibration data, including both resting and non-resting data in a single model. The percentage difference between the measured and predicted heat production for every subject was calculated using each method. This was taken as a measure of the accuracy of the method. The use of correlation coefficients was found to be misleading, since a perfect correlation could be associated with a large mean difference and standard deviation i.e. the method was neither accurate nor precise. The logistic model, was also used by Li, Deurenberg & Huatvast (1993) and has the advantage of fitting the data, without assuming a flex point.

An alternative non-linear model is the Sigmoid model. Like the logistic model, it makes no assumptions about resting heart rate and avoids the use of a flex point. Moon and Butte (1996) compared linear, 2nd order, 3rd order, logistic and sigmoid models of calibrating heart rate monitors. They found that the Sigmoid model had the highest coefficient of determination ($R^2 = 0.91$), but used a two-component model based on RMR and HR^3 to estimate 24-h $\dot{V}O_2$ and $\dot{V}CO_2$ using a combination of heart rate and activity monitors.

1.5.6.4 Generic calibration

It would not be necessary to perform individual heart rate calibrations for each subject, if a generic calibration could be found, scaling $\dot{V}CO_2$ to some allometric parameter. In many studies, scaling to body surface area is used to compare the results from different subjects. This removes the effect of the increase in CO_2 production rate with body size.

The consensus in studies of energy expenditure using heart rate monitors seems to be that individual calibration is necessary to obtain estimates of energy expenditure that are sufficiently accurate to detect small differences in population studies. Spurr *et al.* (1988) obtained estimates from heart rate data that were within 15-20 % of those measured by whole body indirect calorimetry, a method which is clearly unsuitable for studies in free-living individuals. Li *et al.* (1993) obtained inter-individual CV's of 11-20 % and intra-individual CV's of 14-18 %. This level of precision may, however be adequate for ^{13}C breath tests, where the error introduced by using resting $\dot{V}CO_2$, when individuals are not at rest, can be up to 100 %.

Animal studies have attempted to predict energy expenditure from heart rate measurements using a generic calibration (Richards & Lawrence, 1984; Sneddon, Mathers & Thomson, 1985). Richards and Lawrence (1984) found that the rate of energy expenditure of adult cattle pulling loads whilst walking on a treadmill, was related to relative heart rate, defined as the heart rate of a working animal divided by the heart rate at rest. Energy expenditure was normalised to kg body weight$^{0.75}$. A similar relationship was found by Sneddon *et al.* (1985) in young calves.

1.6 Use of deuterium labelled tracers

1.6.1 Introduction

Use of deuterium (^2H) labelled tracers could avoid the problems associated with lack of knowledge of $\dot{V}CO_2$, incomplete recovery of tracer and changes in background ^{13}C abundance. Furthermore, the proportion of label that may be sequestered into organic molecules is small, approximately 4 % (Haggerty, 1990). The volume of distribution of ^2H is total body water, which is not affected by food intake, physical activity or nutritional status over the required time course of 6-8 h, which is similar to the sampling time during

the [^{13}C]MTG breath test. Body water can be sampled in the form of saliva, urine or plasma.

1.6.2 The [^{2}H]MTG test

It is possible to synthesise MTG using [$^2H_{15}$]octanoic acid, rather than [1-^{13}C]octanoic acid. [^{2}H]MTG is not available commercially, but [^{13}C]MTG and [^{2}H]MTG will be digested and absorbed in the same manner. However, the fate of the label is different after β-oxidation. The ^{13}C label on [1-^{13}C]octanoic acid is removed at the first pass through the mitochondrial β-oxidation pathway as [1-^{13}C]acetyl CoA, which enters the TCA cycle for oxidation to $^{13}CO_2$, but the label may be sequestered into other carbon pools during anabolic and anaplerotic processes (Figure 1.11), and thus only approximately 30 % of ingested tracer is recovered in breath CO_2 within 6 h (Amarri *et al.* 1998). By contrast, most of the deuterium exchanges with body water during β-oxidation and sequestration of ^{2}H into body glycogen, protein and lipid stores is small (Haggerty, 1990; Haggerty *et al.* 2000) compared to sequestration of carbon. The ^{2}H non-aqueous exchange factor accepted in the calculation of total body water from deuterium dilution is 1.04 (Schoeller & Jones, 1987) i.e. ~4 % of ingested deuterium is sequestered. Therefore approximately 96 % ingested ^{2}H should be recovered in body water in healthy subjects. There will be small losses in insensible water in faeces, perspiration etc.

To calculate percentage dose recovered in body water from deuterium labelled tracers, a measure or estimate of the tracer distribution volume (total body water) is required. Total body water can be measured independently by ^{18}O-dilution (Schoeller *et al.* 1980), but this would be prohibitively expensive for routine use and supplies of 10 % ^{18}O enriched water are unreliable. In adults, total body water can be estimated using equations based on height and weight (Hume & Weyers, 1971). Estimation of total body water from bioimpedence measurements is possible if suitable equations are available for population being studied (Houtkooper *et al.* 1992; Hannan *et al.* 1994; Berger *et al.* 2000; Sun *et al.* 2003), but these may not be accurate in children (Reilly *et al.* 1996; Parker *et al.* 2003). The simple formula devised by Slater and Preston (2002) to predict total body water from height, based on measurements in subjects aged from 3 to 83, may be sufficiently accurate in this context.

The cost of deuterium analysis has improved considerably since the advent of continuous-flow methods of deuterium analysis (Section 1.4.4). These are much less labour-intensive

than traditional methods, which require off-line preparation of pure hydrogen samples followed by deuterium analysis by dual-inlet IRMS. It is now possible to prepare and analyse many more samples in a day than previously and therefore analytical costs are considerably reduced. However, the body water pool is much larger than the bicarbonate pool, so larger doses of ^{2}H-labelled substrates (10-15 times more than for ^{13}C breath tests) are required to achieve sufficient enrichment for accurate analysis.

Use of [^{2}H]MTG as a test of exocrine pancreatic insufficiency that is not affected by diet or physical activity could prove to be feasible in the near future, if supplies of [^{2}H]MTG can be secured.

1.6.3 Validation of ^{13}C breath tests using ^{2}H-labelled substrates

Bluck *et al.* (2002) used simultaneous doses of [$^{2}H_{15}$]octanoic acid and [1-^{13}C]octanoic acid in their validation study of the octanoic acid test of gastric emptying. The hypothesis was that the majority of the label will be removed during β-oxidation, passing directly into body water and therefore the kinetics observed should be more closely related to the reference method, radioscintigraphy.

Deuterium labelled substrates can also be used to test the assumptions related to recovery of ^{13}C in breath and sequestration within the body. The acetate correction factor accounts for ^{13}C fixation that might occur at any step between the entrance of acetyl-CoA into the TCA cycle until recovery of label in breath CO_2 (Section 1.4.9). Assumptions in its use are that CO_2 production rate is the same on each occasion, that there are no other major routes of sequestration of label, and that oxidation of both tracers take place at the same rate. If these assumptions are true, then recovery in breath corrected for label sequestered in the body should be 95 to 100 % and should be similar to the recovery of ^{2}H in body water following ingestion of [^{2}H]MTG. If recovery is not within 5 % of 95 %, then the assumptions are not valid.

Comparison of recovery of deuterium in body water following ingestion of [^{2}H]MTG and [^{2}H]octanoate would confirm that hydrolysis of the long-chain fatty acids from the *sn*-1 and *sn*-3 position of MTG is the rate-limiting step in its metabolism. Comparison of recovery of deuterium in body water following ingestion of [$^{2}H_{15}$]octanoate and [$^{2}H_{3}$]acetate would confirm that acetate and octanoate are metabolised in the same manner following absorption.

1.7 Summary of the problem

The MTG breath test provides an indirect measure of exocrine pancreatic insufficiency in children with cystic fibrosis and could be used to optimise pancreatic enzyme replacement therapy (PERT) in these children (Amarri *et al.* 1997). However, in validation studies, the test had a sensitivity of 0.89 and specificity of 0.81 resulting in a positive predictive value of 0.63 and negative predictive value of 0.95 (Vantrappen, 1989; Perri & Andriulli, 1998). This implies that there were few false positive results and that the majority of patients with exocrine pancreatic insufficiency were correctly identified, but there were too many false negative results shown by low recovery of ^{13}C in breath CO_2 of healthy subjects. The same pattern was observed by Amarri *et al.* (1997) in children. Large intra-individual variation of $^{13}CO_2$ excretion has also been reported in healthy adult subjects (Kalivianakis *et al.* 1997), with a coefficient of repeatability of cPDR 9h of 22.7 %. Reasons for low recovery in the breath of healthy subjects, and children with cystic fibrosis taking their normal PERT, could be due to one or more of the following:

1. errors in dosage
2. inaccurate ^{13}C measurement
3. loss in stool
4. inaccurate CO_2 production rate measurement
5. sequestration within the body.

Errors in dosage can be controlled by careful weighing to sufficient accuracy, ensuring homogeneous distribution within the test meal, taking account of losses during preparation and adjusting for incomplete consumption of the test meal. The natural ^{13}C abundance of the test meal should also be controlled by using low ^{13}C ingredients.

Inaccurate isotope abundance measurement can be avoided by careful calibration of the IRMS, and frequent checks of linearity and precision. Accuracy of measured enrichment also depends on taking steps to maintain constant background ^{13}C abundance.

Losses in stool and urine have been shown to be small, amounting to less than 5 % of the ingested dose in healthy children and children with cystic fibrosis taking their normal dose of PERT (Slater *et al.* 2002). The vast majority of tracer must thus be exhaled in breath CO_2 or sequestered in metabolic products within the body. Accurate accounting for the sequestered tracer should result in a test with improved discrimination.

Quantitation of tracer excretion requires knowledge of the volume of distribution of the tracer as well as ingested dose and breath ^{13}C abundance. In the case of breath $^{13}CO_2$, the volume of distribution is endogenously produced CO_2 from metabolic processes, which is usually expressed as CO_2 production rate ($\dot{V}CO_2$). A resting value based on BMR is usually assumed, but if subjects are not resting and in the postabsorptive state throughout the test, this will be an underestimate of the true CO_2 production rate.

1.8 Hypothesis and Aims

1.8.1 Global hypothesis

The global hypothesis is that the poor positive predictive value of the ^{13}C-mixed triacylglycerol (MTG) breath test used to assess exocrine pancreatic insufficiency is due to lack of knowledge of the true carbon dioxide production rate ($\dot{V}CO_2$) during the test.

Use of a constant value of resting $\dot{V}CO_2$, whether predicted from body surface area (300 $mmol.h^{-1}.m^{-2}$), calculated from BMR predicted using the Schofield (1985) equations, or measured, underestimates the true CO_2 production rate and does not take account of variations during the test.

This results in an underestimate of the ^{13}C percentage dose recovered, especially in children, who are unable to maintain resting conditions for the six-hour duration of the test.

The solution to this problem is either to measure CO_2 production rate for the duration of the test, or to use an empirically derived correction to eliminate the need for its measurement.

1.8.2 Aim

To improve the positive predictive value of the MTG breath test, either by continuously measuring $\dot{V}CO_2$ during the test, or by using a correction for tracer loss in the products of intermediary metabolism. A series of interrelated experiments and human studies were designed to achieve this aim and to test the hypothesis above.

1.8.3 Objectives

1 Validation of laboratory methods. *To optimise laboratory procedures and thus ensure that mass spectrometric methods provide accurate and precise results.*

2 Measuring CO_2 production rate. *To assess the potential of using heart rate monitors to estimate CO_2 production rate and sources of its variation during ^{13}C breath tests, and to determine the most suitable calibration procedure in healthy adults.*

3 Generic calibration of heart rate monitors. *To assess potential generic calibration methods to predict CO_2 production rate from heart rate during ^{13}C-breath tests.*

4 Development of a test meal. *To design a test meal to carry both hydrophilic ([1-^{13}C]acetate, [$^{2}H_3$]acetate) and lipophilic ([1-^{13}C]octanoic acid, [$^{2}H_{15}$]octanoic acid, [^{13}C]MTG and [^{2}H]MTG) substrates to study intermediary metabolism within the context of the [^{13}C]MTG test.*

5 Investigation of [^{13}C]MTG metabolism. *To investigate aspects of [^{13}C]MTG metabolism by comparing the cumulative percentage dose recovered (cPDR) from the [^{13}C]MTG breath test with that from [1-^{13}C]octanoic acid, [1-^{13}C]acetate and [^{13}C]bicarbonate breath tests in subjects wearing calibrated heart rate monitors.*

6 Intra-individual variation in the MTG test. *To measure the intra-individual variation of the cPDR in the [^{13}C]MTG and [1-^{13}C]acetate breath tests in subjects wearing calibrated heart rate monitors.*

7 Deuterium-labelled MTG test. *To investigate the use of deuterium labelled MTG as a simpler alternative to the ^{13}C-breath test and to validate improvements to the ^{13}C- MTG breath test.*

8 [^{13}C]MTG breath test in healthy adults and children. *To investigate the effect of different levels and patterns of activity by performing [^{13}C]MTG and [1-^{13}C]acetate breath tests in healthy adult volunteers, healthy child volunteers and children with cystic fibrosis, all wearing individually calibrated heart rate monitors.*

9 [^{13}C]MTG breath test using generic heart rate calibration. *To investigate potential generic calibration methods to predict CO_2 production rate from heart rate during ^{13}C breath tests in subjects with a wide range of age and body habitus and to demonstrate their use in the [^{13}C]MTG and [1-^{13}C]acetate breath tests.*

10 Empirical compensation for individual VCO_2. *To investigate the use of an acetate correction as an empirically derived means of compensating for lack of knowledge of CO_2 production rate during the [^{13}C]MTG breath test.*

11 Determination of the cut-off point of the [^{13}C]MTG test. *To determine the appropriate cut-off of the modified MTG breath test using two graph-receiver operator characteristics (TG-ROC), and to calculate the positive and negative predictive values of the new test.*

1.9 Ethical considerations

Ethical approval was obtained from the Yorkhill Research Ethics Committee for the studies involving children and from the University of Glasgow Ethics Committee for Non Clinical Research Involving Human Subjects for the studies involving adults. The purpose of the study was carefully explained and written informed consent was obtained from all subjects (adults and children) taking part in the study, and where appropriate their parents. The study posed no danger to those taking part and subjects were free to drop out at any time.

Appendix 1 contains copies of the letters of approval from the University of Glasgow Ethics Committee for Non Clinical Research Involving Human Subjects and Yorkhill Research Ethics Committee, plus the information sheets for volunteers and a blank consent form.

Chapter 2 Methods

Summary of Chapter 2

In this chapter, the methods used to test the hypothesis and address the aims described at the end of Chapter 1, are described. Each group of experiments or studies was designed to address each of the objectives listed in Section 1.8.3. The results of each set of experiments or studies are reported in Chapter 3.

The experiments described in Sections 2.1 to 2.4 were designed to establish accurate methods of quantifying tracer excretion in breath. Quantitation of tracer excretion requires knowledge of the volume of distribution of the tracer as well as ingested dose and breath ^{13}C abundance. In the case of ^{13}C breath tests, $^{13}CO_2$ originating from oxidation of the tracer is diluted by endogenously produced CO_2 from metabolic processes. Therefore knowledge of CO_2 production rate ($\dot{V}CO_2$) is required. A resting value based on basal metabolic rate is usually assumed, but if subjects are not resting and in the postprandial state throughout the test, this will be an underestimate of the true CO_2 production rate.

There are three alternative approaches to solving this problem:

i. Measure CO_2 production rate throughout the breath-sampling period
ii. Use an empirically derived correction to compensate for the effect of "unknown" CO_2 production
iii. Use a tracer which does not enter the body's CO_2 pool.

Each of these approaches was explored during this study:

i. CO_2 production rate was measured throughout the breath-sampling period using calibrated heart rate monitors. Alternative calibration procedures were investigated and the possibility of using a generic calibration was explored (Sections 2.2, 2.3, 2.8 and 2.9).
ii. Use of an acetate correction to account for ^{13}C retained in the body was explored. This approach requires two breath tests to be performed, as simultaneous use of ^{13}C with the radioisotope ^{14}C is precluded. CO_2 production rate is assumed to be the same on both occasions, but knowledge of the actual value is not required (Sections 2.6 and 2.10).

iii. Use of deuterium (^2H) labelled MTG, rather than ^{13}C-labelled MTG, avoids the need to know CO_2 production rate. ^2H is distributed through the body water pool and therefore requires sampling of urine or saliva, rather than breath, and also a measurement or estimate of total body water (Section 2.7).

Once accurate methods to quantify tracer excretion in breath and other minor losses have been established, mass balance can be used to estimate the quantity of tracer retained within the body using [^{13}C]MTG and its metabolites, [1-^{13}C]octanoate, [1-^{13}C]acetate and [^{13}C]bicarbonate (Sections 2.5 and 2.6). Section 2.7 describes experiments using ^2H-labelled MTG, octanoate and acetate in the same subjects.

Use of heart rate monitors to estimate $\dot{V}CO_2$ during the [^{13}C]MTG test was investigated in eight healthy adults, ten healthy children and seven children with cystic fibrosis (Section 2.8). Cumulative breath $^{13}CO_2$ excretion was calculated using resting and non-resting values of $\dot{V}CO_2$. Physical activity level during the test was defined as non-resting PDR divided by resting PDR. Use of generic heart rate calibration methods, which avoid the need for individual calibration, was also investigated (Section 2.9).

[1-^{13}C]acetate breath tests were performed on eight healthy adults, nine healthy children and three children with cystic fibrosis, who had also performed the [^{13}C]MTG breath test. The cumulative excretion of $^{13}CO_2$ during the [^{13}C]MTG breath test was corrected for label sequestered in the body using the cumulative excretion of $^{13}CO_2$ during the [1-^{13}C]acetate breath test (Section 2.10).

Two graph-receiver operator characteristics (TG-ROC) were used to determine the appropriate cut-off for the [^{13}C]MTG test with a 6 h sampling time. PDR was calculated using both resting and non-resting values of $\dot{V}CO_2$. The positive and negative predictive values of the tests were calculated (Section 2.11).

2.1 Validation of laboratory methods

2.1.1 Introduction

The laboratory methods used to measure isotopic abundance were validated, to ensure that all measurements were accurate (traceable to international standards or gravimetrically prepared standard curves), precise (standard deviation of three replicate analyses < 1 ppm) and linear (the isotope ratio was constant over the expected concentration range). This ensured that measurement of isotopic abundance was not a major source of error in the calculation of cumulative excretion.

The isotopic abundance of ^{13}C in breath CO_2, and ^{2}H and ^{18}O in body water, as represented by urine and saliva, was measured by continuous flow-isotope ratio mass spectrometry (CF-IRMS). This technique measures the abundance of the stable isotopes of carbon, nitrogen, hydrogen and oxygen in simple gases, CO_2, N_2, H_2 in a stream of carrier gas (He). The sample is purified on-line: a water trap removes moisture, and breath CO_2 is separated from N_2 on a GC column in an isothermal oven. The pure gas sample enters the ion source of the mass spectrometer, where in a high vacuum it is ionised by bombardment with electrons from a hot filament. The ions are separated in a magnetic field on the basis of their mass:charge (*m/z*) ratio. The detector in an isotope ratio mass spectrometer is a series of Faraday cups, each of which detects ions of a single mass. For CO_2, the monitored ion beams are *m/z* 44, 45 and 46. For H_2, the monitored ion beams are *m/z* 2 and 3. Specialised instruments are required to measure *m/z* 2 and 3 in the presence of He at *m/z* 4.

The Department of Child Health took delivery of its first IRMS (Hydra 20-20 IRMS with a deuterium spur, PDZ Europa, Crewe, UK) in October 1997, coincident with the start of this project. There were no routine laboratory procedures in place at this time and these had to be developed as part of this study. To ensure that the isotope ratio mass spectrometer gave accurate and precise results, studies involving human subjects were preceded by a series of experiments to optimise IRMS operation and the procedures used to prepare samples and reference gases. The IRMS source tuning was optimised separately for CO_2 and for H_2 analysis. The laboratory CO_2 reference gas (5% CO_2 in N_2) was calibrated against references, which were traceable to the international standards and linearity of CO_2 measurements was checked. The procedure for analysing ^{18}O and ^{2}H in reference waters and clinical samples was optimised. $H_2{}^{18}O$ and $^{2}H_2O$ standard curves were prepared to

check the accuracy of ^{18}O and ^{2}H measurements. The procedure used to fill reference gas vials was optimised to give reproducible results, with a coefficient of variation on the amount of gas in each vial, of less than 1%.

2.1.2 Measurement of ^{13}C and ^{18}O isotopic abundance

The IRMS was composed of a 20-20 IRMS interfaced to an automated breath carbon analyser (ABCA, PDZ Europa, Crewe, UK) and an autosampler capable of holding 204 x 10 ml Exetainer breath sampling vials (Labco, High Wycombe, UK).

2.1.2.1 Procedure for filling reference gas vials

Reference gases were prepared on a 20-place vacuum manifold (PDZ Europa, Crewe, UK) attached to an Edwards two stage rotary pump, model E2M1.5 with an Edwards active pirani gauge and Edwards active gauge controller to monitor the vacuum (all available from Northern Scientific, York, UK). The manifold had 20 ports, each with a luer-lock stopcock (Sigma-Aldrich, Poole, UK) and a 25 gauge needle (Microlance 3, Beckton Dickinson, Cowley, UK). There were isolation taps at either end. Reference gas entered at the left-hand side. The flow of reference gas was controlled by an in-line flow controller, and set to 100 ml min^{-1} as measured by a bubble flow meter. The outlet to the vacuum pump was at the right-hand-side. All reference gas and clinical samples (breath, urine or saliva) were prepared in 10 ml Exetainer gas sampling vials (Labco, High Wycombe, UK). Evacuated vials are supposed to have a 10 ml draw, but the actual volume of the vial is 12 ml. The procedure for filling Exetainers was optimised empirically to minimise the coefficient of variation (standard deviation of total beam / mean total beam x 100). The manifold was evacuated by closing the gas isolation tap and all the stopcocks, and opening the vacuum isolation tap. Exetainers were attached to ports via a needle through the septum, leaving the right hand port free. The stopcocks were opened (except for the last port) and the tubes evacuated. All the stopcocks were closed and the vacuum pump was isolated. The free port was opened and the manifold was flushed with reference gas for 5 min, after which the Exetainers were filled by opening the stopcocks, one at a time starting at the left-hand side, for exactly 10 s. This was timed using a stopwatch to eliminate inter-individual error between operators.

2.1.2.2 Measurement of ^{13}C and ^{18}O in breath CO_2 and CO_2 reference gas

The abundance of ^{13}C and ^{18}O in breath CO_2 was measured by monitoring the ion beams at *m/z* 44, 45 and 46. The IRMS source parameters and resistance of the head amplifiers are shown in Table 2.1. The source was tuned for maximum sensitivity with a broad flat-topped *m/z* 45/44 ratio trace and maximum width in the plateau of the *m/z* 46/44 ratio traces. This was achieved by small adjustment of the HT, ion repeller and beam focus settings. Measurements were made against a reference gas containing 3 % CO_2 in N_2 (Air Products Special Gases, Crewe, UK). This had been calibrated against secondary references that were traceable to the international standards (VPDB, Vienna Pee Dee Belemnite for ^{13}C and VSMOW, Vienna Standard Mean Ocean Water for ^{18}O) (Coplen, 1996) at the Isotope Geosciences Unit, Scottish Universities Environmental Research Centre, East Kilbride. The Craig correction (Craig, 1957), which uses the measured [$^{12}C^{16}O^{18}O$] at *m/z* 46 to account for the presence of [$^{12}C^{16}O^{17}O$] at *m/z* 45, was applied by the manufacturers software. Results were expressed as ppm ^{13}C or ppm ^{18}O. After maintenance periods, the stability of the IRMS was checked by trapping CO_2 reference gas and monitoring the ion beams at *m/z* 44, 45 and 46 and the ratio traces of 45/44 and 46/44.

Table 2.1 Hydra-IRMS source and detector settings for CO_2 and H_2 analysis

	CO_2, $^{13}CO_2$ and $C^{16}O^{18}O$	H_2, [$^2H^1H$]
Magnet Current (A)	12.5	2.6
HT (V)	2520	2723
Trap Current (μA)	200	600
Electron Energy (eV)	-75	-75
Ion Repeller (V)	-11	30
Beam Focus (%)	91	86
Head Amplifier Resistance		
Beam 1 (MΩ)	100	100
Beam 2 (MΩ)	5000	100,000
Beam 3 (MΩ)	5000	Not applicable

2.1.2.3 CO_2 calibration curve and linearity of $^{13}CO_2$ abundance

A standard curve was prepared over the expected range of CO_2 concentration in exhaled breath by preparing tubes of reference gas containing 0.5-10 % CO_2, by injecting pure (100 %) CO_2 (Air Products Special Gases, Crewe, UK) into evacuated Exetainers using a gas-tight syringe (SGE, Burke Analytical, Alva, UK). A measurement is said to be linear, if the isotope ratio (abundance) is constant over the expected concentration range. Linearity of ^{13}C measurements was checked by plotting the abundance of ^{13}C (ppm) against calculated CO_2 concentration. % CO_2 was the independent variable, plotted on the *x*-axis and ppm ^{13}C was the dependent variable plotted on the *y*-axis.

2.1.2.4 Precision of breath $^{13}CO_2$ analysis and inter-laboratory check

A bicarbonate breath test (0.5 mg/kg body weight) was performed on a single subject, and multiple identical breath samples were obtained using the "bag and mask" technique (Weaver *et al.* 1993). Exhaled air was sampled at intervals by blowing through a one-way valve (Ambu, Brondby, Denmark) into a 600 ml gas sampling bag (Laerdal Medical, Orpington, UK), which has been fitted with a 3-way Luer tap to facilitate gas transfer. Breath samples were transferred to an evacuated Exetainer using a syringe. Five identical replicates were prepared at each time point. The abundance of $^{13}CO_2$ was measured as described above (Section 2.1.2.2). Four replicates were analysed on the HYDRA-IRMS in the Department of Child Health, and one was measured on the 20:20-IRMS (Europa Scientific) in the Isotope Biochemistry Laboratory at the Scottish Universities Environmental Research Centre, East Kilbride.

2.1.2.5 Preparation of an ^{18}O standard curve

The accuracy of ^{18}O enrichment measurements was checked by preparing a calibration curve and plotting the enrichment measured by IRMS against that calculated from the weight and the abundance of the stock $H_2{}^{18}O$. The abundance of ^{18}O in the stock $H_2{}^{18}O$ was calibrated against the international standard (VSMOW) at the Isotope Geosciences Unit, Scottish Universities Environmental Research Centre, East Kilbride. Ideally, the gradient of the calibration curve should be 1.0.

A series of gravimetric standards containing 0, 15, 75, 150, 225 and 375 ppm excess ^{18}O was prepared from $H_2{}^{18}O$ (10 atom % ^{18}O, normalised for deuterium concentration, CK Gas Products, Wokingham, UK) diluted with tap-water. Large volumes (1 L) of 0 and 150

ppm excess ^{18}O were prepared to serve as working standards to be analysed with each batch of samples. An aliquot (400 µl) of each sample was pipetted into a 10 ml Exetainer gas testing vial (Labco, High Wycombe, UK). Vials were evacuated for one min, filled with reference gas (3 % CO_2 in nitrogen, Air Products Special Gases, Crewe) as described in section 2.2.2.1 and left to equilibrate with the headspace gas for 24 h at ambient temperature. During this time the ^{18}O in the water phase equilibrated with the CO_2 in the gas phase. The abundance of ^{18}O in the gas phase was measured by CF-IRMS, monitoring *m/z* 44 and 46. The abundance of ^{18}O in standard waters was calculated with reference to the known abundance of ^{18}O in the CO_2 reference gas, which was traceable to international standards. Results were expressed as ppm ^{18}O. The enrichment of water samples was calculated by subtracting the measured abundance of ^{18}O in the 0 reference (tap water) from the measured abundance of ^{18}O in the sample. Results were expressed as ppm excess ^{18}O. Measured enrichment (ppm excess ^{18}O) was plotted against enrichment calculated from the independent analysis of the stock $H_2{}^{18}O$, and the weight of $H_2{}^{18}O$ and tap water used to prepare the reference water. Enrichment calculated from weight was taken as the independent variable and plotted on the *x*-axis.

2.1.2.6 Accuracy and precision of CO_2 measurements

Accuracy of measured $^{13}CO_2$ abundance was ensured by calibrating the reference gas against the international standard and placing references at intervals during each analytical run. The reported isotope ratio was corrected for instrumental drift between references. Precision of $^{13}CO_2$ measurements was checked at intervals by analysing batches of reference gases and calculating the standard deviation (SD) of three replicates. SD < 0.5 ppm ^{13}C (<0.05 ‰) was regarded as acceptable (Preston, 1992).

Accuracy of $H_2{}^{18}O$ measurements was ensured routinely by including working standard waters containing 0 and 150 ppm excess ^{18}O in triplicate at intervals in each batch of samples. The gradient of this two-point calibration curve was used to calculate the isotope abundance in each sample. The reported isotope ratio was corrected for instrumental drift between references as described below (Section 2.1.3.3). The precision of ^{18}O abundance measurements was checked by calculating the standard deviation (n=3) of the standard waters, which were included at intervals in each batch of samples. SD < 0.5 ppm ^{18}O was regarded as acceptable.

2.1.3 Measurement of ^2H isotopic abundance

2.1.3.1 Measurement of ^2H in reference gas

Reference gases (5 % hydrogen in helium, Air Products Special Gases, Crewe, UK) were prepared as described in Section 2.1.2.1. The IRMS source parameters and resistance of the head amplifiers for analysis of deuterium are shown in Table 2.1. The source was tuned for minimum *m/z* 3/2 ratio, with maximum sensitivity. A nominal value for ^2H abundance of –42 δ VSMOW was entered in the manufacturer's software since samples are always analysed with reference to gravimetric standard waters. Data were exported to a "Reprocessor" programme provided by the IRMS manufacturer, where a non-linear least squares regression was applied to determine the contribution of H_3^+ to *m/z* 3.

2.1.3.2 Preparation of a ^2H standard curve

Accuracy of ^2H enrichment measurements was checked by preparing a calibration curve and plotting the enrichment measured by IRMS against that calculated from the weight and certified abundance of the stock ^2H_2O. Ideally, the gradient of the calibration curve should be 1.0.

A series of gravimetric standards containing 0, 15, 30, 75, 100, 150, 250, 300, 750, 1100, 1500 ppm excess ^2H was prepared from ^2H_2O (99.9 atom % ^2H, Isotech, CK Gas Products, Wokingham, UK) diluted with tap water. Large volumes (1 L) of 0 and 75 ppm excess ^2H were prepared to serve as working standards to be analysed with each batch of samples. An aliquot (400 µl) of each sample was pipetted into a 10 ml Exetainer gas testing vial (Labco, High Wycombe, UK). Glass inserts (200 µl, Chromacol, Welwyn Garden City, UK) containing platinum catalyst (platinum 5 % on alumina powder, -325 mesh, surface area > 250 $m^2.g^{-1}$, Sigma Aldrich, Gillingham, UK) were added to each vial, taking great care not to wet the catalyst. Exetainer vials were evacuated for one min, filled with reference gas (5 % hydrogen in helium, Air Products Special Gases, Crewe, UK) for 10 s as described in Section 2.1.2.1, and left to equilibrate at ambient temperature, for 48 h prior to analysis. During this time the deuterium in the vapour phase above the sample equilibrated with the hydrogen in the reference gas. The abundance of deuterium in the gas phase was measured by CF-IRMS (Prosser & Scrimgeour, 1995). The abundance of ^2H in samples was calculated with reference to the known abundance of reference waters, placed at intervals in each batch of samples, and drift corrected between references.

Results were expressed as ppm ^{2}H. The enrichment of reference waters was calculated by subtracting the measured abundance of the tap water (0 reference) from that of the samples. Results were expressed in units of ppm excess ^{2}H.

2.1.3.2 Calculation of abundance of ^{2}H and ^{18}O in water samples

A typical batch of samples had the following pattern:

5 reference gas tubes (to condition the system)

3 natural abundance reference waters (0 ppm excess $^{2}H/^{18}O$ = tap water used to make enriched reference waters)

3 enriched reference waters (75 ppm excess ^{2}H or 150 ppm excess ^{18}O)

2 reference gas tubes

18 sample waters (reference waters, urine or saliva)

2 reference gas tubes

3 natural abundance reference waters

3 enriched reference waters (75 ppm excess ^{2}H or 150 ppm excess ^{18}O)

2 reference gas tubes

18 sample waters (reference waters, urine or saliva) etc....

There were, therefore, 28 samples/standards between the first enriched reference water (1 of 3) and the next occurrence of the enriched references in the sample queue. The first sample is the 6^{th} tube in the queue, if the first enriched reference is number 1 (mid-point of the standards).

To take account of instrumental drift and fractionation during the equilibration period, the output from the 'Reprocessor' must be corrected by reference to the gradient of the two-point calibration curve and the known natural abundance of the 0 ppm excess reference water (150.7 ppm ^{2}H, 1986.4 ppm ^{18}O) to obtain the correct abundance in the sample. This was done, using a spreadsheet, by taking a proportion of gradient from the calibration curve preceding the samples and a proportion from the gradient from the calibration curve following the samples such that the total is 1. The proportion is related to the position of the sample relative to the reference waters in the analytical batch.

The gradient (G) of the 2-point calibration curve is the reported abundance of the enriched reference water minus the reported abundance of the natural abundance reference water, all divided by the actual enrichment of the enriched reference water. The actual enrichment of

the 75 ppm excess ^{2}H reference water was 73.64 ppm excess. The actual enrichment of the 150 ppm excess ^{18}O reference water was 179.78 ppm excess ^{18}O.

$$G = \frac{RA_{EREF} - RA_{0REF}}{E_{REF}} \tag{2.1}$$

where, RA_{EREF} = Reported abundance of ^{2}H or ^{18}O in the enriched reference water (ppm)

RA_{0REF} = Reported abundance of ^{2}H or ^{18}O in the natural abundance reference water (ppm)

E_{REF} = Actual enrichment of ^{2}H or ^{18}O in the enriched reference water (ppm excess)

If N is the number of vials in the repeating pattern (28 in the example above) and n is the number of the vial (sample 1 = 6 in the example above), the drift correction takes (N-n)/(N+1) times the gradient of the calibration curve preceding the group of samples (G_1) and n/(N+1) times the gradient of the calibration curve following the samples (G_2). The actual abundance (AA_{SAMP}, ppm) of ^{2}H or ^{18}O in each sample is calculated as follows,

$$AA_{SAMP} = \frac{\left(RA_{SAMP} - \left(\left(\frac{N-n}{N+1}\right)RA_{0REF1}\right) + \left(\left(\frac{n}{N+1}\right)RA_{0REF2}\right)\right)}{\left(\left(\frac{N-n}{N+1}\right)G_1\right) + \left(\left(\frac{n}{N+1}\right)G_2\right)} + AA_{REF} \tag{2.2}$$

where, RA_{SAMP} = Reported abundance of ^{2}H or ^{18}O in the sample (ppm)

RA_{0REF1} = Reported abundance of the natural abundance reference water preceding the samples (ppm)

RA_{0REF2} = Reported abundance of the natural abundance reference water following the samples (ppm)

G_1 = Gradient of the 2-point calibration curve preceding the samples

G_2 = Gradient of the 2-point calibration curve following the samples

AA_{REF} = Actual abundance of ^{2}H or ^{18}O in the natural abundance reference water (ppm)

Enrichment of ^{2}H or ^{18}O in the sample (ppm excess) is the actual abundance of ^{2}H or ^{18}O in the sample minus the actual abundance of ^{2}H or ^{18}O in the baseline sample.

2.1.3.4 Accuracy and precision of ^{2}H measurements

Accuracy of ^{2}H measurements was checked by preparing gravimetric standards containing 0, 15, 30, 75, 100, 150, 250, 300, 750, 1100, 1500 ppm excess ^{2}H and analysing them with reference to the working standards (0 and 75 ppm excess ^{2}H) as described above (Section 2.1.3.2) and plotting the calibration curve of measured versus calculated enrichment. Enrichment calculated from weight was taken as the independent variable and plotted on the *x*-axis.

Accuracy of ^{2}H measurements was ensured routinely by including standard waters (tap water plus an enriched standard) in triplicate at intervals in each batch of samples. These standards were prepared with the samples and treated in exactly the same way as the samples, as there is a large fractionation factor associated with preparation of samples by the equilibration method (Scrimgeour *et al.* 1993). When samples and standards are treated in exactly the same manner and held at the same temperature, the fractionation factor will be the same for both. The gradient and intercept (natural abundance of the 0 ppm excess reference water = tap water) of this two-point calibration curve were used to calculate the isotope abundance in each sample as described above (Section 2.1.3.3). The reported abundance was corrected for instrumental drift between references. Precision of ^{2}H measurements was checked by analysing groups of reference gases before each batch of samples and by calculating the standard deviation of three replicate analyses of the standard waters, which were included at intervals in each batch of samples.

2.2 Measuring CO_2 production rate

2.2.1 Study design

The aim of this study was to assess the feasibility of using heart rate monitors to estimate CO_2 production rate minute-by-minute during ^{13}C breath tests, and to determine the most suitable calibration procedure. A pilot study was carried out on two healthy, compliant adult volunteers using a [^{13}C]bicarbonate breath test. Sources of variation in $\dot{V}CO_2$ during ^{13}C breath tests were investigated. Heart rate and CO_2 production rate ($\dot{V}CO_2$) were measured simultaneously while resting and at varying levels of activity above resting. Potential methods of calibrating heart rate monitors to predict CO_2 production rate were investigated. The [^{13}C]bicarbonate breath test was performed under fasting, fed, resting and non-resting conditions. The test was repeated three times each under resting (sitting)

and non-resting conditions. $\dot{V}CO_2$ was measured at intervals during each bicarbonate breath test using a ventilated hood indirect calorimeter and heart rate monitors were worn throughout. PDR was calculated using predicted or measured resting $\dot{V}CO_2$, and also using $\dot{V}CO_2$ continuously estimated from heart rate using the best individual calibration method. Urinary loss of ^{13}C as [^{13}C]bicarbonate and [^{13}C]urea was measured during the fasting test.

2.2.2 Predicting and measuring basal/resting metabolic rate

Basal metabolic rate (BMR) is defined as the energy expenditure of a healthy subject lying at rest, in a thermally neutral environment, at least 12 h postprandially (Harris & Benedict, 1919). Resting metabolic rate is defined here as measurement of "basal" metabolism, where these conditions are not met, usually because the measurement took place 3-4 h after the last meal, rather than after an overnight fast.

2.2.2.1 Predicting resting $\dot{V}CO_2$

Resting $\dot{V}CO_2$ can be predicted from basal metabolic rate or from body surface area. The latter is most commonly used in ^{13}C breath tests.

Resting $\dot{V}CO_2$ was assumed to be constant at 300 mmol $CO_2.h^{-1}.m^{-2}$ body surface area (Shreeve *et al.* 1970), which equals 5 $mmol.min^{-1}.m^2$. Body surface area was calculated from height and weight using the Haycock *et al.* (1978) equation (Equation 2.3).

$$\text{Surface area } (m^2) = (\text{weight (kg)}^{0.5378}) \times (\text{height (cm)}^{0.3964}) \times 0.024265 \qquad (2.3)$$

$$\dot{V}CO_2 = 300 \times \text{body surface area mmol. } h^{-1} \qquad (2.4)$$

Basal metabolic rate (MJ/d) was predicted from age, gender, height and weight using the Schofield (1985) equations. Resting $\dot{V}CO_2$ was estimated from BMR by assuming a respiratory quotient, RQ of 0.85 (IDECG, 1990).

$$\dot{V}CO_2 \ (mmol.h^{-1}) = \frac{\text{BMR } (MJ.d^{-1}) \times 1000 \times 1000}{24 \times \text{EE } (kJ.L^{-1}) \times 22.414 \text{ (L)}} \qquad (2.5)$$

where, EE = Energy equivalent of CO_2 $(kJ.L^{-1}) = (15.48/0.85) \div 5.55 = 23.76$ (2.6)

and 22.414 L is the volume occupied by 1 mole of a gas at STP.

2.2.2.2 Measuring resting metabolic rate

Resting metabolic rate was measured after an overnight fast using an open circuit indirect calorimeter with a ventilated hood (GEM, Nutren Technologies, Manchester, UK) in a thermostatically temperature controlled environment at 22 °C. The subjects wore light clothing and measurements were made after 15 min acclimatisation lying on a bed. The flow rate, O_2 and CO_2 analysers were calibrated prior to every measurement using calibration gases (Zero gas: High Purity N_2, 99.999 %. Span gas: gravimetric mix composed of 20 % O_2, 1 % CO_2, balance N_2, Air Products Special Gases, Crewe, UK). The whole system was calibrated every 3 to 4 months by burning ethanol and adjusting the concentration of CO_2 entered in the manufacturer's software for the span gas in to give an RQ of 0.667. The repeatability specified by the manufacturer was 0.01 % absolute for O_2 and 0.02 % absolute for CO_2. The GEM ventilated hood indirect calorimeter has a large canopy attached to the hood, which enables measurements to be made in sitting and standing positions as well as lying on a bed. The flow rate through the hood can be optimised for each individual so that the fraction of CO_2 in expired air ($FeCO_2$) is between 0.6 and 0.7 %. This improves the accuracy of the CO_2 measurements without causing discomfort to the patient.

Oxygen consumption (VO_2) and carbon dioxide production rate (VCO_2) were calculated as follows,

$$VO_2 = (Vi \times FiO_2) - (Ve \times FeO_2) \quad (2.7)$$

$$VCO_2 = (Ve \times FeCO_2) - (Vi \times FiCO_2) \quad (2.8)$$

where: Fi~ indicates the fraction of gas in inspired air

Fe~ indicates the fraction of gas in expired air

and Vi and Ve are inspired and expired flow rates ($L.min^{-1}$).

The Haldane transformation assumes that nitrogen is not produced or consumed in the lungs and any difference in inspired and expired nitrogen must be due to differences in Ve compared to Vi.

$$Vi = Ve \times FeN_2 / FiN_2 \quad (2.9)$$

and

$$FeN_2 / FiN_2 = (1\text{-}FeO_2 - FeCO_2) / (1\text{-}FiO_2 - FiCO_2) \quad (2.10)$$

The Haldane transformation allows gas exchange calculations to be based on the measurement of expired flow only. Thus,

$$\dot{V}O_2 = \dot{V}e\left[\left\{\frac{1-FeO_2-FeCO_2}{1-FiO_2-FiCO_2}FiO_2\right\}-FeO_2\right] \quad (2.11)$$

and

$$\dot{V}CO_2 = \dot{V}e\left[FeCO_2-\left\{\frac{1-FeO_2-FeCO_2}{1-FiO_2-FiCO_2}FiO_2\right\}FiCO_2\right] \quad (2.12)$$

$$RQ = \dot{V}CO_2/\dot{V}O_2 \quad (2.13)$$

$\dot{V}CO_2$ (ml.min^{-1}) was converted to mmol.h^{-1} prior to PDR calculations and mmol.min^{-1}.m^2 body surface area for comparison with predicted values.

$$\dot{V}CO_2\ (mmol.h^{-1}) = \frac{\dot{V}CO_2\ (ml.min^{-1}) \times 60 \times 1000}{1000 \times 22.414} \quad (2.14)$$

where, 22.414 is the volume occupied by 1 mole of a gas at standard temperature and pressure (STP).

Resting heart rate (RHR) was measured simultaneously using a Polar Vantage NV heart rate monitor (Polar Electro Oy, Kempele, Finland). The time in both instruments was synchronised by downloading from the same PC. Data were averaged over one minute intervals and downloaded into a proprietary spreadsheet software (Initially, Lotus 1-2-3 Release 5 for Windows, then Microsoft Excel for Windows 95, version 7a, and finally Microsoft Excel 97 SR2).

2.2.3 Calibration of heart rate monitors

The heart rate calibration procedure was performed after breath sampling had ceased. Oxygen consumption ($\dot{V}O_2$), carbon dioxide production rate ($\dot{V}CO_2$) and heart rate (HR) were measured simultaneously, averaged over one minute intervals, with the subject lying supine on a bed for 10 min, sitting upright on the bed for 6 min and standing at the side of the bed for 6 min. Measurements were made with the subject sitting on a bicycle ergometer. The hood of the calorimeter was suspended from the ceiling and the cape tied around the subject's waist. The subject then began cycling at approximately 50 cycles per

min and 0 resistance. Every 5-6 min the resistance was elevated to increase the workload, until the subject's heart rate increased to approximately 150 beats per min. The aim was to maintain a constant heart rate for 3 min following an equilibration period at each level of work. The subject then lay on the bed and data were collected during the recovery period. Data collection ceased when CO_2 production rate returned to resting levels.

Data (averaged over one-min periods) were downloaded from the heart rate monitor and the indirect calorimeter to a personal computer and read into a proprietary spreadsheet software. Resting data collected earlier in the day were also included. Time data were matched to give simultaneous readings of both heart rate and $\dot{V}CO_2$. $\dot{V}CO_2$ ($mmol.min^{-1}.m^{-2}$) was plotted against heart rate with heart rate the independent variable plotted on the x-axis and $\dot{V}CO_2$ the dependent variable plotted on the y-axis unless otherwise stated. Two linear and four non-linear calibration methods were explored.

The most accurate calibration method has no bias i.e. the mean difference between measured and predicted $\dot{V}CO_2$ is zero. The standard error of this mean is a measure of the precision of the model. Analysis of the residuals i.e. the difference between the measured $\dot{V}CO_2$ at any time point and that predicted by the model allows these values to be quantified. A paired t-test was performed to assess the statistical significance of the bias using a standard statistical software package (Minitab for Windows, Release 11.2).

Effect of smoothing heart rate

Smoothing HR data can be used to account for the sluggish response of exhaled CO_2 to changes in heart rate, which may be due to the size and variability of the bicarbonate pool. Response time differences may, in addition, be due to difference in detector responses between the heart rate monitor and the indirect calorimeter, resulting in an apparent delay between HR rise and $\dot{V}CO_2$ rise, or it could be due to the fact that the output from the indirect calorimeter displays time in integer minutes, whereas the output from the heart rate monitors displays time to the nearest second. Smoothing brings the exercise and recovery data closer to the same line and allows all the calibration data to be included in the model. Several smoothing routines were explored, including averaging one or two points either side of the point of interest and averaging 2, 3 and 4 points forward of the point of interest. The former has no effect on the relative time of heart rate and $\dot{V}CO_2$ detection. The most appropriate smoothing routine was judged to be the one with coefficient of determination, R^2, closest to unity.

2.2.3.1 Linear methods

Linear-flex method (after Spurr *et al.* 1988)

The linear-flex method used resting $\dot{V}CO_2$ below a critical heart rate and a linear model above the critical value. The linear model was the regression line through the exercise data, but omitting the recovery data. The flex heart-rate was defined as the mean of the resting heart rate (lying/sitting) and the first non-resting heart rate (standing) during the calibration exercise. The critical value was taken as the flex heart rate plus 10.

Steady state (after Livingstone *et al.* 1992)

This method also used resting $\dot{V}CO_2$ below a flex point and a linear model above the flex point. Resting $\dot{V}CO_2$ was defined as the mean measured $\dot{V}CO_2$ for all the resting activities (lying, sitting and standing still). An equilibration period was allowed at each work level, followed by a 3-min sampling period. The mean of these three data points was plotted on a calibration curve of $\dot{V}CO_2$ versus heart rate. The flex point was defined as the mean of the highest heart rate for resting activities and the lowest heart rate on the bicycle ergometer. Above the flex point, $\dot{V}CO_2$ was calculated from the calibration curve.

2.2.3.2 Non-linear methods

Non-linear methods were performed on smoothed heart rate data, including both exercise and recovery phases and utilised the "Solver" function of Microsoft Excel (Walsh & Diamond, 1995). This uses the least squares method to determine the line of best fit through a data set, such that the root mean square (RMS) of the difference between the values predicted by the model and the measured values, is a minimum (Motulsky & Ransnas, 1987).

2nd and 3rd order polynomials

A second order polynomial or quadratic fit has the form,

$$\dot{V}CO_2 = a*HR^2 + b*HR \qquad (2.15)$$

A third order polynomial or cubic fit has the form,

$$\dot{V}CO_2 = a*HR^3 + b*HR^2 + c*HR \qquad (2.16)$$

where, a, b & c are constants determined by the model to minimise the root mean square.

Logistic model

The logistic model has the form,

$$VCO_2 = \left(\frac{a}{1+be^{-cHR}}\right)+d \tag{2.17}$$

where, a, b, c & d are constants determined by the model to minimise the root mean square.

Sigmoid Model

The sigmoid model had the form,

$$VCO_2 = \left(\frac{a}{1+e^{-(HR-b)/c}}\right)+d \tag{2.18}$$

where, a, b, c & d are constants determined by the model to minimise the root mean square and a is the amplitude, b is the centre, c is the width and d is the offset in Figure 2.1.

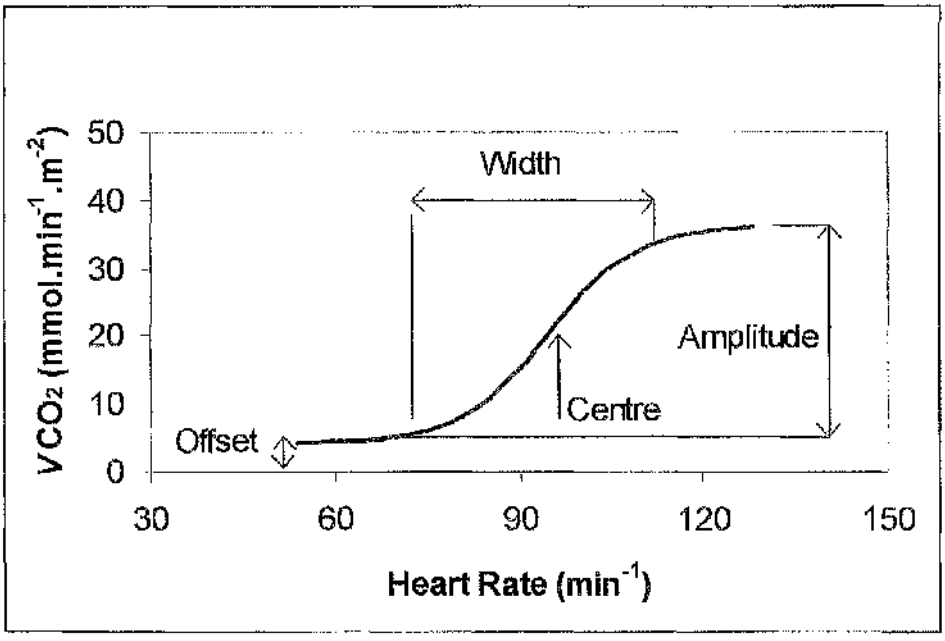

Figure 2.1 Schematic drawing of a sigmoid curve

The Solver options selected for logistic and sigmoid functions are shown in Table 2.2.

Table 2.2 Solver options for curve fitting using logistic and sigmoid models

Option	Value
Maximum time (s)	100
Iterations	100
Precision	0.000001
Tolerance (%)	0.001
Convergence	0.001
Use automatic scaling	✔
Assume non-negative	✔
Estimate	Quadratic
Derivative	Central
Search	Newton

2.2.3.4 Predicting $\dot{V}CO_2$ from $\dot{V}O_2$

The response of $\dot{V}CO_2$ to changes in heart rate may be sluggish due to the size of the bicarbonate pool, and the fact that this is both a source and a sink of CO_2. The body has no stores of molecular O_2, therefore the response to change in demand is virtually immediate. Thus, the calibration curve of $\dot{V}O_2$ versus heart rate should be more precise, than the calibration curve of $\dot{V}CO_2$ versus heart rate. $\dot{V}CO_2$ can be predicted from $\dot{V}O_2$ by assuming an RQ of 0.85 (IDECG, 1990). This approach was explored by plotting heart rate versus $\dot{V}O_2$ and fitting a sigmoid model using the method of least squares, as described above.

2.2.4 [^{13}C]bicarbonate breath tests

Bicarbonate breath tests were used to demonstrate the feasibility of using heart rate monitors to continuously measure $\dot{V}CO_2$ under fasting, fed, resting and non-resting conditions. $\dot{V}CO_2$ was measured at intervals during the test to establish the normal variability under fasting, fed, resting and non-resting conditions encountered during ^{13}C breath tests. PDR was calculated using a constant value of resting $\dot{V}CO_2$ predicted from body surface area (Section 2.2.2.1); a constant value of resting $\dot{V}CO_2$ predicted from basal metabolic rate estimated using the Schofield (1985) equations (Section 2.2.2.1); a constant value of measured resting $\dot{V}CO_2$ (Section 2.2.2.2); and minute-by-minute estimates of $\dot{V}CO_2$ predicted from heart rate (Section 2.2.2.3). Tests were repeated on several occasions

at different levels of physical activity. Urinary loss of tracer as [^{13}C]bicarbonate and [^{13}C]urea were measured.

2.2.4.1 Procedure for [^{13}C]bicarbonate breath tests

Studies were undertaken after an overnight fast. Each subject's body weight was measured to the nearest 0.1 kg using Seca scales (model 707, Seca Ltd., Birmingham, UK), which were calibrated annually. Body height was measured to 0.1 cm using a Holtain stadiometer (Holtain, Crymych, Dyfed, UK). Basal metabolic rate was measured using a ventilated hood indirect calorimeter as described in Section 2.2.2.2. The subjects consumed a cereal-based test meal, which was standardised for each subject. At the end of the test meal sodium [^{13}C]bicarbonate (0.5 mg.kg^{-1} body weight, 99 atom % ^{13}C, Isotech, CK Gas Products, Wokingham, UK) was consumed in ~50 ml semi-skimmed milk (1.8 % fat).

Alveolar breath was sampled by exhalation into an Exetainer breath-sampling vial (Labco, High Wycombe, UK) through a straw until condensation appeared on the side of the vial. The cap was replaced immediately. Breath was sampled at baseline and then every min for the first 15 min, at 20 min, then every 10 min to 1 h post dose. Breath sampling continued every 20 min for 6 h. Breath $^{13}CO_2$ abundance was measured by CF-IRMS as previously described. The subjects wore a heart rate monitor throughout the test. The bicarbonate breath test was repeated on several occasions as described below (Section 2.2.4.3) to determine the effect of fasting, sitting and walking during the test. On each occasion the subjects avoided food naturally enriched with ^{13}C for 3 d prior to the test.

$\dot{V}CO_2$ was measured using a ventilated hood indirect calorimeter as described in Section 2.2.2.2, in the fasting state (before consumption of the test meal), 1 h after the test meal, and 3 h after the test meal during each bicarbonate breath test.

2.2.4.2 Thermogenic effect of the meal

On one occasion, $\dot{V}CO_2$ and $\dot{V}O_2$ were measured for 2 h following the test meal. The thermogenic effect of the meal was taken as the mean $\dot{V}CO_2$ over the 2 h following the test meal divided by the basal rate.

2.2.4.3 Intra-subject variability of breath $^{13}CO_2$ recovery

[^{13}C]bicarbonate breath tests were performed under three different conditions: fasting, resting (R); fed, sitting (S); fed with moderate activity: walking (W). The latter tests were repeated three times.

Fasting, resting PDR

On the fasting occasion, basal metabolic rate was measured, the subject remained lying on the bed and consumed the dose of sodium [^{13}C]bicarbonate dissolved in 50 ml semi-skimmed (1.8 % fat) milk. Breath was sampled as described above and the subjects consumed only water for the remainder of the time. They lay in a supine position, resting, but not sleeping for the whole breath sampling period (6 h). Urine was sampled before measurement of basal metabolic rate and for 36 h following the dose. The volume was measured at each void using a 1L-measuring cylinder. Samples (1 ml) for [^{13}C]bicarbonate analysis were pipetted immediately into a labelled Exetainer breath-sampling vial. A further sample (~20 ml) was transferred to a plastic universal bottle for analysis of [^{13}C]urea (Section 2.2.4.4).

Fed PDR

On the fed occasions, the subjects took the same breakfast each time. This was composed of unsweetened breakfast cereal with semi-skimmed (1.8 % fat) milk and a drink of unsweetened orange juice. A light lunch composed of low ^{13}C foods was taken after 4 h. This meal was the same during each bicarbonate breath test. The subjects sat in an upright position during the test and moved around as little as possible.

Walking PDR

During this test, the subjects walked in the vicinity of the hospital for 1 h following consumption of the dose, otherwise the test was as described for the fed procedure. On one occasion, urine was sampled before measurement of basal metabolic rate and for 36 h following the dose as described above.

2.2.4.4 Calculation of percentage dose recovered (PDR) in breath

The enrichment of $^{13}CO_2$ in post-dose breath samples was calculated by subtracting the abundance of $^{13}CO_2$ in the baseline sample from that of the post-dose samples. Percentage dose recovered (PDR) in each sample was calculated from CO_2 production rate ($\dot{V}CO_2$) and breath CO_2 enrichment as follows:

$$\text{PDR } h^{-1} = \frac{V\!CO_2 \text{ (mmol.h}^{-1}\text{) x breath } CO_2 \text{ enrichment (ppm } ^{13}C \text{ excess) x 100}}{\text{mmol excess } ^{13}C \text{ in dose x } 10^6} \quad (2.19)$$

where, $V\!CO_2$ (mmol.h^{-1}) = $V\!CO_2$ (ml.min^{-1}) x 60 / 22.414 (2.20)

22.414 L is the volume occupied by 1 mole of a gas at STP

and mmol excess ^{13}C in dose = tracer dose (mmol) x tracer atom fraction excess ^{13}C

tracer dose (mmol) = weight substrate (mg) / molecular weight substrate

atom fraction excess ^{13}C = abundance ^{13}C in substrate – natural abundance ^{13}C

usually = (99-1.11)/100 = 0.979

The cumulative per cent dose recovered (cPDR) is calculated by summing individual PDR values averaged over the time interval between samples.

For example, cPDR at time 2 (t_2) = $cPDR_{t1}$ + ((PDR_{t1} + PDR_{t2})/2 x (t_2-t_1)) (2.21)

$cPDR_{t1}$ is cumulative PDR (%) at time1 (t_1 h post dose)

PDR_{t1} is PDR h^{-1} at time 1 (t_1 h post dose)

PDR_{t2} is PDR h^{-1} at time 2 (t_2 h post dose)

The cumulative percentage dose recovered (cPDR) was calculated using a constant value of resting $V\!CO_2$ predicted from body surface area (Section 2.2.2.1); a constant value of resting $V\!CO_2$ predicted from basal metabolic rate estimated using the Schofield equations (Section 2.2.2.1); a constant value of measured resting $V\!CO_2$ (Section 2.2.2.2); and minute-by-minute estimates of $V\!CO_2$ predicted from heart rate (Section 2.2.2.3). For the purposes of this test, physical activity level (PAL) was defined as cPDR calculated using $V\!CO_2$ estimated from heart rate divided by cPDR calculated using $V\!CO_2$ predicted from surface area (Haycock *et al.* 1978; Shreeve *et al.* 1970). This definition is mathematically equivalent to $V\!CO_2$ estimated from heart rate divided by resting $V\!CO_2$ predicted from surface area.

2.2.4.5 Urinary loss of ^{13}C as [^{13}C]bicarbonate and [^{13}C]urea following a bicarbonate breath test

[^{13}C]bicarbonate could be excreted in the urine in the form of unchanged tracer and also in the form of [^{13}C]urea, via the urea cycle. The tracer would be expected to appear as urinary bicarbonate in the first few hours following the dose, but later it would be in the form of [^{13}C]urea.

Urine was sampled at baseline and for 36 h on two occasions: during one of the bicarbonate breath tests with moderate activity and during the fasting, resting test. The volume was measured at each void using a 1 L-measuring cylinder. Aliquots (1 ml in duplicate) for [^{13}C]bicarbonate analysis were pipetted immediately into labelled 10 ml Exetainer breath sampling vials. The volume of these vials is 12 ml, but when evacuated, they have a 10 ml draw. A further aliquot (~20 ml) was transferred to a plastic universal bottle for subsequent analysis of [^{13}C]urea. The remainder of the void was discarded.

[^{13}C]bicarbonate in urine samples taken before and for 12 h following consumption of the dose was quantified by adding 100 µl 3M HCl to the Exetainer immediately prior to analysis. Acidification of the sample releases CO_2 from urinary bicarbonate into the headspace. The $^{13}CO_2$ abundance and CO_2 concentration (%) was analysed by CF-IRMS in the same manner as a breath sample (Section 2.1.2). The enrichment above baseline of each sample was calculated (ppm excess ^{13}C). PDR was calculated as the product of the mean ^{13}C enrichment and the mean amount of carbon in the sample as follows:

$$PDR = \left(\frac{CO_2 \times E \times T_{VOL}}{22.414 \times D \times P_{VOL}} \right) \qquad (2.22)$$

where, CO_2 = mean measured CO_2 volume of the sample (1l/1000 x % CO_2 /100) (L)

E = mean measured enrichment of the sample (atom % excess)

T_{VOL} = total urine volume voided at that time point (L)

22.414 = volume of 1 mole of gas at standard temperature and pressure

D = amount ^{13}C administered (mol)

P_{VOL} = volume urine in Exetainer (L)

The cumulative PDR was calculated by summing the PDR of each sample over the collection period.

[^{13}C]urea in urine samples taken before and for 36 h following the test meal was analysed as described by Morrison *et al.* (1999). Urine (50 µl) was pipetted, in triplicate, into individual Exetainers. The gas phase in each Exetainer was removed using the vacuum manifold described in section 2.1.2.1. The Exetainers were isolated and the manifold flushed with pure nitrogen at a flow rate of 100 ml.min^{-1}, for 5 min. Each Exetainer was opened to the nitrogen stream for 10 s. Type VI jack bean urease (EC 3.5.1.5) (Sigma-Aldrich, Poole, UK) was dissolved in 0.05 M phosphate buffer at pH 7 and flushed with nitrogen. The activity of the reagent was 1 unit of urease activity per ml buffer. One unit

should liberate 0.5 μmole CO_2 from urea per min at pH 7 and 25 °C. Enzyme solution (1 ml) was injected into each Exetainer. The Exetainers were incubated at 37 °C in a shaking water bath for 2 h. The reaction was halted and CO_2 released into the headspace by adding 100 μl 3M HCl (Equation 2.23). CO_2 concentration and $^{13}CO_2$ abundance in the gas phase were analysed by CF-IRMS as previously described (Section 2.1.2). The amount of carbon, in each sample was calculated from the percentage CO_2 produced by enzyme hydrolysis.

$$^{13}CO(NH_2)_2 + H_2O \xrightarrow{pH<2} {}^{13}CO_2 + NH_4^+ \qquad (2.23)$$

The enrichment above baseline of each sample was calculated (ppm excess ^{13}C). PDR was calculated as the product of the mean ^{13}C enrichment and the mean amount of carbon in the sample as above (Equation 2.22). The cumulative PDR was calculated by summing the PDR of each sample over the collection period.

2.3 Generic calibration of heart rate monitors

2.3.1 Study design

The aim of this study was to assess potential generic calibration methods to predict $\dot{V}CO_2$ from heart rate during ^{13}C-breath tests. $\dot{V}CO_2$ was normalised to various body parameters including, height^n, weight^n and surface area. Data from both subjects were combined and a sigmoid model fitted using the least squares method. PDR during the bicarbonate breath tests was calculated using $\dot{V}CO_2$ predicted from heart rate using the generic calibration method for comparison with individual calibration.

2.3.2 Generic calibration methods

Calibration data from both subjects were combined and the effect of scaling $\dot{V}CO_2$ to various body parameters was explored, using the sigmoid model. Normalisation methods included scaling to body surface area, weight, weight$^{3/4}$, height, height^2, height^3 and use of relative heart rate. In each case heart rate (HR) was smoothed relative to $\dot{V}CO_2$ (Section 2.2.3.2). The accuracy and precision of each model were compared as described below to determine the best normalisation method.

Relative heart rate (after Sneddon *et al,* 1985)

Use of relative heart rate should take account of differences in body size. Small children have a greater heart rate than teenagers and adults. Relative heart rate was defined as working heart rate (WHR) divided by resting heart rate (RHR), therefore $\dot{V}CO_2$ was plotted against relative heart rate and a linear regression line was drawn through the data with RHR>1. Above a relative heart rate flex point of 1.05, the linear regression line was used. Below this threshold, resting $\dot{V}CO_2$ (5 $mmol.min^{-1}.m^{-2}$) was used.

A second form of relative heart rate was explored. This was defined as working heart rate minus resting heart rate. $\dot{V}CO_2$ was plotted against heart rate above the resting value, and a linear regression line was plotted through the data with (WHR-RHR)>10. Below this flex point, resting $\dot{V}CO_2$ (5 $mmol.min^{-1}.m^{-2}$) was used, above it the model was used.

2.3.2.1 Accuracy and Precision

Accuracy was defined as the difference between the mean measured $\dot{V}CO_2$ and the mean value predicted from heart rate using the model. A negative value indicated that the model overestimated the true $\dot{V}CO_2$ and would therefore overestimate PDR. Accuracy was expressed as a percentage of the mean measured $\dot{V}CO_2$ so that $\dot{V}CO_2$ normalised to different body parameters could be compared. It was necessary to express the results in percentage terms as the units of $\dot{V}CO_2$ normalised to height^n, weight and surface area are different.

Precision was defined as the coefficient of variation (CV) i.e. the standard deviation (SD) expressed as a percent of the mean measured $\dot{V}CO_2$. Expressing precision as CV, rather than SD, allows comparison between methods with results expressed in different units.

2.4 Development of a test meal

2.4.1 Study design

A test meal was designed to carry both hydrophilic (sodium [1-^{13}C]acetate, sodium [$^{2}H_3$]acetate) and lipophilic ([1-^{13}C]octanoic acid, [$^{2}H_{15}$]octanoic acid, [^{13}C]MTG and [^{2}H]MTG) substrates. Deuterium labelled tracers must be given at ~10 times the dose of ^{13}C-labelled tracers, because of the large pool size of the oxidation product (body water) compared with the bicarbonate pool. The palatability of the test meal containing the expected doses was investigated using unlabelled materials. Experiments were performed *in vitro* to investigate retention of the labelled compound during preparation and within the solid phase of the test meal and to check that distribution of the tracer was homogeneous.

Errors in dosage were controlled by careful weighing to sufficient accuracy, ensuring homogeneous distribution within the test meal, taking account of losses during preparation and adjusting for incomplete consumption of the test meal. The natural ^{13}C abundance of the test meal was controlled by using low ^{13}C ingredients.

2.4.2 The test meal

The proposed test meal was a biscuit (flapjack) composed of 90 g rolled oats, 40 g butter and 40 g honey (weighed to within 1 g). These are all low ^{13}C ingredients (Morrison *et al.* 2000). The honey and butter were melted over a bain-marie. The tracer (weighed to 0.001 g) was stirred into the melted ingredients until dissolved and distributed evenly. The oats were added and the mixture and stirred thoroughly until all the liquid was absorbed. The mixture was spread over the bottom of an aluminium foil-lined tray (160 mm square, surface area 0.0256 m^2 or 170 mm diameter, surface area 0.0227 m^2), and baked at 130 °C for 15 min in a fan-assisted oven. The bowls, spoons, baking tray and foil were weighed before and after use, so that the tracer weight could be corrected for losses during preparation of the test meal.

The nutritional composition of the test meal was calculated from food composition tables (Holland *et al.* 1991). This recipe provides 3.13 MJ and is sufficient for two 75 kg adults or 3-4 children, depending on their age and size. Subjects were given a portion equivalent to 17 to 20 % of their daily energy requirements (Department of Health, 1991) together with a drink of unsweetened orange juice or water, as they preferred. The FQ (food

quotient) of the test meal was calculated from the energy contribution of each nutrient to the total metabolizable energy as follows:

$$FQ - ((p \times 0.81) + (f \times 0.71) + (c \times 1.00))/100 \quad (2.24)$$

Where, p, f and c are the amount of energy from protein, fat and carbohydrate in the test meal, expressed as a percentage of total metabolizable energy, and the constants are the classical values for the FQ of individual fuels (Lusk, 1928, as cited by Black *et al.* 1986).

The ^{13}C abundance of the test meal was calculated from the ^{13}C abundance of the individual ingredients (Morrison *et al.* 2000).

2.4.3 Palatability studies

The palatability of the test meal was investigated using unlabelled substrates at the doses used for ^{13}C-breath tests (~13 $\mu mol.kg^{-1}$ body weight) and also at the doses required for deuterium-labelled tracers (~130 $\mu mol.kg^{-1}$ body weight).

Unlabelled sodium acetate, octanoic acid and tripalmitin were purchased (Sigma-Aldrich, Poole, UK). Tripalmitin was substituted for MTG as unlabelled MTG was not available. Flapjacks were baked containing 150 mg sodium acetate; 300 mg octanoic acid; 300 mg sodium octanoate; 1.4 g tripalmitin, the amount required for two adult subjects in a ^{13}C-breath test. Flapjacks were also prepared containing 12 g unlabelled sodium acetate; 3.8 g sodium octanoate and 20 g tripalmitin, i.e. the amount required for ^{2}H-validation studies to enrich body water by 50 ppm excess ^{2}H. Octanoic acid was converted to sodium octanoate to disguise the unpleasant flavour of octanoic acid (Section 2.4.3.1). The amount of butter in the flapjack containing 20 g tripalmitin was reduced by this amount. Palatability was assessed by the investigators.

2.4.3.1 Conversion of octanoic acid to sodium octanoate

Octanoic acid at the dose required for ^{2}H validation has extremely poor palatability. Conversion of octanoic acid to its sodium salt reduces the unpleasant taste and smell. Octanoic acid was converted to its sodium salt by adding sodium bicarbonate.

$$CH_3(CH_2)_6COOH + NaHCO_3 = CH_3(CH_2)_6COONa + CO_2 + H_2O \quad (2.25)$$

1 mol octanoic acid requires 1 mol sodium bicarbonate to make 1 mol sodium octanoate. MW ^{12}C-octanoic acid = 144, MW sodium bicarbonate = 84. Therefore, 0.583 g sodium bicarbonate is required to neutralise 1 g octanoic acid.

Density of octanoic acid = 0.9 mg.ml^{-1}. Therefore, 3.78 g = 4.22 ml.

Water, 1 ml g^{-1} octanoic acid (3.78 ml) was pipetted into a bowl. 4.22 ml octanoic acid and 2.20 g sodium bicarbonate were added and mixed together by gently swirling the bowl. The reaction to form sodium octanoate was obvious. The honey and butter were added and the flapjack made as before.

The molecular weight and density of [$^{2}H_{15}$]octanoic acid are higher than unlabelled octanoic acid therefore the relative amounts of octanoic acid and sodium bicarbonate must be adjusted when labelled substrates are used (section 2.7.3).

MW [1-^{13}C]octanoic acid = 145 , density = 0.9 mg.ml^{-1}
MW [$^{2}H_{15}$]octanoic acid = 169, density = 1 mg.ml^{-1}
280 mg [1-^{13}C]octanoic acid = 310 µl required 0.28 x (84/145) g bicarbonate = 0.162 g
3.5 g [$^{2}H_{15}$]octanoate = 3.5 ml required 3.3 x (84/169) g bicarbonate = 1.75 g, total 1.912 g

2.4.4 In vitro experiments

Experiments were performed *in vitro* to check that the hydrophilic tracers ([1-^{13}C]acetate, [1-^{13}C]octanoate, sodium salts) and the lipophilic tracers ([1-^{13}C]octanoic acid and [^{13}C]MTG) remained in the biscuit during preparation and to investigate partitioning of the tracer between solid and liquid phases in the acid conditions of the stomach.

A flapjack was prepared containing unlabelled sodium acetate and unlabelled sodium octanoate at the dose used for ^{13}C-breath tests (150 mg CH_3COONa = 0.9 mg.g^{-1} flapjack, cooked weight and 300 mg $CH_3(CH_2)_6COONa$ = 1.9 mg.g^{-1} flapjack). A second flapjack was prepared containing unlabelled acetate at the dose used for ^{2}H-validation studies (12 g CH_3COONa = 70 mg.g^{-1} flapjack). A flapjack was also prepared with no added acetate or octanoate to serve as a control.

2.4.4.1 Analysis of flapjack acetate and octanoate

A weighed portion of flapjack (~20 g) was broken into small pieces and mixed by vigorous swirling with 100 ml 9 $g.L^{-1}$ NaCl in 0.1M HCl, to represent the conditions in the normal acid stomach, in a wide-neck screw cap bottle. The bottle was swirled at intervals for the first 20 min and allowed to settle before sampling. The pH of the supernatant was checked using pH range 1-4 paper. Aliquots (10 ml) were transferred to a plastic universal bottle after 20, 60 and 120 min. These were centrifuged at 1000 *g* (where *g* is the acceleration due to gravity) for 5 min. A volume equivalent to 1 μmole acetate at 100 % release into the aqueous phase was transferred to a 2 ml glass vial (465 μl from the normal dose flapjack and 6 μl from the high dose flapjack). Internal standard (458 nmole 3-methyl valerate = 20 μl 22.875 mM solution in 0.3 M NaOH) was added with enough 1 M NaOH to make the solution alkaline. Working standards were prepared containing 458 nmole 3-methyl valerate and 1 μmole sodium acetate and 2 μmole sodium octanoate. The vials were dried in an oven at 55 °C overnight. The procedure was repeated four times at acid pH (1.5), once using deionised water (pH 6.5) and once using 0.1 M NaOH (pH ~13) to investigate the yield in non-acid conditions. On the day of analysis, 100 μL 3M HCl and 1 ml diethyl ether were added to the vial, which was shaken by vortex mixing. The free acids were thus extracted into the upper ether layer.

The volatile fatty acids were quantified by capillary gas chromatography (GC) using a ZB FFAP megabore column, ID 0.53 mm, length 30 m, film thickness 1 μm (Phenomenex, Macclesfield, UK). The carrier gas was helium set at a flow rate of 7.5 $ml.min^{-1}$ at ambient temperature. The injection volume was 1 μl. The GC temperature program was 80 °C for 3 min, 80-210 °C at 10 °C min^{-1}, hold for 2 min. The injector and detector temperatures were 230 °C.

2.5 Investigation of [^{13}C]MTG metabolism

2.5.1 Study design

Once accurate methods had been established to quantify tracer exhalation in breath and minor losses via other routes, mass balance could be used to estimate the quantity of tracer retained within the body. A series of experiments was undertaken in two compliant healthy subjects to investigate the assumptions associated with the [^{13}C]MTG breath test under fasting, fed, resting and non-resting conditions using [^{13}C]MTG and its metabolites, [1-^{13}C]octanoate, [1-^{13}C]acetate and [^{13}C]bicarbonate. Molar equivalent amounts of [^{13}C]MTG, [^{13}C]octanoate and [1-^{13}C]acetate were baked in the test meal described above, but [^{13}C]bicarbonate was dissolved in a small volume of milk and taken at the end of a cereal based test meal, or without the meal to study the effect of fasting during the test. [1-^{13}C]acetate was also taken in a similar manner to study the effect of fasting, feeding and composition of the test meal on ^{13}C recovery in breath CO_2. Repeatability of the MTG, acetate and bicarbonate tests was measured under ideal conditions i.e. with the subjects sitting throughout the test and wearing heart-rate monitors. The feasibility of performing acetate and MTG tests on the same day was also explored.

Doses of [^{13}C]MTG, [1-^{13}C]octanoic acid and [1-^{13}C]acetate were equivalent, when expressed in moles of substrate per unit body weight (Table 2.3).

Table 2.3 Molar equivalence of tracer doses for ^{13}C breath tests

Tracer	Molecular weight	Dose mg.kg^{-1} body weight	Dose μmol.kg^{-1}
[^{13}C]bicarbonate, Na salt	85	0.5	6
1-[^{13}C]acetate, Na salt	83	1	13
1-[^{13}C]octanoic acid	145	2	13
[^{13}C]MTG	752	10	13

Subjects consumed a diet composed of low ^{13}C foods for three days before each test. Baseline variation of breath ^{13}C abundance was measured under fasting and fed conditions. Subjects wore heart rate monitors during the tests, so that VCO_2 could be predicted continuously from the equations determined in Section 2.2. The effect of the test meal on PDR in the [1-^{13}C]acetate breath test was investigated. The effect of fasting and feeding during the [1-^{13}C]acetate breath test, and the effect of physical activity during the

[^{13}C]MTG breath test were determined. In all tests PDR was calculated using a constant value of resting $V\!CO_2$ predicted from body surface area; a constant value of resting $V\!CO_2$ predicted from basal metabolic rate using the Schofield (1985) equations; a constant value of resting $V\!CO_2$ measured using a ventilated hood indirect calorimeter; and continuously measured $V\!CO_2$ estimated from heart rate using the individual's own calibration. The cPDR values were compared and the physical activity level (PAL) calculated from PDR estimated continuously from heart rate divided by PDR estimated using a constant measured value of resting $V\!CO_2$.

2.5.2 Variation of baseline ^{13}C abundance

Accuracy of breath ^{13}C enrichment measurements depends on constant background ^{13}C abundance as well as accurate isotope abundance measurements. A constant and low ^{13}C background is more important when cPDR (area under curve) is the calculated end-point, rather than for kinetic studies, such as gastric emptying (Maes *et al.* 1998) where the measured end-point is related to rate of ^{13}C appearance. Variation of baseline ^{13}C abundance was studied on two occasions, one fasting and one fed, after three days on a diet low in ^{13}C (Morrison *et al.* 2000). Breath was collected by blowing into an Exetainer breath sampling vial (Labco, High Wycombe, UK) through a straw until condensation appeared on the side of the vial. The cap was replaced immediately. Breath was sampled every 30 min for 8 h and the ^{13}C abundance was measured by CF-IRMS as previously described. The subjects wore a heart rate monitor throughout the test.

On the fasting occasion, subjects stayed in bed for 8 h, drank 50 ml semi-skimmed (1.8 % fat) milk instead of breakfast and consumed only water for the remainder of the time. The milk was taken to make this test comparable with the fasting acetate (Section 2.5.3) and bicarbonate (Section 2.2.4.3) breath tests, where it was used to dissolve the tracer dose. Subjects read or listened to the radio for entertainment, but did not sleep.

On the fed occasion, the subjects took breakfast composed of unsweetened breakfast cereal with semi-skimmed (1.8 % fat) milk and a drink of unsweetened orange juice. A light lunch composed of low ^{13}C foods was taken after 4 h. This meal was the same during each ^{13}C-breath test. The subjects remained seated during the test and moved around as little as possible.

2.5.3 Effect of food intake and test meal on cPDR

To study the effect of food intake and composition of the test meal on cPDR, ^{13}C-acetate breath tests (1 mg.kg^{-1} body weight [1-^{13}C]acetate (sodium salt), 99 atom %, Cambridge Isotope Laboratories, Inc., Andover, MA, USA) were performed under fasting and fed conditions. In the fasting test, subjects took the dose in 50 ml semi-skimmed milk (1.8 % fat) and lay on a bed for 10 h. They consumed only water for the remainder of the time. Subjects listened to the radio for entertainment, but did not sleep. Fed tests compared consumption of labelled acetate dissolved in 50 ml semi-skimmed milk, following the same standard breakfast as the bicarbonate breath tests, and baked in a flapjack (Section 2.2.2). When the tracer was taken in milk, breath was sampled at baseline and at the same intervals as the bicarbonate breath test. When the tracer was taken in a flapjack, breath was sampled at baseline, every 10 min for the first hour, followed by every 20 min for 6 h and then every 30 min for a further 4 h. Subjects remained seated in an upright position during the fed tests and moved around as little as possible. A light lunch composed of low ^{13}C foods was taken approximately 4 h after consumption of the test meal. Basal metabolic rate was measured as described in Section 2.2.2.2, and subjects wore a calibrated heart rate monitor throughout the test. The cPDR was calculated as described in Section 2.2.4.4.

2.5.4 Effect of physical activity during the [^{13}C]MTG breath test

To investigate the effect of physical activity during the [^{13}C]MTG breath test, tests were performed at rest and under non-resting conditions. The resting test was performed in a similar manner to the fed acetate test described above (Section 2.5.3). [^{13}C]MTG (1,3-distearyl, 2[carboxyl-^{13}C]octanoyl glycerol, 99 atom % ^{13}C, Cambridge Isotope Laboratories, Inc. Andover, MA, USA), 10 mg.kg^{-1} body weight (~1.4 g per flapjack) was baked in a flapjack (Section 2.2.2). Breath was sampled at baseline, every 20 min for 6 h and then every 30 min for a further 4 h, 10 h in total. A light lunch composed of low ^{13}C foods was taken 4 h after ingestion of the test meal. Basal metabolic rate was measured as described in Section 2.2.2.2. The cPDR was calculated as described in Section 2.2.4.4.

During the non-resting test, the subjects walked, mainly on the flat for a distance of approximately 19 km (12 miles) at ~3.2 km h^{-1} (2 miles h^{-1}) following ingestion of the test meal. A picnic lunch composed of low ^{13}C foods was taken approximately 4 h after ingestion of the test meal. cPDR was calculated as above using the measured resting VCO_2 from the resting test.

2.6 Intra-individual variation in the MTG test

2.6.1 Study design

The aim of this study was to measure intra-individual variation of the cPDR in the [^{13}C]MTG and [1-^{13}C]acetate breath tests in two healthy adult subjects wearing calibrated heart rate monitors. Each test was performed three times with the subjects sitting upright during the test. Use of an acetate correction, as a mathematical means of compensating for lack of knowledge of CO_2 production rate during the [^{13}C]MTG breath test, was investigated. The feasibility of performing simultaneous MTG and acetate breath tests on the same day was also investigated.

2.6.2 Intra-individual variation

[^{13}C]MTG and [1-^{13}C]acetate breath test were performed three times as described in Sections 2.5.4 and 2.5.3. Subjects sat quietly during the tests in an upright position and moved around as little as possible. The cPDR was calculated as described in Section 2.2.4.4.

2.6.3 Use of acetate and bicarbonate correction factors

Acetate and bicarbonate corrections can account for tracer retained in the body during ^{13}C-breath tests (Section 1.4.9). Acetate and bicarbonate corrections were applied to the 6 h MTG breath PDR (MTG PDR_{6h}).

$$\text{PDR with bicarbonate correction} = \text{MTG } PDR_{6h} / \text{ Bicarbonate } PDR_{6h} \times 100 \quad (2.26)$$

$$\text{PDR with acetate correction} = \text{MTG } PDR_{6h} / \text{ Acetate } PDR_{6h} \times 100 \quad (2.27)$$

2.6.4 MTG and acetate breath tests on the same day

If acetate correction factors proved to be a useful tool, it would be necessary to perform both tests on the same day. The feasibility of doing this was investigated in two healthy adult volunteers. Subjects consumed two test meals. The first was a flapjack containing 10 mg.kg^{-1} body weight [^{13}C]MTG (section 2.4.2) and washed down with unsweetened orange juice. This was taken instead of breakfast. The second test meal was taken 4 h later. This was another flapjack containing 1 mg.kg^{-1} body weight [1-^{13}C]acetate, which

was also taken with a drink of unsweetened orange juice. Breath was sampled at baseline and then every 20 min for 10 h. Water was taken *ad libitum* during the test. PDR h^{-1} was calculated using a constant value of VCO_2 predicted from body surface area (Section 2.2.2.1). Fitting two Maes models (Morrison 2000) deconvoluted the curves. Thus, the area under the acetate curve (cPDR) and the area under the MTG curve could be calculated.

2.7 Deuterium-labelled MTG test

2.7.1 Study design

The aim of this study was to investigate the use of deuterium labelled MTG as a simpler alternative to the ^{13}C-breath test and to validate improvements to the [^{13}C]MTG breath test. Use of deuterium labelled tracers avoids the need to know VCO_2 during the test, if an accurate estimate of the volume of distribution of the product of oxidation, ^2H_2O, i.e. total body water, is available. Deuterium labelled MTG could offer a simpler alternative to the ^{13}C-breath test and can be used to validate improvements to the [^{13}C]MTG breath test. Use of [^2H]MTG was investigated in two healthy adults. [^{13}C] and [^2H]MTG were taken in the same test meal. Breath, saliva and urine were sampled. The volume of distribution of ^2H (total body water) was measured by ^{18}O-dilution and basal metabolic rate was measured prior to consumption of the test meal. Heart rate monitors were worn, so that VCO_2 would be estimated continuously during the test from the subjects' own individual calibration curve. On separate occasions, [^{13}C]/[^2H]octanoate and [^{13}C]/[^2H]acetate tests were performed as above. Urinary losses of [$^2H_3$]acetate were also measured during the dual tracer acetate test. The cumulative percentage dose recovered (cPDR) in urine or saliva was compared with the cPDR from the [^{13}C]MTG or [1-^{13}C]octanoate test with an acetate correction applied. Deuterium labelled MTG is not available commercially, but 20 g [^2H]MTG was kindly donated by Cambridge Isotope Laboratories, Andover, USA.

2.7.2 [^2H]MTG-test

[^2H]MTG (20 g or 140 $mg.kg^{-1}$ body weight) and [^{13}C]MTG (1.4 g or 10 $mg.kg^{-1}$ body weight) were baked in the same flapjack (Section 2.4.3). The amount of butter was reduced by 20 g to compensate for the large amount of lipid added as [^2H]MTG. The [^2H]MTG (1,3-distearyl, 2[$^2H_{15}$]octanoyl glycerol, 97 atom % ^2H) was custom synthesised by Cambridge Isotope Laboratories, Inc. Andover, MA, USA.

Saliva was sampled every 20 min for 6 h and then every 30 min for a further 4 h, starting 10 min after ingestion of the test meal, so that breath and saliva sampling times were offset. Urine was sampled at 2 hourly intervals during the breath test. The dose of $H_2{}^{18}O$ (0.5 $g.kg^{-1}$ body weight) was taken after the end of breath sampling and samples of saliva and urine were collected at the same time on the following nine days. Urine and saliva samples were stored in plastic universal bottles at –20 °C prior to analysis.

The amount of deuterium entering the body water pool was analysed by CF-IRMS after equilibration with 5 % H_2 in He, and the PDR in body water was calculated as described in section 2.7.2.1. Total body water was measured by ^{18}O-dilution as described in Section 2.7.2.2.

PDR ^2H in body water was compared with $cPDR_{10h}$ [^{13}C]MTG with acetate and bicarbonate correction factors (Sections 2.6.2 and 2.6.3).

2.7.2.1 Measurement of ^2H in body fluids

Deuterium-labelled fatty acids and MTG were used in validation studies (Sections 2.7.2, 2.7.3 and 2.7.4). The deuterium is distributed through the body water pool following absorption and oxidation of the fatty acid. Enrichment of ^2H in body water can be measured by CF-IRMS. Samples and reference waters were prepared according to the method of Scrimgeour *et al.* (1993). Urine and saliva samples were thawed completely, shaken, and centrifuged at 1000 *g* for 5 min to ensure that any condensate is mixed into the sample, as this is fractionated relative to the urine or saliva. The sample (400 µl) was pipetted into 10 ml Exetainer gas testing vials (Labco, High Wycombe, UK). Glass inserts (200 µl, Chromacol, Welwyn Garden City, UK) containing platinum catalyst (platinum 5 % on alumina powder, -325 mesh, surface area > 250 $m^2.g^{-1}$, Sigma Aldrich, Gillingham, UK) were added to each vial, taking great care not to wet the catalyst. Reference waters (0 and 75 ppm excess ^2H) were prepared and analysed with each batch as described in Section 2.1.3.2. Exetainer vials were placed on a twenty-tube manifold and were evacuated for 1 min. The manifold was brought to atmospheric pressure prior to flushing with reference gas for 5 min. Samples and reference waters were filled with reference gas (5 % hydrogen in helium, Air Products Special Gases, Crewe, UK) for 10 s. These were left to equilibrate with the head-space gas, at ambient temperature, for a minimum of 48 h prior to analysis. During this time the deuterium in the vapour phase above the sample equilibrated with the hydrogen in the reference gas. The abundance of deuterium in the gas phase was measured

by CF-IRMS as described in Section 2.1.3. The abundance of ^{2}H in samples was calculated with reference to the known abundance of the reference waters. Results were expressed as ppm ^{2}H. The enrichment of the post-dose samples was calculated by subtracting the abundance of the baseline sample from that of the post-dose samples and expressed in units of ppm excess ^{2}H.

Percentage dose recovered in body water was calculated from the ^{2}H enrichment at time 0 and the TBW (kg) measured by ^{18}O-dilution (Section 2.7.2.2). ^{2}H enrichment at time 0 is the *y*-intercept of the elimination rate curve of the natural logarithm of body water enrichment versus time, where time (t) was the independent variable plotted on the *x*-axis and ^{2}H enrichment (ppm excess) was the dependent variable plotted on the *y*-axis.

$$PDR = E_{t0} \text{ (mmol excess } ^{2}H) / D \text{ (mmol excess } ^{2}H_2O \text{ equivalent)} \times 100 \qquad (2.28)$$

where, E_{t0} = enrichment of body water at time 0, mmol excess ^{2}H

= TBW (mmol) x ^{2}H enrichment at t0 (ppm excess) x 1.04 / 10^{6}

1.04 = ^{2}H non-aqueous exchange factor (Schoeller & Jones, 1987)

D = ^{2}H dose, mmol excess $^{2}H_2O$ equivalent

= number ^{2}H atoms in substrate / 2 x mmol excess ^{2}H in dose

mmol excess ^{2}H in dose = tracer dose (mmol) x tracer atom fraction excess ^{2}H

tracer dose (mmol) = weight substrate (mg) / molecular weight substrate

tracer atom fraction excess ^{2}H = abundance ^{2}H in sustrate – natural abundance ^{2}H

for ^{2}H-compounds this is usually (99.8-0.015) / 100 = 0.998

2.7.2.2 Measurement of total body water by ^{18}O dilution in body water

Total body water was measured by ^{18}O dilution in body water (Schoeller *et al.* 1980) to find the volume of distribution of the deuterium labelled tracer, when the test meal contained both ^{13}C- and ^{2}H-labelled tracer. The weighed dose of $H_2{}^{18}O$ (0.5 $g.kg^{-1}$ body weight) ($H_2{}^{18}O$, 10 atom % ^{18}O, normalised for deuterium concentration, CK Gas Products, Wokingham, UK) was taken after completion of breath sampling as breath CO_2 would became enriched with ^{18}O, leading to an error in ^{13}C measurement due to the Craig correction (Section 2.1.2.2), which could not be cancelled in the software used. An aliquot (2 ml) of the stock $H_2{}^{18}O$ was retained for analysis as a 1:500 dilution in tap water. A sample of the tap water was also retained. Baseline samples of saliva and urine were taken before consumption of the ^{18}O-water. Samples were collected at the same time on the

following 10 days, noting the time of each sample and avoiding the early morning urine sample. The ^{18}O abundance in body water (saliva or urine) was measured by CF-IRMS with reference to gravimetric standards (0 and 150 ppm excess ^{18}O, Section 2.1.2.3).

Samples and reference waters were prepared for ^{18}O analysis according to the method of Prosser *et al.* 1991. Urine and saliva samples were thawed completely, shaken, and centrifuged at 1000 *g* for 5 min. The sample (400 µl) was pipetted into 10 ml Exetainer gas testing vials (Labco, High Wycombe, UK). Vials were evacuated for one min and filled with 3 % CO_2 in N_2 (Air Products Special Gases, Crewe). Reference waters (0 and 150 ppm excess ^{18}O) were prepared and analysed with each batch. Samples and reference waters were left to equilibrate with the headspace gas for 24 h at ambient temperature. During this time the ^{18}O in the water phase equilibrated with the CO_2 in the gas phase. The abundance of ^{18}O in the gas phase was measured by CF-IRMS, monitoring *m/z* 44 and 46 (Section 2.1.2). The abundance of samples was calculated with reference to the known abundance of the reference waters and drift corrected between references. Results were expressed as ppm ^{18}O. The enrichment of the post-dose samples was calculated by subtracting the abundance of the baseline sample from that of the post-dose samples and expressed in units of ppm excess ^{18}O.

Total body water was calculated from the *y*-intercept of the decay curve of the natural logarithm of body water enrichment versus time, where time (t) was the independent variable plotted on the *x*-axis and ^{18}O enrichment (ppm excess) was the dependent variable plotted on the *y*-axis using the diluted dose method as follows:

$$TBW\ (mol) = WT_{DD}\ (g) / W^{18}O_{DD}\ (g) \times D\ (g) \times E_{DD} / E^{18}O_{t0} \times 18.0153 / 1.01 \quad (2.29)$$

where,

WT_{DD}	=	weight (g) tapwater in the dose dilution
$W^{18}O_{DD}$	=	weight (g) ^{18}O-water in the dose dilution
D	=	weight (g) ^{18}O-water consumed
E_{DD}	=	enrichment of ^{18}O in the dose dilution (ppm excess ^{18}O)
$E^{18}O_{t0}$	=	enrichment of ^{18}O at time 0 (ppm excess ^{18}O)
18.0153	=	molecular weight water
1.01	=	^{18}O non-aqueous exchange factor (Schoeller & Jones, 1987)

$$TBW\ (kg) = TBW\ (mol) \times 18.0153 / 1000 \quad (2.30)$$

2.7.2.3 Prediction of total body water

In adults, total body water can be estimated from height and weight using the Hume and Weyers (1971) equations or height using the Slater and Preston (2002) equation. Hume and Weyers (1971) give equations for both genders:

Males:

$$TBW\ (kg) = (0.194786 \times height,\ cm) + (0.296785 \times weight,\ kg) - 14.012934 \quad (2.31)$$

Females:

$$TBW\ (kg) = (0.344547 \times height,\ cm) + (0.183809 \times weight,\ kg) - 35.270121 \quad (2.32)$$

According to Slater & Preston (2002),

$$TBW\ (kg) = 7.4 \times (height,\ m)^3 \quad (2.33)$$

The cumulative PDR at the plateau enrichment, calculated using measured TBW, was compared with that using TBW estimated using the Hume and Weyers (1971) equations or the Slater and Preston (2002) equation.

2.7.3 [$^2H_{15}$]octanoate test

The percentage dose recovered from [^{2}H] and [^{13}C]MTG tests were compared with that when the tracer is in the form of free octanoic acid, rather than esterified in the form of a triacylglycerol.

A flapjack was prepared containing [1-^{13}C]octanoic acid (99 atom % ^{13}C, Cambridge Isotope Laboratories, Inc. Andover, MA, USA), 2 mg.kg^{-1} body weight (280 mg per flapjack) and [$^2H_{15}$]octanoic acid (99.8 atom % ^{2}H, Cambridge Isotope Laboratories, Inc. Andover, MA, USA), 25 mg.kg^{-1} body weight (3.5 g per flapjack), converted to their sodium salts by addition of 1.912 g sodium bicarbonate as described in Section 2.4.3.1.

Baseline breath, saliva and urine samples were obtained. Breath was sampled every 20 min for 6 h and then every 30 min for a further 4 h, 10 h in total. Saliva was sampled every 20 min for 6 h and then every 30 min for a further 4 h, starting 10 min after ingestion of the test meal, so that breath and saliva sampling times were offset. Urine was sampled at two hourly intervals during the breath test. Total body water was measured by ^{18}O-dilution at the end of the breath sampling period as described in Section 2.7.2.2.

Samples of saliva and urine were collected at the same time on the following nine days. Urine and saliva samples were stored in plastic universal bottles at –20 °C prior to analysis.

The amount of deuterium entering the body water pool was analysed by CF-IRMS after equilibration with 5 % H_2 in He, and the PDR in body water was calculated as described in Section 2.7.2.1.

The cumulative PDR in breath and body water following the octanoate test was compared with that from the mixed triacylglycerol test.

2.7.4 [$^2H_3$]acetate test

The cPDR from [^{2}H] and [^{13}C]MTG and octanoate tests were compared with that from the [$^2H_3$] and [1-^{13}C]acetate tests.

[1-^{13}C]acetate, sodium salt (1 mg.kg^{-1} body weight, ~140 mg per flapjack) and [$^2H_3$]acetate, sodium salt (80 mg.kg^{-1} body weight, 12 g per flapjack, 99.8 atom %, Cambridge Isotope Laboratories, Inc., Andover, MA, USA) were baked in the same flapjack. Urine and breath samples were collected. Breath was sampled at baseline, then every 10 min for the first hour and every 20 min for 5 h and finally every 30 min for a further 4 h, 10 h in total. Urine was sampled at baseline and for 24 h following the test meal. The volume of urine was measured at each void and three aliquots retained in plastic universal bottles. Urine samples were stored at –20 °C until analysis. Breath $^{13}CO_2$ abundance was analysed by CF-IRMS as described in section 2.1.1.2. The amount of deuterium entering the body water pool was analysed by CF-IRMS as described in section 2.7.2.1, after equilibration with 5 % H_2 in He. The amount of tracer excreted in urine as [$^2H_3$]acetate was analysed as its *tert.*-butyldimethylsilyl (TBDMS) derivative by GC/MS (Morrison *et al.* 2003a) after purification by solid phase extraction (Waldron & Preston, 2001). Recovery of ^{2}H as ^{2}HOH in body water (at the plateau enrichment) was compared with that following the [^{2}H]MTG test using a two-sample t-test. Recovery of ^{13}C in breath CO_2 (cPDR 10 h) was compared with that following the [^{13}C]MTG test.

2.7.4.1 Analysis of [$^2H_3$]acetate in urine

Precautions were taken to minimise the blank in this assay. All glassware was acid washed in 0.1 M HCl and rinsed in deionised, distilled water (DDW) before use. The ultrafiltration devices were rinsed with 1 % phosphoric acid. All reagents and solvents were analytical grade or better. Volatile fatty acids (VFA) were purchased from Sigma-Aldrich (Poole, UK). Solutions (20 mM in aqueous sodium hydroxide) were prepared to serve as internal and external standards. Reagent blanks were prepared with each batch of samples. Internal standard, 0.4 μmol 3-methylvaleric acid (20 μl of a 20 mM solution in $NaOH_{(aq)}$) was added to 10 ml urine. The pH was measured and if <7 adjusted to 7-8 by adding 1 M NaOH. NaCl (1.17 g) was dissolved in the sample and this was poured into an ultrafiltration unit (Amicon Centriplus centrifugal filter device YM-30, 30 kDa cut-off, Millipore (UK) Ltd., Watford, UK) and centrifuged at 3000 *g* for 2 h to remove proteins and other high molecular weight components. The resulting filtrate was acidified to pH 2 by adding concentrated phosphoric acid (~20 μl at a time). VFA were concentrated by solid phase extraction (SPE). The SPE cartridges (Bakerbond SPE column, 200 mg SDB, 3 ml capacity, Mallinckrodt Baker UK, Milton Keynes, UK) were conditioned with 2 x 2 ml methanol, followed by 1 x 2 ml deionised water and 1 x 2 ml dilute phosphoric acid (prepared by adding 15 μl concentrated phosphoric acid to 10 ml deionised water, pH 2) before loading the samples. The acidified ultrafiltrate was added to the conditioned SPE column and the VFA eluted with 3 x 400 μl methanol. Sodium salts of the VFA were prepared by adding 100 μl 1M NaOH. The sample was divided between two 2 ml crimp-cap vials (2-CV, Chromacol, Welwyn Garden City, UK). The solvent was removed by drying in an oven at 55 °C overnight.

VFA were extracted into 500 μl ether upon addition of 100 μL 3M HCl and with vortex mixing. The ether phase (200 to 400 μl) was decanted and dried over anhydrous Na_2SO_4. An aliquot (100 μl) of the ether phase was added to 100 μl acetonitrile. The TBDMS (*tert.*-butyldimethylsilyl) VFA derivatives were formed by addition of 20 μl MTBSTFA (Sigma-Aldrich, Poole, UK) and heating at 60 °C for 60 min. TBDMS-acetate enrichment and concentration were analysed by GC/MS (Hewlett Packard 5890 II GC with an Optic temperature programmable injector and Fisons Instruments A200S autosampler + VG Trio-1000 quadrupole MS with electron impact ionisation). The GC operated in splitless mode with helium (CP grade) as carrier gas. The injector temperature was ramped from 60 °C to 300 °C at 16 °C s^{-1} and the transfer line between the GC and the MS was operated

at 300 °C. The analytical column was a DB5ms (J & W Scientific, Folsom, CA, USA), length: 30 m, internal diameter 0.25 mm, film thickness 0.25 µm. The temperature program started at 50 °C and held for 0.2 min then ramped to 200 °C at 10 °C min^{-1}, then from 200 °C to 300 °C at 30 °C min^{-1}, followed by 2 min at 300 °C. The solvent delay was 5 min and the injection volume was 0.5 µl.

The Trio-1000 quadrupole mass spectrometer with electron impact ionisation, was operated with a trap current of 150 µA and electron energy of 70 eV. The ion source temperature was 200 °C, and the detector multiplier was operated at 500 V. The TBDMS derivative has a prominent ion at M-57, i.e. M-(C-$(CH_3)_3$). The quantitation masses for acetate were *m/z* 117, 118, 119, 120 (M-57). [$^2H_3$]acetate enrichment was determined from the ratio (119 + 120)/117, after blank subtraction. The isotopomer at *m/z* 119, corresponding to [$^2H_2$]acetate, was included in the enrichment calculation because the analysis of the [$^2H_3$]acetate tracer showed that it contained a significant amount of [$^2H_2$]acetate. Acetate concentration was determined with reference to the internal standard, 3-methylvalerate, quantitation ion *m/z* 173. The response factors of each VFA, relative to 3-methyl valerate, were determined by analysing a VFA blend of known molar composition. The dwell time on each mass was 0.04 s, with a span of ± 0.2 amu.

2.8 [^{13}C]MTG breath test in healthy adults and children

2.8.1 Study design

The aim of this study was to investigate the effect of different levels and patterns of activity on the cumulative percentage dose recovered during [^{13}C]MTG and [^{13}C]acetate breath tests. [^{13}C]MTG and [1-^{13}C]acetate breath tests were performed in a group of compliant subjects (healthy adult volunteers), a group of subjects with varying levels of activity (healthy child volunteers) and a group of children with cystic fibrosis, all wearing individually calibrated heart rate monitors. This study included more healthy control subjects than children with cystic fibrosis because previous studies in children (Amarri *et al.* 1997) lacked specificity and had a low positive predictive value, due to low recovery in some healthy children. Adults were asked to consume a diet composed of low ^{13}C foods for 3 d before the test, and children for 24 h before the test. The cPDR was calculated using a constant value of resting $V\!CO_2$ predicted from body surface area; a constant value of resting $V\!CO_2$ predicted from basal metabolic rate using the Schofield (1985) equations;

a constant value of resting $\dot{V}CO_2$ measured using a ventilated hood indirect calorimeter; and $\dot{V}CO_2$ estimated from heart rate on a minute-by-minute basis using the individual's own calibration. The cPDR values were compared and the physical activity level (PAL) calculated from PDR estimated continuously from heart rate divided by PDR estimated using a constant measured value of resting $\dot{V}CO_2$. Use of an acetate correction factor was also explored.

2.8.2 Recruitment of subjects

Eight healthy adults, ten healthy children and seven children with cystic fibrosis were recruited. [^{13}C]MTG and [1-^{13}C]acetate breath tests were performed on healthy adults at the Department of Child Health, Yorkhill Hospital and on healthy children in their own homes. Adults were recruited from amongst the members of staff at the Department of Child Health. Eight healthy children were recruited from the families of members of staff. Two additional children were friends or siblings of children with cystic fibrosis, who did the test at the same time as their friend or sibling. All subjects gave written informed consent to take part in the study.

2.8.3 Calibration of heart rate monitors

Heart rate monitors were calibrated as described in Section 2.2. Calibration procedures were compared by analysing the residuals, i.e. the difference between measured $\dot{V}CO_2$ and $\dot{V}CO_2$ estimated from heart rate using the model. The bias i.e. the mean of the residuals, the standard error of this mean and the 95 % confidence interval were calculated using a standard statistical software package (Minitab for Windows, Release 11.2). A paired t-test was performed on the residuals to determine whether the bias was statistically significant.

2.8.4 Comparison of methods of estimating resting metabolic rate

2.8.4.1 Estimating RMR

$\dot{V}CO_2$ estimated from height and weight using the Schofield (1985) equations and assuming a constant value of 5 mmol.min^{-1}.m^{-2} (Section 2.2.2.1) were compared with that measured at rest using a ventilated hood indirect calorimeter (Section 2.2.2.2). $\dot{V}CO_2$ estimated from heart rate during the RMR measurement, using the preferred model, was also compared with the measured value. The mean difference between the measured and

predicted value of resting $\dot{V}CO_2$ was calculated for each group of subjects and for the whole study group.

2.8.4.2 Effect of position on measured RMR

One of the criteria for measuring basal metabolic rate is that the subject should be lying in a supine position (Section 2.2.2.2). Resting metabolic rate is normally measured in this position, however it was noted during the heart rate calibration procedure that children with cystic fibrosis had an elevated CO_2 production rate, when lying compared to sitting. This was investigated further by comparing lying $\dot{V}CO_2$ with sitting $\dot{V}CO_2$ in healthy subjects and in children with cystic fibrosis. The mean difference, standard error of this mean and the 95 % confidence interval were calculated using a standard statistical software package (Minitab for Windows, Release 11.2). A paired t-test was performed to determine whether the difference was statistically significant between healthy control subjects and children with cystic fibrosis.

2.8.5 Postprandial or diet-induced thermogenesis

The thermogenic effect of a cereal-based meal was measured in seven adult subjects, following measurement of basal metabolic rate. Subjects came to the hospital after an overnight fast. They rested on a bed for 20 min preceding measurement of basal metabolic rate as previously described (Section 2.2.2.2). The hood of the indirect calorimeter was removed, but subjects remained on the bed in a semi-recumbent position. They consumed a meal composed of unsweetened wheat- or rice-based breakfast cereal with semi-skimmed (1.8 % fat) milk and a glass of unsweetened orange juice and the hood was replaced. $\dot{V}CO_2$ and $\dot{V}O_2$ measurements continued for 2 h until they had returned to basal levels. The subjects watched videos for entertainment during this time. The thermogenic effect of the meal was calculated by dividing the mean $\dot{V}CO_2$ over the 2 h following the meal by the basal value and expressing it as a percentage of the basal rate.

2.8.6 Procedure for [^{13}C]MTG and [1-^{13}C]acetate breath tests

2.8.6.1 [^{13}C]MTG breath test in healthy subjects

The test started at 8 am, after an overnight fast. Heart rate monitors were fitted and baseline breath samples obtained by the subjects blowing through a straw into an Exetainer breath sampling tube until condensation appeared on the side of the tube. The tracer was baked in a flapjack as described in Section 2.4. The test meal was taken instead of breakfast. Subjects were given a portion in proportion to their body weight such that the dose of [^{13}C]MTG was approximately 10 mg.kg^{-1} body weight and the energy intake was about 17 % of their estimated daily energy needs. A drink of unsweetened orange juice was taken with the meal in adults. Some children preferred water or milk. Breath was sampled at baseline and then every 20 min for 6 h, followed by every 30 min for 3 h (9 h in total). Adult subjects sat in an upright position during the test and moved around as little as possible. Children took part in "rainy day" activities of their choice including watching television, watching videos, doing homework, playing board games, playing computer games and playing quietly in their room. A light lunch of rolls, ham, cheese, potato crisps, fruit and unsweetened fruit juice (apple or orange, according to preference) was taken approximately 4 h after the test meal. Water was consumed *ad libitum* during the test. Children were given the option of flavouring this with sugar-free cordial.

Heart rate data were downloaded to a PC immediately after the test, but the calibration procedure and measurement of RMR took place on a separate occasion. Breath $^{13}CO_2$ abundance (ppm ^{13}C) was measured by CF-IRMS as previously described (Section 2.1.2.2). Enrichment of post-dose samples was calculated by subtracting the abundance of the baseline sample from that of the post-dose sample. Enrichment was expressed in units of ppm excess ^{13}C. The PDR h^{-1} from each sample was calculated using Equation 2.17 (Section 2.2.4.4). PDR was calculated using the following estimates of $\dot{V}CO_2$:

1) Constant value of resting $\dot{V}CO_2$ predicted from body surface area (Section 2.2.2.1)
2) Constant value of resting $\dot{V}CO_2$ using the Schofield (1985) equations to predict basal metabolic rate, and hence resting $\dot{V}CO_2$, as described in Section 2.2.2.1
3) Constant value of measured resting $\dot{V}CO_2$ (Section 2.2.2.2)
4) $\dot{V}CO_2$ predicted from heart rate around the time of each breath sample using individually calibrated heart rate monitors (Section 2.2.3)

5) $\dot{V}CO_2$ predicted from heart rate around the time of each breath sample using generic calibrations normalised to body surface area and height^3 (Section 2.9).

Physical activity level (PAL) during the test was defined as cPDR 6 h calculated using method 4 divided by cPDR 6 h calculated using method 3. This is mathematically equivalent to non-resting $\dot{V}CO_2$ divided by resting $\dot{V}CO_2$, as the breath enrichment and dose terms are the same in both calculations and cancel out in the calculation of PAL. Non-resting $\dot{V}CO_2$ divided by resting $\dot{V}CO_2$ = TEE/REE = PAL.

2.8.6.2 [^{13}C]MTG breath test in children with cystic fibrosis

The consultant paediatrician responsible for the care of children with cystic fibrosis identified suitable children from the list of those attending the clinic at the Royal Hospital for Sick Children, Glasgow. Families were initially approached by a consultant paediatric gastroenterologist, to establish their interest in taking part in the study. If they were interested, a researcher contacted them by telephone to confirm the procedure and establish a suitable date for the test to take place. Information sheets and consent forms were posted to their home with ample time for them to withdraw if they changed their mind.

On the day of the test, the children came to the ambulatory day care unit at the Royal Hospital for Sick Children, Glasgow, without having breakfast. Two subjects preferred to do the test when they were in hospital for routine intravenous antibiotic treatment and one preferred to do the test in her own home. The procedure was explained to the children and baseline breath samples were obtained. Heart rate monitors were fitted and the test meal consumed without any pancreatic enzyme replacement therapy (PERT). Breath was sampled every 20 min for 6 h.

Resting metabolic rate was measured between 3 and 4 h after consumption of the test meal as described in Section 2.2.2.2. Separate hoods and air filters for the indirect calorimeter were reserved for healthy control subjects, for children with cystic fibrosis who have never had antibiotic resistant *Pseudomonas aeruginosa* isolated from sputum, and for children with cystic fibrosis, who have had *Pseudomonas aeruginosa* colonisation. This information was retrieved from the cystic fibrosis clinic database for each subject before they came to the hospital. The inside of the hoods were wiped thoroughly with chlorhexidine gluconate 0.5 % w/v in industrial methylated spirits BP70 % v/v (Hydrex DS Pink, Adams Health Care, Leeds, UK) between subjects.

A light lunch composed of the same low ^{13}C foods offered to the healthy children was taken with the usual PERT after the RMR measurement. Children were entertained by playing computer games, watching videos, playing board games with the researcher or colouring, depending on their age and interests. At the end of the breath-sampling period, the children took part in the heart rate calibration procedure described in Section 2.2.3 before returning home.

2.8.6.3 [1-^{13}C]acetate breath test

All of the healthy subjects and three of the children with cystic fibrosis performed a [1-^{13}C]acetate breath test (1 mg.kg^{-1} body weight) within one month of the MTG test. The tracer was baked in a flapjack as described in Section 2.4. The dose of [1-^{13}C]acetate was of equivalent molarity to that of MTG. The test took place in the same place and in a similar manner to the MTG test. Children with cystic fibrosis did not take their usual PERT with the test meal, but did take their usual dose with lunch. Breath was sampled at baseline, every 10 min for the first hour during the acetate test, followed by every 20 min until 6 h after the test meal. Adults and healthy children continued sampling every 30 min for a further 3 to 4 h. PDR was calculated using a constant value of resting $\dot{V}CO_2$ predicted from body surface area, a constant value of resting $\dot{V}CO_2$ predicted from basal metabolic rate using the Schofield (1985) equations, the measured resting value of $\dot{V}CO_2$, and continuously measured $\dot{V}CO_2$ estimated from heart rate using the individual's own calibration.

2.9 [^{13}C]MTG tests using generic heart rate calibration

2.9.1 *Study design: search for a generic calibration*

Use of a generic calibration, which could be applied to subjects of all ages and size, would greatly simplify the breath test procedure by avoiding the need for individual calibration of heart rate monitors. Therefore, the aim of this study was to investigate potential generic calibration methods to predict CO_2 production rate from heart rate during ^{13}C breath tests in subjects with a wide range of age and body habitus and to demonstrate their use in the [^{13}C]MTG and [1-^{13}C]acetate breath tests. Heart rate calibration data from all subjects were included representing subjects aged from 5 to 47 years, with BMI 21 to 34 kg.m^{-2} in adults and BMI SD score –1.0 to +2.5 in children. Generic calibration methods to predict $\dot{V}CO_2$ from heart rate included normalising $\dot{V}CO_2$ from the heart rate calibration procedure

to body surface area, height^2, height^3 and weight. Data from all subjects were combined and a sigmoid model fitted using the least squares method (Section 2.2.3).

Potential generic calibration methods were initially compared by considering the accuracy, defined as the mean measured $\dot{V}CO_2$ minus mean $\dot{V}CO_2$ predicted from 2-point smoothed heart rate, and expressed as a percentage of the mean measured value. This is a measure of the overall bias of the method. Precision was defined as the standard deviation of the residuals expressed as a percentage of the mean measured $\dot{V}CO_2$ i.e. the coefficient of variation. Accuracy and precision are expressed as percentages to enable comparisons between normalisation methods with results expressed in different units.

Univariate analysis of variance of the relationship between age and each of the constants in the sigmoid model for each normalisation method was investigated using the regression analysis tool in the data analysis tools of Microsoft Excel 97. In individual subjects, normalisation methods were compared by analysing the residuals, i.e. the difference between measured $\dot{V}CO_2$ and $\dot{V}CO_2$ estimated from heart rate using the generic model. The bias, i.e. the mean of the residuals, the standard error of this mean and the 95 % confidence interval were calculated using a standard statistical software package (Minitab for Windows, Release 11.2). A good model has no bias i.e. the mean of the residuals is zero. A paired t-test was performed on the residuals to determine whether the bias was statistically significant. The effect of using a generic rather than an individual calibration was demonstrated by calculating the PDR in the [^{13}C]MTG and [1-^{13}C]acetate breath tests using $\dot{V}CO_2$ predicted from heart rate using each of the generic methods.

2.9.2 Use of a generic calibration or assumed PAL: a pragmatic approach

Individual calibration of heart rate monitors is not practical for a routine test, but heart rate could be used to predict $\dot{V}CO_2$ if a suitable generic calibration was available, or alternatively individually calibrated heart rate monitors could be used to determine the reference range in healthy subjects and the physical activity level (PAL) under the normal conditions of the test. Data were obtained from a previous study (Amarri *et al.* 1997), in which a [^{13}C]MTG breath test was performed on 45 children with cystic fibrosis, who had not taken their usual pancreatic enzyme replacement therapy with the test meal. The tests were performed under similar conditions to the current study. The PAL measured in this study was applied to the cPDR 6 h data from the previous study and the results compared with those obtained in the current study.

2.10 Empirical compensation for individual $\dot{V}CO_2$

2.10.1 Introduction

Use of an acetate correction as an empirically derived means of compensating for lack of knowledge of $\dot{V}CO_2$ during the [^{13}C]MTG breath test was investigated by dividing the cPDR at 6 h, calculated assuming a constant value of 5 mmol.min^{-1}.m^{-2}, in the MTG test by that in the acetate test (Equation 2.27). In this way, the $\dot{V}CO_2$ terms cancel out, as they are assumed to be the same for each test, even if the exact value is unknown. The procedure was repeated using cPDR calculated using $\dot{V}CO_2$ predicted from heart rate using the subject's own individual calibration. The $cPDR_{6h}$ acetate was plotted against $cPDR_{6h}$ MTG for each group of subjects, with MTG PDR_{6h} the independent variable plotted on the x-axis and Acetate PDR_{6h} the dependent variable plotted on the y-axis. The line of unity was included.

2.11 Determination of the cut-off point of the [^{13}C]MTG test

2.11.1 Introduction

To establish whether use of a minute-by-minute estimate of $\dot{V}CO_2$ rather than a constant resting value of $\dot{V}CO_2$ improved the discrimination of the MTG breath test, data for cumulative percentage dose recovered in 6 h using $\dot{V}CO_2$ predicted from heart rate in healthy children and children with cystic fibrosis were combined. Two graph-receiver operator characteristics (TG-ROC) was used to determine the appropriate cut-off for the new test with a 6 h sampling time. The positive and negative predictive values of the test were calculated. The procedure was repeated for cPDR calculated using a constant resting value of $\dot{V}CO_2$.

2.11.2 Determination of cut-off

The appropriate cut-off for each test above was determined using TG-ROC (Greiner, 1995) at the 95% accuracy level. The cut-off point, d0; sensitivity, which equals specificity, θ_0; intermediate range, IR; valid range proportion, VRP were tabulated.

2.11.3 Positive and negative predictive values

The positive and negative predictive values for each MTG test were calculated using the equations shown in section 1.4.2.4 and using a prevalence of pancreatic insufficiency in the study population of 0.24 (6 out of 25 subjects, who normally took pancreatic enzyme replacement therapy). These were compared with the values obtained by Vantrappen *et al.* (1989) in their validation study of the MTG test in adult patients with pancreatic disease.

Chapter 3 Results

Summary of Chapter 3

In this chapter, the results of the experiments and studies outlined in Chapter 2 are reported. Accurate quantification of tracer excretion in breath requires accurate measurement of breath $^{13}CO_2$ enrichment, accurate measurement of dose ingested and accurate measurement of $\dot{V}CO_2$. If the aim is to account for all fates of ingested tracer, then account must be made for loss of tracer in stool and urine, and tracer sequestration within the body.

Accurate measurement of breath $^{13}CO_2$ enrichment relies on accurate measurement of breath $^{13}CO_2$ abundance and control of background $^{13}CO_2$ abundance, including the composition of the test meal. Accuracy and precision of isotope abundance measurements were established (Section 3.1) and variation of background ^{13}C abundance was quantified (Section 3.5). The homogeneity of labelled substrate distribution within the test meal and losses during preparation were checked *in vitro* (Section 3.4).

The three alternative approaches of addressing the problem of lack of knowledge of true $\dot{V}CO_2$ during ^{13}C breath tests were initially explored in two healthy adult subjects (Sections 3.2 to 3.7). The most promising methods were then applied to a larger group of subjects, including eight healthy adults, ten healthy children and seven children with cystic fibrosis (Sections 3.8 to 3.11). Methods of predicting and measuring resting $\dot{V}CO_2$ were compared (Sections 3.2.2 and 3.8.3) and the contribution of postprandial thermogenesis to total $\dot{V}CO_2$ was measured in adult subjects (Sections 3.2.4 and 3.8.4). Individually calibrated heart rate monitors were used to estimate total $\dot{V}CO_2$ continuously during ^{13}C breath tests (Sections 3.2, 3.5, 3.6, 3.8 and 3.9). Use of a generic calibration was explored (Sections 3.3 and 3.9).

Two healthy adults took part in additional studies using [^{13}C]MTG and its labelled metabolites, to study the effect of factors including rest, exercise, fasting and feeding on the recovery of $^{13}CO_2$ in breath. Simultaneous use of ^{13}C- and ^{2}H-labelled tracers (MTG, octanoate and acetate) was also investigated (Sections 3.5 to 3.7). ^{2}H-labelled tracers are potentially advantageous as food intake and physical activity do not affect recovery, and relatively little is sequestered into organic compounds.

3.1 Validation of laboratory methods

The laboratory methods used to measure isotopic abundance were validated. Thus, ensuring that all measurements were accurate (traceable to international standards or gravimetrically prepared standard curves), precise (SD of three replicate analyses < 1 ppm) and linear (the isotope ratio was constant over the expected concentration range of 0.5-5 % CO_2). This ensured that measurement of isotopic abundance was not a major source of error in the calculation of cumulative excretion.

3.1.1 Measurement of ^{13}C and ^{18}O isosotopic abundance

3.1.1.1 Reproducibility of filling reference gases

The procedure for filling Exetainers was optimised empirically to minimise the coefficient of variation (CV). Using the procedure described in Section 2.1.2.1, it was possible to achieve a CV on the total beam (equivalent to peak area) of ~1 %.

3.1.1.2 CO_2 calibration curve and linearity of $^{13}CO_2$ abundance

The CO_2 calibration curve, prepared by injecting known amounts of pure CO_2 into an evacuated Exetainer, is shown in Figure 3.1, R^2 = 1.0. Linearity of CO_2 abundance measurements is shown in Figure 3.2. Measured ^{13}C abundance was constant (SD = 1.1 ppm ^{13}C) over a ten-fold range of sample size corresponding to the range expected from breath samples (0.5 to 5 %).

3.1.1.3 Precision of breath $^{13}CO_2$ analysis and inter-laboratory check

The precision of replicate analyses of breath $^{13}CO_2$ enrichment is shown in Figure 3.3. The mean standard deviation of $^{13}CO_2$ abundance in breath CO_2 was 2 ppm excess ^{13}C over the range 30 to 620 ppm excess ^{13}C (n = 4 analyses on the instrument used for this work). The enrichment of samples analysed in the Isotope Biochemistry Laboratory at the Scottish Universities Environmental Research Centre (SUERC) is also shown.

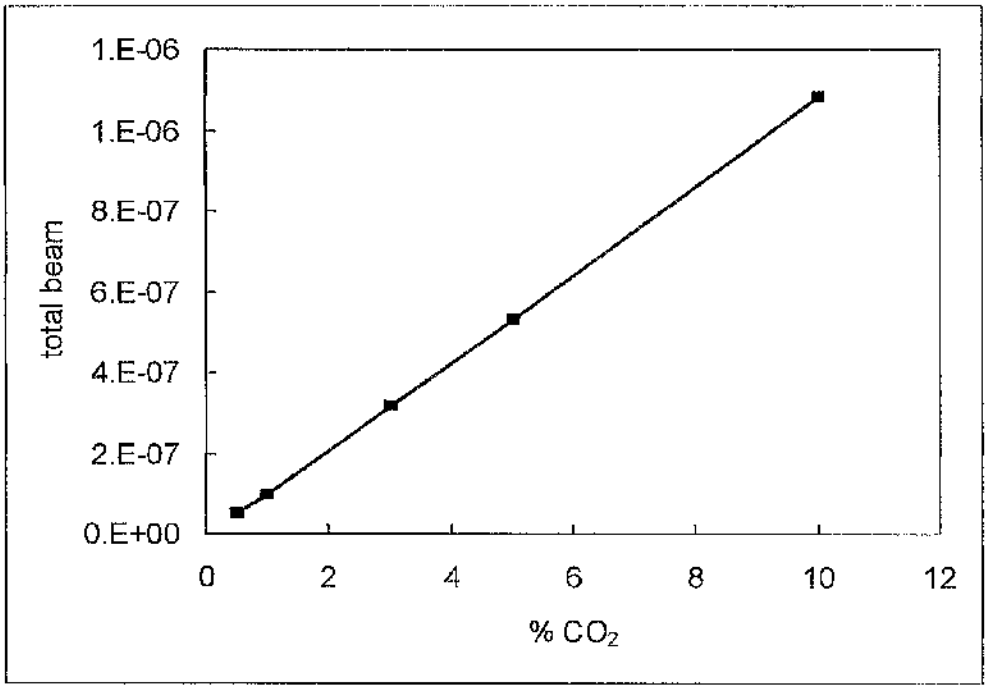

Figure 3.1 CO_2 standard curve

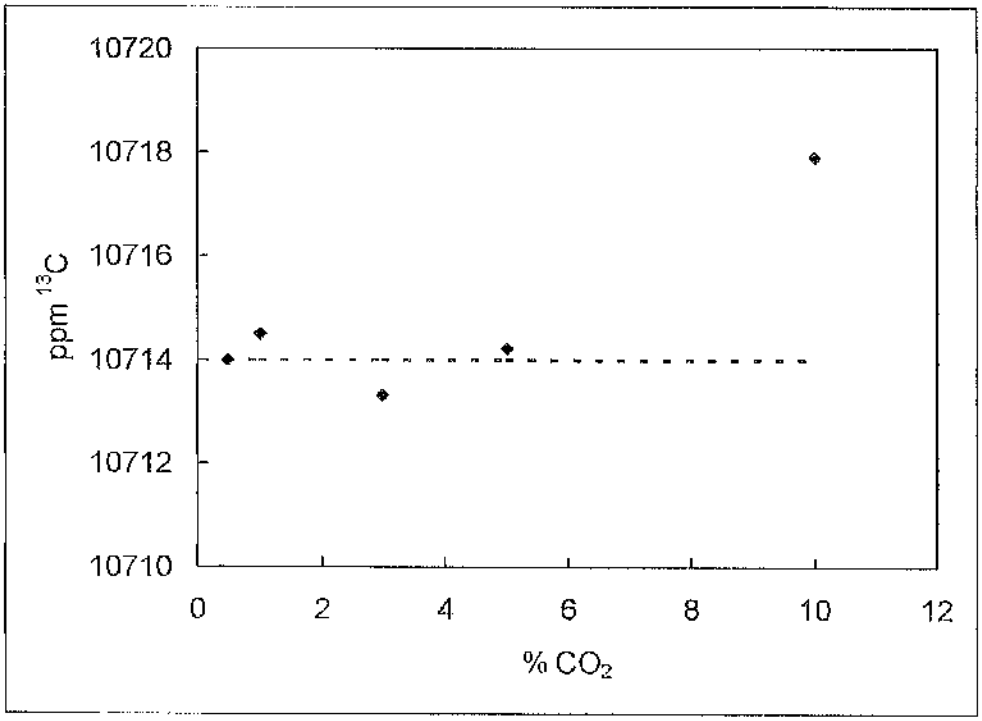

Figure 3.2 Linearity of $^{13}CO_2$ measurements

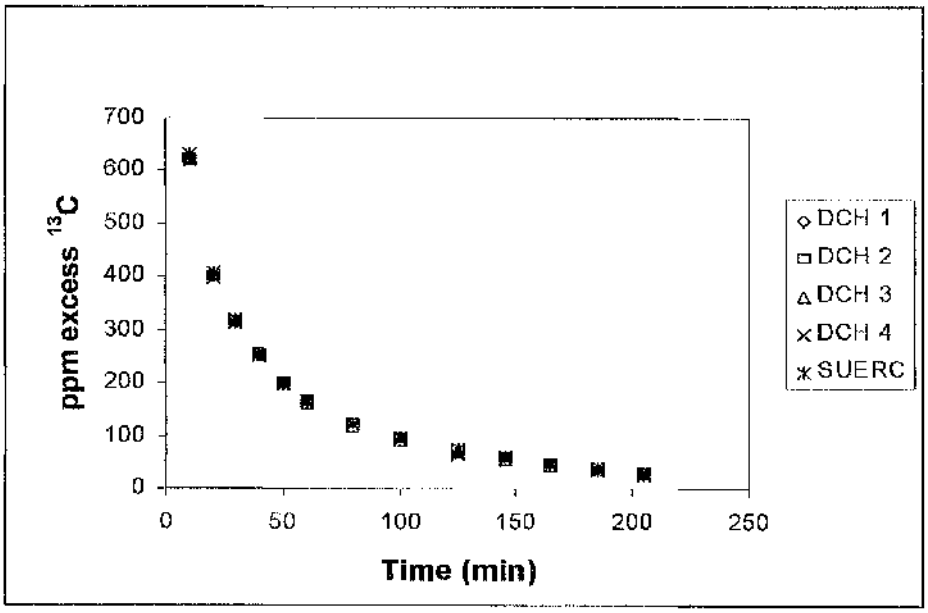

Figure 3.3 Precision of breath $^{13}CO_2$ measurements and inter-laboratory comparison

3.1.1.4 ^{18}O standard curve

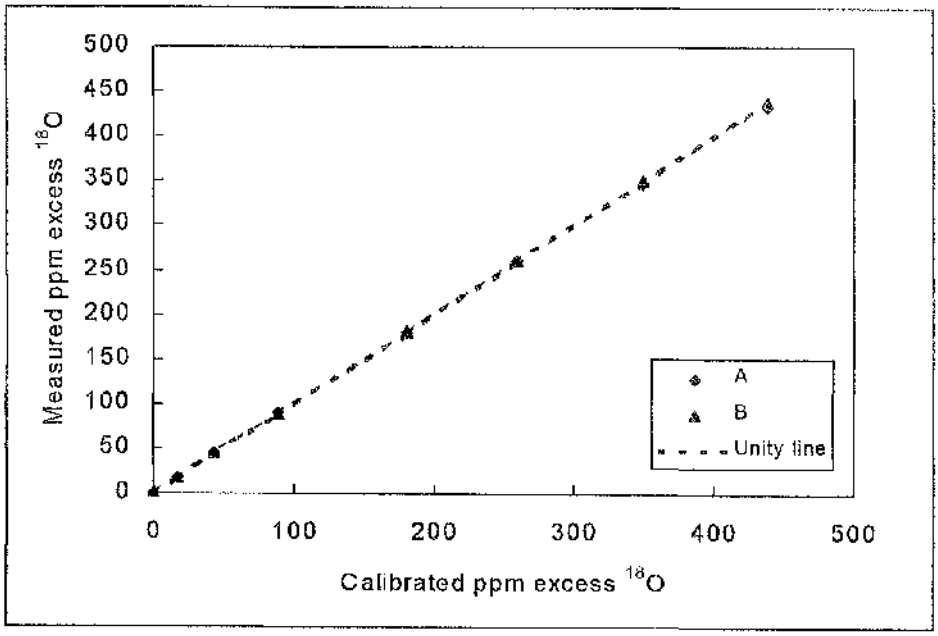

Figure 3.4 ^{18}O standard curve

Initially, the enrichment of the gravimetric standards was calculated based on the weight of $H_2{}^{18}O$, the weight of added tapwater and the abundance of ^{18}O as stated on the manufacturer's Certificate of Analysis. However, independent analysis of the stock $H_2{}^{18}O$

against the international standard (VSMOW) showed that it contained more ^{18}O than stated on the manufacturer's Certificate of Analysis. Therefore, the enrichment of the standards was recalculated and the nominal 150 ppm excess ^{18}O standard was found to contain 179.8 ppm excess ^{18}O. The ^{18}O calibration curve is shown in Figure 3.4. Calibrated ppm excess ^{18}O on the *x*-axis is the enrichment calculated from the independent analysis of the stock solution, which is traceable to the international standard. Unlike deuterium, there is not a large fractionation factor associated with preparation of samples for ^{18}O analysis by the equilibration method. The gradient of the two-point calibration curve, before drift correction was typically ~1.03. The gradient of the ^{18}O calibration curve after applying the drift correction (as described in Section 2.1.3.3) was 1.0, $R^2 = 1.0$.

3.1.1.5 Accuracy and precision of ^{13}C and ^{18}O abundance measurements

Accuracy of ^{13}C and ^{18}O abundance measurements was ensured by calibrating the reference gas against the international standards (VPDB for ^{13}C and VSMOW for ^{18}O) and placing references at intervals in each batch of samples. Reported abundances were drift corrected between references. The abundance of ^{13}C in the reference gas was –37.95 δ ^{13}C VPDB = 10695.1 ppm ^{13}C. The abundance of ^{18}O in the reference gas was +12.57 δ ^{18}O VSMOW = 2100.7 ppm ^{18}O.

Precision of ^{13}C measurements was checked at intervals by analysing batches of reference gases and calculating the standard deviation of three replicates. SD <0.5 ppm ^{13}C was routinely achieved.

Precision of ^{18}O measurements was checked by calculating the standard deviation of the three replicate analyses of the reference waters. SD <0.5 ppm ^{18}O was routinely achieved on both enriched and natural abundance waters.

3.1.2 Measurement of ^2H isotopic abundance

3.1.2.1 ^2H standard curve

Figure 3.5 shows the standard curve of deuterium enrichment over the whole measured range. Figure 3.6 shows the range between 0 and 200 ppm excess, which is the range of interest in this study.

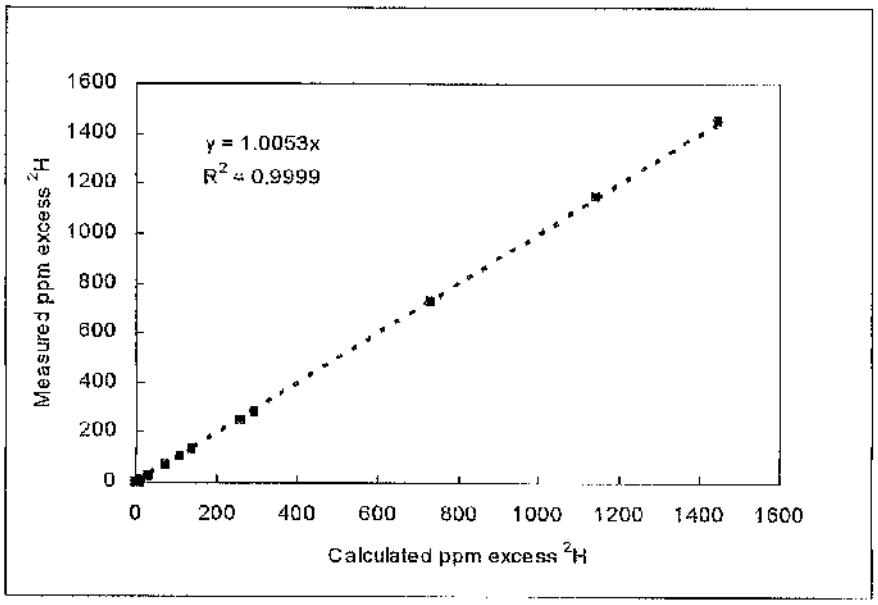

Figure 3.5 ^{2}H standard curve

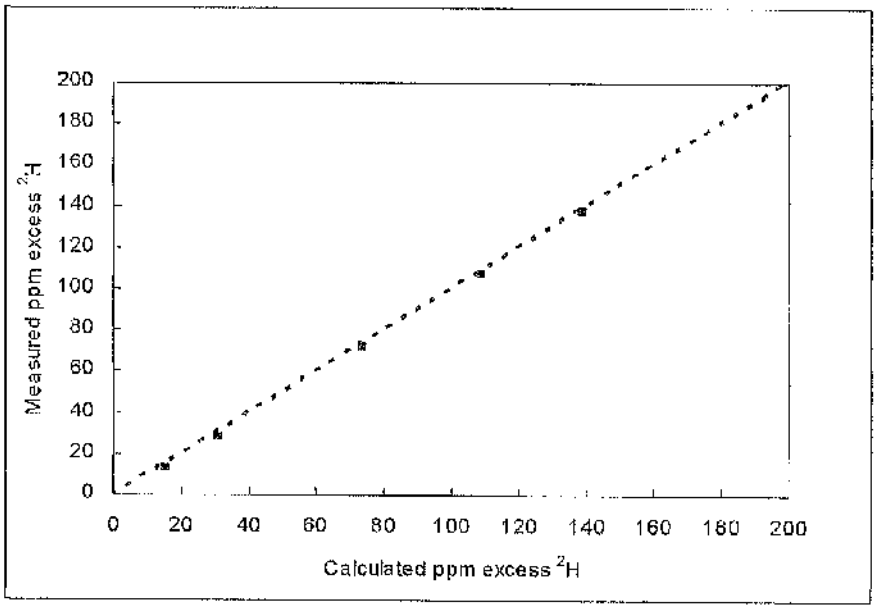

Figure 3.6 Lower region of ^{2}H standard curve

3.1.2.2 Accuracy and precision of ^{2}H measurements

Accuracy of ^{2}H measurements was ensured by including working standards (0 and 75 ppm excess ^{2}H) at intervals in each analytical run. These standards were prepared with the samples and treated in exactly the same way as the samples, as there is a large fractionation factor associated with preparation of samples by the equilibration method (Scrimgeour *et al.* 1993). The gradient of the two-point calibration curve using the ^{2}H abundance reported

by the 'Reprocessor' was approximately 0.37. The enrichment of the reference waters was calculated using this correction factor and the natural abundance of the tap-water sample (150.5 ppm ^{2}H) after drift-correction between the standards as described in section 2.1.3.3. The gradient of the calibration curve was 1.0053, R^2= 0.9999. Precision of ^{2}H measurements was checked by calculating the standard deviation of the three replicate analyses of the reference waters. SD < 1 ppm ^{2}H was routinely achieved.

3.2 Measuring CO_2 production rate

3.2.1 Subject characteristics

Two healthy adults took part in a series of experiments to test the feasibility of using heart rate monitors to measure $\dot{V}CO_2$ continuously during ^{13}C-breath tests. The characteristics of the subjects are shown in Table 3.1.

Table 3.1 Details of subjects who took part in the pilot study

	Subject 1	Subject 2
Gender	Female	Male
Age	44	46
Weight (kg)	55	75
Height (m)	1.59	1.83
BMI ($kg.m^{-2}$)	21.7	22.4

3.1.3 Predicting and measuring basal/resting metabolic rate

Resting/basal metabolic rate was determined as described in section 2.2.2. The results for $\dot{V}CO_2$ are shown in Table 3.2.

The Shreeve value of 5 mmol $CO_2.min^{-1}.m^{-2}$ body surface area was close to the measured value in Subject 1, but prediction of $\dot{V}CO_2$ from BMR estimated using the Schofield equations based on height and weight was closer to the measured value in Subject 2.

Table 3.2 Predicted and measured resting $\dot{V}CO_2$ normalised to body surface area

$\dot{V}CO_2$ method	Subject 1 $mmol.min^{-1}.m^{-2}$	Subject 2 $mmol.min^{-1}.m^{-2}$
Shreeve (1970) predicted	5	5
Schofield (1985) predicted	4.5	4.8
Measured	4.9	4.7
Predicted from HR*	4.9	4.5

* using sigmoid model

3.2.3 Calibration of heart rate monitors

Figure 3.7 shows time matched heart rate (HR) and $\dot{V}CO_2$ data from the heart rate calibration procedure in a healthy adult subject. Note that at low levels of energy expenditure heart rate increases, whilst $\dot{V}CO_2$ remains relatively unchanged. The two then rise in parallel before returning to resting levels when the exercise stopped.

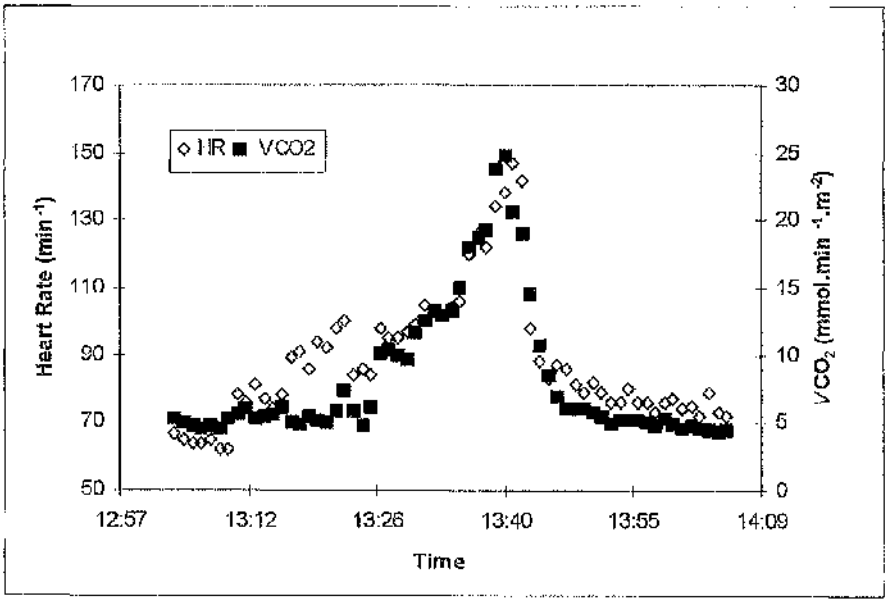

Figure 3.7 Time matched data from the heart rate calibration procedure

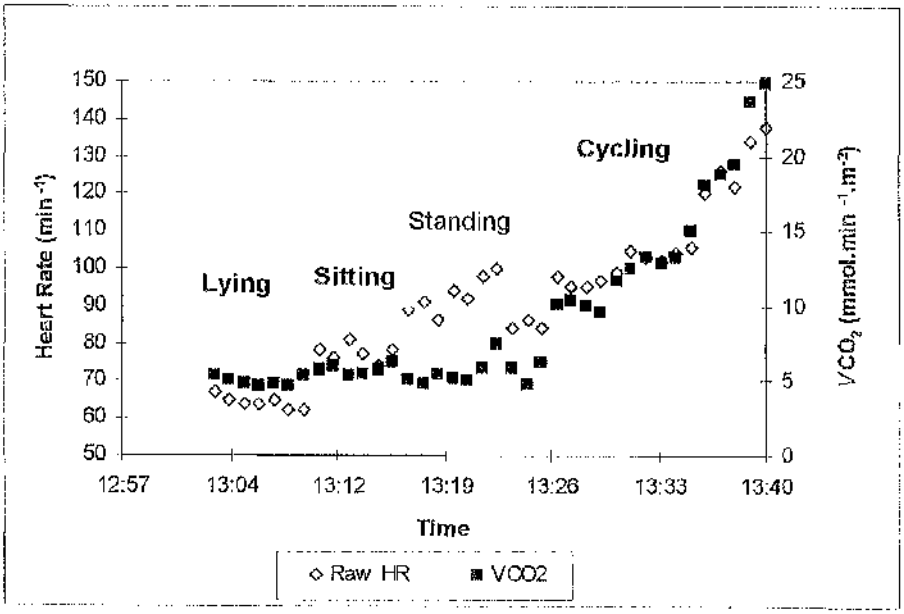

Figure 3.8 Region of increasing energy expenditure showing equilibration periods

The best calibration method has no bias i.e. the mean difference between measured and predicted $\dot{V}CO_2$ is zero. This is conveniently displayed using a Bland-Altman plot (Bland & Altman, 1986) of the residual (difference between measured and predicted values) versus the mean of the measured and predicted values. The standard error of this mean is a measure of the precision of the model. Analysis of the residuals i.e. the difference between the measured $\dot{V}CO_2$ at any time point and that predicted by the model allows these values to be quantified. A paired t-test was performed to assess the statistical significance of the bias. The results of the analysis of residuals are tabulated in Appendix 2 for all subjects studied. Subjects 1 and 2 are the ones who took part in the pilot study.

Effect of smoothing heart rate

Averaging heart rate one or two points either side of the point of interest had no effect on the calibration as it has no effect on the relative time of heart rate and $\dot{V}CO_2$ detection. However, averaging 2, 3 and 4 points forward of the point of interest proved to be useful as illustrated in Figure 3.9. The most appropriate smoothing routine was judged to be the one with coefficient of determination, R^2, closest to unity. The coefficients of determination for the calibration data in Figures 3.9 to 3.11 are tabulated in Table 3.3.

Table 3.3 Coefficient of Determination (R^2) for smoothing routines

Smoothing routine	Subject 1 A	Subject 1 B	Subject 2
Raw HR data	0.84	0.84	0.71
2 points forward	0.89	0.86	0.78
3 points forward	0.91	0.84	0.83
4 points forward	0.92	0.80	0.86

The effect of smoothing was markedly different between individuals on different occasions. This may be due to biological variation, but some part of it could be due to the fact that the indirect calorimeter has a slower response and its output displays time in integer minutes, whereas the output from the heart rate monitors displays time to the nearest second. This could result in almost a minute error in matching the output from two instruments. Subject 1 performed the heart rate calibration procedure as part of the pilot study (Subject 1A) and again two years later (Subject 1B). On the second occasion, smoothing had a much less marked effect than on the first.

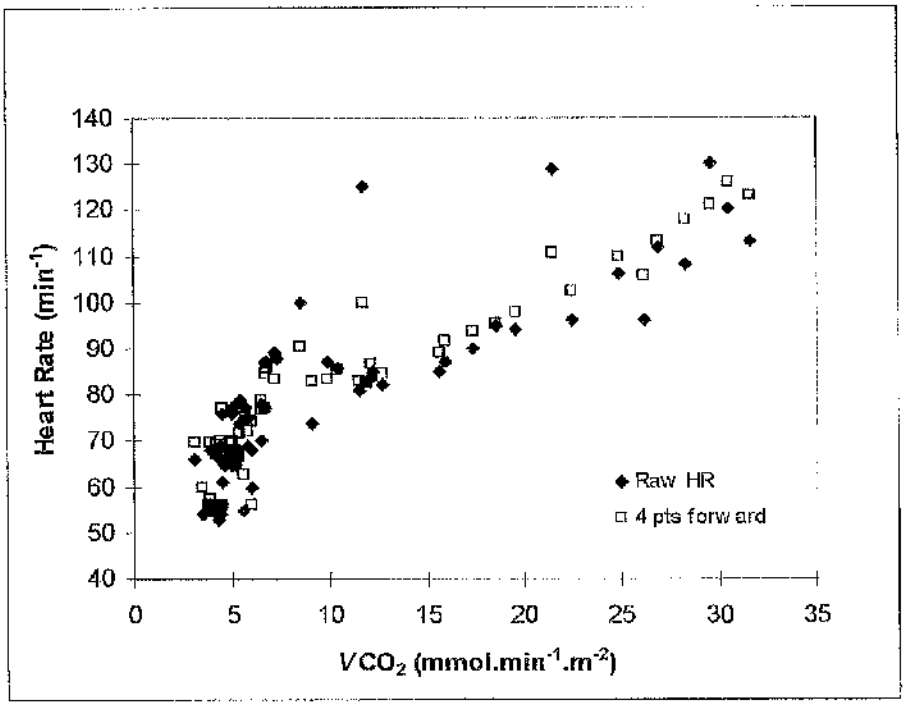

Figure 3.9 Effect of smoothing heart rate by averaging four points forward on Subject 2, including both exercise and recovery data

Smoothing heart rate forwards moves heart rate relative to $\dot{V}CO_2$ and brings data closer to a straight line, so that all data (during exercise and recovery) can be included in the model, and not just data collected after equilibration at each level of energy expenditure.

3.2.3.1 Linear methods

Linear calibration methods have two components. A resting value of $\dot{V}CO_2$ is assumed below a critical point and a linear model is used above the critical point. Linear calibration methods used raw (unsmoothed) heart rate data as in the published methods.

Figure 3.10 shows the calibration curve fitted to the data shown in Figure 3.7 using the linear flex method of Spurr *et al.* (1988) as described in Section 2.2.3.1. Open symbols are the measured data. Filled symbols are the data predicted from heart rate using the linear model. Resting heart rate was 69 min^{-1}, the flex point was 76 and therefore the critical value, above which the linear model was used, was 86 min^{-1}. Resting $\dot{V}CO_2$ was 4.54 $mmol.min^{-1}.m^{-2}$. Figure 3.11 shows the Bland-Altman residual plot of the bias between measured $\dot{V}CO_2$ and $\dot{V}CO_2$ predicted using the linear model shown in Figure 3.10 applied to the whole data set. In this case, the bias was 0 (95 % confidence interval −0.43, 0.44) and there was no significant difference between the measured and predicted values of $\dot{V}CO_2$ ($P = 0.99$, Appendix 2, adult Subject 1).

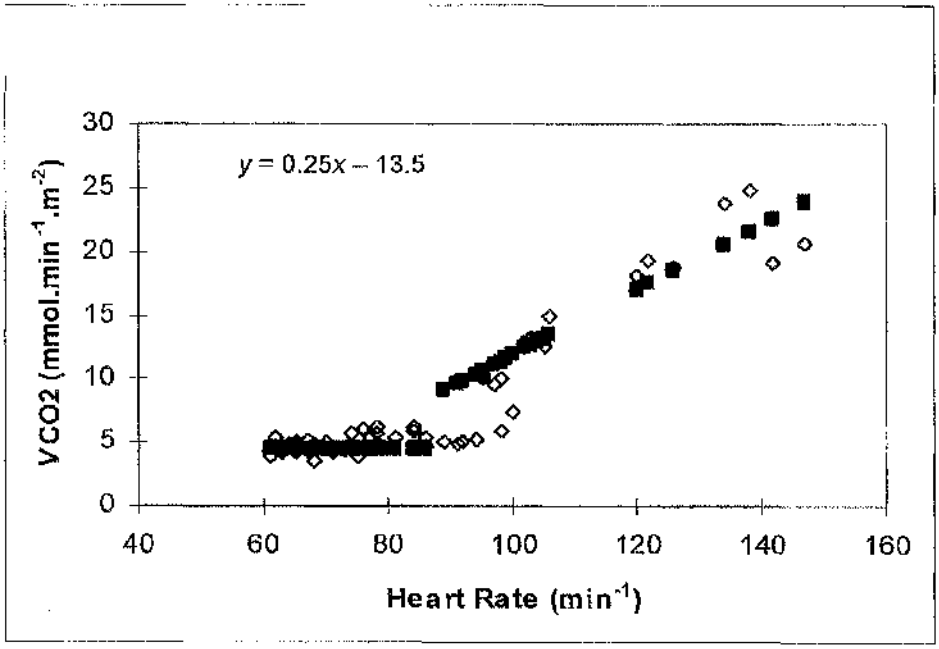

Figure 3.10 Linear-flex calibration fitted to data from Figure 3.7

Resting HR = 67, flex point = 76, critical value = 86 min^{-1}. Resting $\dot{V}CO_2$ = 4.54 $mmol.min^{-1}.m^{-2}$

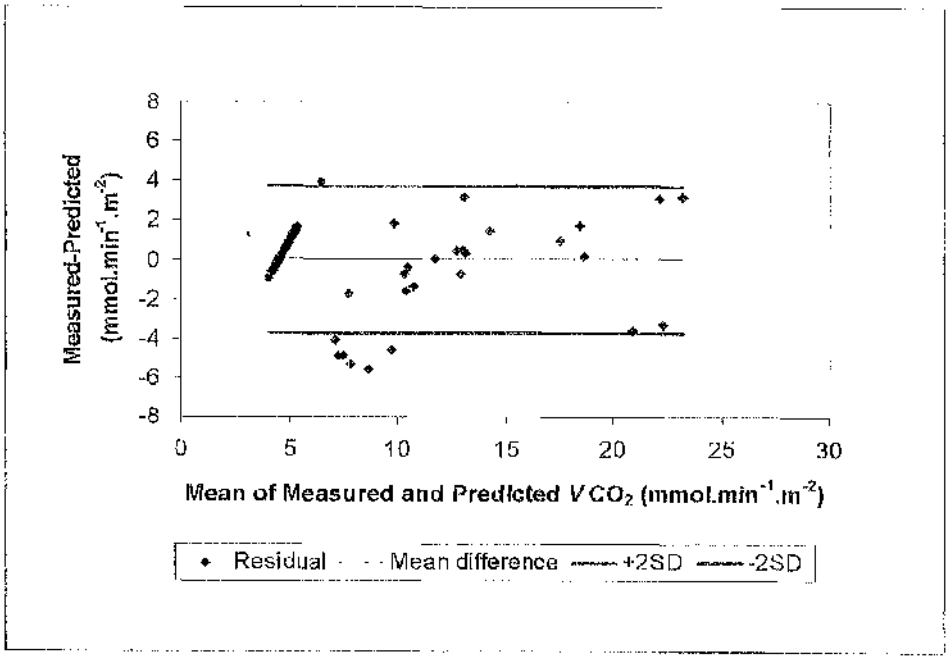

Figure 3.11 Residual plot of data from Figure 3.10

Figure 3.12 shows the calibration curve using the mean steady state values according to the method of Livingstone *et al.* (1992) as described in Section 2.2.3.1. Heart rate at the flex point was 73 min^{-1} and the mean $\dot{V}CO_2$ when the subject was lying, sitting and standing,

was 4.9 mmol.min^{-1}.m^{-2}. Figure 3.13 shows the Bland-Altman residual plot of the bias between measured $\dot{V}CO_2$ and $\dot{V}CO_2$ predicted using the linear model shown in Figure 3.12 applied to the whole data set. The bias was 0.54 (95 % confidence interval –0.01, 1.07) and there was a significant difference between the measured and predicted values of $\dot{V}CO_2$ ($P = 0.045$, Appendix 2, adult Subject 1).

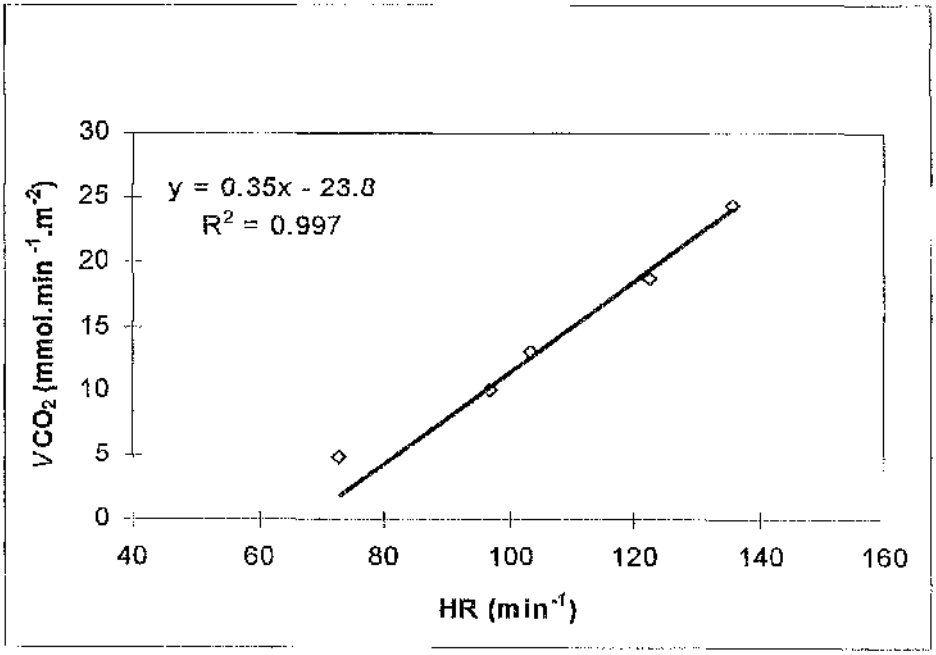

Figure 3.12 Steady-state calibration curve from data in Figure 3.8

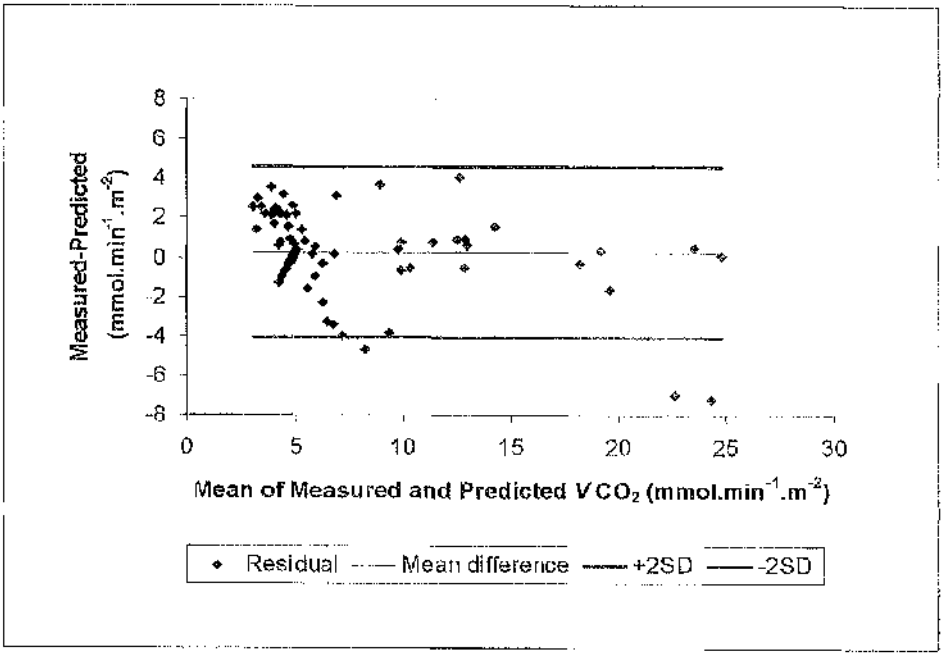

Figure 3.13 Residual plot of data from Figure 3.12

3.2.3.2 Non-linear methods

Non-linear methods were performed on smoothed heart rate data, including both exercise and recovery phases as described in Section 2.2.3.2. Figures 3.14-3.17 show calibration curves using 2nd and 3rd order polynomials, logistic and sigmoid models fitted to the data shown in Figure 3.7, as described in Section 2.2.3.2. Open symbols are the measured data. Filled symbols are the data predicted from heart rate using the model. Second and third order polynomials did not fit the data well at low levels of activity (lying, sitting and standing) and will not be discussed further. The bias was 0 (95 % confidence interval –0.34, 0.34) and there was no significant difference between the measured and predicted values of $\dot{V}CO_2$ as the model was established using the method of least squares (see Appendix 2, adult Subject 1).

3.2.2.3 Predicting $\dot{V}CO_2$ from $\dot{V}O_2$

Figure 3.18 shows the calibration curve for $\dot{V}O_2$ predicted from heart rate (HR) in Subject 1. Although, the standard error of the bias for $\dot{V}O_2$ predicted from heart rate was slightly less than for $\dot{V}CO_2$ predicted from heart rate (0.15 compared to 0.17), there was no advantage in predicting $\dot{V}CO_2$ from $\dot{V}O_2$. Use of an assumed RQ of 0.85 (IDECG, 1990), which was also the FQ of the test meal, introduces a very large error. The mean bias in Subject 1 was 0.82 mmol $CO_2.min^{-1}.m^{-2}$ (95 % confidence interval 0.44, 1.19, $P < 0.001$) and in Subject 2 was 1.10 mmol $CO_2.min^{-1}.m^{-2}$ (95 % confidence interval 0.10, 1.92, $P = 0.03$).

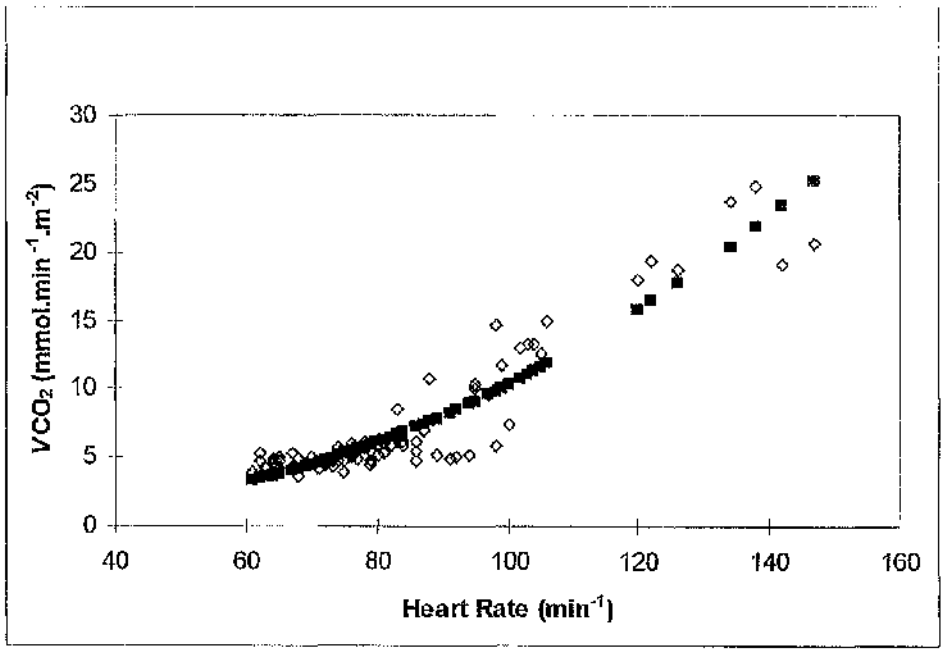

Figure 3.14 Second order polynomial fitted to the data in Figure 3.7

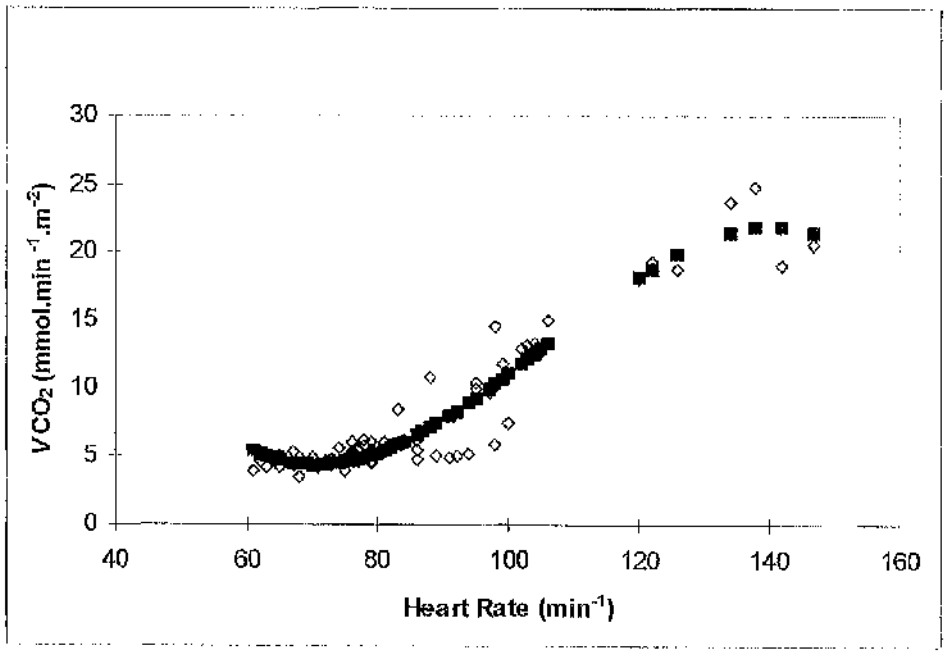

Figure 3.15 Third order polynomial fitted to the data in Figure 3.7

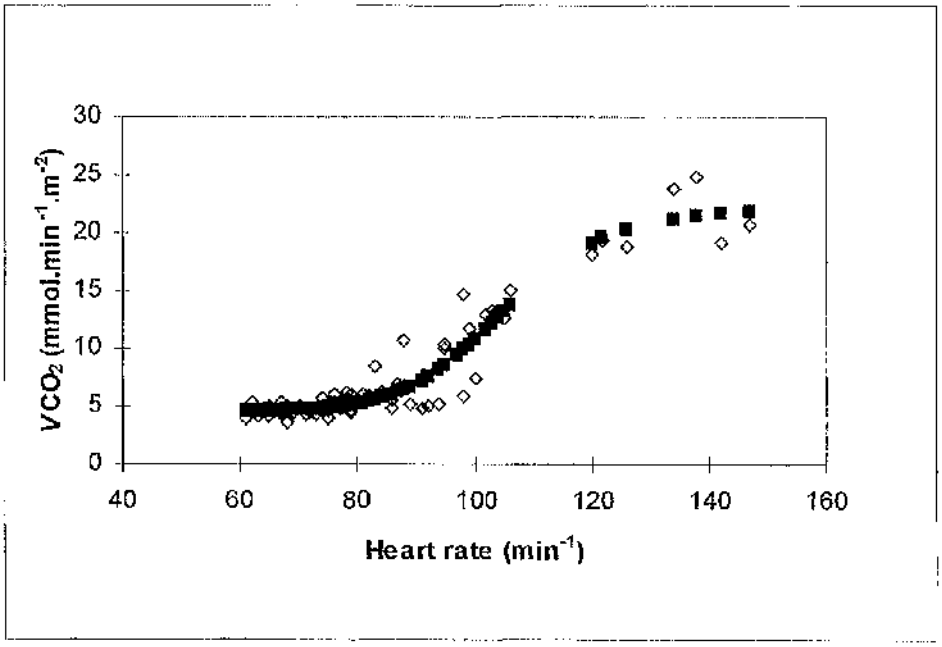

Figure 3.16 Logistic model fitted to the data in Figure 3.7

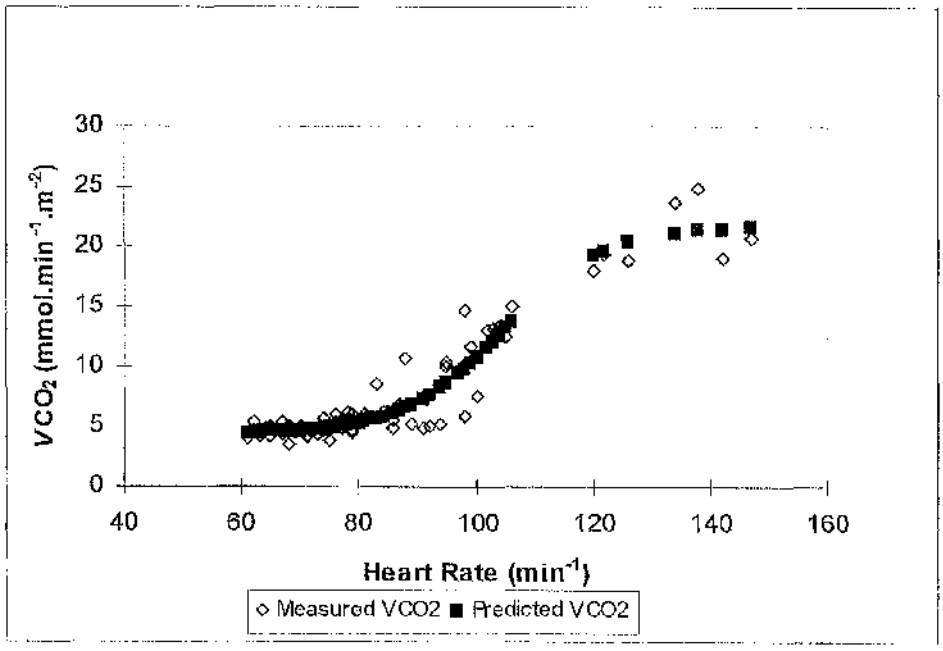

Figure 3.17 Sigmoid model fitted to the data in Figure 3.7

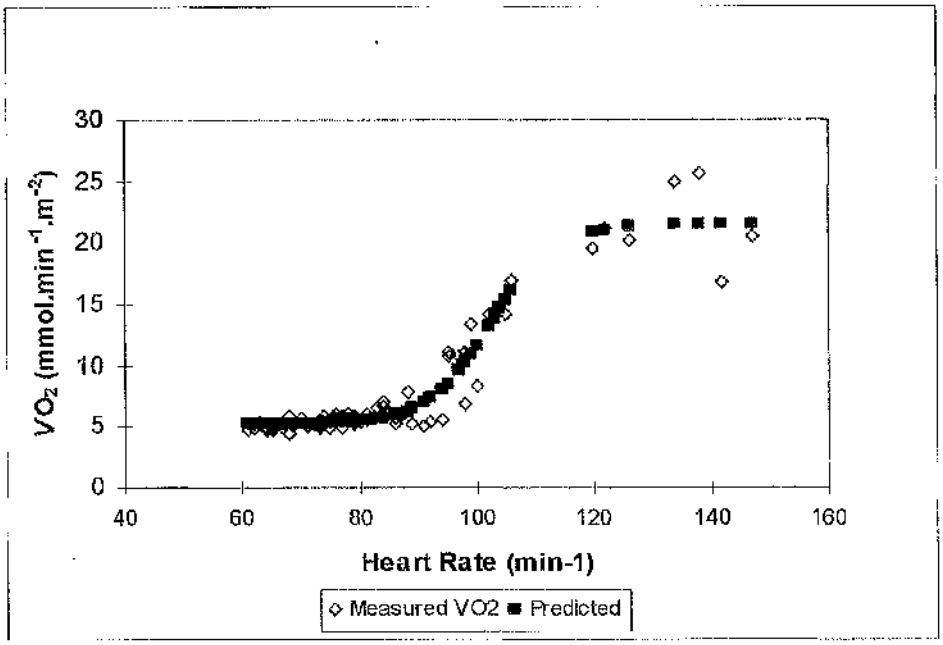

Figure 3.18 Calibration curve for $\dot{V}O_2$ predicted from heart rate (sigmoid model)

3.2.4 [^{13}C]bicarbonate breath tests

3.2.4.1 Variation of measured $\dot{V}CO_2$ during the bicarbonate breath test

$\dot{V}CO_2$ (mmol.min^{-1}.m^{-2} body surface area) was measured in the fasting condition, 1 h after the test meal and 3 h after the test meal during each bicarbonate breath test. Tests were performed once a week over a six-week period to allow breath $^{13}CO_2$ abundance to return to baseline levels between tests. Results are shown in Tables 3.4 and 3.5.

Subjects chose their preferred breakfast of unsweetened breakfast cereal, semi-skimmed milk and unsweetened orange juice, which was the same for each test. The meal chosen by Subject 1 provided 18 % of her estimated daily energy requirements (Department of Health, 1991), whereas the meal chosen by Subject 2 provided only 12 % of his energy needs. This may have caused the low $\dot{V}CO_2$ of Subject 2 at 2 to 3 h following breakfast.

In both subjects the RQ fell during the fasting test, reflecting the switch towards oxidation of the body's lipid reserves, when there was no food intake. There was a difference between subjects in the response to sitting or walking during the test. In both subjects, $\dot{V}CO_2$ increased following the meal (by a factor of ~1.2, when the subjects were sitting

still) and returned towards basal levels (6 % above basal in Subject 1 and 6 % below basal in Subject 2) by 2 to 3 h after the meal. However, when subjects were not resting, the changes in $\dot{V}CO_2$ in the female subject (Subject 1) were very similar to when she was resting. $\dot{V}CO_2$ increased by a factor of 1.25 compared to 1.21 and then returned to 1.07 and 1.06 times basal levels by 3 h after the meal. In Subject 2 (male), the response to exercise was different. $\dot{V}CO_2$ increased to 1.35 times basal at one h after the meal, with a gentle walk in the intervening period, and was still 1.22 times basal 3 h after the meal. Data are summarized in Table 3.6.

3.2.4.2 Thermogenic effect of the test meal

The thermogenic effect of the cereal based breakfast taken before the [^{13}C]bicarbonate dose was 1.2 x BMR in Subject 1 and 1.3 x BMR in Subject 2 over two hours.

Table 3.4 Changes in measured $\dot{V}CO_2$ during bicarbonate breath tests: Subject 1

	BMR		1 h after breakfast		$\dot{V}CO_2$	2-3 h after breakfast		$\dot{V}CO_2$
	$\dot{V}CO_2$	RQ	$\dot{V}CO_2$	RQ	1 h:BMR	$\dot{V}CO_2$	RQ	3 h:BMR
Fasting, resting	5.12	0.83	4.65	0.77	0.91	4.51	0.75	0.88
Fed, sitting 1	4.74	0.82	6.08	0.83	1.28	5.37	0.81	1.13
Fed, sitting 2	5.01	0.83	5.93	0.86	1.18	4.70	0.81	1.02
Fed, sitting 3	4.86	0.79	5.62	0.88	1.16	4.97	0.86	1.02
Fed, walking 1	5.32	0.75	6.49	0.86	1.22	6.29	0.84	1.18
Fed, walking 2	5.15	0.78	6.49	0.84	1.26	5.23	0.75	1.01
Fed, walking 3	4.57	0.88	5.80	0.86	1.27	4.72	0.82	1.03
Mean (ex fasting)	**4.94**	0.81	**6.07**	0.86	**1.23**	**5.21**	0.82	**1.07**
CV (%)	5.6	5.6	5.9	2.1	4.1	11.3	4.6	6.7

$\dot{V}CO_2$ (mmol.min^{-1}.m^{-2} body surface area)

Table 3.5 Changes in measured $\dot{V}CO_2$ during bicarbonate breath tests: Subject 2

	BMR		1 h after breakfast		$\dot{V}CO_2$	2-3 h after breakfast		$\dot{V}CO_2$
	$\dot{V}CO_2$	RQ	$\dot{V}CO_2$	RQ	1 h:BMR	$\dot{V}CO_2$	RQ	3 h:BMR
Fasting, resting	4.95	0.90	5.09	0.81	1.03	4.20	0.75	0.84
Fed, sitting 1	5.10	0.88	6.56	0.93	1.29	5.01	0.80	0.98
Fed, sitting 2	5.11	0.92	5.50	0.89	1.08	4.33	0.79	0.85
Fed, sitting 3	4.79	0.84	5.93	0.87	1.24	4.82	0.82	1.00
Fed, walking 1	5.16	0.88	6.83	0.96	1.34	5.49	0.84	1.06
Fed, walking 2	4.99	0.81	7.34	0.94	1.47	6.53	0.82	1.31
Fed, walking 3	4.64	0.81	5.80	0.84	1.25	5.98	0.87	1.29
Mean (ex fasting)	**4.97**	0.86	**6.33**	0.91	**1.28**	**5.36**	0.82	**1.08**
CV (%)	4.2	5.2	11.1	5.1	10.0	15.0	3.5	16.9

$\dot{V}CO_2$ (mmol.min^{-1}.m^{-2} body surface area)

Table 3.6 Ratio of non-resting VCO_2 to resting VCO_2 (mean of 3 different days)

	Subject 1 (female)		Subject 2 (male)	
Time after meal	1 h	3h	1h	3h
Sitting	1.21	1.06	1.20	0.94
Walking	1.25	1.07	1.35	1.22

3.2.4.3 Intra-subject variability of breath $^{13}CO_2$ recovery

Figures 3.19 to 3.24 show the percentage dose recovered (PDR) in 6 h following a [^{13}C]bicarbonate breath test. PDR was calculated as described in Section 2.2.4.4 using five different ways of estimating VCO_2:

1. Shreeve: a constant value of 5 mmol.min^{-1}.m^{-2} body surface area
2. MR0: a constant value of VCO_2 measured under resting, fasting conditions
3. MR1: a constant value of VCO_2 measured one h after the test meal
4. MR3: a constant value of VCO_2 measured three h after the test meal
5. HR: variable VCO_2 predicted from heart rate using a sigmoid model

Figures 3.19 and 3.20 show the cumulative dose excreted in breath when the test was performed under resting, fasting conditions i.e. with the subject lying on a bed and with no food intake. The 6 h PDR is approximately 60 % in Subject 1 and 80 % in Subject 2. There is no difference between using a constant value of 5 mmol.min^{-1}.m^{-2} body surface area, measured VCO_2 in basal conditions and VCO_2 predicted from heart rate under these conditions.

Figures 3.21 and 3.22 show the cumulative dose excreted in breath when the test is performed with a test meal and the subject sitting in an upright position during the test. A second meal composed of low ^{13}C foods was taken 4 h after the test meal.

Figures 3.23 and 3.24 show the cumulative dose excreted in breath when the test is performed with a test meal and the subject walking during the first hour following the test meal. A second meal composed of low ^{13}C foods was taken 4 h after the test meal.

The fed tests were repeated three times on each subject. Data are summarised in Tables 3.7 and 3.8. These experiments illustrate the problem with ingesting doses of [^{13}C]bicarbonate by mouth, as it is prone to loss by eructation.

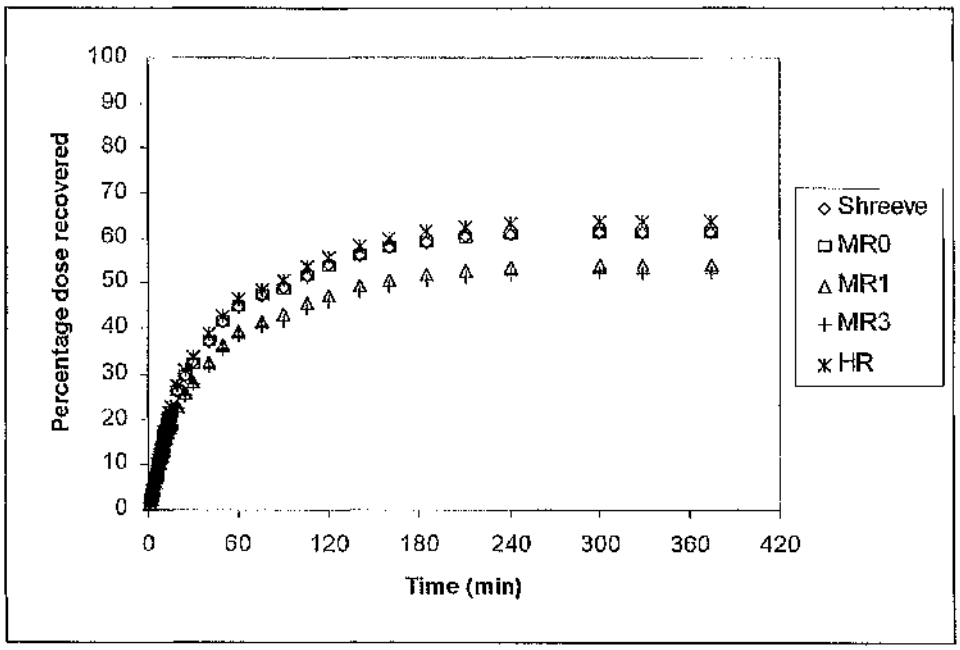

Figure 3.19 Percentage dose recovered in breath CO_2 during a [^{13}C]bicarbonate breath test (Subject 1) under fasting, resting conditions (R)

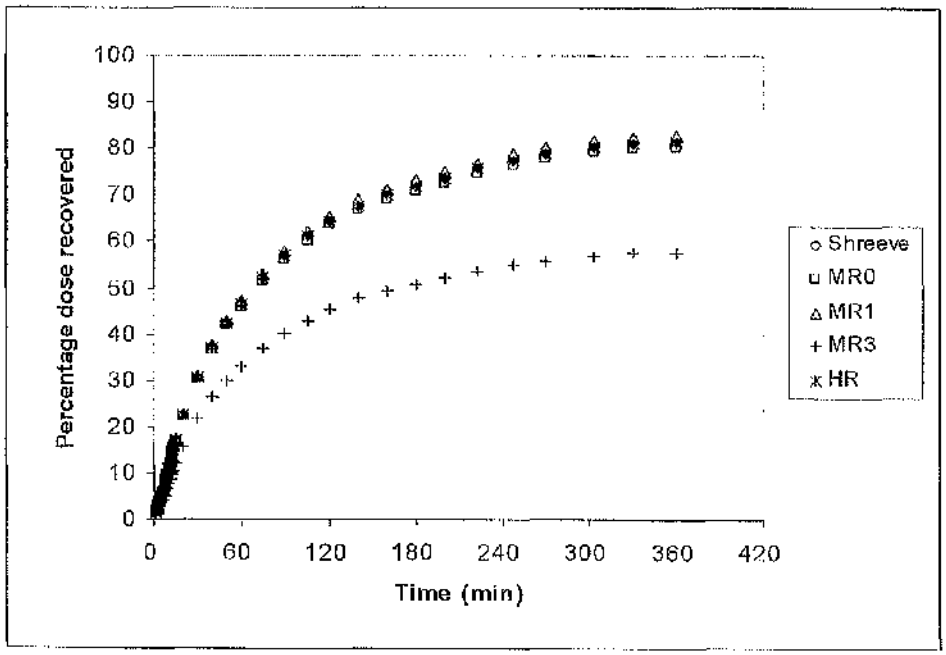

Figure 3.20 Percentage dose recovered in breath CO_2 during a [^{13}C]bicarbonate breath test (Subject 2) under fasting, resting conditions (R)

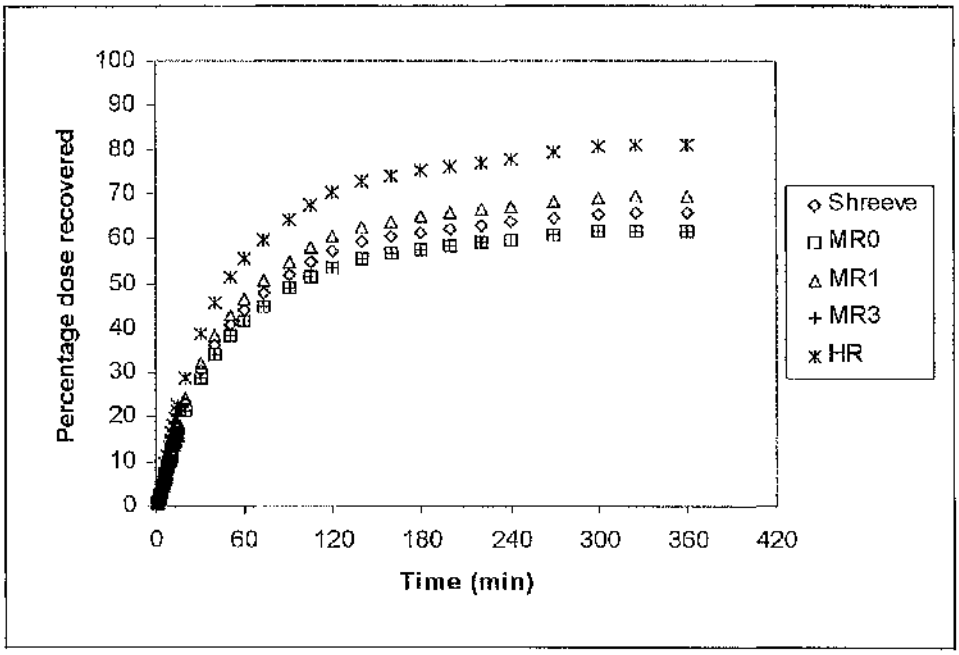

Figure 3.21 Percentage dose recovered in breath CO_2 during a [^{13}C]bicarbonate breath test (Subject 1) under fed, sitting conditions (S)

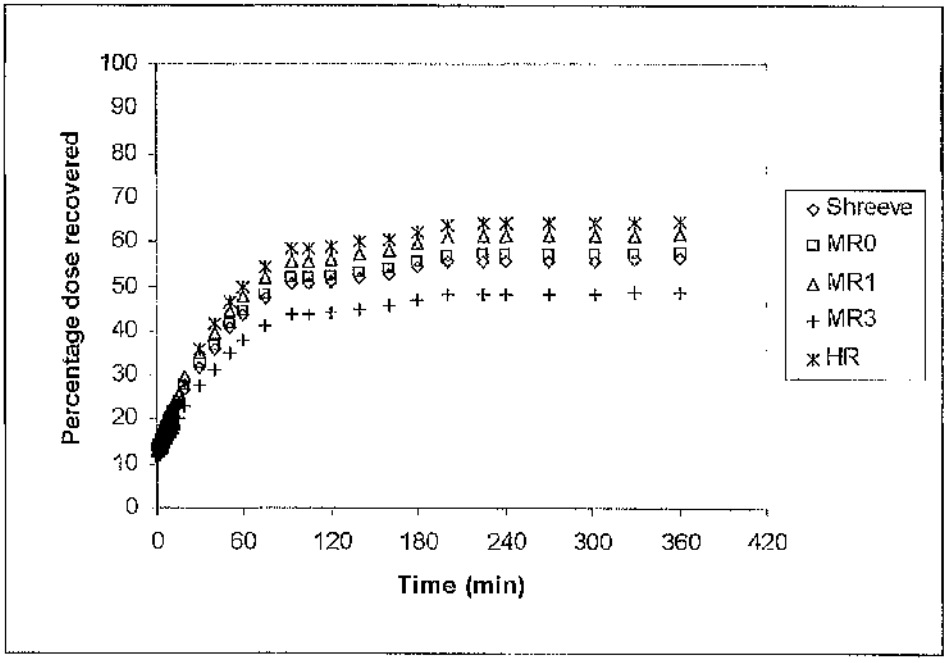

Figure 2.22 Percentage dose recovered in breath CO_2 during a [^{13}C]bicarbonate breath test (Subject 2) under fed, sitting conditions (S)

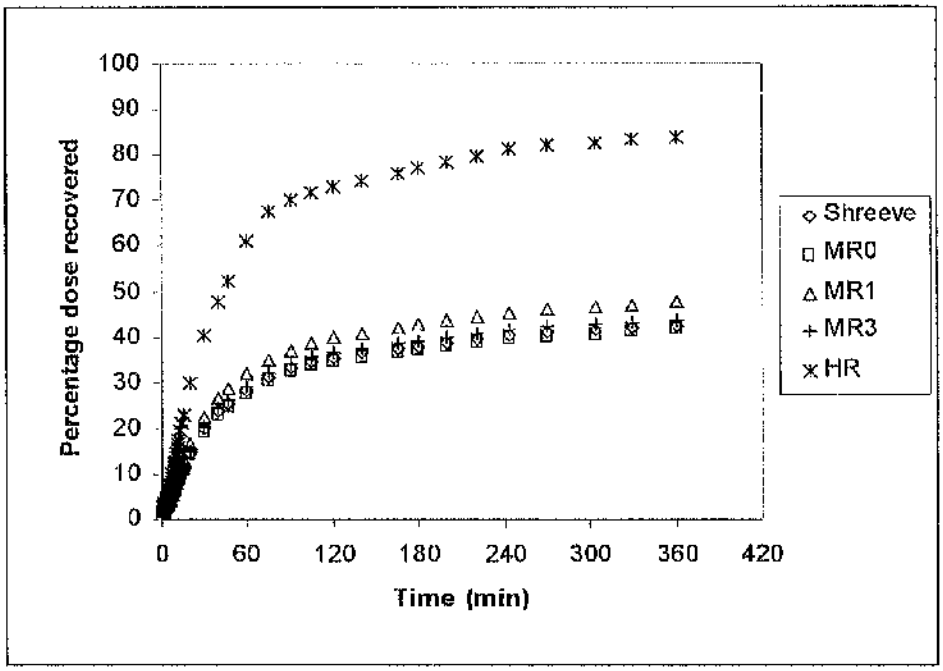

Figure 3.23 Percentage dose recovered in breath CO_2 during a [^{13}C]bicarbonate breath test (Subject 1) under fed, walking conditions (W)

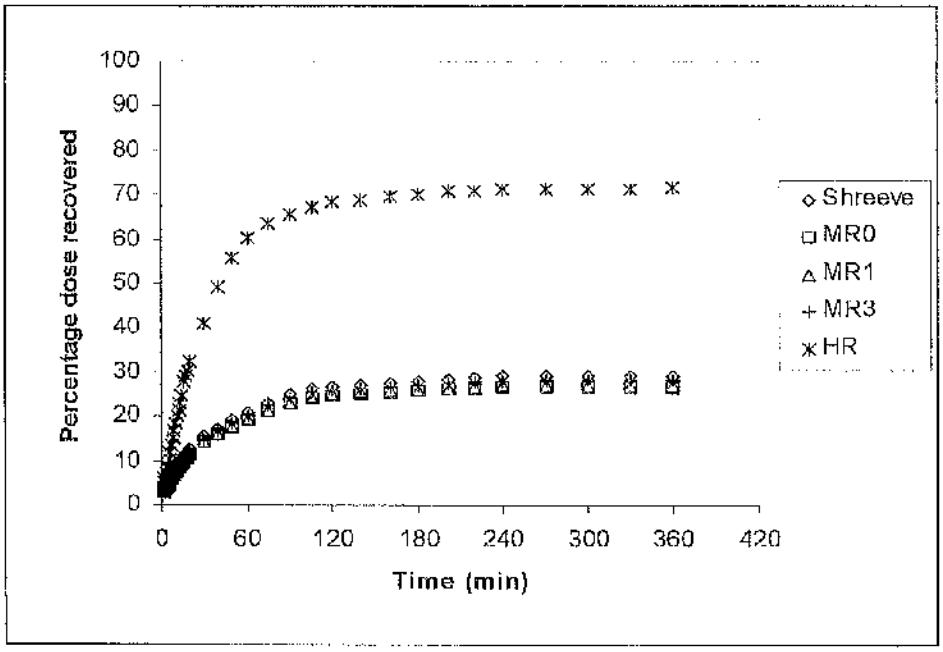

Figure 3.24 Percentage dose recovered in breath CO_2 during a [^{13}C]bicarbonate breath test (Subject 2) under fed, walking conditions (W)

Table 3.7 Summary of 6 h cPDR from [^{13}C]bicarbonate breath tests on Subject 1

	Shreeve	MR0	MR1	MR3	HR	PAL
R 1	61.3	61.2	53.8	52.4	63.7	1.0
S 1	65.7	61.7	69.4	61.7	80.9	1.2
S 2	49.2*	46.7*	59.9*	52.8*	[60.6]*	
S 3	44.2*	44.3*	52.4*	41.5*	[54.4]*	
W 1	19.5*	17.5*	21.2*	18.6*	38.5*	2.0
W 2	42.5	41.8	47.7	43.8	[83.9]	
W 3	30.0	28.0	35.2	27.3	[59.2]	

HR, $\dot{V}CO_2$ estimated from heart rate or [ ] during a test with matched diet and activity; *Subject reported eructation; PAL = HR cPDR / Shreeve cPDR

Table 3.8 Summary of 6 h cPDR from [^{13}C]bicarbonate breath tests on Subject 2

	Shreeve	MR0	MR1	MR3	HR	PAL
R 1	81.5	80.3	82.9	57.6	81.4	1.0
S 1	58.2	54.2	65.8	56.0	64.0	1.1
S 2	32.8*	33.4*	43.0*	32.8*	[36.9]*	
S 3	56.2	57.5	61.9	48.8	64.7	1.2
W 1	29.1	26.4	27.1	28.3	71.5	2.5
W 2	36.4	35.7	40.0	33.7	69.7	2.0
W 3	24.3	22.3	29.3	22.0	61.1	2.5

HR, $\dot{V}CO_2$ estimated from heart rate or [ ] during a test with matched diet and activity; *Subject reported eructation; PAL = HR cPDR / Shreeve cPDR

3.2.4.4 Urinary loss of ^{13}C as [^{13}C]bicarbonate and [^{13}C]urea following a bicarbonate breath test

Less than 5 % of ingested tracer was recovered in urine as either as [^{13}C]bicarbonate or as [^{13}C]urea. The results are shown in Table 3.9 and are in accordance with published values (Elia, 1991) following an intravenous infusion of labelled bicarbonate in which approximately 2 % of the infused label was recovered in urine, mainly in urea.

Table 3.9 Urinary loss of ^{13}C as [^{13}C]bicarbonate and [^{13}C]urea (Subject 1)

Test	[^{13}C]bicarbonate (%)	[^{13}C]urea (%)	Total (%)
R1 (fasting)	1.8	2.9	4.7
W2 (fed, walking)	0.2	2.0	2.2

3.3 Generic calibration of heart rate monitors

Measured $\dot{V}CO_2$ was normalised to the body parameters shown in Table 3.10 before combining data from both subjects. A sigmoid model was fitted by the method of least squares, therefore the mean difference between the measured and predicted values (accuracy) is 0. The best generic calibration method was judged to be the one with highest precision i.e. the smallest CV. Table 3.10 shows that there was no advantage in using a relative heart rate (after Sneddon *et al.* 1985). Normalisation to height^2 or height^3 and surprisingly, weight had the best precision, but both of these subjects were lean (BMI ~22 kg.m^{-2}).

Table 3.10 Comparison of normalisation methods for a potential generic calibration method to predict $\dot{V}CO_2$ from HR (n = 2 subjects)

Normalisation method	Accuracy (%)	Precision (%)
Relative HR (WHR/RHR)*	0.00	31.1
Relative HR (WHR-RHR)*	0.00	28.4
Surface area (m^2)	0.00	24.0
Weight (kg)	0.00	20.6
Weight$^{3/4}$ (kg$^{3/4}$)	0.00	23.4
Height (m)	0.00	26.6
Height^2 (m^2)	0.00	21.9
Height^3 (m^3)	0.00	20.1

* $\dot{V}CO_2$ normalised to body surface area

3.4 Development of a test meal

3.4.1 Nutritional composition and isotopic abundance of the test meal

The ^{13}C abundance of the test meal was calculated from the abundance of ^{13}C in the individual ingredients (Morrison *et al.* 2000) and is shown in Table 3.11 together with the energy content of the meal. The nutritional composition of the test meal is shown in Table 3.12.

Table 3.11 Energy content and ^{13}C abundance of test meal

Ingredients	Energy (kJ)	$\delta^{13}C_{VPDB}$	Atom % ^{13}C
90 g Rolled Oats	1428	-28.07	1.080
40 g Honey	492	-25.01	1.084
40 g Butter	1212	-29.08	1.079
Whole meal	3132	-28.08	1.080

Table 3.12 Nutritional composition of the test meal

	Per 100 g Wet Weight	% Energy
Protein (g)	6	6
Carbohydrate (g)	53	45
Fat (g)	24	49
Energy (MJ)	1.84	100

The FQ (food quotient) of the test meal was calculated from the energy contribution of each nutrient to the total metabolizable using Equation 2.23.

Thus, $FQ = ((5.6 \times 0.81) + (49.3 \times 0.71) + (45.1 \times 1.00))/100$ (3.1)

$FQ = 0.85$

3.4.2 *Palatability studies*

The palatability of all the flapjacks containing the amount of substrate required to achieve sufficient enrichment of $^{13}CO_2$ in breath was considered acceptable for subjects of all ages. The flapjack containing sodium octanoate was much more palatable than that containing

octanoic acid, with just a hint of 'goaty' flavour. The palatability of the flapjacks containing the high dose of acetate and tripalmitin was acceptable. The flapjack containing the high dose of sodium octanoate was tolerable for adults, but not very pleasant and probably not palatable for children.

3.4.3 In vitro experiments

3.4.3.1 Analysis of flapjack acetate and octanoate

The control flapjack contained 2 nmol acetate/g flapjack, which is approximately 20 % of the normal dose of ^{13}C-acetate. There was no octanoate in the control flapjack.

The results are shown in Tables 3.13 and 3.14. Analysis of acetate from a low pH (pH 1.5) has a high coefficient of variation (~23 %), possibly due to the volatility of the protonated compounds under these conditions. Acetate is in the form of volatile acetic acid, rather than its non-volatile sodium salt under acidic conditions, and is therefore prone to loss to the atmosphere. Nearly 80 % of the acetate dose was found in the aqueous phase at acid pH, rather than the solid phase. All the dose was in the aqueous phase after 1 h at neutral and alkaline pH. At the high dose required for ^{2}H tests, all of the acetate was in the aqueous phase after 1 h at pH 1.5. Octanoate was retained in the solid phase at low pH (~8 % release), but was released at high pH (~40 % release). More octanoate was released in neutral and alkaline conditions, as this is more water soluble in the form of its sodium salt.

Table 3.13 Yield of acetate from flapjack, % normal ^{13}C-breath test dose (1-4) or high dose, after subtraction of the blank

	Normal dose				Mean	CV (%)	High dose	Normal dose	Normal dose
	1	2	3	4					
pH	1.5	1.5	1.5	1.5			2.5	6.5	13
20 min	72	65	75	48	**65**	19	70	52	46
60 min	68	84	105	91	**87**	18	106	104	101
120 min	54	95	124	71	**86**	35	117		
Mean	65	81	101	70	**79**	24	98		
CV (%)	15	19	24	30	22		25		

Table 3.14 Yield of octanoate from flapjack, % normal ^{13}C-breath test dose

	Normal dose			Mean	CV (%)	Normal dose	
	1	2	3				
pH	1.5	1.5	1.5			6.5	13
20 min	9	10	8	**9**	11	20	24
60 min	8	8	7	**8**	8	25	36
120 min	7	10	9	**9**	18	33	50
Mean	8	9	8	**8**	12	26	37
CV (%)	13	12	13	13			

3.5 Investigation of [^{13}C]MTG metabolism

3.5.1 Variation of baseline ^{13}C abundance

Baseline variation in breath $^{13}CO_2$ abundance was measured under fasting and fed conditions in two healthy adults. The results are shown in Table 3.15. Lower breath ^{13}C abundance under fasting conditions is a reflection of lipid oxidation under these circumstances. There was less variation in background ^{13}C abundance under fasting conditions than fed conditions.

The maximum enrichment in a ^{13}C-breath test is usually not more than 100 ppm excess ^{13}C. Even in compliant subjects, under the normal conditions of a test in children i.e. with food and sitting, the standard deviation of the background breath $^{13}CO_2$ abundance was more than 5 ppm excess. Therefore, it is important to give enough substrate for the peak enrichment to be well above the background noise.

Table 3.15 Variation of baseline ^{13}C abundance (ppm) over 8 h in fasting and fed conditions after 3 d on a low ^{13}C diet

	Subject 1		Subject 2	
	Mean (ppm ^{13}C)	SD	Mean (ppm ^{13}C)	SD
Fasted	10819	1.3	10819	1.1
Fed	10828	7.0	10824	5.2

3.5.2 Effect of food intake and the test meal on cPDR

The cumulative percentage dose recovered in 6 h, calculated using different estimates of $\dot{V}CO_2$, is shown in Table 3.16. Figure 3.25 shows the recovery of $^{13}CO_2$ in breath following ingestion of 1 mg kg^{-1} body weight [1-^{13}C]acetate under fasting and fed conditions. PDR was calculated using a variable value of $\dot{V}CO_2$ estimated from HR (smoothed). The bumps in the graphs after approximately 6 h show the tendency to move around more later during prolonged breath tests. This would not be obvious if a constant value of $\dot{V}CO_2$ was used to calculate PDR.

^{13}C appeared in breath CO_2 faster when the tracer was taken in milk (both fasting and following the breakfast cereal), than when it was baked in a biscuit. This is possibly due to the faster rate of gastric emptying of the liquid meal, and thus earlier arrival at the liver. More ^{13}C was recovered in breath when the tracer was given in milk than when it was baked in a flapjack.

3.5.3 Effect of physical activity during the [^{13}C]MTG breath test

The effect of physical activity during the [^{13}C]MTG breath test was different between subjects and different from that observed during the bicarbonate breath test, where increasing physical activity tended to increase the cumulative excretion of $^{13}CO_2$ in breath. This was the case for Subject 2 (Table 3.17), but not for Subject 1. Figure 3.26 shows the excretion of $^{13}CO_2$ in breath following ingestion of 10 mg [^{13}C]MTG kg^{-1} body weight, when subjects sat still during the test and when they walked at a fairly slow pace for 7 h. The break for lunch, when the subjects stopped walking, 4 h after the test meal, can be clearly seen from the data calculated using $\dot{V}CO_2$ predicted from heart rate. There was a small increase in recovery following the second meal, when subjects remained seated. This is due to the increase in $\dot{V}CO_2$ following the meal due to diet-induced thermogenesis.

A relatively small error (< 20 %) is observed when a constant value of resting $\dot{V}CO_2$ is used to calculate PDR, if subjects remain seated throughout the test. However, use of resting $\dot{V}CO_2$ when subjects are not resting, results in a gross error, which could amount to several hundred percent in extreme cases.

Table 3.16 Effect of test meal on 6 h cPDR following 1 mg kg^{-1} [1-^{13}C]acetate

VCO_2 prediction	Subject 1			Subject 2		
Method	Fasting	Milk	Flapjack	Fasting	Milk	Flapjack
Shreeve (constant)	71.7	49.7	44.6	50.2	39.0	29.8
Schofield (constant)	64.1	44.5	39.9	48.6	37.7	28.8
Measured (constant)	61.4	39.9	38.3	46.4	33.9	27.5
HR* (variable)	63.1	46.1	41.5	36.8	34.8	26.1
PAL (HR/Measured)	1.0	1.2	1.1	0.8	1.0	1.0

* HR 2 point smoothed

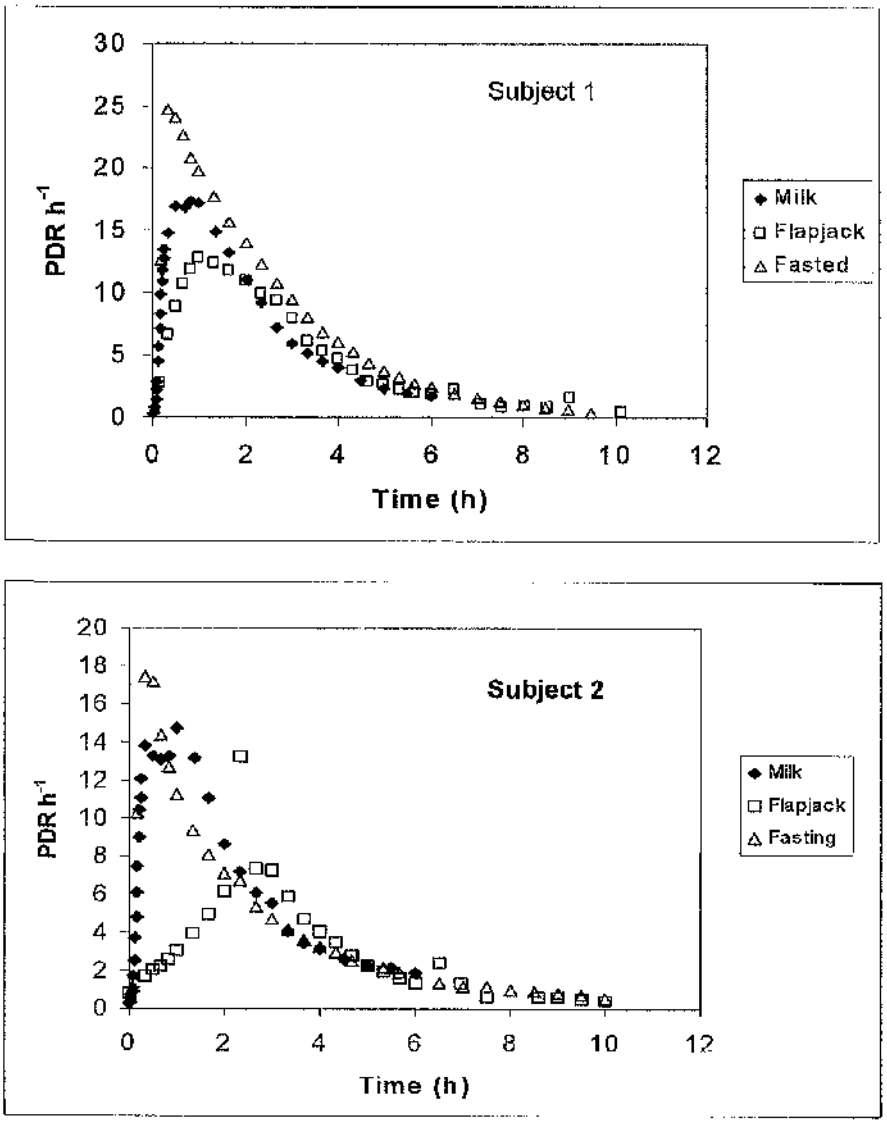

Figure 3.25 Effect of test meal on recovery of ^{13}C in breath CO_2 following ingestion of 1 mg.kg^{-1} [1-^{13}C]acetate

PDR was calculated using a variable value of VCO_2 estimated from smoothed HR.

Table 3.17 Effect of physical activity on 6 h cPDR following 10 mg kg^{-1} [^{13}C]MTG

VCO_2 prediction	Subject 1				Subject 2			
Method	Sitting		Walking		Sitting		Walking	
	6 h	10 h	6 h	8 h	6 h	10 h	6 h	10 h
Shreeve (constant)	43.1	50.4	22.2	22.8	29.2	37.0	18.1	21.8
Schofield (constant)	38.4	44.9	19.8	20.4	28.3	35.8	17.5	21.1
Measured (constant)	31.0	36.3	16.1	16.6	25.5	32.4	15.6	18.8
HR* (variable)	38.6	45.5	36.8	37.7	25.8	33.3	69.7	80.9
PAL (HR/Measured)	1.2	1.2	2.3	2.3	1.0	1.0	4.5	4.3

* HR 2 point smoothed

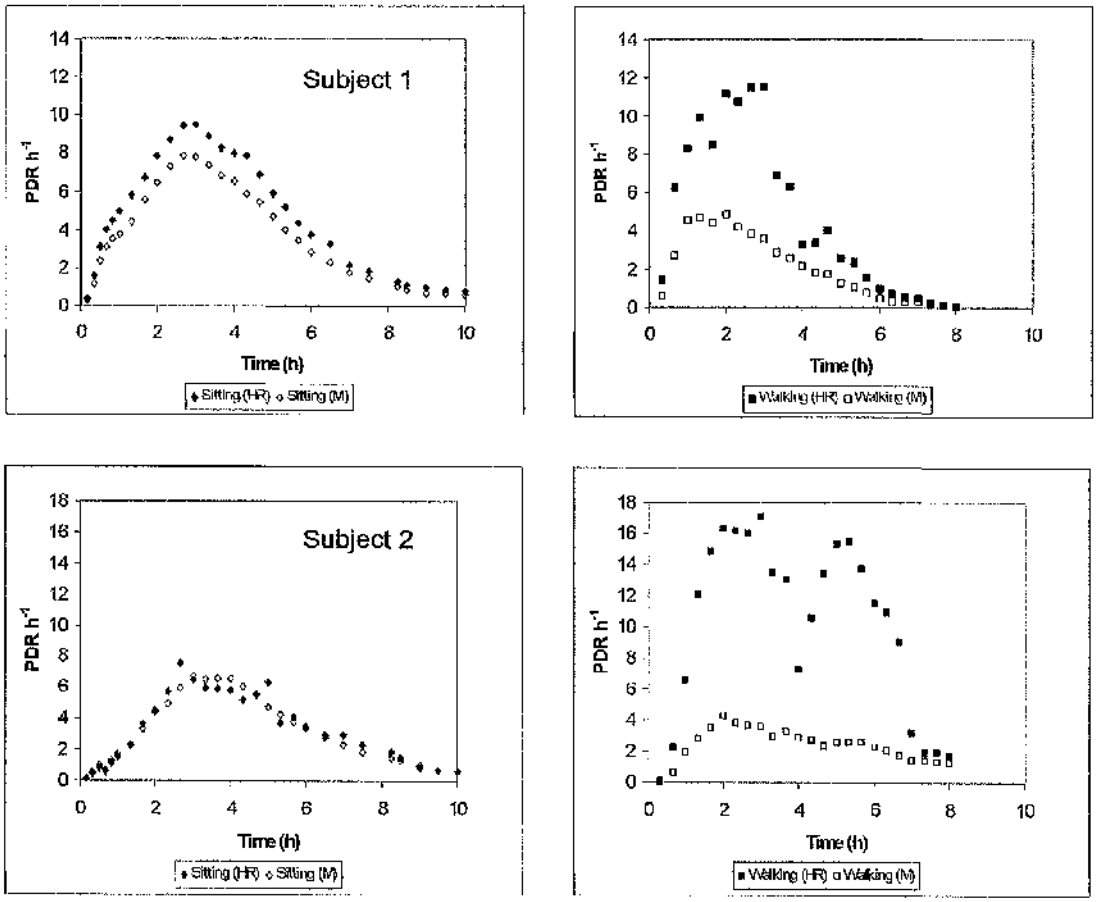

Figure 3.26 Recovery of $^{13}CO_2$ in breath (PDR h^{-1}) following ingestion of 10 mg kg^{-1} [^{13}C]MTG under resting (sitting) and non-resting (walking) conditions

PDR was calculated using VCO_2 estimated from 2 point smoothed HR using a sigmoid model (HR) or using resting VCO_2 measured by indirect calorimetry (M).

3.6 Intra-individual variation in the MTG test

3.6.1 Intra-individual variation

Intra-individual variation of breath $^{13}CO_2$ recovery was typically <7 % and judged to be within the normal limits of biological variation in these two compliant subjects, no matter which estimate of VCO_2 was used (Tables 3.18 and 3.19). The measured physical activity level was 1.0 to 1.2.

Table 3.18 Intra-individual variation of recovery of $^{13}CO_2$ in breath 6 h following ingestion of 10 mg [^{13}C]MTG kg^{-1} body weight baked in a flapjack

VCO_2 prediction	Subject 1				Subject 2			
Method	1	2	3	CV (%)	1	2	3	CV (%)
Shreeve (constant)	43.1	40.0	38.5	5.8	29.2	28.7	25.9	6.4
Schofield (constant)	38.4	35.9	34.4	5.6	28.3	27.8	25.1	6.4
Measured[$] (constant)	31.0	29.4	27.9	5.3	25.5	25.1	22.4	6.9
HR* (variable)	38.6	34.2	34.5	6.9	25.8	25.4	20.5	12.3
PAL (HR/measured)	1.2	1.2	1.2	3.7	1.0	1.0	1.0	5.7

[$]Resting VCO_2 measured using a ventilated hood indirect calorimeter. * HR 2 point smoothed

Table 3.19 Intra-individual variation of recovery of $^{13}CO_2$ in breath 10 h following ingestion of 10 mg [^{13}C]MTG kg^{-1} body weight baked in a flapjack

VCO_2 prediction	Subject 1				Subject 2			
Method	1	2	3	CV (%)	1	2	3	CV (%)
Shreeve (constant)	50.4	48.2	45.4	5.2	37.0	37.6	35.0	3.7
Schofield (constant)	44.9	43.2	40.6	5.0	35.8	36.4	33.8	3.9
Measured[$] (constant)	36.3	35.4	32.9	5.1	32.4	32.9	30.2	4.5
HR* (variable)	45.5	41.0	40.8	6.3	33.3	33.2	28.5	8.7
PAL (HR/measured)	1.2	1.2	1.2	4.2	1.0	1.0	1.0	4.4

[$]Resting VCO_2 measured using a ventilated hood indirect calorimeter. * HR 2 point smoothed

In normal healthy subjects longer sampling time results in a lower CV, as breath $^{13}CO_2$ enrichment has almost returned to baseline levels. This will not be the case for patients with impaired exocrine pancreatic function, who have not taken their PERT.

Results of [1-^{13}C]acetate breath tests were very similar to those of [^{13}C]MTG tests. Excretion of $^{13}CO_2$ in breath during 6 h following ingestion of [1-^{13}C]acetate (1 mg.kg^{-1} body weight) or [^{13}C]MTG (10 mg.kg^{-1} body weight) is shown in Tables 3.20 and 3.21.

Table 3.20 Subject 1: Intra-individual variation of $cPDR_{6h}$ following ingestion of either 1 mg [^{13}C]acetate or 10 mg [^{13}C]MTG per kg body weight

VCO_2 prediction	[^{13}C]acetate				[^{13}C]MTG			
Method	1	2	3	CV (%)	1	2	3	CV (%)
Shreeve (constant)	44.6	41.8	49.3	8.4	43.1	40.0	38.5	5.8
Schofield (constant)	39.9	37.5	44.0	8.1	38.4	35.9	34.4	5.6
Measured[$] (constant)	38.3	40.6	40.3	3.1	31.0	29.4	27.9	5.3
HR* (variable)	41.5	41.4	43.0	2.1	38.6	34.2	34.5	6.9
PAL (HR/measured)	1.1	1.0	1.1	3.1	1.2	1.2	1.2	3.7

[$]Resting VCO_2 measured using a ventilated hood indirect calorimeter. * HR 2 point smoothed

Table 3.21 Subject 2: Intra-individual variation of $cPDR_{6h}$ following ingestion of either 1 mg [^{13}C]acetate or 10 mg [^{13}C]MTG per kg body weight

VCO_2 prediction	[^{13}C]acetate				[^{13}C]MTG			
Method	1	2	3	CV (%)	1	2	3	CV (%)
Shreeve (constant)	29.8	29.3	31.4	3.6	29.2	28.7	25.9	6.4
Schofield (constant)	28.8	28.4	30.3	3.4	28.3	27.8	25.1	6.4
Measured[$] (constant)	27.5	26.8	28.5	3.1	25.5	25.1	22.4	6.9
HR* (variable)	26.1	23.3	25.0	5.7	25.8	25.4	20.5	12.3
PAL (HR/measured)	1.0	0.9	0.9	4.9	1.0	1.0	1.0	5.7

[$]Resting VCO_2 measured using a ventilated hood indirect calorimeter. * HR 2 point smoothed

3.6.2 Use of acetate and bicarbonate correction factors

The full recovery of $^{13}CO_2$ from a normal healthy subject undergoing a [^{13}C]MTG breath test with the appropriate correction factor should be close to 100 %, assuming losses in urine and faeces are small and the same for both tracers. Use of a bicarbonate correction factor underestimates oxidation of tracer, because it underestimates fixation of tracer via the TCA cycle. It is an implicit assumption that endogenous CO_2 production is the same during each test and therefore the actual values will cancel out, so it should not matter which estimation of $\dot{V}CO_2$ is used to calculate PDR. The first two MTG and the first two acetate breath tests, performed in a sitting position with the tracer baked in a flapjack, all took place within a six-month period. Therefore a 'Latin Square' design was used to calculate the recovery of tracer at 6 h in each MTG test using each acetate recovery factor from the data in Tables 3.20 and 3.21. PDR calculated using a constant value of $\dot{V}CO_2$ (300 mmol.m^{-2}.h^{-1}, after Shreeve, 1970) was used in each case. A bicarbonate recovery factor (65.7 % for Subject 1 and 58.2 % for Subject 2, from Tables 3.7 and 3.8) was also applied. The results are summarised in Table 3.22, and show that an acetate recovery factor and not a bicarbonate recovery factor is appropriate.

Table 3.22 Results of [^{13}C]MTG breath tests with acetate and bicarbonate recovery factors

Subject 1	Acetate			Bicarbonate
MTG	1	2	Mean	1
1	96.6	103.1	99.9	65.6
2	89.7	95.7	92.7	60.9
Mean	93.2	99.4	**96.3**	63.2

Subject 2	Acetate			Bicarbonate
MTG	1	2	Mean	1
1	98.0	99.7	98.8	50.2
2	96.3	98.0	97.1	49.3
Mean	97.1	98.8	**98.0**	49.7

3.6.3 MTG and acetate breath tests on the same day

Figure 3.27 shows the measured recovery of $^{13}CO_2$ in breath, together with the deconvoluted curves obtained using the Maes (1998) model, as described by Morrison (2000). Peak 1 is the MTG recovery and Peak 2 is the acetate recovery. When the total area under the curve was calculated from the model to 16 h, substrate oxidation was overestimated in both subjects. This is because recovery of ^{13}C following acetate ingestion was less than that following MTG ingestion, implying that there are additional loss routes when the label is on acetate, compared to when the label is on octanoate. The recovery of ^{13}C in 6 h was similar for both tracers in these two subjects (Table 3.23). However, it is not really feasible to perform both tests on the same day in the clinical situation, and the assumptions associated with the use of an acetate correction may not be valid. This will be discussed further in Section 4.7.

Table 3.23 Substrate oxidation (%) calculated from cPDR MTG with an acetate correction (data shown in Figure 3.27)

	Subject 1	Subject 2
Area under MTG curve (cPDR 0-16 h)	50.9	43.4
Area under Acetate curve (cPDR 0-16 h)	38.8	33.8
MTG with acetate recovery	131.1	128.3
MTG cPDR 6 h	40.7	30.6
Acetate cPDR 6 h	36.3	32.9
MTG (6 h) with acetate recovery (6 h)	112.0	93.1

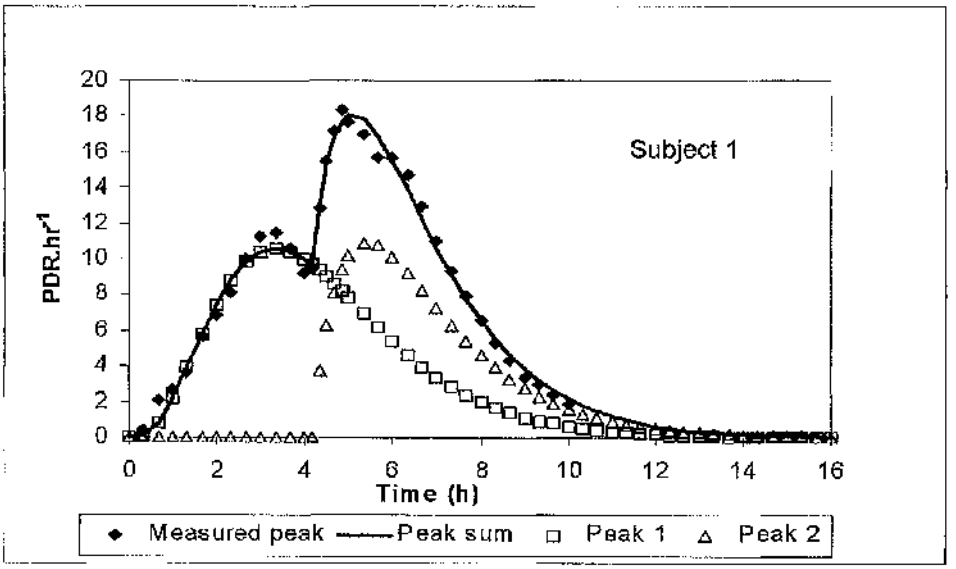

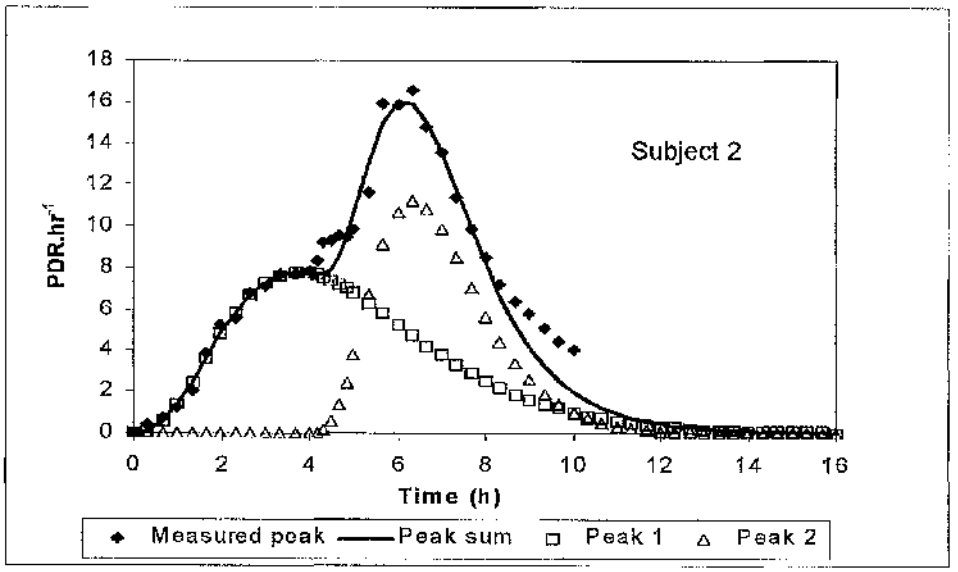

Figure 3.27 Measured and modelled MTG (peak 1) and acetate (peak 2) recovery

[^{13}C]MTG (10 mg.kg^{-1} body weight) was taken at time 0 and [1-^{13}C]acetate (1 mg.kg^{-1} body weight) was taken 4 h later.

3.7 Deuterium-labelled MTG test

3.7.1 [^{2}H]MTG-test

3.7.1.1 Recovery of tracer in breath and body water following ingestion of [^{13}C]MTG and [^{2}H]MTG in the same test meal

The rate of excretion of tracer in saliva was faster than breath (Figure 3.28) following ingestion of [^{13}C]MTG and [^{2}H]MTG. The appearance of ^{2}H in urine was slower than in saliva, as expected.

Recovery of ^{2}H in body water following ingestion of [^{2}H]MTG was compared with recovery of ^{13}C in breath CO_2 following ingestion of [^{13}C]MTG with an acetate correction and also with a bicarbonate correction. Over 90 % of the tracer was accounted for with the acetate correction, but only 40-50 % with the bicarbonate correction. The results are summarised in the Table 3.24. Breath ^{13}C recovery with bicarbonate and acetate correction factors taken from Tables 3.7 & 3.8 and 3.20 & 3.21 (cPDR calculated using $\dot{V}CO_2$ estimated from HR, when subjects were sitting quietly during the test). PDR ^{2}H was calculated from the plateau enrichment in saliva and urine. The plateau enrichment was the mean enrichment for all samples collected between 6 and 10 h after consumption of the test meal.

Table 3.24 Recovery of tracer in breath (6 h) and body water following ingestion of [^{13}C]MTG and [^{2}H]MTG in the same test meal

Test	Tracer	cPDR Calculation Method	Subject 1	Subject 2
1	^{13}C-MTG	Measured fasting, resting $\dot{V}CO_2$	31.0	25.5
2	^{13}C-MTG	Variable $\dot{V}CO_2$ estimated from HR	38.6	25.8
3	^{13}C-MTG	As 2 with bicarbonate correction	47.7	40.1
4	^{13}C-MTG	As 2 with acetate correction	91.9	104.0
5	^{2}H-MTG	Saliva	95.9	99.2
6	^{2}H-MTG	Urine	92.9	99.8

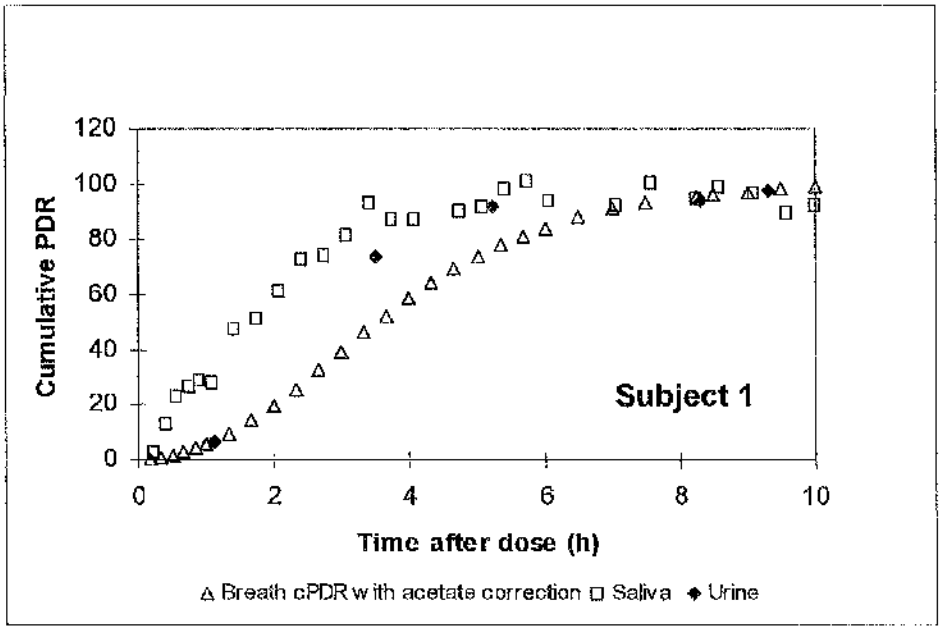

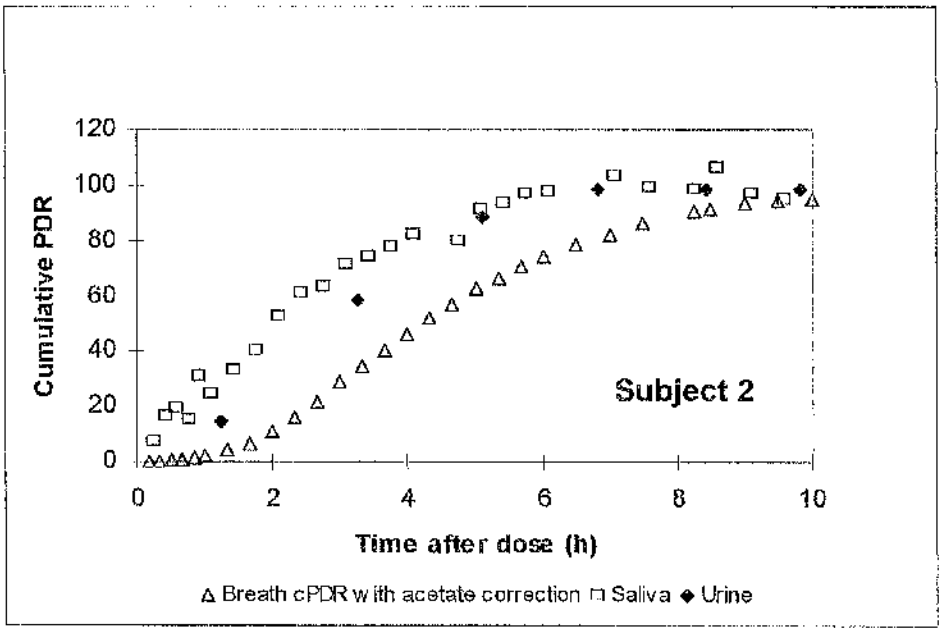

Figure 3.28 Recovery of tracer in breath, saliva and urine following ingestion of [^{13}C] and [^{2}H]MTG in the same test meal

3.7.1.2 Measurement of total body water (TBW) by ^{18}O dilution in body water

Total body water measured by ^{18}O dilution was 30.9 kg, 52.3 % body weight in Subject 1 and 42.9 kg, 53.1 % body weight in Subject 2.

3.7.2 [^{2}H]octanoate test

3.7.2.1 Recovery of tracer in breath and body water following ingestion of [^{13}C]octanoate and [^{2}H] octanoate in the same test meal

Recovery of tracer in breath, saliva and urine following ingestion of [^{13}C]octanoate and [^{2}H]octanoate in the same test meal was similar to that observed following ingestion of MTG (Table 3.35). The bicarbonate correction factor was 80.9 % for Subject 1 and 64.4 % for Subject 2. The acetate correction factor was 42.0 % for Subject 1 and 24.8 % for Subject 2.

Table 3.25 Recovery of tracer in breath (6 h) and body water following ingestion of [1-^{13}C]octanoate and [$^2H_{15}$] octanoate in the same test meal

Test	Tracer	cPDR Calculation Method	Subject 1	Subject 2
1	^{13}C-MTG	Measured fasting, resting $V\!CO_2$	33.1	32.2
2	^{13}C-MTG	Variable $V\!CO_2$ estimated from HR	42.2	30.7
3	^{13}C-MTG	As 2 with bicarbonate correction	52.2	47.7
4	^{13}C-MTG	As 2 with acetate correction	100.5	122.8
5	^{2}H-MTG	Saliva	93.1	96.2
6	^{2}H-MTG	Urine	94.2	101.4

3.7.3 [^{2}H]acetate test

3.7.3.1 Recovery of tracer in breath and body water following ingestion of [^{13}C]acetate and [^{2}H]acetate in the same test meal

Recovery of ^{13}C in breath was similar to that previously observed. PDR using $V\!CO_2$ estimated from HR was 43 % in Subject 1 and 25 % in Subject 2. PDR ^{2}H in urine was 87.3 % in Subject 1 and 90.8 % in Subject 2. This was lower than observed during the [$^2H_{15}$]MTG or [$^2H_{15}$]octanoate tests (Table 3.26).

3.7.3.2 Comparison of MTG, octanoate and acetate recovery

Differences in recovery at the plateau enrichment (6 to 12 h) were compared using a two-sample t-test (Table 3.27).

Table 3.26 Comparison of recovery of [^{2}H] in body water following ingestion of [$^2H_{15}$]MTG, [$^2H_{15}$]octanoate and [$^2H_3$]acetate

	[$^2H_{15}$]MTG	[$^2H_{15}$]octanoate	[$^2H_3$]acetate
Subject 1	92.9 (0.9)	94.2 (1.7)	87.3 (0.6)
Subject 2	99.8 (0.2)	101.4 (1.0)	90.8 (0.2)

Mean (SEM)

Table 3.27 Confidence interval (95%) for the difference in the mean recovery of [$^2H_{15}$]MTG versus [$^2H_{15}$]octanoate and [$^2H_{15}$]MTG versus [$^2H_3$]acetate

	[$^2H_{15}$]MTG v [$^2H_{15}$]octanoate		[$^2H_{15}$]MTG v [$^2H_3$]acetate	
	95% CI	P	95% CI	P
Subject 1	-6.7, 4.0	0.52	2.6, 8.6	0.007
Subject 2	-6.5, 2.4	0.19	7.1, 10.8	0.002

There was no significant difference in recovery between [$^2H_{15}$]MTG and [$^2H_{15}$]octanoate, but differences between [$^2H_{15}$]MTG and [$^2H_3$]acetate were significant at the 99 % confidence level, with subject 2 showing the greater difference. The same pattern of recovery was displayed in the ^{13}C breath tests for Subject 2, although not for Subject 1 (Table 3.28).

Table 3.28 Comparison of recovery of ^{13}C in breath CO_2 10 h after ingestion of [^{13}C]MTG and [1-^{13}C]acetate

	[^{13}C]MTG	[1-^{13}C]acetate	[^{13}C]MTG v [1-^{13}C]acetate	
	Mean (SEM)	Mean (SEM)	95% CI	P
Subject 1	45.6 (0.3)	46.6 (0.2)	-2.0, -0.2	0.03
Subject 2	32.5 (0.3)	27.9 (0.2)	3.7, 5.5	<0.001

3.7.3.3 Prediction of total body water

In the current study, TBW was measured twice by ^{18}O dilution and predicted using the Hume and Weyers (1971) or the Slater and Preston (2002) equations. Table 3.29 compares the cPDR calculated using measured TBW and predicted TBW in each of the ^{2}H tests.

Table 3.29 Comparison of TBW prediction methods to calculate cPDR in ^{2}H tests

	Measured by ^{18}O dilution		Predicted	
Subject 1 (F)	1	2	Hume & Weyers	Slater & Preston
TBW (kg)	30.9	32.5	30.2	29.7
cPDR: MTG	90.5	95.2	88.9	87.0
cPDR: octanoate	91.8	96.6	89.5	88.2
cPDR: acetate	85.1	89.5	83.2	81.7
	Measured by ^{18}O dilution		Predicted	
Subject 2 (M)	1	2	Hume & Weyers	Slater & Preston
TBW (kg)	42.9	42.7	46.3	45.4
cPDR: MTG	99.3	98.9	107.1	105.0
cPDR: octanoate	100.5	100.0	108.4	106.2
cPDR: acetate	91.0	90.6	98.2	96.2

The prediction equations slightly underestimated TBW in Subject 1 and overestimated TBW in Subject 2. The Slater & Preston (2002) equation based on height only was just as accurate as the Hume & Weyers (1971) equations based on height and weight. In the context of a non-invasive test of fat digestion, use of predicted TBW with [^{2}H]MTG may suffice.

3.7.3.3 Analysis of [$^{2}H_3$]acetate in urine

<0.5% ingested [$^{2}H_3$]acetate was excreted as [$^{2}H_3$]acetate in urine. Therefore loss of tracer via this route does not explain the differences observed above.

3.8 [^{13}C]MTG breath test in healthy adults and children

3.8.1 Recruitment of subjects

Eight healthy adults, ten healthy children and seven children with cystic fibrosis (CF) took part in the study. Their age, gender and anthropometry are shown in Table 3.30. Individual data are given in Appendix 2.

Table 3.30 Subject Characteristics

	Adult	Child	CF
N	8	10	7
Age (y)	26 (21 - 47)	10 (5 - 15)	13 (6 - 15)
Gender (M:F)	6:2	5:5	2:5
Height (cm)	179 (159 - 187)	135 (108 - 178)	146 (116 - 176)
Weight (kg)	70 (57 - 108)	38 (20 - 62)	37 (24 - 58)
BMI (kg.m^{-2})	23.1 (20.7 - 34.3)		
BMI SD score		0.89 (-0.96 to +2.54)	-0.52 (-0.87 to +1.54)

Median (range)

There was no significant difference in age or height between healthy control children and children with cystic fibrosis, but children with cystic fibrosis had a significantly lower BMI SD score ($P = 0.05$), as might be expected.

3.8.1.1 Problems of recruitment of children with cystic fibrosis

Twelve children expressed an interest in taking part in the study when initially contacted by the consultant paediatric gastroenterologist. Three withdrew after being contacted by the researcher, either because of the time commitment required or because of illness within the family. Two (siblings) failed to arrive on the day of the test. A second appointment was made, but the family cancelled this when they were contacted on the day before the test. Seven children with cystic fibrosis performed MTG breath tests, but a heart rate monitor could not be fitted to one child, who was in hospital for routine intravenous antibiotic therapy, because of the position of her portacath. There was a problem recording the HR data during the breath test in a second child, but he did complete the calibration procedure. Therefore heart rate data were only available for five children with cystic

fibrosis during the breath test, but data from the calibration procedure were obtained from six subjects. There were no problems with the calibration procedure in any child with cystic fibrosis.

3.8.2 Calibration of heart rate monitors

Results of the residual analysis of heart rate calibration methods for individual subjects are shown in Appendix 2. $\dot{V}CO_2$ was expressed as $mmol.min^{-1}.m^{-2}$ body surface area. Accuracy was defined as the difference between measured and modelled $\dot{V}CO_2$ (i.e. bias) expressed as a percentage of mean measured $\dot{V}CO_2$ for each subject. A negative bias indicates an overestimation of $\dot{V}CO_2$ by the model. Precision was defined as the standard deviation of the residuals expressed as a percentage of mean measured $\dot{V}CO_2$ i.e. the coefficient of variation. Table 3.31 shows the mean and standard error on the mean for all 24 subjects.

Table 3.31 Comparison of heart rate calibration methods

	Accuracy (%)		Precision (%)	
$\dot{V}CO_2$ prediction method	Mean	SEM	Mean	SEM
Linear-flex	-1.9	1.6	29.4	2.9
Steady-state	-7.8	2.0	35.1	3.4
3rd Order Polynomial (raw HR)	0.1	0.2	28.1	1.4
3rd Order Polynomial (smoothed HR)	-0.1	0.3	23.8	1.3
Sigmoid (raw HR)	- 0.04	0.04	26.7	1.8
Sigmoid (smoothed HR)	-0.0002	0.0002	23.2	1.5
From $\dot{V}O_2$, sigmoid raw HR, RQ=0.85	0.04	0.1	27.6	2.0

There was a significant difference (at the 95 % confidence level) between measured and predicted $\dot{V}CO_2$ using the linear flex method in 4 out of 24 subjects (17 %, 3 adults and 1 child with cystic fibrosis). The steady-state method consistently overestimated $\dot{V}CO_2$, giving significantly different estimates in 50 % of subjects (four adults, three control children and five children with cystic fibrosis). Non-linear methods, which do not make assumptions about resting metabolic rate were more accurate than linear methods. The most accurate and precise calibration method was the sigmoid model with smoothed heart rate, closely followed by the 3rd order polynomial, but the latter has the disadvantage of

overestimating $\dot{V}CO_2$ at low heart rate, therefore the sigmoid model is the preferred model. By definition, there was no significant difference between the measured and predicted $\dot{V}CO_2$, when a non-linear model was fitted to individual calibration data using the method of least squares. There were problems fitting the model to raw heart rate data in two subjects, but a solution was found for all subjects using smoothed heart rate. There was no advantage in predicting $\dot{V}CO_2$ from $\dot{V}O_2$ by assuming an RQ of 0.85. This method gave significantly different estimates of $\dot{V}CO_2$ in 50 % of subjects (five adults, five control children and two children with cystic fibrosis).

3.8.3 Comparison of methods of estimating resting metabolic rate

3.8.3.1 Estimating RMR

Insufficient resting data were obtained from the heart rate calibration procedure to adequately predict resting $\dot{V}CO_2$ in one healthy control subject (Child 2). Data from this child were excluded from the statistical analysis using heart rate calibration, but included in the rest. Resting $\dot{V}CO_2$ data was available for one child with cystic fibrosis (CF7), who could not be fitted with a heart-rate monitor. Therefore seven children with cystic fibrosis are included in comparisons which do not require heart rate data. Overall, there was no difference between using a constant value of 5 $mmol.min^{-1}.m^{-2}$ and predicting $\dot{V}CO_2$ from height and weight (Table 3.32). Use of smoothed heart rate gave a more accurate estimate of resting $\dot{V}CO_2$, than raw heart rate. Resting $\dot{V}CO_2$ estimated from raw heart rate was significantly different from the measured value at the 95 % confidence level.

Table 3.32 Difference between measured resting $\dot{V}CO_2$ and predicted resting $\dot{V}CO_2$ ($mmol.min^{-1}.m^{-2}$) including all subject groups

Prediction method	N	Mean	SEM	95 % CI	P
Shreeve	25	0.22	0.17	-0.13, 0.57	0.21
Schofield	25	-0.21	0.14	-0.49, 0.07	0.14
Raw HR*	23	-0.21	0.06	-0.38, -0.04	0.02
Smoothed HR*	23	-0.09	0.07	-0.22, 0.05	0.19

* Sigmoid model, Control child 2 and CF 7 excluded

When considering only the children, the Schofield equations gave a more accurate estimate of resting $\dot{V}CO_2$ in children with cystic fibrosis than the Shreeve method (Table 3.33). The

assumed value of 5 mmol.min^{-1}.m^2 was significantly different from resting $V\dot{C}O_2$ measured in the usual supine position. Resting $V\dot{C}O_2$ estimated from smoothed heart rate using the sigmoid model was very close to the measured value in both groups of children. This is a very important observation, because it is hoped that $V\dot{C}O_2$ will be close to resting for the majority of the time during a ^{13}C-breath test.

Table 3.33 Difference between measured resting $V\dot{C}O_2$ and predicted resting $V\dot{C}O_2$. Comparison of healthy children and children with cystic fibrosis

Prediction method	N	Mean difference mmol.min^{-1}.m^{-2}	SEM	95 % CI	P
Shreeve Control	10	0.30	0.24	-0.25, 0.85	0.25
Shreeve CF lying	7	0.92	0.23	0.35, 1.50	0.01
Shreeve CF sitting	6	0.32	0.29	-0.42, 1.06	0.32
Schofield Control	10	-0.38	0.23	-0.89, 0.14	0.13
Schofield CF lying	7	0.29	0.21	-0.22, 0.80	0.21
Schofield CF sitting	6	-0.26	0.35	-1.15, 0.64	0.50
Raw HR* Control	9	-0.28	0.18	-0.69, 0.12	0.15
Raw HR* CF	6	-0.06	0.11	-0.35, 0.22	0.59
Smoothed HR* Control	9	-0.01	0.13	-0.30, 0.28	0.95
Smoothed HR* CF	6	-0.04	0.10	-0.31, 0.22	0.68

* Sigmoid model, Control child 2 and CF 7 excluded

3.8.3.2 Effect of position on measured RMR

Resting $\dot{V}CO_2$ measured in a supine (lying) and sitting position is shown for all subjects in Appendix 3 (Table A3.1). There was no significant difference (at the 95 % confidence level) between resting $\dot{V}CO_2$ measured in a supine position and resting $\dot{V}CO_2$ measured in a sitting position in healthy subjects (Table 3.34). However, differences were significant in children with cystic fibrosis, who had a lower measured resting $\dot{V}CO_2$ in the sitting position than in the usual supine position.

Table 3.34 Results of paired t-tests on difference between resting $\dot{V}CO_2$ measured in a supine and sitting position

	N	Mean difference mmol.min^{-1}.m^{-2}	SEM	95 % CI	P
All controls	18	-0.12	0.16	-0.46, 0.22	0.46
Adult controls	8	-0.04	0.19	-0.48, 0.40	0.83
Child controls	10	-0.19	0.26	-0.77, 0.40	0.49
Children with CF	6	0.70	0.23	0.11, 1.30	0.03

The mean ± SD resting $\dot{V}CO_2$ in healthy control children (measured in a supine position) was 5.4 ± 0.7 mmol.min^{-1}.m^2. That in children with cystic fibrosis was 6.1 ± 0.5 mmol.min^{-1}.m^2. This difference was significant at the 95 % confidence level when assessed using a two-sample t-test. The 95 % CI for the difference was −1.34, -0.03. P = 0.04. However, when the measurements were made in a sitting position, there was no significant difference between $\dot{V}CO_2$ in healthy control children and $\dot{V}CO_2$ in children with cystic fibrosis. The mean $\dot{V}CO_2$ in healthy controls, who were sitting, was 5.6 ± 1.0 mmol.min^{-1}.m^2 and that in children with cystic fibrosis was 5.4 ± 0.8 mmol.min^{-1}.m^2. The 95 % CI for the difference was −0.79, 1.19. P = 0.67.

3.8.4 Postprandial or diet-induced thermogenesis

CO_2 production rate was measured in seven healthy adult subjects for 2 h following a cereal based test meal (Table 3.35). The mean $\dot{V}CO_2$ during this two-hour period (DIT) was 116 % of the fasting, resting rate (RMR) measured immediately before the meal.

Table 3.35 Effect of diet-induced thermogenesis on $\dot{V}CO_2$ following consumption of a cereal based test meal

Subject No.	Age (y)	Gender	BMI ($kg.m^{-2}$)	DIT (% RMR)
1	46	F	22.8	22.3
2	47	M	22.2	31.7
3	21	M	23.4	10.3
4	22	F	25.2	15.4
5	32	M	21.7	-0.3
6	26	M	20.7	24.1
7	26	M	34.3	8.4
Mean	31		24.3	16.0
SD	11		4.6	10.9

3.8.5 [^{13}C]MTG and [1-^{13}C]acetate breath tests

The cumulative excretion of ^{13}C in breath CO_2 at 6 h following ingestion of the test meal containing [^{13}C]MTG or [1-^{13}C]acetate is summarised in Tables 3.36 and 3.37. Cumulative PDR was calculated using a constant value of $\dot{V}CO_2$ either 5 $mmol.min^{-1}.m^{-2}$ body surface area (Shreeve), predicted from BMR (Schofield) or measured, or a variable value estimated from heart rate (HR predicted). Data from individual subjects are shown in Appendix 3 (Tables A3.2 and A3.3). Pancreatic sufficient (PS) children include all the healthy controls and one child with cystic fibrosis who did not normally take pancreatic enzyme replacement therapy. The remainder of the children with cystic fibrosis are included in the pancreatic insufficient (PI) group. Children with cystic fibrosis appear to have normal acetate metabolism. There was no significant difference between PDR calculated using measured resting $\dot{V}CO_2$ and PDR calculated using a predicted value of resting $\dot{V}CO_2$.

Table 3.36 Cumulative PDR at 6 h during the [^{13}C]MTG breath test

		Cumulative 6 h PDR (median, range)			
Subject	N	Shreeve	Schofield	Measured	HR predicted
Adults	8	33.6 (29-43)	33.1 (28-38)	30.5 (26-33)	41.5 (27-45)
PS Children	11	28.6 (18-40)	31.5 (20-40)	28.2 (17-43)	42.0 (33-62)
PI Children	5	10.5 (4-20)	12.1 (5-21)	11.2 (5-20)	16.8 (6-25)

Table 3.37 Cumulative PDR at 6 h during the [1-^{13}C]acetate breath test

		Cumulative 6 h PDR (median, range)			
Subject	N	Shreeve	Schofield	Measured	HR predicted
Adults	8	32.1 (22-45)	32.9 (23-40)	29.2 (21-38)	36.2 (27-42)
Children	9	27.0 (19-32)	33.2 (22-40)	27.8 (20-34)	44.6 (33-64)
Children with CF	3	26.1 (20-27)	30.7 (24-31)	24.6 (22-32)	37.2 (33-41)

Table 3.38 Summary of physical activity level (PAL) during the [^{13}C]MTG test

	Healthy adults	Healthy children	Children with CF
Median	1.3	1.6	1.3
Minimum	1.0	1.0	1.2
Maximum	1.6	2.2	1.5

Table 3.39 Summary of physical activity level (PAL) during the [1-^{13}C]acetate test

	Healthy adults	Healthy children	Children with CF
Median	1.2	1.7	1.4
Minimum	1.1	1.0	1.3
Maximum	1.4	2.5	1.5

All of the healthy control children and one child with cystic fibrosis performed the tests in the familiar surroundings of their own home, where there was a greater choice of activities than at the ambulatory day care unit, Royal Hospital for Sick Children, Glasgow. Two of the control children and the remainder of children with cystic fibrosis performed the test at the Royal Hospital for Sick Children. The median (range) PAL in children who performed

the test at home was 1.7 (1.1 to 2.2). The median (range) PAL in children who performed the test at the hospital was 1.3 (1.2 to 1.5).

All of the adult subjects, nine of the healthy control children and three of the children with cystic fibrosis performed both [1-^{13}C]acetate and [^{13}C]MTG tests. There was little difference in the PAL on each occasion (Tables 3.38 and 3.39), but the summary data mask individual differences in physical activity (see Tables A3.2 and A3.3). Five of the adults and six of the children had a PAL within 0.1 units on each occasion i.e. they were compliant subjects. Three of the adults, the youngest (mean age 21.3), and five of the healthy control subjects had a PAL that varied by more than 0.1 units (mean difference 0.3 units). This was consistent with the observed behaviour in these subjects.

3.9 [^{13}C]MTG tests using generic heart rate calibration

3.9.1 Search for a generic calibration

Table 3.40 Comparison of normalisation methods for a potential generic calibration method to predict $\dot{V}CO_2$ from HR (n = 24 subjects)

Normalisation method	Accuracy (%)	Precision (%)
Surface area (m^2)	0.00	49.5
Weight (kg)	0.00	46.5
Height^2 (m^2)	0.00	48.6
Height^3 (m^3)	0.00	42.7
Surface area (m^2) and age	0.00	40.8
Height^3 (m^3) and age	0.00	40.5

All methods were equally accurate as the model was fitted using the method of least squares. Normalisation to height^3 was the most precise (Table 3.40). Univariate analysis of variance revealed that age was significantly related to amplitude (constant a in equation 2.16) of the sigmoid curves fitted to data normalised to body surface area (P = 0.01) and height^3 (P = 0.06), but to no other constant. Therefore age was included in the prediction equation to estimate $\dot{V}CO_2$ from heart rate using the generic calibration for $\dot{V}CO_2$ normalised to surface area and height^3. Height^3 is an unbiased predictor of lean body mass (LBM) in all age groups (Slater & Preston, 2002). LBM comprises the major

metabolically active tissues in the body, therefore it is not surprising that it is also related to $\dot{V}CO_2$.

The results of applying generic calibrations normalised to surface area, surface area and age, height^3 and height^3 & age to each individual's heart rate (two point smoothed) during the calibration procedure are shown in Appendix 2 and summarised in Table 3.41. The ideal generic calibration would have no significant difference between measured $\dot{V}CO_2$ and $\dot{V}CO_2$ predicted using the generic calibration.

Table 3.41 Accuracy and precision of generic calibration when applied to each individual's heart rate calibration data: all subjects (n = 24)

	Accuracy (%)		Precision (%)	
$\dot{V}CO_2$ normalisation method	Mean (SEM)	Range	Mean (SEM)	Range
Surface area	-10.6 (7.2)	-104, 35	44.4 (5.0)	17, 116
Surface area and age	-7.6 (6.7)	-100, 37	42.8 (4.5)	19, 115
Height^3	-8.4 (6.6)	-96, 32	41.8 (4.5)	19, 106
Height^3 and age	-3.2 (6.2)	-84, 38	41.3 (4.1)	22, 96

Apparently reasonable mean accuracy (height^3 and age) masks an unacceptably high range, which grossly overestimates $\dot{V}CO_2$ in some subjects. This is shown by a high negative value for accuracy. This problem is worse in children than in adults. Tables 3.42 to 3.44 show accuracy and precision of the generic calibration in adults, healthy children and children with cystic fibrosis. The bias is worse in children with cystic fibrosis than healthy children, but there is a wide range in all children, compared to adults.

In adults, normalisation to surface area and age is the most accurate. This level of accuracy is acceptable for ^{13}C breath tests, but assumption of resting $\dot{V}CO_2$ should not introduce as large an error in adults as in children, as adults should be more compliant.

Table 3.42 Accuracy and precision of generic calibration when applied to each individual's heart rate calibration data: adults only (n = 8)

	Accuracy (%)		Precision (%)	
$\dot{V}CO_2$ normalisation method	Mean (SEM)	Range	Mean (SEM)	Range
Surface area	6.8 (5.7)	-15, 32	43.8 (9.8)	26, 71
Surface area and age	1.3 (6.6)	-20, 36	42.2 (9.6)	23, 72
Height^3	-3.4 (6.3)	-24, 28	41.4 (8.8)	24, 66
Height^3 and age	-4.9 (6.1)	-25, 30	39.6 (8.0)	24, 69

Table 3.43 Accuracy and precision of generic calibration when applied to each individual's heart rate calibration data: healthy children only (n = 10)

	Accuracy (%)		Precision (%)	
$\dot{V}CO_2$ normalisation method	Mean (SEM)	Range	Mean (SEM)	Range
Surface area	-14.6 (11.7)	-96, 35	43.4 (7.7)	17, 106
Surface area and age	-6.5 (10.9)	-78, 37	43.3 (6.1)	19, 86
Height^3	1.6 (11.0)	-84, 32	40.2 (7.0)	19, 100
Height^3 and age	9.5 (10.4)	-74, 38	41.8 (6.2)	22, 94

Table 3.44 Accuracy and precision of generic calibration when applied to each individual's heart rate calibration data: healthy children with cystic fibrosis (n = 6)

	Accuracy (%)		Precision (%)	
$\dot{V}CO_2$ normalisation method	Mean (SEM)	Range	Mean (SEM)	Range
Surface area	-27.3 (18.4)	-104, 20	51.8 (13.7)	22, 116
Surface area and age	-21.4 (18.5)	-100, 25	50.5 (13.6)	23, 115
Height^3	-31.7 (14.4)	-96, -3	50.7 (11.8)	24, 106
Height^3 and age	-22.1 (13.8)	-84, 4	46.1 (10.4)	23, 96

3.9.2 Use of generic calibration to estimate VCO_2 from heart rate

Cumulative percentage dose recovered in 6 h from [^{13}C]MTG and [1-^{13}C] acetate breath tests for individual subjects is shown in Appendix 3 (Figures A3.1-A3.5). Data are summarised below in Tables 3.45 and 3.46. Summary data masks the huge errors in some individuals, which is introduced by using a generic calibration method. These are more obvious in the figures in Appendix 3.

Table 3.45 cPDR (6 h) in breath CO_2 following ingestion of [^{13}C]MTG

	VCO_2 estimate				
Subject Group	IIR individual calibration	IIR generic surface area (sa)	HR generic sa & age	HR generic height^3	HR generic height^3 & age
Adults	41.5 (27-45)	42.6 (29-53)	39.7 (28-50)	47.2 (33-54)	42.3 (34-51)
PS Children	42.2 (33-62)	47.2 (31-68)	43.0 (28-64)	40.7 (26-54)	37.2 (24-47)
PI Children	16.8 (6-25)	25.4 (6-34)	21.6 (6-34)	25.4 (7-32)	22.1 (6-30)

Adults n = 8, pancreatic sufficient children n = 11 (10 healthy controls and 1 child with cystic fibrosis), pancreatic insufficient children with cystic fibrosis n = 5. Median (range)

Table 3.46 cPDR (6 h) in breath CO_2 following ingestion of [1-^{13}C]acetate

	VCO_2 estimate				
Subject Group	HR individual calibration	IIR generic surface area (sa)	HR generic sa & age	HR generic height^3	HR generic height^3 & age
Adults	36.2 (27-42)	39.9 (27-48)	37.5 (25-46)	40.0 (29-50)	37.7 (28-48)
Children	40.9 (33-64)	49.1 (30-81)	44.5 (27-76)	41.0 (25-66)	37.1 (22-63)

Adults n = 8, children n = 11 (9 healthy controls and 2 child with cystic fibrosis). Median (range)

3.9.3 Use of a generic calibration or assumed PAL: a pragmatic approach

Use of individually calibrated heart rate monitors led to complete discrimination between children with pancreatic insufficiency and those without. There was no advantage in using heart rate monitors with a generic calibration over simply assuming resting $\dot{V}CO_2$. However, if individually calibrated heart rate monitors were used to determine the reference range in healthy subjects and to estimate physical activity level during the test under realistic conditions i.e. non-resting and with food intake, then this PAL could be applied in the calculation of PDR in children with cystic fibrosis. The mean PAL in children, who performed the test at the hospital was 1.3 in this study (see Table 3.37). This PAL was applied to the cPDR calculated assuming a constant value of 5 $mmol.min^{-1}.m^{-2}$ in children with cystic fibrosis and the results compared with using an individual heart rate calibration and generic heart rate calibrations (Figure 3.29).

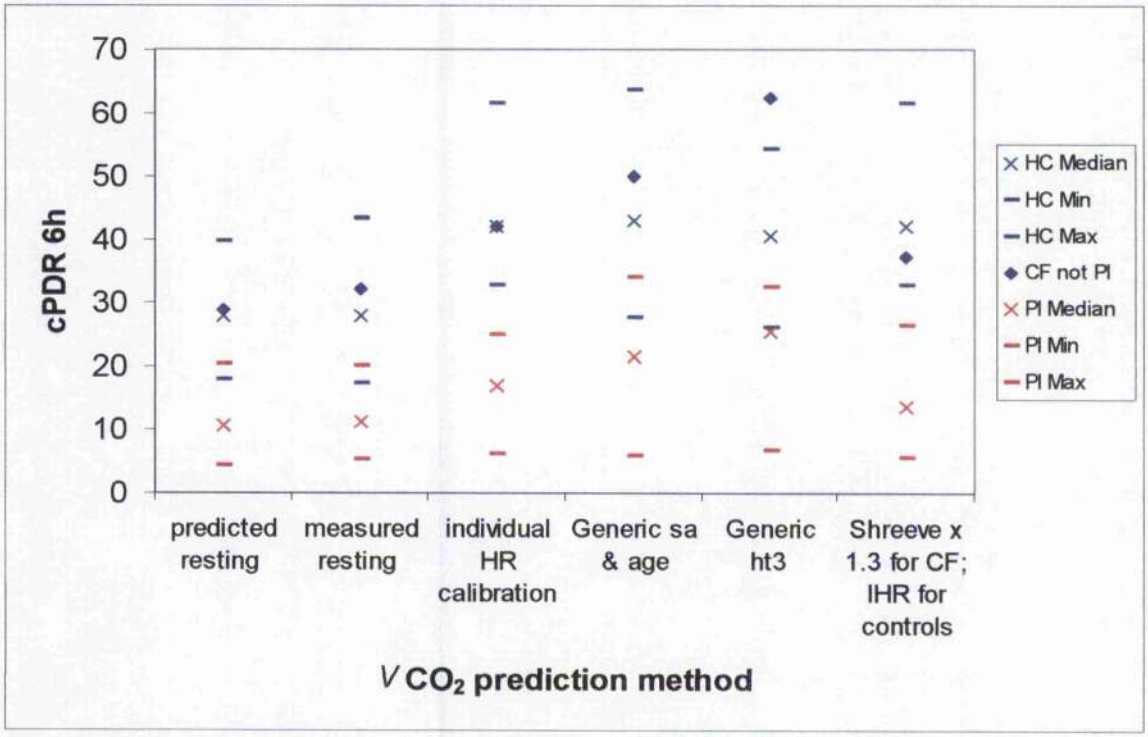

Figure 3.29 Effect of generic calibration on cPDR 6 h during [^{13}C]MTG breath test

Key: HC, healthy control subjects; PI, pancreatic insufficient; IHR, individual heart rate calibration.

The mean cPDR (6 h) in pancreatic sufficient subjects, calculated using non-resting $\dot{V}CO_2$ estimated from heart rate, was 41.5 %, standard deviation 8.5 %. Therefore, the reference range in pancreatic sufficient subjects was 25 to 58 % (mean ± 2SD, n=19). The mean

cPDR (6 h) in pancreatic insufficient subjects (n=6) was 16.1 %, standard deviation 6.0 %. When data from Amarri *et al.* (1997) were included, assuming a PAL of 1.3, the mean cPDR (6 h) in pancreatic sufficient subjects was 39.9 %, standard deviation 8.1 %, and therefore the reference range was 24 to 56 % in pancreatic sufficient subjects (n = 26). The mean cPDR (6 h) in pancreatic insufficient subjects (n = 44) was 7.7 %, standard deviation 8.7 %.

3.10 Empirical compensation for individual $\dot{V}CO_2$

When the cumulative percentage dose recovered in 6 h (cPDR 6 h) from the [1-^{13}C]acetate breath test is plotted against cPDR 6 h from the [^{13}C]MTG test, the results of subjects with normal digestion and absorption should lie either side of the line of unity. Children with exocrine pancreatic insufficiency due to cystic fibrosis have impaired digestion of triacyglycerol, but not impaired absorption and metabolism of medium- and short-chain fatty acids. Therefore, data from pancreatic insufficient subjects should lie above the unity line. This assumes that CO_2 production rate is the same during both tests. Figure 3.30 shows cPDR 6 h calculated using a constant value of resting $\dot{V}CO_2$ (5 mmol.min^{-1}.m^{-2} body surface area). The data are in Appendix 3 (Table A3.4). Figure 3.31 shows cPDR 6 h from the same subjects calculated using a variable value of non-resting $\dot{V}CO_2$ estimated from heart rate. This should take into account differences in PAL between the two breath tests and improve the discrimination of the test. Data are in Appendix 3 (Table A3.5).

Use of variable non-resting $\dot{V}CO_2$ estimated from heart rate improved the discrimination of the test, but introduced a further level of complexity over simply using the heart rate monitor to estimate physical activity level during the test. Use of $\dot{V}CO_2$ estimated from heart rate introduced a greater spread of data than use of a constant resting value. The greater range in healthy children than in healthy adults is a reflection of the more variable PAL in this group.

In some healthy subjects use of heart rate monitors brought the recovery closer to the expected value of 100 %, but not all. Children 2, 5 and 7 showed low values indicating that the recovery of acetate was higher than MTG. Four healthy subjects (two young adults and two children) had much lower recovery of acetate than MTG. These differences could be explained by differences in nutritional status on the day of the test causing a change in the balance between oxidation and lipogenesis.

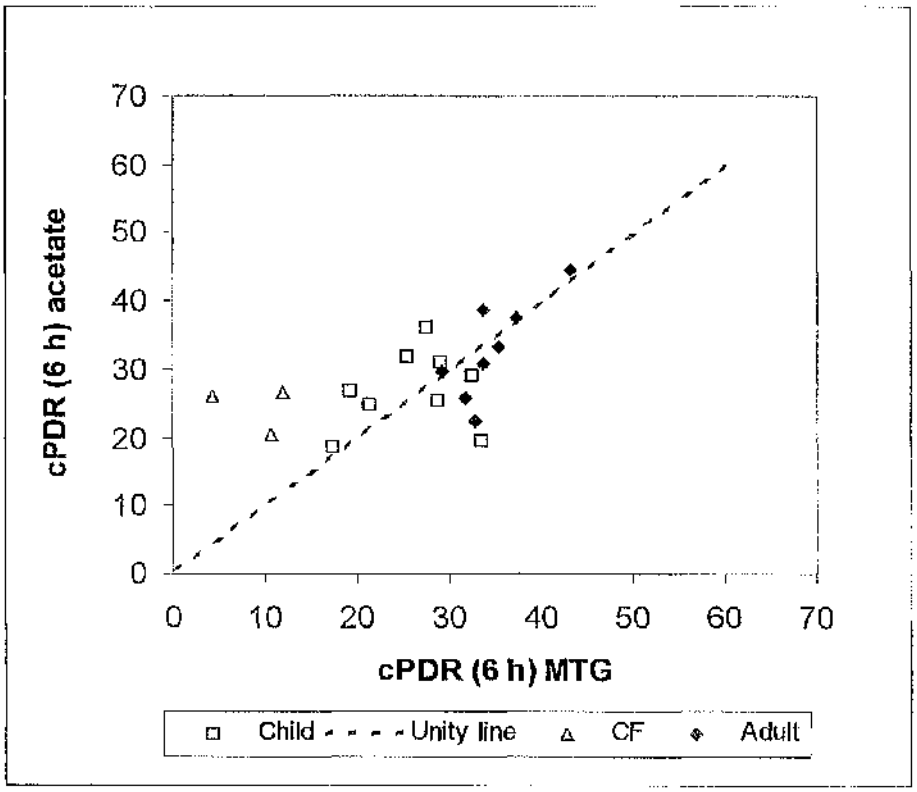

Figure 3.30 cPDR (6 h) calculated using a constant value of resting $\dot{V}CO_2$

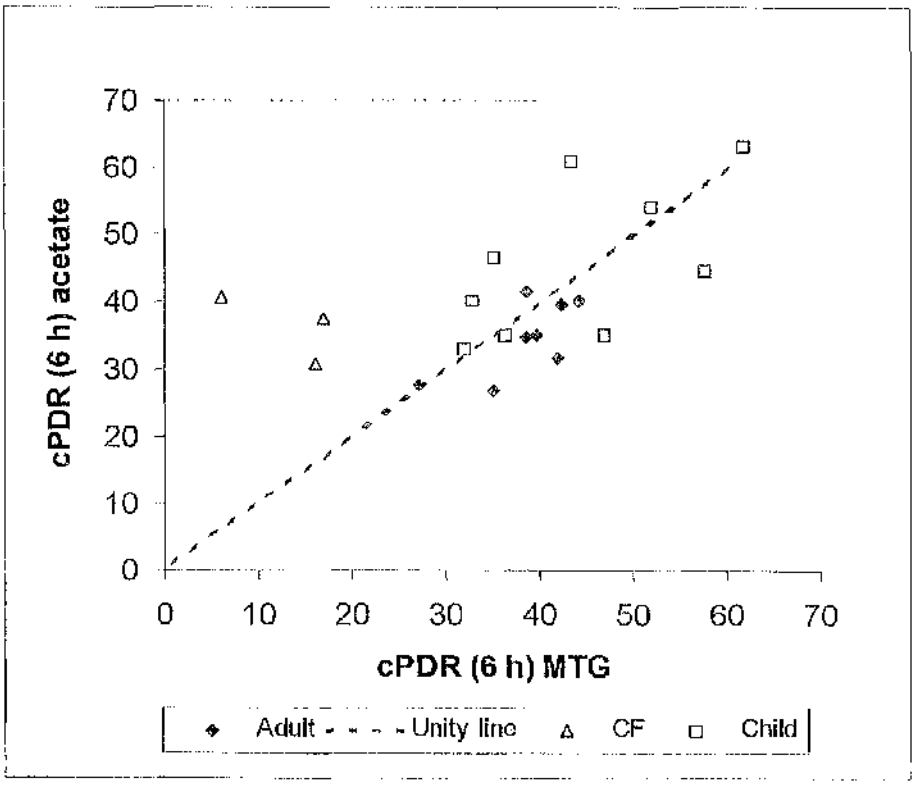

Figure 3.31 cPDR (6 h) calculated using a variable value of non-resting $\dot{V}CO_2$ estimated from heart rate

3.11 Determination of the cut-off point of the [^{13}C]MTG test

3.11.1 Determination of cut-off

The cut-off for a positive test was determined using two graph-receiver operator characteristics (TG-ROC) with non-parametric statistics, as data from the pancreatic insufficient (PI, test positive) subjects were not normally distributed. Results are shown in Tables 3.47 and 3.48.

Table 3.47 Results of TG-ROC analysis (children only, 11 PS, 6PI). PDR 6 h using $\dot{V}CO_2$ values as stated

TG-ROC output	Predicted resting	Measured resting	Predicted from HR (IHRC)	Control IHRC, CF PAL=1.3
N	17	17	17	17
Cut-off (d0, %)	20	20	30	30
Sensitivity/specificity, θ_0	0.83	0.83	1.00	1.00
Intermediate range	17, 20	18, 20		
Valid range proportion	0.92	0.95	1.0	1.0

Key: IHRC = individual heart rate calibration

Table 3.48 Results of TG-ROC analysis (adults and children, 19 PS, 6PI, except where stated otherwise). PDR 6 h using $\dot{V}CO_2$ values as stated

TG-ROC output	Predicted resting	Measured resting	Predicted from HR (IHRC)	Control IHRC, CF PAL=1.3*
N	25	25	25	70
Cut-off (d0, %)	20	20	25	26
Sensitivity/specificity, θ_0	0.86	0.86	1.00	1.00
Intermediate range	18, 20	17, 20		
Valid range proportion	0.94	0.93	1.0	1.0

Key: IHRC = individual heart rate calibration.
* combining data from this study with data from Amarri *et al.* (1997), total 26 PS, 44 PI.

3.11.2 Positive and negative predictive values

The sensitivity and specificity of the [^{13}C]MTG breath test were calculated using the cut-off points determined by TG-ROC (Table 3.48). The positive predictive value (PPV) and negative predictive value (NPV) were calculated using a disease prevalence i.e. prevalence of pancreatic insufficiency in the study population of 0.24 (6 out of 25 subjects). Results are shown in Tables 3.49 to 3.51 for PDR calculated using a constant value of resting $\dot{V}CO_2$ of 5 mmol.min^{-1}.m^{-2} (Table 3.49), constant value of measured resting $\dot{V}CO_2$ (Table 3.50) and a variable value of non-resting $\dot{V}CO_2$ predicted from heart rate (Table 3.51). Vantrappen *et al.* (1989) had a sensitivity of 0.89, specificity of 0.81, PPV of 0.63 and NPV of 0.95 in their MTG validation study in adults with pancreatic disease.

Table 3.49 Sensitivity, specificity, PPV and NPV of the [^{13}C]MTG test using a cut-off of 20 % cPDR 6 h, assuming a constant value of resting $\dot{V}CO_2$ of 5 mmol.min^{-1}.m^{-2}

	Disease +	Disease –	Total	Sensitivity	Specificity	PPV	NPV
Test +	5	2	7	0.83	0.89	0.71	0.94
Test –	1	17	18				
Total	6	19	25				

Table 3.50 Sensitivity, specificity, PPV and NPV of the [^{13}C]MTG test using a cut-off of 20 % cPDR 6 h, assuming a constant value of measured resting $\dot{V}CO_2$

	Disease +	Disease –	Total	Sensitivity	Specificity	PPV	NPV
Test +	5	2	7	0.83	0.89	0.71	0.94
Test –	1	17	18				
Total	6	19	25				

Table 3.51 Sensitivity, specificity, PPV and NPV of the [^{13}C]MTG test using a cut-off of 25 % cPDR 6 h, using variable non-resting $\dot{V}CO_2$ predicted from heart rate

	Disease +	Disease –	Total	Sensitivity	Specificity	PPV	NPV
Test +	6	0	6	1.00	1.00	1.00	1.00
Test –	0	19	19				
Total	6	19	25				

Chapter 4 Discussion

Summary of Results

The experiments described in Chapters 2 and 3 were designed to address the problem summarised at the end of Chapter 1 (Section 1.7). The hypothesis governing these studies was that the poor positive predictive value of the [^{13}C]MTG breath test for intraluminal fat digestion was due to lack of knowledge of the true CO_2 production rate during the test, assuming the accuracy of tracer dosage and isotope abundance measurements, and there were no unaccounted losses in stool or urine.

All measurements of isotope abundance and enrichment were traceable to international standards or gravimetrically prepared standard curves. *In vitro* experiments confirmed that the dose of labelled material was homogeneously distributed throughout the test meal, and there were no major losses during preparation. Urinary losses of ^{13}C as [^{13}C]bicarbonate, [^{13}C]urea and [^{13}C]acetate amounted to <5 % of the ingested dose. Loss in stool had previously been shown to be negligible in lipase sufficient subjects (Slater *et al.* 2002).

Lack of knowledge of the true CO_2 production rate can be addressed either by measuring it continuously during the test or by using an empirically derived correction to eliminate the need for its measurement. Both of these approaches were investigated. A third approach is to use a substrate that is not sequestered into the body's carbon pools. Use of deuterium labelled MTG was also investigated.

[^{13}C]Bicarbonate breath tests were used to demonstrate the feasibility of using calibrated heart rate monitors to estimate $\dot{V}CO_2$ minute-by-minute during ^{13}C breath tests. Calibrated heart rate monitors were used to estimate $\dot{V}CO_2$ during fasting, fed, resting and non-resting ^{13}C-breath tests in two healthy adults. The CV was <10 % in three [^{13}C]MTG breath tests and <5 % in three [1-^{13}C]acetate breath tests performed over an 18-month period with the same test meal, plus a second meal four hours later, and subjects sitting still as much as possible during the test.

Individually calibrated heart rate monitors were used to estimate $\dot{V}CO_2$ continually during ^{13}C breath tests in eight healthy adults, ten healthy children and six children with cystic fibrosis. The most accurate and precise method of estimating $\dot{V}CO_2$ from heart rate was use of a sigmoid model on smoothed heart rate data. Both resting and non-resting $\dot{V}CO_2$

can be estimated using this model. Over all levels of energy expenditure, the sigmoid model gave an accurate estimate of $\dot{V}CO_2$ i.e. there was no difference between measured $\dot{V}CO_2$ and $\dot{V}CO_2$ predicted using the sigmoid model, and the precision (mean CV ± SD) was acceptable (23.2 ± 7.1 %). Use of a generic calibration, to avoid the need for individual calibration, introduced unacceptably large errors.

Use of individually calibrated heart rate monitors to estimate $\dot{V}CO_2$ improved the positive predictive value of the [^{13}C]MTG test from 0.71 using resting $\dot{V}CO_2$ to 1.0 using non-resting $\dot{V}CO_2$ estimated from heart rate, and provided a way of determining the reference range of 6 h cumulative ^{13}C excretion in pancreatic sufficient subjects (24 to 58 %). The cut-off point determined using TG-ROC on data from 25 subjects was 25 %, with sensitivity, specificity, positive and negative predictive values all = 1.0. For comparison, the reference range calculated using a constant value of $\dot{V}CO_2$ of 5 mmol.min^{-1}.m^{-2} was 18 to 43 % and using a constant value of measured resting $\dot{V}CO_2$ was 17 to 40 %. In both cases the cut-off point was 20 % with sensitivity and specificity = 0.86, giving an equivocal range of 17 to 20 %. The positive predictive value was 0.71 and the negative predictive value was 0.94, which is similar to previous studies.

The mean physical activity level (PAL) in tests that were performed under clinical conditions was 1.3 times resting metabolic rate. This factor was applied to the cumulative recovery in six hours during the [^{13}C]MTG breath test data from children with cystic fibrosis (n = 45), who took part in a previous study. The results were compared with the reference range established in this study with no loss of specificity. This approach could be adopted in future [^{13}C]MTG tests, undertaken under clinical conditions, thus avoiding the need for individual heart rate calibration. The mean PAL in children who performed the tests in the familiar surroundings of their own home was 1.7, reflecting the greater choice of activities available to these children.

Acetate correction factors have been used to account for ^{13}C sequestered into body pools during studies of substrate oxidation. Children with cystic fibrosis have normal acetate metabolism. The cumulative 6 h excretion was 20 to 27 % when calculated using resting $\dot{V}CO_2$ and 33 to 41 % when calculated using non-resting $\dot{V}CO_2$ estimated from heart rate, compared with 19 to 45 % and 27 to 64 % in healthy control subjects. The median (range) recovery of ^{13}C with an acetate correction was 45 (16 to 52) % in children with cystic fibrosis and 98 (71 to 170) % in control subjects, when PDR was calculated using a

constant value of resting $\dot{V}CO_2$. It was 45 (15 to 52) % in children with cystic fibrosis and 104 (71 to 144) % in control subjects, when PDR was calculated using non-resting $\dot{V}CO_2$.

Use of acetate correction factors is not recommended as it requires two breath tests on separate occasions, and the assumptions that any deviations from basal $\dot{V}CO_2$ are the same on each occasion and that both tracers are metabolised in an identical manner following absorption, may not be valid.

Approximately 95 % ingested ^2H was recovered in body water following ingestion of [^{2}H]MTG by two healthy adults. This was compared with recovery of ^2H in body water following ingestion of [$^2H_{15}$]octanoate and [$^2H_3$]acetate by the same subjects to test the assumption that MTG, octanoate and acetate are all metabolised in the same manner. Less ^2H was recovered in body water following ingestion of [$^2H_3$]acetate (87 & 91 %) than [^{2}H]MTG (93 & 98 %) or [$^2H_{15}$]octanoate (94 & 101 %), suggesting that a greater proportion of [$^2H_3$]acetate may be sequestered, most probably during lipogenesis.

4.1 Validation of laboratory methods

Methods were established that were accurate (traceable to international standards or gravimetrically prepared standard curves), precise (SD of three replicate analyses < 1 ppm) and linear (the isotope ratio was constant over the expected concentration range). Thus, measurement of isotopic abundance could be excluded as a source of error in determining the percentage dose excreted in breath.

4.2 Measuring CO_2 production rate

4.2.1 Predicting and measuring basal/resting metabolic rate

4.2.1.1 Comparison of methods

When considering only the children, the Schofield equations predicting BMR from height and weight gave a more accurate estimate of resting $\dot{V}CO_2$ in children with cystic fibrosis than the Shreeve method (Table 3.33). The Schofield height and weight equations have been shown to be superior to the FAO/WHO/UNU and Harris-Benedict equations (Section 1.4.3.1) in children with failure to thrive (Kaplan *et al.* 1995) and in obese children (Kaplan *et al.* 1995; Rodriguez *et al.* 2002). Resting $\dot{V}CO_2$ predicted from smoothed heart

rate using a sigmoid model, was not significantly different from measured resting $\dot{V}CO_2$ in any group, but resting $\dot{V}CO_2$ predicted from raw heart rate was significantly different (Table 3.31). There are no published papers, which smooth heart rate prior to fitting a model to predict energy expenditure, and the technique has been criticised because of the failure of linear models to adequately predict low levels of energy expenditure, close to the flex point (Livingstone *et al.* 1992). This is the first study that has attempted to predict CO_2 production rate from heart rate during ^{13}C breath tests.

4.2.1.2 RQ and FQ

The mean RQ for adult subjects (n = 8) was 0.87, which is close to the assumed average value of 0.85 used to calculate $\dot{V}CO_2$ from BMR using the Schofield (1985) equations and recommended by IDECG (1990). The food quotient of the test meal, calculated as described in Section 2.4.2 from its nutritional composition and the FQ of individual fuels (Black *et al.* 1986), was also 0.85. However, the mean RQ for all subjects (n = 25) was 0.90. Children had a higher RQ than adults. The mean RQ for control children was 0.93 (n = 10) and that for children with cystic fibrosis was 0.90 (n = 7). A high RQ usually implies carbohydrate oxidation. The higher value in children may be a reflection of the fact that measurements were made approximately 3 h after their last meal, whereas adults were measured after an overnight fast. Three hours after a meal containing carbohydrate, the RQ will be closer to 1.0 because the carbohydrate in a meal is preferentially oxidised over the fat (Stubbs, 1998). After a period of starvation, such as overnight, the RQ will drop towards 0.7, as lipid replaces carbohydrate as the main energy source (Black, 1986).

Knowledge of RQ during the [^{13}C]MTG breath test would only be necessary if $\dot{V}CO_2$ were to be predicted from $\dot{V}O_2$ estimated from heart rate (Section 2.2.3.4), but data shown in Section 3.8.2 suggests that this is no more accurate or precise than estimating $\dot{V}CO_2$ directly from heart rate.

4.2.1.4 Effect of position on measured $\dot{V}CO_2$

It has been reported in the literature (Girardet *et al.* 1994; Amarri *et al.* 1998; Castro *et al.* 2002 and others) that children with cystic fibrosis have elevated resting metabolic rate compared with healthy control children. Resting metabolic rate is measured with subjects lying in a supine position. Children with cystic fibrosis had a higher CO_2 production rate when lying than when sitting (Table 3.3, Section 3.8.3.2). Resting $\dot{V}CO_2$ was significantly

higher in children with cystic fibrosis than control subjects when measurements were made in the supine position, but the difference disappeared when measurements were made in the sitting position. Children with cystic fibrosis may have greater difficulty breathing in the supine position than when sitting. Therefore, apparently elevated REE in children with cystic fibrosis may be due to the fact that REE measurements are made while subjects are lying on their back, but children with CF are not truly at rest in this position.

Girardet *et al.* (1994) found no difference in REE, expressed as kJ per day, between infants with cystic fibrosis and controls, but REE was significantly elevated in children with cystic fibrosis when expressed per kg body weight or per kg fat-free mass. A similar conclusion was reached by Bronstein *et al.* (1995) with respect to TEE in infants with presymptomatic cystic fibrosis. An apparent difference, when EE was expressed per kg body weight, disappeared once differences in body composition were taken into account by expressing EE per kg fat free mass per day or simply as kJ per day. In this study $\dot{V}CO_2$ was expressed in relation to body surface area, which takes some account of differences in body size and composition. The differences observed here cannot be explained by changes in body composition, as REE measurements were made continuously over a 30-minute interval. The elevated EE observed when children with cystic fibrosis were lying compared to sitting deserves further investigation in a larger number of children, as the supine position is rarely adopted during daily living activities, even when sleeping.

If $\dot{V}CO_2$, measured in the supine position, in children with cystic fibrosis is higher than $\dot{V}CO_2$ when these children are sitting quietly during a ^{13}C-breath test, then use of the measured "resting $\dot{V}CO_2$" to calculate PDR will slightly overestimate the cumulative excretion. There may be no advantage in using a measured value of resting $\dot{V}CO_2$ compared to a predicted value using the Schofield (1985) equations (Table 3.33). However, the magnitude of this error is small compared to other errors associated with estimation of $\dot{V}CO_2$ during the [^{13}C]MTG test, and will not make a difference to the outcome of the test in pancreatic insufficient subjects, who have little capacity for triacylglycerol hydrolysis.

4.2.2 Postprandial or diet-induced thermogenesis

The mean $\dot{V}CO_2$ during the two-hour period following the test meal was 116 % of the fasting, resting rate (RMR) measured immediately before the meal. Weststrate (1993) found that 86 % of the total observed thermic effect (over 3.5 h) was observed in the first

2 h of the postprandial period following ingestion of a test meal containing 1.9 MJ in men or 1.3 MJ in women. The energy content of the cereal-based test meal consumed in this study was approximately 1.5 MJ. In five of the seven adults, $\dot{V}CO_2$ in the last 10 min of the DIT measurement was within ±7 % of the basal value. In two subjects, $\dot{V}CO_2$ was still ~20 % above basal 2 h after the meal. DIT is usually assumed to be ~10 % TEE, which is 14 % REE, assuming PAL = 1.4, the Department of Health estimate of energy requirement for non-active activities in adults (Department of Health, 1991), and therefore REE is 71 % TEE. The thermogenic effect of the test meal is close to what would be expected for an average Western Diet, and the test meal alone could account for a PAL of 1.1 to 1.2 during the breath-sampling period. However, there is great variability between individuals, ranging from 1.0 to 1.3. Ignoring DIT would result in an underestimation of up to 30 % in the cumulative PDR during the [^{13}C]MTG breath test.

4.2.3 Calibration of heart rate monitors

4.2.3.1 Individual calibration of heart rate monitors

In this study, the accuracy of the linear calibration methods was similar to that reported in the original papers by Spurr *et al.* (1988) and Livingstone *et al.* (1992), who measured TEE using calibrated heart rate monitors. The mean difference between measured and predicted $\dot{V}CO_2$ using the liner-flex method was –1.9 % ranging from –19 to +9 % in this study, compared to an error of –2.4 % ranging from –15 to +20 % in the original study of Spurr *et al.* (1988). Using the modified linear-flex method of Livingstone *et al.* (1992), the mean difference in this study was -7.8 % ranging from –23.2 to +18.5 %, compared to –3.2 % ranging from –16.7 to + 18.8 % in the study of Livingstone *et al.* (1992). Strath *et al.* (2002), also found that the linear-flex method overestimated energy expenditure in young adults, aged 23 to 29 y.

Non-linear methods were more accurate and did not rely on assumptions about resting metabolic rate. Dauncey and James (1979) compared a logistic function with several linear calibration methods to determine energy expenditure by calibrating heart rate against heat production in a calorimeter. Use of the logistic function reduced the error for 24 h heat production from >10 % to approximately 5 %. Exponential functions (logistic and sigmoid) using smoothed heart rate gave an accurate estimate of resting $\dot{V}CO_2$ and non-resting $\dot{V}CO_2$, using a single function. This was not possible using the flex methods, because of the uncertainty at low levels of energy expenditure around the flex point

(Dauncey and James, 1979; Spurr *et al.* 1988; Livingstone *et al.* 1992). The mean difference between measured resting VCO_2 and VCO_2 predicted from smoothed heart rate using a sigmoid model was – 0.09 mmol.min^{-1}.m^{-2} body surface area (n = 23). An accurate estimate of VCO_2 at low levels of energy expenditure is especially important in the context of ^{13}C breath tests.

A third order polynomial has been used in studies of TEE in children (Beghin *et al.* 2000, 2001, 2002; Ribeyre *et al.* 2000b) , but this method overestimates energy expenditure at low levels of activity e.g. sleeping and fasting, and a second function must be used under these circumstances to avoid overestimating TEE (Beghin *et al*, 2000 and Figure 3.15). There are no published studies using a sigmoid model to predict energy expenditure from heart rate and only two, Dauncey and James (1979) and Li *et al.* (1993), using a logistic model.

All of the curve fitting in this study was done using the Solver add-in to Microsoft Excel, which is provided as part of the standard Microsoft Excel package, and is therefore widely available. Once the calculations have been set up in the spreadsheet, curve fitting in this manner is easy for a novice to learn. The residuals are determined as part of the least squares regression analysis and therefore calculation of the accuracy and precision of the model is trivial.

4.2.3.2 Generic calibration of heart rate monitors

There is a loss of precision when a generic calibration is used to estimate energy expenditure compared to using individual calibrations. An acceptable generic calibration must have a low coefficient of variation (CV). For individual heart rate calibration, the mean inter-subject precision of different calibration methods ranged from 23 to 35 %, which is similar to the CV on the slope (~22 %) and intercept (~30 %) of the linear calibration curves in the Livingstone *et al.* (1992) study. Li *et al.* (1993) obtained inter-individual CV's of 11 to 20 % using a logistic model to estimate energy expenditure in forty female cotton mill workers in Beijing. In the current study, the smallest mean inter-subject CV was obtained for the sigmoid model using smoothed heart rate (23 %, median, 22 %, range 13 to 35 % in individual subjects). The broader range of precision here is probably explained by the fact that Li *et al.* (1993) used the average steady state at each energy level to establish their model, whereas all data were included in the present study. When the generic calibration was applied to each individual's calibration data, the mean

precision in subjects aged from 5 to 47 y, was 44 % (median, 35 %, range 17 to 116 %), when $\dot{V}CO_2$ was normalised to surface area. When $\dot{V}CO_2$ was normalised to height^3, the mean precision was 42 % (median, 38 %, range 19 to 106 %).

Two studies of energy expenditure in farm animals have used a generic calibration to predict energy expenditure from heart rate in working cattle and buffalo (Richards & Lawrence, 1984; Sneddon *et al.* 1985). Richards and Lawrence (1984) found a correlation coefficient for the linear regression of energy expenditure (Watts per kg$^{0.75}$) versus relative heart rate (RHR), i.e. working heart rate/resting heart rate in two cattle and two buffalo of 0.91 with n = 49 data points. Similar results were obtained by Sneddon *et al.* (1985). In this study, the correlation coefficient for the linear regression of $\dot{V}CO_2$ (mmol.min^{-1}.m^{-2} body surface area) versus relative heart rate was 0.73 in eight adults with n = 593 data points. Although the calibration procedure for the cattle covered a fairly wide range of heart rate, RHR from 1.0 to 2.2, the live weight of the animals was only 510 kg to 630 kg. This may explain the much poorer correlation in this study, where relative heart rate was similar (1.0 to 2.4), but there was relatively a much greater range of body size (weight 57 to108 kg, BMI 21 to 34 kg.m^{-2}).

The only study in humans that has published data attempting to use a generic heart rate calibration is that of Li *et al.* (1993). They used a group calibration obtained by combining data (energy expenditure, kJ.min^{-1} and heart rate, beats min^{-1}) from half of their subjects (n– 20) and applying it to individual heart rate data from the other half. Although the mean difference in energy expenditure was fairly small (approximately 2 % of the daytime energy expenditure), there was great individual variation ranging from approximately -63 % to + 68 %, and the method was deemed to be unsatisfactory. A similar result was found in this study (Table 3.41) when the generic calibration was applied to individual heart rate data. In subjects aged from 5 to 47 y, normalisation to height^3 and age gave the most accurate generic calibration. The mean difference between measured and predicted $\dot{V}CO_2$ was –3.2 % (median +2.2 %, range –84 % to + 38 %), but the range was much smaller when only adults were considered (-25 % to +30 %). In adults, normalisation to surface area and age gave the most accurate generic calibration. The mean difference between measured and predicted $\dot{V}CO_2$ was 1.3 % (median 0.9 %, range –20 % to + 36 %), and the mean precision was 42 % (median 32 %, range 23 % to 72%). Therefore, there may be some scope for the use of heart rate monitors with a generic calibration as a compliance test in adults during ^{13}C-breath tests that last for extended periods of time, such

as studies of oro-caecal transit time and starch fermentation in the colon (Christian *et al.* 2002; Morrison *et al.* 2003b).

An alternative approach is now available, which was not on the market when this study commenced. Electronic motion sensors are now available that can apparently monitor low levels of activity e.g. the activePAL™ professional (PAL Technologies, Glasgow, UK). These were developed for use in sedentary populations, including joint-replacement and stroke patients, and could prove to be a useful tool to estimate PAL during ^{13}C-breath tests. The sensor is strapped to the upper part of the leg and can detect the duration of periods of sitting, standing and moving around. This type of device could be a useful means of testing compliance, so that the recovery of ^{13}C in each breath sample could be corrected for physical activity level. No calibration is necessary as the output is given in relative MET units (Ainsworth *et al.* 2000).

4.2.4 [^{13}C]Bicarbonate breath tests

4.2.4.1 Recovery of $^{13}CO_2$ in breath

Bicarbonate breath tests were performed to demonstrate the feasibility of using heart rate monitors to continuously measure VCO_2 under fasting, fed, resting and non-resting conditions. Recovery of labelled CO_2 after intravenous infusion of sodium [^{13}C]bicarbonate is often assumed to be ~80 % (Hoerr *et al.* 1989), but published values range from ~50 % to 100 %, depending on the length of infusion time, whether the test is performed under fasting or fed conditions and under resting or non-resting conditions. Leijssen & Elia (1996) reviewed 34 human bicarbonate studies involving 480 subjects. Overall, continuous infusions tended to have higher recovery than bolus doses (84 ± 11 % versus 69 ± 11 %). No significant differences in recovery were found between ^{14}C and ^{13}C studies, children and adults or lean and obese subjects. Higher recoveries were found during feeding than during fasting (84 ± 8 % versus 74 ± 7 %). Barstow *et al.* (1990) studied the influence of increased metabolic rate on [^{13}C]bicarbonate wash-out kinetics. Under fasting, resting conditions 67 ± 5 % of the intravenous bolus dose was recovered in breath over a four-hour period. This increased to 80 ± 11 % in two hours during light exercise. Leese *et al.* (1994) found no difference between recovery following an oral bolus dose and an intravenous bolus dose of [^{13}C]bicarbonate (63 ± 3 %, versus 62 ± 1 %). However, Meineke *et al.* (1993) observed much greater variation in recovery following administration of oral doses of [^{13}C]sodium bicarbonate in the fasted state. The mean

recovery in four hours was 64 %, but ranged from 49 % to 73 %. The authors did not attribute this variability to losses due to eructation, but low levels of eructation were observed during the present study following oral doses of bicarbonate.

When PDR was calculated using $\dot{V}CO_2$ predicted from HR (Figures 3.19-3.24 and Tables 3.7 and 3.8), the results were in line with published studies using an intravenous bolus dose of labelled tracer. Therefore individually calibrated heart rate monitors could be used to estimate $\dot{V}CO_2$ during ^{13}C-breath tests under resting and non-resting conditions. Use of resting $\dot{V}CO_2$ when subjects were not at rest underestimated the true breath excretion rate.

4.2.4.2 Recovery of ^{13}C in urine and stool

Excretion of ^{13}C in urine as [^{13}C]bicarbonate and [^{13}C]urea was measured following ingestion of [^{13}C]bicarbonate. The total urinary loss of ^{13}C was higher in fasting conditions (4.7 %) than in fed (2.2 %). This is in accordance with published values (Elia, 1991) following an intravenous infusion of labelled bicarbonate in which approximately 2 % of the infused label was recovered in urine, mainly in urea. Excretion of labelled acetate in urine following [^{13}C]acetate and [^{13}C]octanoate breath tests was also measured (data not included) and found to be < 0.5 % ingested dose.

Any [^{13}C]MTG or [^{13}C]diacylglycerol (DAG), which escapes digestion or absorption in the small intestine will enter the colon, where it may become a substrate for fermentation by colonic microflora or it may be excreted in stool. These two fates have been shown by us to be negligible in healthy children and children with cystic fibrosis taking their normal enzyme supplement (Ling *et al.* 1998, Slater *et al.* 2002).

Urinary excretion of ^{13}C is not a major pathway of loss and the sum of urinary and stool excretion probably accounts for less than 5 % ingested tracer in the [^{13}C]MTG test in healthy individuals and also children with cystic fibrosis taking their normal enzyme supplement.

4.3 Development of a test meal

A test meal was developed that could carry [^{13}C]MTG, [^{13}C]octanoate or [1-^{13}C]acetate or their deuterium labelled analogues. This was a biscuit (flapjack) composed of oats, butter and honey, which are all have low ^{13}C natural abundance so that the test meal would not

perturb the background breath ^{13}C abundance. *In vitro* experiments confirmed that the labelled material was homogeneously distributed throughout the test meal and there were no unaccounted losses during preparation.

The recipe given in Section 2.4.2 provides 3.13 MJ or approximately 17 % of the daily energy needs of two adults. Children were given a portion amounting to approximately 20 % of their estimated energy requirements. Subjects of all ages found the test meal acceptable. It was also gluten-, lactose- and egg-free, and could therefore be used in tests on subjects with special dietary needs and subjects following a vegetarian diet.

In vitro experiments showed that approximately 80 % of the acetate entered the aqueous phase under the normal acid conditions found in the stomach and all of it under neutral and alkaline conditions. These findings agree with the results of Braden *et al.* (1995), where 85 % of [^{13}C]acetate and 77 % ^{99m}Tc remained in the liquid phase after incubation of an oat-based semi-solid meal with HCl for 30 min, and are in line with the partitioning expected between aqueous and other phases. Partitioning of the tracer between solid and liquid phases of the test meal, or in the stomach, is more important in the context of gastric emptying tests than the current study, where the end point is calculation of area under the recovery curve, rather than time to some threshold. The results shown in Tables 3.13 and 3.14 suggest that the tracer was homogeneously distributed in the flapjack and not lost during preparation, implying that errors in dosage are unlikely to be a major source of error using this test meal.

4.4 Investigation of [^{13}C]MTG metabolism

4.4.1 Variation of baseline ^{13}C abundance

Calculation of cumulative $^{13}CO_2$ excretion requires knowledge of the enrichment of breath $^{13}CO_2$ above background levels. Constant background ^{13}C abundance is assumed, which requires careful control of diet on the days preceding the test and during the test to avoid foods, which are naturally enriched in ^{13}C. Background $^{13}CO_2$ abundance also depends on the nutritional status of the individual. If a person is oxidising glycogen derived glucose as their main energy substrate, breath $^{13}CO_2$ abundance will be higher than if they are oxidising lipids, assuming these macronutrients were from the same dietary source (Schoeller *et al.* 1977; Schoeller *et al.* 1984). ^{13}C-breath tests are usually performed in the resting state after an overnight fast. The change from glycogen to lipid as a fuel source is

sometimes observed as a falling baseline prior to the test. In this study, breath ^{13}C abundance was lower under fasting conditions than with food intake and is a reflection of lipid oxidation under fasting circumstances. There was less variation in background ^{13}C abundance under fasting conditions than fed conditions, but it is impractical to perform ^{13}C breath tests in children under fasting conditions.

4.4.2 Effect of food intake and the test meal on PDR in [1-^{13}C]acetate breath test

Recovery of ^{13}C in breath CO_2 following ingestion of [1-^{13}C]acetate is higher under fasting conditions than fed (Tables 3.16 and 4.1), as acetate is oxidised under fasting conditions, whereas it is directed towards lipogenic pathways under well-nourished conditions (Frayn, 1996, Mittendorfer *et al.* 1998). This is contrary to the situation following ingestion of [^{13}C]bicarbonate, where more ^{13}C is recovered in breath under fed conditions than fasted conditions (Leijssen & Elia, 1996).

Table 4.1 cPDR in 6 h following 1 mg kg^{-1} body weight [1-^{13}C]acetate under fasting and fed conditions

	Subject 1	Subject 2
Fasting	63.1	36.8
Liquid meal	46.1	34.8
Solid meal	41.5	26.1

Following a mixed meal, the carbohydrate component of the meal will be preferentially oxidised (Stubbs, 1998) and the lipids will be stored either as triacylglycerol in adipose tissue, in the case of dietary long-chain fatty acids, or incorporated into newly formed long-chain fatty acids in the case of acetate. Under normal circumstances the rates of glycolysis and of the TCA cycle are integrated, so that only as much glucose is metabolised to pyruvate as is needed to supply the TCA cycle with acetyl-CoA. Pyruvate and acetyl-CoA are normally maintained at steady-state concentrations (Nelson & Cox, 2000). But demand for energy is higher following a meal, than under fasting conditions and thus, more unlabelled CO_2 from glucose metabolism will equilibrate with the labelled bicarbonate and flush the latter from the body following a meal. When the ^{13}C label is on acetate, it is more likely to enter lipogenic pathways in the fed condition and be

sequestered in the body, whereas under fasting conditions, when glucose is in short supply, acetate is more likely to be oxidised or form ketone bodies. Ketone bodies are an important supply of fuel to muscle and brain under fasting conditions, therefore under these circumstances the label will be oxidised and appear in breath CO_2.

The form of the test meal affects gastric emptying rate and hence the time it takes for the tracer to reach the liver. If the tracer is taken in a liquid, following a solid meal, the liquid (aqueous) phase leaves the stomach first (Maes *et al.* 1996). Therefore, the labelled material will reach the liver faster when it is taken in milk (either alone or following breakfast cereal), than when it is baked in a biscuit. When the labelled material is incorporated into a solid meal, this must be broken down into smaller particles by the process of trituration, before it can leave the stomach. The amount of acetate oxidised will depend on the nutritional state of the individual and the energy provided by the meal relative to their needs.

The breakfast preceding the ingestion of [1-^{13}C]acetate dissolved in milk (liquid meal), which was composed of cereal with semi-skimmed milk and a glass of unsweetened orange juice, provided 1600 kJ (~18 % daily energy needs) for Subject 1, but only 1440 kJ (~12 % daily energy needs) for Subject 2. When the test meal was flapjack with unsweetened orange juice, it provided ~17 % of the daily energy needs of both subjects (1480 kJ for Subject 1 and 2110 kJ for Subject 2). Therefore, the energy content of the meals were similar for Subject 1 (17 versus 18 % estimated daily energy requirements) and so was the amount of tracer oxidised. However, the cereal breakfast provided less energy than the flapjack to Subject 2 (12 versus 17 % estimated daily energy requirements) and more acetate was oxidised.

A small increase in recovery was observed following the second meal in both acetate and MTG tests, even when subjects remained seated. This is due to the increase in the rate of $\dot{V}CO_2$ following the meal due to diet-induced thermogenesis (DIT), and results in ^{13}C still incorporated in TCA cycle intermediates being flushed from the body.

4.4.3 Effect of physical activity during the [^{13}C]MTG breath test

There was a difference between subjects in the metabolism of [^{13}C]MTG during gentle exercise. Subject 1, female, increased VCO_2 during exercise (PAL 2.3 compared to 1.2), but not oxidation of [^{13}C]MTG, (PDR_{6h} 38.6 % when resting compared to 36.8 % when walking). Subject 2, male, increased VCO_2 during exercise (PAL 4.5 compared to 1.0) and also substrate oxidation (PDR_{6h} 25.8 % when resting compared to 69.7 % when walking) in a similar manner to the bicarbonate breath test (PDR_{6h} in the bicarbonate breath test under non-resting conditions ~70 %). Thus, in Subject 1, [1-^{13}C]acetate produced during β-oxidation of labelled octanoate must have entered lipogenic pathways under both circumstances, whereas in Subject 2, the labelled acetate was stored under resting conditions, but oxidised during exercise. These results probably reflect inter-individual variation and depend on the nutritional status (and general fitness) of the individuals, rather than gender, as a similar observation was made by Kalivianakis *et al.* (1997), who measured recovery of ^{13}C in breath following ingestion of 4 mg [^{13}C]MTG kg^{-1} body weight in adults, who cycled at 25 to 35 % VO_{2max} for 5 h and then rested for 4 h. PDR_{9h} ranged from 25.3 % to 85.3 % and was not gender related.

The PAL of 2.3 in Subject 1 is consistent with walking at 2 mile h^{-1} at a slow pace on a firm, level surface, which has a MET intensity of 2.5 (Ainsworth *et al.* 2000). Subject 2 carried a backpack containing waterproof clothing and a snack for both subjects (approximate weight, 7 kg or 15 lb). The average pace over 8 h was approximately 3.2 km h^{-1} (2 mile h^{-1}). Walking, carrying a 15 lb load on level ground has a MET intensity of 3.5 and increases to 5 going uphill and 7.5 climbing hills with 10-20 pound load. The PAL in subject 2 was 4.5. The amount of time spent walking uphill was not noted, but there were short stretches of steep ascent. Although the PAL could not be calculated using the factorial method (FAO/WHO/UNU, 1985; Ainsworth *et al.* 2000), the PAL measured using VCO_2 estimated from heart rate is close to what might be expected and confirms that heart rate monitors can be used to estimate VCO_2 during the [^{13}C]MTG test under non-resting conditions.

4.4.4 Intra-individual variation in the MTG test

The intra-individual variation of PDR_{10h} in these two subjects was less than 10 %, which is better than 22.7 % reported by Kalivianakis *et al.* (1997). This is probably due subject compliance as repeatability was much better in some individuals than others in the

Kalivianakis study. Kalivianakis *et al.* (1999) did not state whether subjects were asked to refrain from vigorous exercise on the day before the test, as this could affect RMR (van Raaij, 2002), and therefore PDR even if subjects were compliant during the test.

4.5 [^{13}C]MTG tests using calibrated heart rate monitors

The recovery of ^{13}C, calculated using a constant value of resting $\dot{V}CO_2$, during the MTG test was in the same range as has been reported previously (Amarri *et al.* 1997; Wutzke *et al.* 1999; van Dijk-van Aalst *et al.* 2001; Slater *et al.* 2002). No matter whether resting $\dot{V}CO_2$ was measured or predicted, there was an overlap between pancreatic sufficient and pancreatic insufficient subjects in the cumulative amount of ^{13}C excreted in breath CO_2, when resting $\dot{V}CO_2$ was used in the calculation of PDR. The child with cystic fibrosis, who was not pancreatic insufficient, had cumulative excretion in the middle of the normal range. When a variable non-resting value of $\dot{V}CO_2$, predicted from heart rate was used, the populations of pancreatic sufficient and pancreatic insufficient subjects were completely resolved (Table 3.36 and Figure 3.29).

The sensitivity and specificity of the [^{13}C]MTG test, when PDR_{6h} was calculated using a constant value of resting $\dot{V}CO_2$ was 86 %, which is similar to the validation study of Vantrappen *et al.* (1989), which had a sensitivity of 89 % and specificity of 81 %. Löser *et al.* 1998 performed a validation study of the [^{13}C]MTG breath test on 27 healthy adults, 26 patients with chronic pancreatitis (13 of whom had mild and 13 severe exocrine pancreatic insufficiency), and 25 patients with non-pancreatic gastrointestinal disease. The results of the MTG breath test were compared with the results from other non-invasive tests- faecal elastase 1 concentration and faecal chymotrypsin activity. The sensitivity and specificity of the [^{13}C]MTG test for area under the curve at 5 h (PDR_{5h}) was calculated. The report does not mention CO_2 production rate, but it can probably be assumed that a constant value of 300 $mmol.h^{-1}.m^{-2}$ body surface area was assumed in the calculation of PDR. The sensitivity of the MTG test in patients with severe exocrine pancreatic insufficiency was 100 %, but it was only 46 % in patients with mild exocrine pancreatic insufficiency. Overall the sensitivity was 73 % and the specificity was 69 %, which is worse than the present study and Vantrappen's (1989) study. The faecal elastase test had a sensitivity of 92 % and specificity of 90 %, and the faecal chymotrypsin test had a sensitivity of 56 % and specificity of 82 %.

The poor sensitivity and specificity of the Löser *et al.* (1998) [^{13}C]MTG test could be due to non-compliance of some of the control subjects, with respect to remaining seated throughout the test, in which case use of resting $\dot{V}CO_2$ in the calculation of PDR is inappropriate. The cumulative excretion of ^{13}C in the breath of healthy controls ranged from ~5 to 35 %, whereas that from patients with non-pancreatic gastrointestinal disease ranged from ~15 to 35 %. Amarri *et al.* (1997) showed that children with non-pancreatic gastrointestinal disease have similar breath ^{13}C excretion to healthy controls during the [^{13}C]MTG test (20 to 35 % recovery after 6 h compared with 20 to 42 % in controls).

In the study reported in this thesis, use of individually calibrated heart rate monitors to estimate $\dot{V}CO_2$ during the [^{13}C]MTG test improved the positive predictive value of the test from 0.71, when resting $\dot{V}CO_2$ was used, to 1.0 when non-resting $\dot{V}CO_2$ estimated from heart rate was used to calculate PDR.

Individually calibrated heart rate monitors are a useful tool to determine the reference range of cumulative ^{13}C excretion in healthy children during the [^{13}C]MTG breath test. Knowledge of the reference range in healthy children is necessary to assess exocrine pancreatic insufficiency in children with cystic fibrosis. Calibrated heart rate monitors can also be used to measure physical activity during the test, so that cumulative excretion in children with cystic fibrosis can be corrected for non-resting CO_2 production rate. There was no loss of specificity when this approach was adopted using [^{13}C]MTG breath test data from children with cystic fibrosis (n = 45), who took part in a previous study (Amarri *et al.* 1997).

The measured physical activity during the MTG breath test was 1.3 in healthy adults and children with cystic fibrosis and 1.7 in healthy children, who performed the test in the familiar surroundings of their own home, where there was a greater choice of activities. The PAL measured here is closer to what would be calculated from METs (Ainsworth, 2000), than PARs (Department of Health, 1991) (see Section 1.4.3.5), reflecting the fact that the denominator is RMR, rather than BMR. Examples of MET intensities for the activities carried out during ^{13}C-breath tests are shown in Table 4.2.

Table 4.2 MET intensity (for adults) of activities carried out during ^{13}C-breath tests

Code	METS	Specific activity	Example
07010	1.0	Inactivity	Lying quietly, watching television
07011	1.0	Inactivity	Lying quietly, in bed, listening to music, not talking or reading
07020	1.0	Inactivity	Sitting quietly, watching television
07030	0.9	Inactivity	Sleeping
07070	1.0	Inactivity	Reclining - reading
09010	1.5	Miscellaneous	Sitting - playing cards, playing board games
09020	1.3	Miscellaneous	Sitting – reading book, newspaper etc.
09040	1.8	Miscellaneous	Sitting – writing, desk work, typing
09050	1.8	Miscellaneous	Standing – talking or talking on the phone
09060	1.8	Miscellaneous	Sitting – studying including reading or writing
09071	2.0	Miscellaneous	Standing
09075	1.5	Miscellaneous	Sitting-arts and crafts, light effort
09085	1.8	Miscellaneous	Standing-arts and crafts, light effort
09100	1.5	Miscellaneous	Sitting, relaxing, talking, eating
17070	3.0	Walking	Downstairs
17130	8.0	Walking	Upstairs
17150	2.0	Walking	Houschold
17152	2.5	Walking	Walking, 2 mph, slow pace, firm surface
05170	2.5	Home activities	Sitting, playing with children, light, only active periods
05175	4.0	Home activities	Walk/run, playing with children, light, only active periods

From Ainsworth *et al.* (2000)

The measured physical activity level in individual breath tests was in accordance with the observed behaviour, although activity diaries were not kept. The MET intensities shown above indicate that even short bursts of activity can lead to an underestimation of the percentage dose recovered in breath at that time if a resting value is erroneously assumed.

4.6 [^{13}C]MTG tests using generic heart rate calibration

Use of generic calibration methods appears to have more potential in adults than in children (Appendix 3, Figures A3.1 to A3.5). The generic calibration using height^3 and age proved to be useful in the healthy control child with a poor heart rate calibration that overestimated resting VCO_2 (Section 3.8.3.1), but overestimated VCO_2 in one healthy child and two children with cystic fibrosis. It also underestimated VCO_2 in one healthy child. Normalisation to surface area was no better than height^3 in the children with cystic fibrosis and grossly overestimated VCO_2 in two healthy control children for whom normalisation to height^3 gave a more accurate estimate of VCO_2. There was no advantage in using a generic calibration to estimate VCO_2 from heart rate over using a constant PAL (Section 3.9.2).

4.7 Sequestration of ^{13}C within the body

4.7.1 Empirical compensation for individual VCO_2

Once accurate methods had been established to quantify tracer exhalation in breath and other minor losses, mass balance could be used to estimate the quantity of tracer retained within the body. If oral doses of acetate are assimilated in the same manner as other fatty acids, then all the processes that occur after β-oxidation of octanoic acid are common to both labelled substrates and recovery of ^{13}C in breath CO_2 from the [1-^{13}C]acetate breath test can be used to correct the recovery from the [^{13}C]MTG test for label that is retained in the body.

The acetate correction factor accounts for label fixation that might occur at any step between the entrance of acetyl-CoA into the TCA cycle until recovery of label in breath CO_2. [1-^{13}C]acetate is the appropriate form for use with fatty acids labelled at C1. An assumption in its use is that there are no other major routes of sequestration of label and that oxidation of acetate and octanoate take place at the same rate. Less than 5 % of ingested ^{13}C is excreted in stool and urine in healthy subjects and children with cystic fibrosis taking their normal pancreatic enzyme replacement therapy (Sections 3.2.4.4, 3.7.3.3 and Slater *et al.* 2002), assuming that excretion of label as [^{13}C]bicarbonate and [^{13}C]urea is similar during the [1-^{13}C]acetate and [^{13}C]MTG breath tests as during a bicarbonate breath test (Leijssen & Elia, 1996). If these assumptions are true, then recovery in breath corrected for label sequestered in the body should be 95 to 100 % and should be similar to the recovery of ^{2}H in body water following ingestion of [^{2}H]MTG.

There was a wide range of recovery of ^{13}C, when the acetate correction factor was applied to the recovery of ^{13}C from the MTG test. Recovery ranged from 71 to 170 % of the ingested dose, with a median of 98 %, when PDR was calculated using a constant value of resting VCO_2 (i.e. the same value for each breath sample in both tests). It was 71 to 144 % with a median of 104 %, when PDR was calculated using non-resting VCO_2 estimated from heart rate, suggesting that PAL and therefore VCO_2 was not identical during both tests. In some healthy subjects use of heart-rate monitors brought the recovery closer to the expected value of almost 100 %, but not all. Four healthy subjects (two young adults and two children) had very high recovery after applying the acetate correction. This occurs when there is much lower recovery of ^{13}C following ingestion of [1-^{13}C]acetate than [^{13}C]MTG. Three healthy children showed low values after applying the acetate correction, indicating that the recovery during the acetate breath test was higher than the MTG test. These differences could be explained by differences in nutritional status on the day of the test causing a change in the balance between oxidation and lipogenesis. *De novo* lipogenesis can be fairly important on a high carbohydrate diet and might vary from one individual to another, depending on their dietary profile.

In lipogenic states, some acetate may be incorporated into newly synthesised fatty acids (Hellerstein *et al.* 1991). Thus, some label may be lost before the possible exchange with TCA cycle intermediates and/or bicarbonate. Under these circumstances the acetate correction factor overestimates substrate oxidation, because *de novo* lipogenesis occurs in the cytosol of the hepatocyte and oxidation of exogenous acetate occurs in tissues other than the liver (Gurr *et al.* 2002). The extent of overestimation depends on the rate of *de novo* fatty acid synthesis (Mittendorfer *et al.* 1998). In addition, under conditions of negative energy balance, the opposite may be true. Acetate is released from the test meal under the acid conditions of the stomach (Section 3.4.3), and is rapidly absorbed and available for oxidation in tissues other than the liver. MTG has to reach the small intestine for digestion by pancreatic lipase before the labelled octanoate can be absorbed. The labelled molecule has to enter the mitochondrion for β-oxidation prior to release of the label during the TCA cycle. Therefore, the acetate correction, in the context of ^{13}C-breath tests, depends on the nutritional status of the individual, as well as physical activity during the test, being the same on each test day. This is hard to control in free-living subjects.

Use of acetate correction factors is not recommended, as it requires two breath tests on separate occasions and the assumptions that VCO_2 is the same on each occasion, and that both tracers are metabolised in an identical manner may not valid. Ideally, the tracer used

to correct for sequestration within the body, should be administered simultaneously with [^{13}C]MTG and be subject to the same metabolic processes following absorption. Use of [1-^{14}C]octanoate, sodium salt, with [^{13}C]MTG would be better than [1-^{13}C]acetate, but this option is not available in children for ethical reasons, because of the radiation hazard involved with the use of ^{14}C, and the taste of octanoate would be unacceptable to children. From the point of view of minimising radiation dose, it would be better to use [1-^{13}C]octanoate and [^{14}C]MTG, as less radioactivity would be absorbed in the target population with pancreatic disease and most of the tracer would be excreted in stool, but this would also introduce palatability problems.

The radioactivity in breath-CO_2 resulting from the oxidation of ^{14}C-labelled tracers can be measured by liquid scintillation counting after trapping in hyamine hydroxide containing an indicator (Ozker *et al.* 1977). Maes *et al.* (1996) used simultaneous doses of [1-^{13}C]octanoate and [^{14}C]MTG to correct the rate of intraluminal lipolysis for differences in gastric emptying rate in adults, but they did not calculate percentage dose recovered for either tracer. This approach might be acceptable in adult pancreatitis patients, but not in children with cystic fibrosis.

4.7.2 Comparison of MTG, octanoate and acetate metabolism

Deuterium labelled tracers showed that recovery of label following ingestion of [$^{2}H_3$]acetate was lower than [$^{2}H_{15}$]MTG, which was similar to [$^{2}H_{15}$]octanoate. This suggests that MTG is handled in the same way as octanoate once the long chain fatty acids at the *sn*-1 and *sn*3 positions of MTG have been hydrolysed by pancreatic enzymes, but the assumption that octanoic acid is metabolised in an identical manner to exogenous acetate may be false.

In the discussion that follows, it is necessary to distinguish between exogenous acetate, which is acetate derived from the diet or from fermentation of carbohydrates in the colon, and endogenous acetate, which is acetate derived intracellularly from intermediary metabolism.

Neither exogenous acetate nor octanoate are esterified into triacylglycerol within enterocytes during absorption, because the specific acyl-CoA synthetases required for their activation are not present (Frayn, 1996). Activation is necessary before any further metabolism can take place. Therefore exogenous acetate is carried to the liver, where

acetyl-CoA synthetase (EC 6.2.1.1) is present in the cytosol. Pouteau *et al.* (1996) found that 60 % (range 42 to 79 %) of an intragastric infusion (lasting three hours) of [1-^{13}C]acetate was removed from the circulation during first-pass metabolism in the splanchnic bed of healthy human volunteers in the post absorptive state. Approximately 70 % of the tracer dose was oxidised. Recovery was less in the current study; the median (range) recovery of ^{13}C in breath CO_2 in six hours was 36 % (15 to 42 %) in adults and 41 % (33 to 64 %) in children. This is probably because the tests were performed in the fed state and therefore more tracer would be directed towards lipogenesis than oxidation.

Acetate is activated by acetyl-CoA synthetase (EC 6.2.1.1). A cytosolic acetyl-CoA synthetase is present in the cytosol of some tissues, including the liver, where it functions by activating acetate for fatty acid synthesis (Section 1.3.6.1). Carnitine acetyl-transferase (CAT) catalyses the interconversion between acetyl-CoA and acetylcarnitine. In rat liver, CAT is found in the lumen of mitochondria and peroxisomes, but is absent from the cytosol or cytosol-facing membranes and is therefore not available to cytosolic acetyl-CoA (Zammit, 1999a). The absence of a cytosolic (or cytosol-facing) CAT in the liver and acetyl-CoA synthetase in liver mitochondria, allows acetate to be transported from this tissue and to be activated and oxidised in the mitochondria of other tissues (Gurr *et al.* 2002). Therefore the main site of exogenous acetate oxidation is not the liver. Breath $^{13}CO_2$ following ingestion of [1-^{13}C]acetate arises from oxidation of the substrate in tissues other than the liver, such as skeletal muscle. In the liver, the likely fate of exogenous acetate is incorporation into long-chain fatty acids by *de novo* lipogenesis, but chain elongation in the smooth endoplasmic reticulum is also possible.

In contrast, octanoic acid is activated in the mitochondrial matrix (Zammit, 1984) prior to β-oxidation, therefore octanoic acid cannot take part in lipogenic reactions in the cytosol. Oral doses of [1-^{13}C]octanoate are rapidly oxidised to [1-^{13}C]acetyl-CoA at the first pass through the mitochondrial β-oxidation pathway (Section 1.3.5.4), mainly in the hepatocyte. [1-^{13}C]acetyl-CoA reacts with oxaloacetate to form citrate in the TCA cycle (Section 1.3.5.5). The label may eventually appear in breath CO_2, or be sequestered into organic compounds by the biosynthetic pathways and anaplerotic reactions shown in Figure 1.11. Under conditions of high rates of fatty acid oxidation, the production of [1-^{13}C]acetyl-CoA can exceed the capacity of the TCA cycle and the excess is converted by CAT to [1-^{13}C]acetylcarnitine, which must be exported from the hepatocyte or cross the endoplasmic reticular or peroxisomal membranes, for activation to [1-^{13}C]acetyl-CoA prior to further metabolism (Section 1.3.5.5). The fact that elevated acetylcarnitine

concentrations are observed in plasma under these conditions, whereas cytosolic CoA content remains sufficiently high to enable continued activation of fatty acids, suggests that very little metabolism of the acetyl units exported from the mitochondria occurs prior to its release from the cell (Zammit, 1999a). Under these conditions endogenous acetate can be metabolised in tissues other than the liver, such as skeletal muscle.

Pakula *et al.* (1997) studied the incorporation of [1-^{14}C]acetate and [1-^{14}C]octanoate into cellular lipids by HepG-2 cells. They found that the radioactivity was recovered mainly in phospholipids, rather than triacylglycerol, and was recovered exclusively in long-chain fatty acids. There would be additional fates *in vivo*. Indeed, Carnielli *et al.* (1994) found 12 % dietary octanoate in plasma triacylglycerol in premature infants fed a formula containing medium-chain triacylglycerol, suggesting that most of the octanoic acid was absorbed via the hepatic route. Label was also recovered in long-chain fatty acids (C14:0, C16:0, C18:0 and C18:1) from plasma triacylglycerol, although only C14:0 (5.3 ± 2.8 %) and C16:0 (9.1 ± 4.8 %) could be quantified due to incomplete chromatographic separation of C18:0 and C18:1. It is not possible to determine the location of the label within the molecule, when enrichment is measured by GC-combustion-IRMS.

Under the conditions of a [^{13}C]MTG breath test i.e. mainly resting and with food intake, label from both [1-^{13}C]acetate and [1-^{13}C]octanoate can be incorporated into long-chain fatty acids, but the rate will not be the same. *De novo* lipogenesis using exogenous sources of [1-^{13}C]acetate occurs in the cytosol of hepatocytes, whereas octanoate must undergo β-oxidation in the mitochondria (Figure 1.9). For the label to be incorporated into long-chain fatty acids, acetyl-CoA must be transferred from the mitochondria to the cytosol, but the mitochondrial membrane is not permeable to acetyl CoA, therefore acetyl groups cross the mitochondrial membrane in the form of citrate (Figure 1.12) or acetylcarnitine. Citrate is formed in the mitochondrial matrix by the condensation of acetyl-CoA with oxaloacetate. It can continue in the TCA cycle, but when present at high levels, citrate is transported to the cytosol, where it is cleaved by citrate lyase (EC 4.1.3.6) activity to regenerate acetyl-CoA and oxaloacetate (Stryer, 1988). The cytosolic acetyl-CoA can enter lipogenic pathways in the same way as exogenous acetate. Oxaloacetate is recycled via pyruvate.

Label from [1-^{13}C]octanoate can be incorporated into monounsaturated long-chain fatty acids after mitochondrial β-oxidation of the label from octanoic acid. There is a fatty acid chain elongation system in the mitochondria of mammalian liver, which occurs by the

addition of 2C units from acetyl-CoA to monoenoic acyl-CoAs (Gurr *et al.* 2002), but this is a minor route of endogenous fatty acid synthesis, as the products are 20:1(n-9), 22:1(n-9) and 24:1(n-9), which are not major components of body tissues (Montgomery *et al.* 2003). The more likely metabolic fate of the tracer is incorporation into amino acids via the TCA cycle or export from the mitochondrion and incorporation into long chain fatty acids via *de novo* lipogenesis in the cytosol followed by chain elongation in the endoplasmic reticulum.

4.8 The deuterium-labelled MTG test

The deuterium labelled MTG test could be a useful test of exocrine pancreatic insufficiency in its own right. Sequestration of deuterium into organic compounds is low compared to ^{13}C (Figures 4.1 and 4.2) and the test is not affected by physical activity and food intake, both of which give rise to uncertainty about the volume of distribution of the tracer in ^{13}C breath tests.

The protocol adopted here was more complex than necessary for a routine test. Firstly, as [^{13}C]MTG and [^{2}H]MTG were being used simultaneously and it was also desirable to measure TBW, the $H_2{}^{18}O$ dose was given after the ^{13}C breath test was completed in order to avoid ^{18}O interference during $^{13}CO_2$ analysis. Far more saliva samples were taken than strictly necessary so that the absorption kinetics could be compared with those of free octanoic acid and acetic acid. TBW was deliberately measured over a much longer period than necessary. The plateau formed in saliva after 4-8 h and in urine after 6-10 h would be sufficient.

The rate of excretion of tracer in saliva was faster than breath following ingestion of [^{2}H]MTG and [^{13}C]MTG (Figure 3.28). The same was observed following ingestion of [1-^{13}C]octanoate and [$^{2}H_{15}$]octanoate. The appearance of ^{2}H in urine was slower than in saliva, as expected. If [^{2}H]MTG were to be used as a routine test, an 8 h urine or saliva collection period would suffice, as the enrichment of both had reached a plateau by this time, and in children the equilibration time is faster than in adults due to their smaller body size and faster water turnover. Hourly saliva collections would be sufficient or aliquots of each urine sample passed for 6 to 8 h. It is only necessary to save 10 to 20 ml for analysis. Urine collections have the advantage that there is a large excess of sample over that required for analysis, allowing repeat analysis as necessary. They are also less prone to evaporative loss, which will cause isotope fractionation. It is difficult to collect more than 1 ml saliva at any time point, and subjects must not drink within half an hour of sampling,

therefore any food or fluid intake must be taken immediately after sampling saliva, which is particularly difficult to achieve in children. For these reasons, urine sampling is preferred over saliva sampling of the body water pool. The minimum number of samples required is one baseline sample and one post-dose sample 6 to12 h later.

The calculated PDR for both ^{2}H and ^{13}C labelled tracers depends on the accuracy of the measured, or predicted, volume of distribution of the tracer. The volume of distribution of ^{2}H is total body water (TBW) and of ^{13}C is endogenous production of CO_2 from metabolic processes. Measuring TBW during ^{2}H tests by ^{18}O dilution routinely would be impractical because of the scarcity and expense of $H_2{}^{18}O$ (~£6,000 per litre for 10% enriched $H_2{}^{18}O$, which is ~£200 per measurement for an adult subject, less for a child, but availability is unpredictable at the current time), although no additional samples would be required. Total body water could be assumed to be a fixed percentage of body weight (ICRP, 1975), but this would introduce large errors in lean or overweight adults, and in children. Prediction from height and weight (Hume & Weyers, 1971) is a possibility in adults. Alternatively, TBW can be estimated from bioelectrical impedance measurements (Hannan *et al*, 1994), but equations to calculate TBW from impedance need to be established for each group of subjects. They have not been properly validated in children (Reilly *et al.* 1996; Parker *et al.* 2003).

Slater & Preston (2002) found that TBW could be estimated from height^3 with reasonable accuracy in a wide variety of subjects (135 males and 126 females), aged from 3 to 87 y. Subjects included healthy adults, wasted cancer patients, obese adults, children with HIV and healthy children. The mean bias compared to TBW measured by isotope dilution was 0.5 kg (95 % CI 0.1 to 1.0 kg) and was less than other methods applied in this wide range of subjects as shown in Table 4.3.

Figure 4.1 Summary of loss processes of ^2H during the [^2H]MTG test

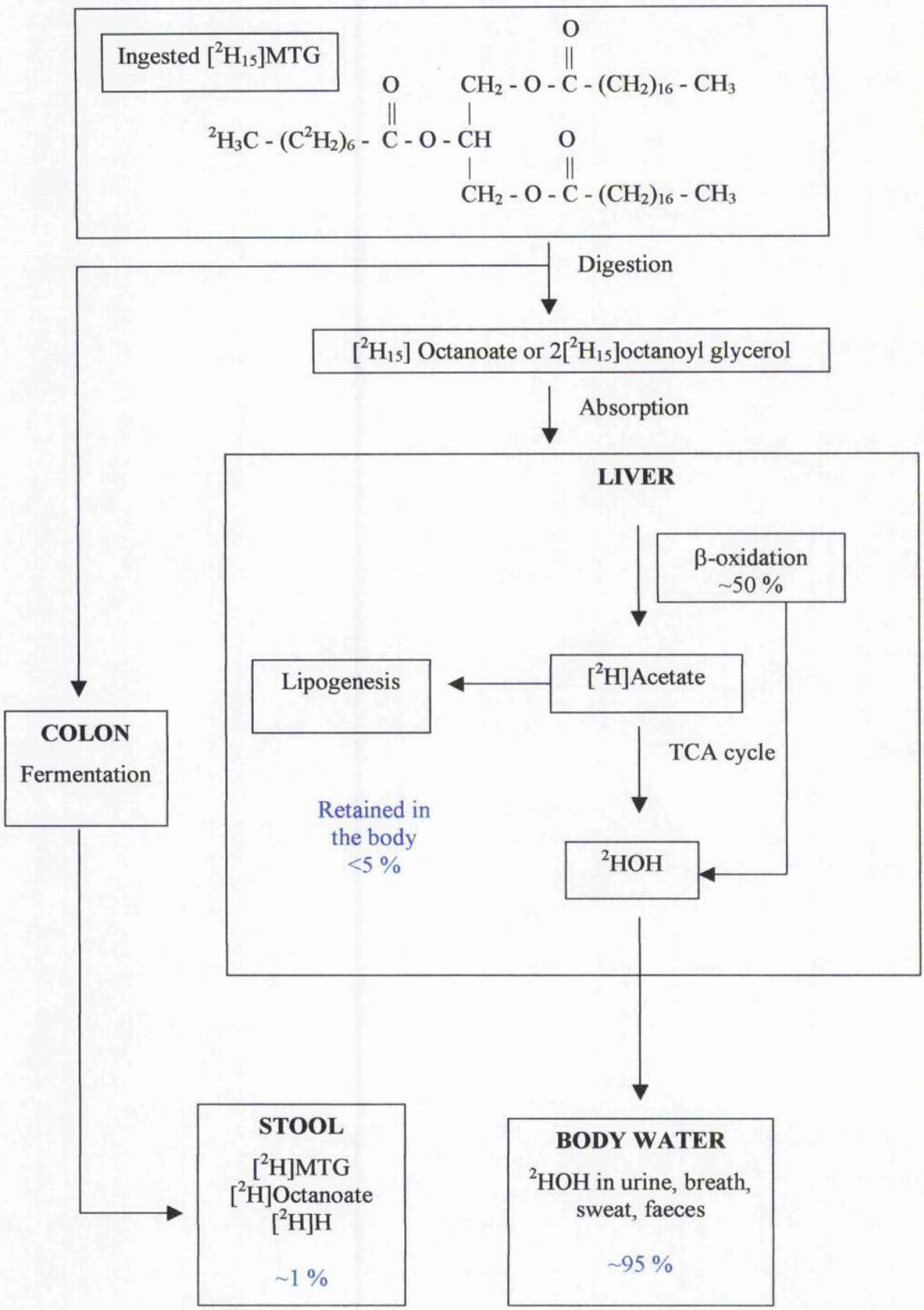

Figure 4.2 Summary of loss processes of ^{13}C during the [^{13}C]MTG breath test

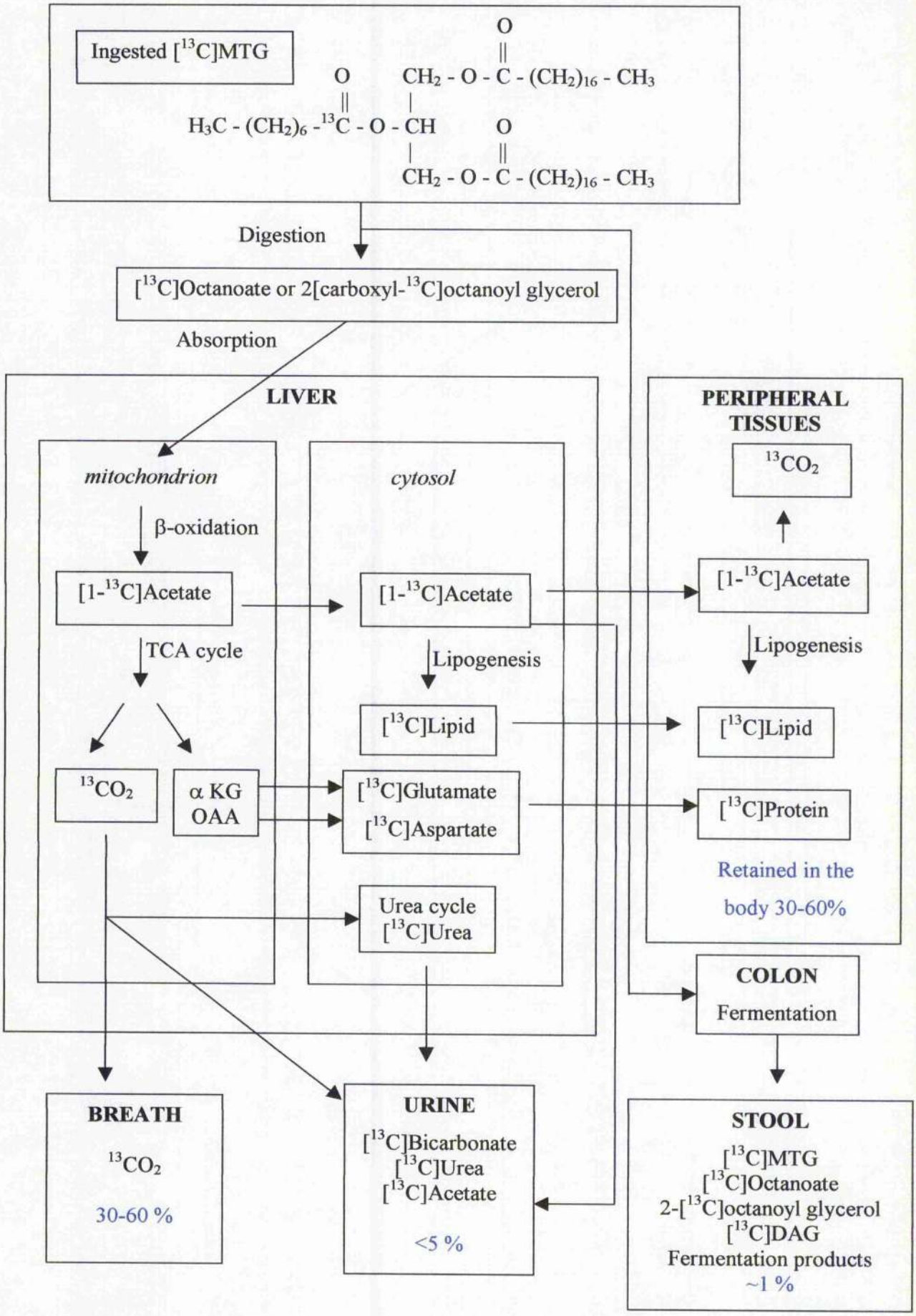

Table 4.3 Comparison of TBW prediction methods

TBW prediction method	Mean difference (kg)*	SEM	95% CI
TBW = 7.4 x Ht^3	0.55	0.22	0.11, 0.99
TBW = 0.55 x body weight	-1.95	0.28	-2.51, -1.40
Hume & Weyers	-1.20	0.26	-1.70, -0.69
BIA (n=108)	-2.12	0.22	-2.55, -1.69

*Measured TBW minus predicted TBW for all 261 subjects, unless stated otherwise.

from Slater & Preston (2002)

Table 3.28 shows that the error introduced by using a predicted value of TBW is relatively small and therefore use of a predicted value of TBW might be good enough in the context of a non-invasive test of fat digestion (~5 % error), but the problem remains that [^{2}H]MTG is not yet commercially available and ~10 times as much [^{2}H]MTG is required to label body water, as [^{13}C]MTG to label the bicarbonate pool. However, only one baseline and a minimum of one, but preferably two or three post dose urine samples are required over a period of 8 to10 h in adults and 6 to 8 h in children. Therefore the test could be performed as part of the routine annual assessment of children with cystic fibrosis to either assess the need for PERT or check that the current dose is adequate. The test could be performed overnight, if this was more practical. In this case, the test meal would be consumed in the evening and urine samples would be obtained at baseline and the following morning, as the plateau enrichment of body water is maintained for approximately 16 h.

The abundance of ^{2}H in body water spaces has been measured using Fourier transform infrared spectrophotometry (Jennings *et al.* 1999), which is less expensive instrumentation than IRMS, but studies measuring deuterium dilution by this technique have used ten times the normal dose of ^2H_2O to achieve sufficient analytical precision (Wells *et al.* 1999, Cisse *et al.* 2002). It would be prohibitively expensive to use doses of [^{2}H]MTG at this level, which would amount to approximately 50 g for a child weighing 30 kg.

The advantages and disadvantages of the [^{2}H]MTG test and [^{13}C]MTG test are compared in Figure 4.3, but the [^{2}H]MTG test could be a simpler, more robust non-invasive test of fat digestion, if the tracer were available at a reasonable cost. Both tests avoid the need for stool sampling, which is greatly disliked by patients and their parents.

Advantages of the [^{13}C]MTG breath test

1. Requires 10-15 times less tracer than the [^{2}H]MTG test
2. No sample preparation prior to analysis
3. Continuous flow IRMS gives fast, accurate ^{13}C analysis in breath CO_2
4. Relatively inexpensive in terms of tracer and analytical costs

Disadvantages of the [^{13}C]MTG breath tests

1. The volume of distribution of the tracer is subject to fluctuation due to physical activity and postprandial thermogenesis

Advantages of the [^{2}H]MTG test

1. Only one pre-dose and one post-dose sample of urine taken between 6 and 16 h post-dose are necessary to calculate PDR
2. Total body water can be estimated from height

Disadvantages of the [^{2}H]MTG test

1. Tracer cost is very high, although $^{2}H_2O$ is relatively inexpensive, therefore the cost of [^{2}H]MTG per gram could be cheaper than [^{13}C]MTG. Lower tracer dosage would be possible but may result in greater analytical cost.

Figure 4.3 Comparison of [^{13}C] and [^{2}H]MTG tests

An ideal pancreatic function test would be inexpensive, easily performed, repeatable and reliable (Couper *et al.* 2002). It should be specific for pancreatic disease and able to define the exact level of pancreatic function in subjects with pancreatic insufficiency in whom partial impairment of exocrine function is present, but nutrient assimilation is unaffected. There should be no interference from pancreatic enzyme supplements. Unfortunately, the ideal test does not exist, but the [^{2}H]MTG test may come close.

Chapter 5 Conclusions

- Use of individually calibrated heart rate monitors to estimate $\dot{V}CO_2$ during the [^{13}C]MTG test increased the positive predictive value of the test from 0.71 using resting $\dot{V}CO_2$ to 1.0 using non-resting $\dot{V}CO_2$ estimated from heart rate.

- Individually calibrated heart rate monitors can be used to estimate the physical activity level during tests that are performed under realistic conditions, which did not require children to sit absolutely still for six hours and include a second meal during the test.

- Individually calibrated heart rate monitors are a useful tool to determine the reference range of cumulative ^{13}C excretion in healthy children during the [^{13}C]MTG breath test.

- The cumulative excretion of ^{13}C in the breath of children with cystic fibrosis can be corrected for non-resting CO_2 production rate once the physical activity level during the test has been determined. There was no loss of specificity when this approach was adopted using [^{13}C]MTG breath test data from children with cystic fibrosis (n = 45), who took part in a previous study in the same clinical setting.

- Use of an acetate correction factor to account for tracer sequestered in the body during [^{13}C]MTG breath tests is not recommended as it requires two breath tests on separate occasions, and the assumptions that $\dot{V}CO_2$ is the same on each occasion and both tracers are metabolised in an identical manner following absorption may not be valid.

- The [^{2}H]MTG test may provide a simpler, more robust non-invasive test of fat digestion, if supplies of this novel stable isotope labelled tracer are secured. The test could be performed during the annual assessment of children with cystic fibrosis, as the results are not affected by physical activity or food intake during the test.

- A major advantage of both MTG tests of fat digestion, and therefore indirectly of exocrine pancreatic function, is the avoidance of stool sampling, which is necessary for the other commonly used tests i.e. faecal elastase test and fat balance measurements.

Chapter 6 Recommendations for further work

6.1 Clinical validation studies

A clinical validation study comparing simultaneous [^{13}C]MTG and [^{2}H]MTG tests with the best currently available non-invasive test of exocrine pancreatic function in children with cystic fibrosis, i.e. the faecal elastase-1 test (Löser *et al.* 1998; Nousia-Arvanitakis, 2003) is recommended.

Use of recently introduced "intelligent" electronic motion sensors that can monitor low levels of activity, but do not require calibration should be investigated. These could be used to estimate the physical activity level around the time of each breath sample, so that the recovery in the [^{13}C] test can be adjusted for non-resting conditions as necessary.

The sensitivity and specificity of the faecal elastase test should be compared with the new [^{13}C]MTG test that includes a compliance test for physical activity during the MTG test and a second meal to avoid problems associated with falling background $^{13}CO_2$ abundance in fasted subjects.

The sensitivity and specificity of the faecal elastase test should be compared with that of the [^{2}H]MTG test.

A clinical validation study of the improved [^{13}C]MTG test versus the [^{2}H]MTG test and faecal elastase test should be carried out in adults with pancreatic disease, who display a wider range of pancreatic insufficiency than children with cystic fibrosis.

6.2 Macronutrient metabolism

6.2.1 Lipid metabolism

[1-^{13}C]acetate has been used in an analogous way to that described in this thesis to provide acetate correction factors in studies of lipid metabolism (Sidossis, 1995a). Mass isotopomer distribution analysis (MIDA) is a technique for studying the biosynthesis and turnover of macronutrients *in vivo* (Hellerstein & Neese, 1992; 1999). The method has potential for measuring fatty acid and cholesterol metabolism (Hellerstein, 1995) and has been used to measure *de novo* lipogenesis and re-esterification of fatty acids (Hellerstein *et*

al. 1993), but large quantities of very expensive tracers are required. Recently, a method was introduced using a very inexpensive tracer (^2H_2O) to measure triglyceride synthesis and turnover *in vivo* (Turner *et al.* 2003). Methods utilising [1,2-^{13}C]acetate or [$^2H_3$]acetate and MIDA may have potential for studying the effect of exogenous acetate production on lipid metabolism *in vivo*, and hence investigation of mechanisms of prevention of coronary heart disease.

6.2.2 Protein metabolism

Some of the current problems of protein metabolism concern the quantitation of the breakdown rate of key proteins, particularly in inflammatory disease (Preston *et al*, 1998). [1-^{13}C]acetate can be used as an intrinsic tracer delivering labelled carbon atoms to aspartate and glutamate through TCA cycle intermediates. Because these labels are either rapidly exchanged or incorporated into protein, they can potentially be used to measure protein degradation (Millward, 1970).

6.2.3 Carbohydrate metabolism

Acetate is as important an intermediate in carbohydrate metabolism as it is in lipid metabolism. Oral doses of [^{13}C]acetate can be used to measure total acetate production in studies of colonic fermentation of carbohydrate. Carbohydrates that are not digested by small intestinal enzymes reach the colon, where they are substrates for fermentation by the colonic microflora. The products of carbohydrate fermentation are short-chain fatty acids, principally acetate, propionate and butyrate. Intravenous administration of labelled acetate will underestimate total acetate production, because no account is taken of endogenous acetate removed during first pass metabolism in the splanchnic bed. For instance, Wolever *et al.* (1995) found significantly more ^{13}C in serum lipids after rectal than intravenous adminstration of [1,2-^{13}C]acetate.

The potential health benefits of foods containing slowly digestible and resistant starch, and the effect of food processing on the digestion and metabolism of starchy foods is an area of active research interest e.g. the EU Eurostarch project (www.eurostarch.org), "Stable isotope applications to monitor starch digestion and fermentation for the development of functional foods". Consumption of plant-based cereal foods containing slowly digestible and resistant starch could be beneficial in the prevention of colon cancer and the prevention and treatment of obesity and type 2 diabetes, which are major issues of public

health concern. Chronic diseases such as the metabolic syndrome and cancer have been attributed to the "Western Lifestyle" with lack of physical activity and a diet containing too much fat and refined carbohydrates.

Bibliography

Ainsworth BE, Haskell WL, Whitt MC, Irwin MA, Swartz AM, Strath SJ, O'Brien WL, Bassett DRJr, Schmitz KH, Emplaincourt PO, Jacobs DRJr & Leon AS (2000) Compendium of physical activities: an update of activity codes and MET intensities. *Medicine & Science in Sports & Exercise* **32,** S498-S516.

Ainsworth BE, Haskell WL, Leon AS, Jacobs DRJr, Montoye HJ, Sallis JF & Paffenbarger RSJr (1993) Compendium of physical activities: classification of energy costs of human physical activities. *Medicine & Science in Sports & Exercise* **25,** 71-80.

Alton EWFW & Smith SN (2000) Applied cell biology. In *Cystic fibrosis,* 2nd edition, pp. 61-80. [ME Hodson & DM Geddes, editors]. London: Arnold.

Amarri S, Coward WA, Harding M & Weaver LT (1998) Importance of measuring CO_2-production rate when using ^{13}C-breath tests to measure fat digestion. *British Journal of Nutrition* **79,** 541-545.

Amarri S, Harding M, Coward WA, Evans TJ & Weaver LT (1997) ^{13}Carbon mixed triglyceride breath test and pancreatic enzyme supplementation in cystic fibrosis. *Archives of Disease in Childhood* **76,** 349-351.

Amarri S & Weaver LT (1995) ^{13}C-breath tests to measure fat and carbohydrate digestion in clinical practice. *Clinical Nutrition* **14,** 149-154.

Armon Y, Cooper DM, Springer C & Barstow TJ (1990) Oral [^{13}C]bicarbonate measurement of CO_2 stores and dynamics in children and adults. *Journal of Applied Physiology* **69,** 1754-1760.

Bach AC, Ingenbleek Y & Frey A (1996) The usefulness of dietary medium-chain triglycerides in body weight control: fact or fancy? *Journal of Lipid Research* **37**(4), 708-726.

Bar-Or T, Bar-Or O, Waters H, Hirji A & Russel S (1996) Validity and social acceptability of the Polar Vantage XL for measuring heart rate in preschoolers. *Pediatric Exercise Science* **8,** 115-121.

Barber MD, Ross JA, Voss AC, Tisdale MJ & Fearon KCH (1999) The effect of an oral nutritional supplement enriched with fish oil on weight-loss in patients with pancreatic cancer. *British Journal of Cancer* **81,** 80-86.

Barr RG, Perman JA, Schoeller DA & Watkins JB (1978) Breath tests in pediatric gastrointestinal disorders: new diagnostic opportunities. *Pediatrics* **62,** 393-401.

Barstow TJ, Cooper DM, Sobel EM, Landaw EM & Epstein S (1990) Influence of increased metabolic rate on [^{13}C]bicarbonate washout kinetics. *American Journal of Physiology* **259,** R163-R171.

Beghin L, Budniok T, Vaksman G, Boussard-Delbecque L, Michaud L, Turck D & Gottrand F (2000) Simplification of the method of assessing daily and nightly energy expenditure in children, using heart rate monitoring calibrated against open circuit indirect calorimetry. *Clinical Nutrition* **19,** 425-435.

Beghin L, Guimber D, Hankard R, Michaud L, Marinier E, Hugo JP, Cezard JP, Turck D, & Gottrand F (2001) Total energy expenditure and its components in children treated with home parenteral nutrition. *Clinical Nutrition* **20**, 64.

Beghin L, Michaud L, Guimber D, Vaksmann G, Turck D & Gottrand F (2002) Assessing sleeping energy expenditure in children using heart-rate monitoring calibrated against open-circuit indirect calorimetry: a pilot study. *British Journal of Nutrition* **88,** 533-543.

Bell GH, Emslie-Smith D, & Paterson CR (1976) *Textbook of Physiology and Biochemistry*, 9th Edition. Edinburgh: Churchill Livingstone.

Benedict FG (1907) Carnegie Institution Publication Washington: Carnegie Institute.

Berger VA, Rousset P, MacCormack C & Ritz P (2000) Reproducibility of body composition and body water spaces measurements in healthy elderly individuals. *Journal of Nutrition and Health in Aging* **4,** 243-245.

Bernstein M, Sloutskis D, Kumanyika S, Schutz Y & Morabia A (1998) Data-based approach for developing a physical activity frequency questionnaire. *American Journal of Epidemiology* **147,** 147-154.

Bitar A, Vermorel M, Fellmann N, Bedu M, Chamoux A & Coudert J (1996) Heart-rate recording method validated by whole-body indirect calorimetry in 10-year-old children. *Journal of Applied Physiology* **81,** 1169-1173.

Black AE, Coward WA, Cole TJ & Prentice AM (1996) Human energy expenditure in affluent societies: an analysis of 574 doubly-labelled water measurements. *European Journal of Clinical Nutrition* **50,** 72-92.

Black AE, Prentice A & Coward A (1986) Use of food quotients to predict respiratory quotients for the doubly-labelled water method of measuring energy expenditure. *Human Nutrition: Clinical Nutrition* **40C,** 381-391.

Bland M (1995) *An Introduction to Medical Statistics,* 2nd Edition. Oxford: Oxford University Press.

Bland JM & Altman DG (1986) Statistical methods for assessing agreement between two methods of clinical measurement. *The Lancet* 1 (8476), 307-310.

Bluck LJC, Harding M, French S, Wright A, Halliday D & Coward WA (2002) Measurement of gastric emptying in man using deuterated octanoic acid. *Rapid Communications in Mass Spectrometry* **16,** 127-133.

Boeck WG, Adler GM & Gress TM (2001) Pancreatic function tests: when to choose, what to use. *Current Gastroenterology Reports* **3,** 95-100.

Bohinski RC (1983) Lipids and Biomembranes. In *Modern Concepts in Biochemistry,* 4th Edition, pp. 224-253. Boston: Allyn and Bacon.

Boirie Y, Fauquant J, Rulquin H, Maubois JL & Beaufrere B (1995) Production of large amounts of [^{13}C] leucine enriched milk proteins by lactating cows. *Journal of Nutrition* **125,** 92-98.

Bond JH & Levitt DG (1975) Investigations of small bowel transit time in man utilizing pulmonary hydrogen (H_2) measurements. *Journal of Laboratory and Clinical Medicine* **85,** 546-565.

Booyens J & Hervey GR (1960) The pulse rate as a means of measuring metabolic rate in man. *Canadian Journal of Biochemistry and Physiology* **38,** 1301-1309.

Borowitz D, Baker RD & Stallings V (2002) Consensus report on nutrition for pediatric patients with cystic fibrosis. *Journal of Pediatric Gastroenterology and Nutrition* **35,** 246-259.

Bouten CV, Westerterp KR, Verduin M & Janssen JD (1994) Assessment of energy expenditure for physical activity using a triaxial accelerometer. *Medicine and Science in Sports and Exercise* **26,** 1516-1523.

Boutton TW (1991) Stable carbon isotope ratios of natural materials: II. Atmospheric, terrestrial, marine and freshwater environments. In *Carbon Isotope Techniques,* pp. 173-185. [DC Coleman & B Fry, Editors]. San Diego: Academic Press.

Bowtell JL, Leese GP, Smith K, Watt PW, Nevill A, Rooyackers O, Wagenmakers AJM & Rennie MJ (2000) Effect of oral glucose on leucine turnover in human subjects at rest and during exercise at two levels of dietary protein. *Journal of Physiology* **525,** 271-281.

Braden B, Adams S, Duan L-P, Orth KH, Maul FD, Lembcke B, Hor G & Caspary WF (1995) The ^{13}C-acetate breath test accurately reflects gastric emptying of liquids in both liquid and semi-solid meals. *Gastroenterology* **108,** 1048-1055.

Bradfield RB, Huntzicker PB & Fruehan GJ (1969) Simultaneous comparison of respirometer and heart-rate telemetry techniques as measures of human energy expenditure. *American Journal of Clinical Nutrition* **6,** 696-700.

British Nutrition Foundation (1992) *Unsaturated fatty acids: Nutritional and Physiological Significance,* London: Chapman & Hall.

Bronstein MN, Davies PSW, Hambridge KM & Accurso FJ (1995) Normal energy expenditure in the infant with presymptomatic cystic fibrosis. *Journal of Pediatrics* **126,** 28-33.

Brydon WG, Kingstone K & Ghosh S (2004) Limitations of faecal elastase-1 and chymotrypsin as tests of exocrine pancreatic disease in adults. *Annals of Clinical Biochemistry* **41,** 78-81.

Carey MC & Hernell O (1992) Digestion and absorption of fat. *Seminars in Gastrointestinal Disease* **3,** 189-208.

Carnielli VP, Sulkers EJ, Moretti C, Wattimena JLD, van Goudoever JB, Dagenhart HJ, Zacchello F & Sauer PJJ (1994) Conversion of octanoic acid into long-chain saturated fatty acids in premature infants fed a formula containing medium-chain triglycerides. *Metabolism* **43,** 1287-1292.

Castro M, Diamanti A, Gambarara M, Bella S, Lucidi V, Papadatou B, Ferretti F, Rosati P & Rupi E (2002) Resting energy expenditure in young patients with cystic fibrosis receiving antibiotic therapy for acute respiratory exacerbations. *Clinical Nutrition* **21,** 141-144.

Ceesay SM, Prentice AM, Day KC, Murgatroyd PR, Goldberg GR & Scott W (1989) The use of heart rate monitoring in the estimation of energy expenditure: a validation study using indirect whole-body calorimetry. *British Journal of Nutrition* **61,** 175-186.

Child Growth Foundation. (1996) *The British 1990 Growth Reference. Revised September 1996.* London: Child Growth Foundation.

Christensen CC, Frey HMM, Foenstelien E, Aadland E & Refsum HE (1983) A critical evaluation of energy expenditure estimates based on individual O_2 consumption/heart rate curves and averages of daily heart rate. *American Journal of Clinical Nutrition* **37,** 468-472.

Christian MT, Amarri S, Franchini F, Preston T, Morrison DJ, Dodson B, Edwards CA & Weaver LT (2002) Modeling ^{13}C-breath curves to determine site and extent of starch digestion and fermentation in infants. *Journal of Pediatric Gastroenterology and Nutrition* **34,** 158-164.

Cisse AS, Bluck L, Diaham B, Dossou N, Guiro AT & Wade S (2002) Use of Fourier transformed infrared spectrophotometer (FTIR) for determination of breastmilk output by the deuterium dilution method among Senegalese women. *Food and Nutrition Bulletin* **23** (3, Suppl), 138-141.

Coplen TB (1995) Discontinuance of SMOW and PDB. *Nature* **375,** 285.

Coplen TB (1996) New guidelines for reporting stable hydrogen, carbon, and oxygen isotope-ratio data. *Geochimica et Cosmochimica Acta* **60,** 3359-3360.

Couper R, Belli D, Durie P, Gaskin K, Sarles J & Werlin S (2002) Pancreatic disorders and cystic fibrosis: working group report of the First World Congress of Pediatric Gastroenterology, Hepatology, and Nutrition. *Journal of Pediatric Gastroenterology and Nutrition* **35,** S213-S223.

Coward WA (1988) The doubly-labelled-water ($^2H_2{}^{18}O$) method: principles and practice. *Proceedings of the Nutrition Society* **47,** 209-218.

Craig H (1957) Isotopic standards for carbon and oxygen and correction factors for mass-spectrometric analysis of carbon dioxide. *Geochimica et Cosmochimica Acta* **12,** 133-149.

Dauncey MJ & James WPT (1979) Assessment of the heart-rate method for determining energy expenditure in man, using a whole body calorimeter. *British Journal of Nutrition* **42,** 1-13.

Davidson AGF (2000) Gastrointestinal and pancreatic disease in cystic fibrosis. In *Cystic fibrosis,* 2nd edition, pp. 261-288. [ME Hodson & DM Geddes, editors]. London: Arnold.

Davidson L, McNeill G, Haggarty P, Smith JS & Franklin MF (1997) Free-living energy expenditure of adult men assessed by continuous heart-rate monitoring and doubly-labelled water. *British Journal of Nutrition* **78,** 695-708.

De Bièvre P & Barnes IL (1985) Table of the isotopic composition of elements as determined by mass spectrometry. *International Journal of Mass Spectrometry and Ion Processes* **65,** 211-230.

de Boeck K, Delbeke I, Eggermont E, Veereman-Wauters G & Ghoos Y (1998) Lipid digestion in cystic fibrosis: comparison of conventional and high lipase enzyme therapy using the mixed-triglyceride breath test. *Journal of Pediatric Gastroenterology and Nutrition* **26,** 408-411.

Department of Health (1991) *Dietary Reference Values for Food Energy and Nutrients for the United Kingdom. Report of the Panel on Dietary Reference Values of the Committee on Medical Aspects of Food Policy.* London: HMSO.

Desnuelle P & Savery P (1963) Specificity of lipases. *Journal of Lipid Research* **4,** 369-384.

Durant RH, Baranowski T, Davis H, Rhodes T, Thompson WO, Greaves KA & Puhl J (1993) Reliability and variability of indicators of heart-rate monitoring in children. *Medicine & Science in Sports & Exercise* **25,** 389-395.

Durnin JVGA, Blake EC, Allan MK, Shaw EJ & Blair S (1961a) Food intake and energy expenditure of elderly women with varying-sized families. *Journal of Nutrition* 75, 73.

Durnin JVGA, Blake EC & Brockway JM (1957) The energy expenditure and food intake of middle-aged Glasgow housewives and their adult daughters. *British Journal of Nutrition* **11,** 85.

Durnin JVGA, Blake EC, Brockway JM & Drury EA (1961b) The food intake and energy expenditure of elderly women living alone. *British Journal of Nutrition* **15,** 499.

Durnin JVGA & Brockway JM (1959) Determination of total daily energy expenditure in man by indirect calorimetry: Assessment of the accuracy of a modern technique. *British Journal of Nutrition* **13,** 41.

Eaton S, Bartlett K & Pourfarzam M (1996) Mammalian mitochondrial β-oxidation. *Biochemical Journal* **320,** 345-357.

Edwards CA, Zavoshy R, & Preston T (1998) Pea flour digestibility and fermentability measured with ^{13}C isotopes. *Biochemical Society Transactions* **26** , S185.

Edwards CA, Zavoshy R, Khanna S, Slater C, Morrison DJ, Preston T & Weaver LT (2002) Production of ^{13}C labelled pea flour for use in human digestion and fermentation studies. *Isotopes in Environmental and Health Studies* **38,** 139-147.

Ekelund U, Aman J, Yngve A, Renman C, Westerterp K & Sjöström M (2002) Physical activity but not energy expenditure is reduced in obese adolescents: a case-control study. *American Journal of Clinical Nutrition* **76,** 935-941.

Elia M (1990) Converting carbon dioxide production to energy expenditure. In *The Doubly-labelled Water Method for Measuring Energy Expenditure,* pp. 193-211. [AM Prentice, Editor]. Vienna: IAEA.

Elia M (1991) Estimation of short-term energy expenditure by the labeled bicarbonate method. In *New Techniques in Nutritional Research,* pp. 207-227. [RG Whitehead & A Prentice, Editors]. London: Academic Press.

Emons HJG, Groenenboom DC, Westerterp KR & Saris WHM (1992) Comparison of heart rate monitoring combined with indirect calorimetry and the doubly labelled water ($^2H_2{}^{18}O$) method for the measurement of energy expenditure in children. *European Journal of Applied Physiology* **65,** 99-103.

Eston RG, Rowlands AV & Ingledew DK (1998) Validity of heart rate, pedometry, and accelerometry for predicting the energy cost of children's activities. *Journal of Applied Physiology* **84,** 362-371.

Evenepoel P, Luypaerts A, Geypens B, Buyse J, Decuypere E, Rutgeerts P & Ghoos Y (1997) Production of egg proteins, enriched with L-leucine-$^{13}C_1$, for the study of protein assimilation in humans using the breath test technique. *Journal of Nutrition* **127,** 327-331.

FAO/WHO/UNU (1985) *Energy and protein requirements.* Report of a Joint FAO/WHO/UNU Expert Consultation. Technical Report Series 724, Geneva: WHO.

Fearon KCH, Richardson RA, Hannan J, Cowen S, Watson W, Shenkin A & Garden OJ (1992) Bioelectrical impedance analysis in the measurement of body composition of surgical patients. *British Journal of Surgery* **799,** 421-432.

Frayn KN (1996) *Metabolic Regulation: A Human Perspective,* London: Portland Press.

Freedson PS (1991) Electronic motion sensors and heart rate as measures of physical activity in children. *Journal of School Health* **61,** 220-223.

Frohnert BI & Bernlohr DA (2000) Regulation of fatty acid transporters in mammalian cells. *Progress in Lipid Research* **39,** 83-107.

Garlick PJ, McNurlan MA, McHardy KC, Calder AG, Milne E, Fearns LM & Broom J (1987) Rates of nutrient utilization in man measured by combined respiratory gas analysis and stable isotopic labelling: effect of food intake. *Human Nutrition: Clinical Nutrition* **41C,** 177-191.

Garry RC, Passmore GM, Warnock GM, & Durnin JVGA (1955) *Studies on expenditure of energy and consumption of food by miners and clerks, Fife, Scotland, 1952.* London: Medical Research Council Special Report Service.

Gaskin KJ, Durie PR, Lee L, Hill R & Forstner GG (1984) Colipase and lipase secretion in childhood-onset pancreatic insufficiency. Delineation of patients with steatorrhea secondary to relative colipase deficiency. *Gastroenterology* **86,** 1-7.

Ghoos YF, Geypens BJ, Maes BD, Hiele MI, Vantrappen G, & Rutgeerts PJ (1993) Breath tests in gastric emptying and transit studies: technical aspects of $^{13}CO_2$-breath tests. In *Progress in Understanding and Management of Gastro-intestinal Motility Disorders,* pp. 169-180. [J Janssens, editors]. Leuven: Dept. Medicine, Division of Gastroenterology, K.U. Leuven.

Ghoos YF, Vantrappen G, Rutgeerts PJ & Schurmans PC (1981) A mixed-triglyceride breath test for intraluminal fat digestive activity. *Digestion* **22,** 239-247.

Gilliam TB, Freedson PS, Geenan DL & Shahraray B (1980) Physical activity patterns determined by heart rate monitoring in 6-7 year-old children. *Medicine and Science in Sports and Exercise* **13,** 65-67.

Girardet JP, Tounian P, Sardet A, Veinberg F, Grimfeld A, Tournier G & Fontaine JL (1994) Resting energy metabolism in infants with cystic fibrosis. *Journal of Pediatric Gastroenterology and Nutrition* **18,** 214-219.

Graham DY, Evans DJJr, Alpert LC, Klein PD, Evans DG, Opekun AR & Boutton TW (1987) *Campylobacter pylori* detected non-invasively by the ^{13}C-urea breath test. *Lancet* **1,** 1174-1177.

Graham DY & Klein PD (1991) What you should know about the methods, problems, interpretations and uses of urea breath tests. *American Journal of Gastroenterology* **86,** 1118-1122.

Greiner M (1995) Two-graph receiver operating characteristic (TG-ROC) - a Microsoft-Excel template for the selection of cut-off values in diagnostic tests. *Journal of Immunological Methods* **185,** 145-146. Can be downloaded free-of-charge from http://city.vetmed.fu-berlin.de/~mgreiner/TG-ROC/tgroc.htm

Greiner M, Sohr D & Göbel P (1995) A modified ROC analysis for the selection of cut-off values and the definition of intermediate results of serodiagnostic tests. *Immunological Methods* **185,** 123-132.

Groot PH & Hulsmann WC (1973) The activation and oxidation of octanoate and palmitate by rat skeletal muscle mitochondria. *Biochimica et Biophysica Acta* **316,** 124-135.

Guillot E, Vaugelade P, Lemarchal P & Rérat A (1993) Intestinal absorption and liver uptake of medium-chain fatty acids in non-anaesthetized pigs. *British Journal of Nutrition* **69,** 431-442.

Gurr MI, Harwood JL, & Frayn KN (2002) *Lipid Biochemistry: An Introduction,* 5th Edition. Oxford: Blackwell Science.

Haggarty P (1990) The effect of isotope sequestration and exchange. In *The Doubly-labelled Water Method for Measuring Energy Expenditure: Technical recommendations for use in humans,* pp. 114-146. [AM Prentice, Editors]. NAHRES-4, Vienna: IAEA.

Haggarty P, Shetty P, Thangam S, Kumar S, Kurpad A, Ashton J, Milne E & Earl C (2000) Free and esterified fatty acid and cholesterol synthesis in adult males and its effect on the doubly-labelled water method. *British Journal of Nutrition* **83,** 227-234.

Hannan WJ, Cowen SJ, Fearon KCH, Plester CE, Falconer JS & Richardson RA (1994) Evaluation of multi-frequency bio-impedance analysis for the assessment of extracellular and total body water in surgical patients. *Clinical Science* **86,** 479-485.

Harding M, Coward WA, Weaver LT, Sweet JB & Thomas JE (1994) Labelling wheat flour with ^{13}C. *Isotopenpraxis* **30,** 1-8.

Harris J & Benedict F (1919) *A biometric study of basal metabolism in man*. Washington DC: Carnegie Institution.

Harro M (1997) Validation of a questionnaire to assess physical activity of children ages 4-8 years. *Research Quarterly for Exercise and Sport* **68,** 259-268.

Haycock G, Schwartz G & Wisotsky G (1978) Geometric method for measuring body surface area: a height-weight formula validated in infants, children and adults. *Journal of Pediatrics* **93,** 62-66.

Heini A, Schutz Y, Diaz E, Prentice AM, Whitehead RG & Jequier E (1991) Free-living energy expenditure measured by two independent techniques in pregnant and nonpregnant Gambian women. *American Journal of Physiology* **261,** E9-E17.

Hellerstein MK (1995) Methods for measurement of fatty acid and cholesterol metabolism. *Current Opinion in Lipidolgy* **6** (3), 172-181.

Hellerstein MK, Christiansen M, Kaempfer S, Kletke C, Wu K, Reid JS, Mulligan K, Hellerstein NS & Shackleton CHL (1991) Measurement of de novo hepatic lipogenesis in humans using stable isotopes. *Journal of Clinical Investigation* **87,** 1841-1852.

Hellerstein MK & Neese RA (1992) Mass isotopomer distribution analysis: a technique for measuring biosynthesis and turnover of polymers. *American Journal of Physiology* **263,** E988-E1001.

Hellerstein MK & Neese RA (1999) Mass isotopomer distribution analysis at eight years: theoretical, analytic, and experimental considerations. *American Journal of Physiology* **276,** E1146-E1170.

Hellerstein MK, Neese RA & Schwarz JM (1993) Model for measuring absolute rates of hepatic de novo lipogenesis and reesterification of free fatty acids. *American Journal of Physiology* **265**, E814-E820.

Henderson Y & Prince AL (1914) . *American Journal of Physiology* **35,** 106.

Hernell O (2001) Assessing fat absorption. *Journal of Pediatrics* **135,** 407-409.

Hoerr RA, Yu Y-M, Wagner DA & Burke JF (1989) Recovery of ^{13}C in breath from $NaH^{13}CO_3$ infused by gut and vein: effect of feeding. *American Journal of Physiology* **257,** E426-E438.

Holland B, Welch AA, Unwin ID, Buss DH, Paul AA, & Southgate DAT (1991) *McCance and Widdowson's, The Composition of Foods,* Fifth. Cambridge: The Royal Society of Chemistry.

Houtkooper LB, Going SB, Lohman TG, Roche AF & Van Loan M (1992) Bioelectrical impedance estimation of fat-free body mass in children and youth: a cross-validation study. *Journal of Applied Physiology* **72,** 366-373.

Hume R & Weyers E (1971) Relationship between total body water and surface area in normal and obese subjects. *Journal of Clinical Pathology* **24,** 234-238.

ICRP 23 (1975) *Report on the Task Group on Reference Man. Report prepared by a Task Group Committee 2 of the International Commission on Radiological Protection.* Oxford: Pergamon Press.

IDECG (1990) *The Doubly-labelled Water Method for Measuring Energy Expenditure: Technical recommendations for use in humans.* NAHRES-4, Vienna: IAEA.

Irving CS, Lifschitz CH, Wong WW, Boutton TW, Nichols BL & Klein PD (1985) Characterization of HCO_3^-/CO_2 pool sizes and kinetics in infants. *Pediatric Research* **19,** 358-363.

Irving CS, Wong WW, Shulman RJ, Smith EO & Klein PD (1983) [^{13}C]bicarbonate kinetics in humans: intra- vs interindividual variations. *American Journal of Physiology* **245,** R190-R202.

Irving CS, Wong WW, Wong WM, Boutton TW, Shulman RJ, Lifschitz CL, Malphus EW, Helge II & Klein PD (1984) Rapid determination of whole-body bicarbonate kinetics by use of a digital infusion. *American Journal of Physiology* **247,** R709-R716.

Jackson DM, Reilly JJ, Kelly LA, Montgomery C, Grant S & Paton JY (2003) Objectively measured physical activity in a representative sample of 3- to 4- year old children. *Obesity Research* **11,** 420-425.

Jacobson BS, Smith BN, Epstein S & Laties GG (1970) The prevalence of carbon-13 in respiratory carbon dioxide as an indicator of the type of endogenous substrate. *Journal of General Physiology* **55,** 1-17.

James WPT, Ferro-Luzzi A & Waterlow JC (1988) Definition of chronic energy deficiency in adults. Report of a working party of the International Dietary Energy Consultancy Group. *European Journal of Clinical Nutrition* **42,** 969-981.

Janz KF (1994) Validation of the CSA accelerometer for assessing children's physical activity. *Medicine and Science in Sports and Exercise* **26,** 369-375.

Janz KF, Golden JC, Hansen JR & Mahoney LT (1992) Heart rate monitoring of physical activity in children and adolescents: the Muscatine Study. *Pediatrics* **89,** 256-261.

Jennings G, Bluck L, Wright A & Elia M (1999) The use of infrared spectrophotometry for measuring body water spaces. *Clinical Chemistry* **45** (7), 1077-1081.

Johnson LR (1997) *Gastrointestinal Physiology,* 5th Edition. London: Mosby.

Johnson RK, Russ J & Goran MI (1998) Physical activity related energy expenditure in children by doubly labeled water as compared with the Caltrac accelerometer. *International Journal of Obesity* **22,** 1046-1052.

Jones PJH, Pencharz PB, Bell L & Clandinin MT (1985) Model for determination of ^{13}C substrate oxidation rates in humans in the fed state. *American Journal of Clinical Nutrition* **41,** 1277-1282.

Jorge JM, Wexner SD & Ehrenpreis ED (1994) The lactulose hydrogen breath tests as a measure of orocaecal transit time. *European Journal of Surgery* **160,** 409-416.

Kalivianakis M, Minich DM, Bijleveld CM, van Aalderen WMC, Stellaard F, Laseur M, Vonk RJ & Verkade HJ (2000) Fat malabsorption in cystic fibrosis patients receiving enzyme replacement therapy is due to impaired intestinal uptake of long-chain fatty acids. *American Journal of Clinical Nutrition* **69** (1), 127-134.

Kalivianakis M, Verkade HJ, Stellaard F, van der Werf M, Elzinga H & Vonk RJ (1997) The ^{13}C-mixed triglyceride breath test in healthy adults: determinants of the $^{13}CO_2$ response. *European Journal of Clinical Investigation* **27,** 434-442.

Kaplan AS, Zemel BS, Neiwender KM & Stallings VA (1995) Resting energy expenditure in clinical pediatrics: measured versus prediction equations. *Journal of Pediatrics* **127,** 200-205.

Kato S, Ozawa K, Konno M, Tajiri H, Yoshimura N, Shimizu T, Fujisawa T, Abukawa D, Minoura T & Iinuma K (2002) Diagnostic accuracy of the ^{13}C-urea breath test for childhood *Helicobacter pylori* infection: a multicentre Japanese study. *American Journal of Gastroenterology* **97,** 1668-1673.

Kien CL (1989) Isotopic dilution of CO_2 as an estimate of CO_2 production during substrate oxidation studies. *American Journal of Physiology* **257,** E296-E298.

Kimball JW (1978) *Biology*, 4th Edition. London: Addison Wesley.

King CE & Toskes PP (1979) Small intestine bacterial overgrowth. *Gastroenterology* **76,** 1035-1055.

Klein PD (1991) Nutritional applications of ^{13}C:strategic considerations. In *New Techniques in Nutritional Research*, pp. 73-94. [RG Whitehead & A Prentice, editors]. London: Academic Press.

Klein PD & Helge H (1998) Methodology for the study of metabolism: breath testing. In *Principles of Perinatal-Neonatal Metabolism*, 2nd Edition, pp. 17-25. [RM Cowett, editors]. New York: Springer-Verlag.

Klein PD & Klein ER (1982) Stable isotopes in biomedical research. *Spectra* **8,** 9-12.

Klein PD & Klein ER (1985) Applications of stable isotopes to pediatric nutrition and gastroenterology: measurement of nutrient absorption and digestion using ^{13}C. *Journal of Pediatric Gastroenterology and Nutrition* **4,** 9-19.

Kriemler S, Hebestreit H, Mikami S, Bar-Or T, Ayub BV & Bar-Or O (1999) Impact of a single exercise bout on energy expenditure and spontaneous physical activity of obese boys. *Pediatric Research* **46,** 40-44.

Leese GP, Nicoll AE, Varnier M, Thompson J, Scrimgeour CM & Rennie MJ (1994) Kinetics of $^{13}CO_2$ elimination after ingestion of ^{13}C bicarbonate: the effects of exercise and acid base balance. *European Journal of Clinical Investigation* **24,** 818-823.

Leijssen DPC & Elia M (1996) Recovery of $^{13}CO_2$ and $^{14}CO_2$ in human bicarbonate studies: a critical review with original data. *Clinical Science* **91,** 665-677.

Li R, Deurenberg P & Huatvast JGAJ (1993) A critical evaluation of heart rate monitoring to assess energy expenditure in individuals. *American Journal of Clinical Nutrition* **58,** 602-607.

Liang X, Le W, Zhang D & Schulz H (2001) Impact of the intramitochondrial enzyme organization on fatty acid oxidation. *Biochemical Society Transactions* **29,** 279-282.

Lindhard J (1913) . *Scandanavian Archives of Physiology* **30,** 395.

Ling SC, Amarri S, Slater C, Hollman AS, Preston T & Weaver LT (2000) Liver disease does not affect lipolysis as measured with the ^{13}C-mixed triacylglycerol breath test in children with cystic fibrosis. *Journal of Pediatric Gastroenterology and Nutrition* **30,** 368-372.

Ling SC, Slater C, Preston T, & Weaver LT (1998) The fate of fat in the colon. *Gut* **42,** A55.

Littlewood JM (1996) Commentary: Fibrosing colonopathy in cystic fibrosis. *Archives of Disease in Childhood* **74,** 466-468.

Livesey G & Elia M (1988) Estimation of energy expenditure, net carbohydrate utilization and net fat oxidation and synthesis by indirect calorimetry: evaluation of errors with special reference to detailed composition of fuels. *American Journal of Clinical Nutrition* **47,** 608-628.

Livingstone MBE, Coward WA, Prentice AM, Davies PSW, Strain JJ, McKenna PG, Mahoney CA, White JA, Stewart CM & Kerr M-JJ (1992) Daily energy expenditure in free-living children: comparison of heart-rate monitoring with doubly labeled water ($^2H_2{}^{18}O$) method. *American Journal of Clinical Nutrition* **56,** 243-352.

Livingstone MBE, Prentice AM, Coward WA, Ceesay SM, Strain JJ, McKenna PG, Nevin GB, Barker ME & Hickey RJ (1990) Simultaneous measurement of free-living energy expenditure by the doubly labeled water method and heart-rate monitoring. *American Journal of Clinical Nutrition* **52,** 65.

Löser C, Brauer C, Aygen S, Hennemann O & Fölsch UR (1998) Comparative clinical evaluation of the ^{13}C-mixed triglyceride breath test as an indirect pancreatic function test. *Scandanavian Journal of Gastroenterology* **33,** 327-334.

Lusk G (1928) *The Elements of the Science of Nutrition.* New York: Johnson Reprint Corporation. Reprinted 1976.

Maes B, Ghoos YF, Geypens BJ, Hiele MI & Rutgeerts PJ (1996) Relation between gastric emptying rate and rate of intraluminal lipolysis. *Gut* **38,** 23-27.

Maes BD, Ghoos YF, Rutgeerts PJ, Hiele MI, Geypens BJ & Vantrappen G (1994) [*C]octanoic acid breath test to measure gastric emptying rate of solids. *Digestive Diseases and Sciences* **39,** 104S-106S.

Maes BD, Mys G, Geypens BJ, Evenepoel P, Ghoos YF & Rutgeerts PJ (1998) Gastric emptying flow curves separated from carbon-labeled octanoic acid breath test results. *American Journal of Physiology* **275,** G169-G175.

Maffeis C, Schutz Y, Micciolo R, Zoccante L & Pinelli L (1993) Resting metabolic rate in six- to 10-year-old obese and non-obese children. *Journal of Pediatrics* **122,** 556-562.

Manefield M, Whiteley AS, Ostle N, Ineson P & Bailey MJ (2002) Technical considerations for RNA-based stable isotope probing: an approach to associating microbial diversity with microbial community function. *Rapid Communications in Mass Spectrometry* **16** (23), 2179-2183.

Manson WG, Coward WA, Harding M & Weaver LT (1999) Development of fat digestion in infancy. *Archives of Disease in Childhood Fetal and Neonatal Edition* **80,** F183-F187.

Marinetti GV (1990) Disorders of lipid digestion and absorption. In *Disorders of Lipid Metabolism,* pp. 7-47. New York: Plenum Press.

Martinez-Costa C, Aparisi L, Rosello P, Calabuig M, Brines J, & Rodrigo M (2002) Simultaneous quantification of faecal elastase-1 and chymotrypsin in the diagnosis and control of exocrine pancreatic function in children. *Pancreatology* **2,** 167-187.

McGarry JD & Foster DW (1980) Regulation of hepatic fatty acid oxidation and ketone body production. *Annual Reviews of Biochemistry* **49,** 395-420.

McMillan DC, Preston T & Taggart DP (1989) Analysis of ^{18}O enrichment in biological fluids by continuous flow-isotope ratio mass spectrometry. *Biomedical and Environmental Mass Spectrometry* **18,** 543-546.

Meijer GA, Westerterp KR, Koper H & Hoor FT (1989) Assessment of energy expenditure by recording heart rate and body acceleration. *Medicine and Science in Sport and Exercise* **21,** 343-347.

Meineke I, de Mey C, Eggers R & Bauer FE (1998) Evaluation of the $^{13}CO_2$ kinetics in humans after oral application of sodium bicarbonate as a model for breath testing. *European Journal of Clinical Investigation* **23,** 91-96.

Melanson EL Jr & Freedson PS (1995) Validity of the Computer Science and Applications, Inc. (CSA) activity monitor. *Medicine & Science in Sports & Exercise* **27,** 934-940.

Millward DJ (1970) Protein turnover in skeletal muscle. I. The measurement of rates of synthesis and catabolism of skeletal muscle protein using [^{14}C]Na_2CO_3 to label protein, *Clinical Science* **59** (5), 577-590.

Mittendorfer B, Sidossis LS, Walser E, Chinkes DL & Wolfe RR (1998) Regional acetate kinetics and oxidation in human volunteers. *American Journal of Physiology* **274,** E978-E983.

Montgomery C, Speake BK, Cameron A, Sattar N & Weaver LT (2003) Maternal docosahexaenoic acid supplementation and fetal accretion. *British Journal of Nutrition* **90,** 1350145.

Moon JK & Butte NF (1996) Combined heart rate and activity improve estimates of oxygen consumption and carbon dioxide production rates. *Journal of Applied Physiology* **81,** 1754-1761.

Morio B, Ritz P, Verdier E, Montaurier C, Beaufrere B & Vermorel M (1997) Critical evaluation of the factorial and heart-rate recording methods for determination of energy expenditure of free-living elderly people. *British Journal of Nutrition* **78,** 709-722.

Morrison DJ (2000) Investigation of oro-caecal transit time and colonic fermentation using lactose [^{13}C]ureide and mathematical modelling of ^{13}C-breath test curves. Ph.D thesis. University of Strathclyde.

Morrison DJ, Dodson B & Preston T (1999) Measurement of urinary total ^{13}C and ^{13}C urea by isotope ratio mass spectrometry after administration of lactose [^{13}C]-ureide. *Rapid Communications in Mass Spectrometry* **13,** 1252-1256.

Morrison DJ, Dodson B, Preston T & Weaver LT (2001) Rapid quality control analysis of ^{13}C-enriched substrate synthesis by isotope ratio mass spectrometry. *Rapid Communications in Mass Spectrometry* **15,** 1282.

Morrison DJ, Dodson B, Slater C & Preston T (2000) ^{13}C natural abundance in the British diet: implications for ^{13}C breath tests. *Rapid Communications in Mass Spectrometry* **14,** 1321-1324.

Morrison DJ, Preston T, Cooper K, Waldron S, Slater C, & Weaver LT (2003a) Quantitation of ^{2}H/^{13}C-volatile fatty acids by GC-MS and of ^{13}C-volatile fatty acids by GC-C-IRMS. In *Proceedings of SIMSUG 2003,* pp. 53 [Bristol: University of Bristol, School of Chemistry Proceedings of SIMSUG 2003.

Morrison DJ, Preston T, Dodson B & Weaver LT (2003b) Gastrointestinal handling of glycosyl [^{13}C]ureides. *European Journal of Clinical Nutrition* **57,** 1017-1024.

Morrison DJ, Zovoshy R, Edwards CA, Dodson B, Preston T, & Weaver LT (1998) Lactose [^{13}C]-ureide as a marker for colonic fermentation and the deconvolution of a complex $^{13}CO_2$ breath test curve. *Biochemical Society Transactions* **26,** S184.

Motulsky HJ & Ransnas LA (1987) Fitting curves to data using nonlinear regression: a practical and nonmathematical review. *FASEB Journal* **1,** 365-374.

Murlin JR & Greer JR (1914) . *American Journal of Physiology* **33,** 253.

Murphy JL, Laiho KM, Jones AE & Wootton SA (1998) Metabolic handling of ^{13}C labelled tripalmitin in healthy controls and patients with cystic fibrosis. *Archives of Disease in Childhood* **79,** 44-47.

Nelson DL & Cox MM (2000) *Lehninger Principles of Biochemistry,* 3rd Edition. New York: Worth.

Newsholme EA & Leech AR (1983) *Biochemistry for the Medical Sciences,* Chichester: John Wiley & Sons.

Nousia-Arvanitakis S (2003) Fecal elastase-1 concentration: an indirect test of exocrine pancreatic function and a marker of enteropathy regardless of cause. *Journal of Pediatric Gastroenterology and Nutrition* **36,** 314-315.

O'Leary MH (1981) Carbon isotope fractionation in plants. *Phytochemistry* **20,** 533-567.

Odle J (1997) New insights into the utilization of medium-chain triglycerides by the neonate: observations from a piglet model. *Journal of Nutrition* **127,** 1061-1067.

Pakula R, Rubin M, Moser AM, Lichtenberg D & Tietz A (1997) Biosynthesis of medium-chain triacylglycerols and phospholipids by HepG-2 cells. *Lipids* **32,** 489-495.

Pambianco G, Wing RR & Robertson R (1990) Accuracy and reliability of the Caltrac accelerometer for estimating energy expenditure. *Medicine and Science in Sports and Exercise* **22,** 858-862.

Parker AC, Preston T, Heaf D, Kitteringham NR & Choonara I (1994) Inhibition of caffeine metabolism by ciprofloxacin in children with cystic fibrosis as measured by the caffeine breath test. *British Journal of Clinical Pharmacology* **38,** 573-576.

Parker AC, Pritchard P, Preston T, Dalzell AM & Choonara I (1997a) Lack of inhibitory effect of cimetidine on caffeine metabolism in children using the caffeine breath test. *British Journal of Clinical Pharmacology* **45,** 467-470.

Parker AC, Pritchard P, Preston T, Smyth RL & Choonara I (1997b) Enhanced drug metabolism in young children with cystic fibrosis. *Archives of Disease in Childhood* **77,** 239-241.

Parker L, Reilly JJ, Slater C, Wells JCK & Pitsiladis Y (2003) Validity of six field and laboratory methods for measurement of body composition in 10-14 year old boys. *Obesity Research* **11,** 852-858.

Pate RR, Baranowski T, Dowda M & Trost SG (1996) Tracking of physical activity in young children. *Medicine and Science in Sport and Exercise* **28,** 92-96.

Perri F & Andriulli A (1998) *Clinical Application of Breath Tests in Gastroenterology and Hepatology,* Rome: International University Press.

Perri F & Andriulli A (1998) Mixed triglyceride breath test: methodological problems and clinical applications. *Reviews of the Medical University of Navarra* **42,** 99-103.

Perri F, Pastore M, Festa V, Clemente R, Quitadamo M, D'Altilia MR, Niro G, Paolucci P & Andriulli A (1998) Intraduodenal lipase activity in celiac disease assessed by means of ^{13}C mixed-triglyceride breath test. *Journal of Pediatric Gastroenterology and Nutrition* **27,** 407-410.

Pouteau E, Piloquet H, Maugeais P, Champ M, Dumon H, Nguyen P & Krempf M (1996) Kinetic aspects of acetate metabolism in healthy humans using [1-^{13}C]acetate. *American Journal of Physiology* **271,** E58-E64.

Preston T (1992) The measurement of stable isotope natural abundance variations. *Plant, Cell and Environment* **15**, 1091-1097.

Preston T & McMillan DC (1988) Rapid sample throughput for biomedical stable isotope tracer studies. *Biomedical and Environmental Mass Spectrometry* **16,** 229-235.

Preston T & Slater C (1994) Mass spectrometric analysis of stable isotope labelled amino acid tracers. *Proceedings of the Nutrition Society* **53,** 363-372.

Preston T, Slater C, McMillan DC, Falconer JS, Shenkin A & Fearon KCH (1998) Fibrinogen synthesis is elevated in fasted cancer patients with an acute phase response. *Journal of Nutrition* **128**, 1355-1360.

Prosser SJ, Brookes ST, Linton A & Preston T (1991) Rapid, automated analysis of ^{13}C and ^{18}O of CO_2 in gas samples by continuous-flow, isotope ratio mass spectrometry. *Biological Mass Spectrometry* **20,** 724-730.

Prosser SJ & Scrimgeour CM (1995) High-precision determination of $^{2}H/^{1}H$ in H_2 and H_2O by continuous-flow isotope ratio mass-spectrometry. *Analytical Chemistry* **67,** 1992-1997.

Rating D & Langhans CD (1997) Breath tests: concepts, applications and limitations. *European Journal of Pediatrics* **156,** S18-S23.

Reilly JJ, Jackson D, Montgomery C, Kelly LA, Slater C, Grant S & Paton JY (2004) Total energy expenditure and physical activity in young Scottish children: mixed longitudinal study. *The Lancet* **363**, 211-212.

Reilly JJ, Wilson J, McColl JH, Carmichael M & Durnin JVGA (1996) Ability of bioelectric impedance to predict fat-free mass in prepubertal children. *Pediatric Research* **39,** 176-179.

Ribeyre J, Fellmann N, Montaurier C, Delaître M, Vernet J, Coudert J & Vermorel M (2000a) Daily energy expenditure and its main components as measured by whole-body indirect calorimetry in athletic and non-athletic adolescents. *British Journal of Nutrition* **83,** 355-362.

Ribeyre J, Fellmann N, Vernet J, Delaître M, Chamoux A, Coudert J & Vermorel M (2000b) Components and variations in daily energy expenditure of athletic and non-athletic adolescents in free-living conditions. *British Journal of Nutrition* **84,** 531-539.

Richards JI & Lawrence PR (1984) The estimation of energy expenditure from heart-rate measurements in working oxen and buffalo. *Journal of Agricultural Science* **102,** 711-717.

Rodriguez G, Beghin L, Michaud L, Moreno LA, Turck D & Gottrand F (2002) Comparison of the TriTrac-R3D accelerometer and a self-report activity diary with heart-rate monitoring for the assessment of energy expenditure in children. *British Journal of Nutrition* **87,** 623-631.

Rodriguez G, Moreno LA, Sarria A, Fleta J & Bueno M (2000) Resting energy expenditure in children and adolescents: agreement between calorimetry and prediction equations. *Clinical Nutrition* **21,** 255-260.

Rowland M, Lambert I, Gormally S, Daly LE, Thomas JE, Hetherington C, Durnin M & Drumm B (1997) Carbon ^{13}-labeled urea breath test for the diagnosis of *Helicobacter pylori* infection in children. *Journal of Pediatrics* **131,** 815-820.

Saggerson ED & Carpenter CA (1981) Carnitine palmitoyltransferase and carnitine octanoyltransferase activities in the liver, kidney cortex, adipocyte, lactating mammary gland, skeletal muscle and heart. *FEBS Letters* **129,** 229-232.

Sallis JF, Buono MJ, Roby JJ, Carlson D & Nelson JA (1990) The caltrac accelerometer as a physical activity monitor for school-age children. *Medicine and Science in Sports and Exercise* **22,** 698-703.

Sanders T (1994) *Dietary fats,* London: Health Education Authority.

Savarino V, Vigneri S & Celle G (1999) The ^{13}C urea breath test in the diagnosis of *Helicobacter pylori* infection. *Gut* **45,** I18-I22.

Schoeller DA, Brown C, Nakamura K, Nakagawa A, Mazzeo RS, Brooks GA & Budinger TF (1984) Influence of metabolic fuel on the $^{13}C/^{12}C$ ratio of breath CO_2. *Biomedical Mass Spectrometry* **11,** 557-561.

Schoeller DA & Jones PJH (1987) Measurement of total body water by isotope dilution: a unified approach to calculations. In *In Vivo Body Composition Studies,* pp. 131-137. [KJ Ellis, S Yasumura, & WD Morgan, editors]. London: Institute of Physical Sciences in Medicine.

Schoeller DA, Schneider JF, Solomons NW, Watkins JB & Klein PD (1977) Clinical diagnosis with the stable isotope ^{13}C in CO_2 breath tests: methodology and fundamental considerations. *Journal of Laboratory and Clinical Medicine* **90,** 412-421.

Schoeller DA, van Santen E, Peterson DW, Dietz W, Jaspan J & Klein PD (1980) Total body water measurement in humans with ^{18}O and ^{2}H labeled water. *American Journal of Clinical Nutrition* **33,** 2686-2693.

Schofield WN (1985) Predicting basal metabolic rate, new standards and review of previous work. *Human Nutrition: Clinical Nutrition* **39C,** 5-41.

Schulz S, Westerterp KR & Bruck K (1989) Comparison of energy expenditure by the doubly labeled water technique with energy intake, heart rate, and activity recording in man. *American Journal of Clinical Nutrition* **49,** 1146-1154.

Scrimgeour CM, Rollo MM, Mudambo S, Handley L & Prosser SJ (1993) A simplified method for deuterium/hydrogen isotope ratio measurements on water samples of biological origin. *Biological Mass Spectrometry* **22,** 383-387.

Shepherd RW, Cleghorn G, Ward LC, Wall CR & Holt TL (1991) Nutrition in cystic fibrosis. *Nutrition Research Reviews* **4,** 51-67.

Shreeve VW, Cerasi E & Luft R (1970) Metabolism of [2-^{14}C]pyruvate in normal, acromegalic and HGH-treated human subjects. *Acta Endocrinologica* **65,** 155-169.

Sidossis LS, Coggan AR, Gastaldelli A & Wolfe RR (1995a) A new correction factor for use in tracer estimations of plasma fatty acid oxidation. *American Journal of Physiology* **269,** E649-E656.

Sidossis LS, Coggan AR, Gastaldelli A & Wolfe RR (1995b) Pathway of free fatty acid oxidation in human subjects. Implications for tracer studies. *Journal of Clinical Investigation* **95,** 278-284.

Slater C, Hardiek M, Preston T & Weaver LT (1998) Analysis of TBDMS 1-^{13}C-palmitic acid in stool samples by gas chromatography-mass spectrometry with electron impact ionisation: comparison with combustion isotope-ratio mass spectrometry. *Journal of Chromatography B: Biomedical Sciences and Applications* **716,** 1-6.

Slater C, Ling SC, Preston T & Weaver LT (2002) Analysis of ^{13}C-mixed triacylglycerol in stool by bulk (EA-IRMS) and compound specific (GC-MS) methods. *Isotopes in Environmental and Health Studies* **38,** 79-86.

Slater C & Preston T (2002) Total body water = 7.4 x height cubed: a simple formula to aid quality control and economic tracer use in studies of body composition and total energy expenditure in children and adults. *Proceedings of the Nutrition Society* **61,** 159A.

Slater C, Preston T & Weaver LT (2001a) Stable isotopes and the International System of Units. *Rapid Communications in Mass Spectrometry* **15,** 1270-1273.

Slater C, Preston T, & Weaver LT (2001b) Validation of the ^{13}C-mixed triacylglycerol breath test using a deuterium labelled tracer. *Clinical Nutrition* **20,** 39-40.

Slater C, Preston T & Weaver LT (2004) Is there an advantage in normalising the results of the *Helicobacter pylori* [^{13}C]urea breath test for CO_2 production rate in children? *Isotopes in Environmental and Health Studies* **40** (1), 89-98.

Smyth RL (1996) Fibrosing colonopathy in cystic fibrosis. *Archives of Disease in Childhood* **74,** 464-468.

Smyth RL, Ashby D, O'Hea U, Burrows E, Lewis P, van Velzen D & Dodge JA (1995a) Fibrosing colonopathy in cystic fibrosis: results of a case-control study. *Lancet* **346,** 1247-1251.

Smyth RL, van Velzen D, Smyth AR, Lloyd DA & Heaf DP (1994b) Strictures of ascending colon in cystic fibrosis and high strength pancreatic enzymes. *Lancet* **343,** 85-86.

Sneddon JC, Mathers JC, & Thomson CJ (1985) Prediction of energy expenditure from heart rate measurements in exercising cattle. *Proceedings of the Nutrition Society* **44,** A33.

Sprecher H, Luthria DL, Mohammed BS & Baykousheva SP (1995) Reevaluation of the pathways for the biosynthesis of polyunsaturated fatty acids. *Journal of Lipid Research* **36,** 2471-2477.

Spurr GB, Prentice AM, Murgatroyd PR, Goldberg GR, Reina JC & Christman NT (1988) Energy expenditure from minute-by-minute heart-rate recording: comparison with indirect calorimetry. *American Journal of Clinical Nutrition* **48,** 552-559.

Stellaard F & Geypens B (1998) European interlaboratory comparison of breath $^{13}CO_2$ analysis. *Gut* **43,** S2-S6.

Stenesh J (1998) *Biochemistry,* III Metabolism, London: Plenum.

Strath SJ, Bassett DR Jr, Thompson DL & Swartz AM (2002) Validation of the simultaneous heart-rate motion sensor technique for measuring energy expenditure. *Medicine & Science in Sports & Exercise* **34,** 888-894.

Stryer L (1988) Fatty acid metabolism. In *Biochemistry,* 3, pp. 469-493. New York: W.H.Freeman.

Stubbs RJ (1998) Appetite, feeding behaviour and energy balance in human subjects. *Proceedings of the Nutrition Society* **57,** 341-356.

Sun SS, Chumlea WC, Heymsfield SB, Lukaski HC, Schoeller DA, Friedl K, Kuczmarski RJ, Flegal KM, Johnson CL & Hubbard VS (2003) Development of bioelectrical impedance analysis prediction equations for body composition with the use of a multicomponent model for use in epidemiologic surveys. *American Journal of Clinical Nutrition* **77,** 331-340.

Swart GR, Baartman EA, Wattimena JL, Rietveld T, Overbeek SE & Van den Berg JW (1997) Evaluation studies of the ^{13}C-mixed triglyceride breath test in healthy controls and adult cystic fibrosis patients with exocrine pancreatic insufficiency. *Digestion* **58,** 415-420.

Thomas JE (1998) ^{13}C urea breath test. *Gut* **43,** S7-S12.

Thomas JE, Dale A, Harding M, Coward WA, Cole TJ, Sullivan PB, Campbell DI, Warren BF & Weaver LT (1999) Interpreting the ^{13}C-urea breath test among a large population of young children from a developing country. *Pediatric Research* **46,** 147-151.

Treuth MS, Adolph AL & Butte NF (1998) Energy expenditure in children predicted from heart rate and activity calibrated against respiration calorimetry. *American Journal of Physiology* **275,** E12-E18.

Trieber FA, Musante L, Hartdagan S, Davis H, Levy M & Strong WB (1989) Validation of a heart rate monitor with children in laboratory and field settings. *Medicine and Science in Sports and Exercise* **21,** 338-342.

Trost SG, Ward DS, Moorehead SM, Watson PD, Riner W & Burke JR (1998) Validity of the computer science and applications (CSA) activity monitor in children. *Medicine & Science in Sports & Exercise* **30,** 629-633.

Turner SM, Murphy EJ, Neese RA, Antelo F, Thomas T, Agarwal A, Go C & Hellerstein MK (2003) Measurement of TG synthesis and turnover in vivo by $^{2}H_2O$ incorporation into the glycerol moiety and application of MIDA. *American Journal of Physiology* **285,** E790-E803.

Van de Kamer JH, Huinick H & Weyers HA, (1949) Rapid method for determination of fat in feces. *Journal of Biological Chemistry* **177,** 347-355.

van Dijk-van Aalst K, Van Den Driessche MI., van der Schoor S, Schiffelers S, Van't Westeinde T, Ghoos Y & Veereman-Wauters G (2001) ^{13}C mixed triglyceride breath test: a noninvasive method to assess lipase activity in children. *Journal of Pediatric Gastroenterology and Nutrition* **32,** 579-585.

van Hall G (1999) Correction factors for ^{13}C-labelled substrate oxidation at whole-body and muscle level. *Proceedings of the Nutrition Society* **58,** 979-986.

van Raaij J (2002) Energy. In *Essentials of Human Nutrition,* Second Edition, pp. 79-96. [J Mann & AS Truswell, editors]. Oxford: Oxford University Press.

Vantrappen GR, Rutgeerts PJ, Ghoos YF & Hiele MI (1989) Mixed triglyceride breath test: a noninvasive test of pancreatic lipase activity in the duodenum. *Gastroenterology* **96,** 1126-1134.

Ventham JC & Reilly JJ (1999) Reproducibility of resting metabolic rate measurement in children. *British Journal of Nutrition* **81,** 435-437.

Vermorel M, Vernet J, Bitar A, Fellmann N & Coudert J (2002) Daily energy expenditure, activity patterns, and energy costs of the various activities in French 12-16-y-old adolescents in free living conditions. *European Journal of Clinical Nutrition* **56,** 819-829.

Wareham NJ, Hennings SJ, Prentice AM & Day NE (1997) Feasibility of heart-rate monitoring to estimate total level and pattern of energy expenditure in a population-based epidemiological study: the Ely young cohort feasibility study 1994-5. *British Journal of Nutrition* **78,** 889-900.

Waldron S & Preston T (2001) Compound specific stable isotope characterisation of volatile fatty acids (C2-C6). *Abstracts of the American Chemical Society* **221,** 92-GEOC.

Walsh S & Diamond D (1995) Non-linear curve fitting using Microsoft Excel *Solver*. *Talanta* **42,** 561-572.

Weaver LT (1998) Stable Isotope Breath Tests. *Nutrition* **14,** 826-829.

Weaver LT, Manson WG & Amarri S (1997) Measuring fat digestion in early life using stable isotope breath tests. *Prenatal and Neonatal Medicine* **2,** 116-123.

Weaver LT, Thomas JE, McClean P, Harding M, & Coward WA (1993) Stable isotope breath tests: their use in paediatric practice. In *Progress in understanding and management of gastrointestinal motility disorders,* pp. 155-168. [J Janssens, editors]. Leuven: KU Leuven, Department of Medicine, Division of Gastroenterology.

Weir JBV (1949) New methods for calculating metabolic rate with special reference to protein metabolism. *Journal of Physiology* **109,** 1-9.

Welk GJ & Corbin CB (1995) The validity of the Tritrac-R3D activity monitor for the assessment of physical activity in children. *Research Quarterly for Exercise and Sport* **66,** 202-209.

Wells JCK, Fuller NJ, Dewit O, Fewtrell MS, Elia M & Cole TJ (1999) Four-compartment model of body composition in children: density and hydration of fat-free mass and comparison with simpler models. *American Journal of Clinical Nutrition* **69,** 904-912.

Weststrate JA (1993) Resting metabolic rate and diet induced thermogenesis: a methodological reappraisal. *American Journal of Clinical Nutrition* **58,** 592-601.

Wigmore SJ, Falconer JS, Plester CE, Ross JA, Maingay JP, Carter DC & Fearon KCH (1995) Ibuprofen reduces energy-expenditure and acute-phase protein production compared with placebo in pancreatic-cancer patients. *British Journal of Cancer* **72,** 185-188.

Wilson DJ & Pencharz PB (1998) Nutrition and cystic fibrosis. *Nutrition* **14,** 792-795.

Wolever, TMS, Spadafora, PJ, Cunnane,SC & Pencharz PB (1995) Proprionate inhibits incorporation of colonic [1,2-^{13}C]acetate into plasma lipids in humans. *American Journal of Clinical Nutrition* **61**, 1241-1247.

Wong L, Turtle S & Davidson A (1982) Secretin pancreozymin stimulation test and confirmation of the diagnosis of cystic fibrosis. *Gut* **23,** 744-750.

Woodward J & Colagiovanni L (1998) Feed the patient, fool the pancreas. *Nursing Times* **94,** 65-69.

Wutzke KD, Radke M, Breuel K, Gurk S, Lafrenz J-D & Heine WE (1999) Triglyceride oxidation in cystic fibrosis: a comparison between different ^{13}C-labeled tracer substances. *Journal of Pediatric Gastroenterology and Nutrition* **29,** 148-154.

Wyse CA, Murphy DM, Preston T, Sutton DG, Morrison DJ, Christley RM & Love S (2001a) The ^{13}C-octanoic acid breath test for detection of effects of meal composition on the rate of solid-phase gastric emptying in ponies. *Research in Veterinary Science* **71,** 81-83.

Wyse CA, Preston T, Love S, Morrison DJ, Cooper JM & Yam PS (2001b) Use of the ^{13}C-octanoic acid breath test for assessment of solid-phase gastric emptying in dogs. *American Journal of Veterinary Research* **62,** 1939-1944.

Young VR & Ajami AM (1999) 1999 Jonathan E. Rhoads Lecture. Isotopic metaprobes, nutrition, and the roads ahead. *Journal of Parenteral & Enteral Nutrition* **23,** 175-194.

Zammit VA (1984) Mechanisms of regulation of the partition of fatty acids between oxidation and esterification in the liver. *Progress in Lipid Research* **23,** 39-67.

Zammit VA (1999a) Carnitine acyltransferase: functional significance of subcellular distributions and membrane topology. *Progress in Lipid Research* **38,** 199-224.

Zammit VA (1999b) The malonyl-CoA-long chain acyl-CoA axis in the maintenance of mammalian cell function. *Biochemical Journal* **343,** 505-515.

Appendix 1 Copies of Ethical Approval Letters

Administrative Assistant:
Ms Deborah Maddern

DM/dm

UNIVERSITY
of
GLASGOW

20 January 2000

Ms Christine Slater
Department of Child Health
RHSC Yorkhill
Glasgow G3 8SJ

Dear Ms Slater

Ethics Committee for Non Clinical Research Involving Human Subjects

Validation study of the mixed triglyceride breath test for assessing fat digestion

Thank you for your recent submission to the Ethics Committee. I am pleased to inform you that the Committee has approved this project.

Yours sincerely

COURT OFFICE
University of Glasgow, Main Building, Glasgow G12 8QQ
Secretary of Court: Mr Dugald Mackie, *Direct Line:* 0141-330 4266
~~*Academic Secretary:* Miss Fiona Aikon, *Ext* 4243/4102~~
Administrative Assistant: Ms Deborah Maddern, *Ext* 5853/4120
Telephone: 0141-339 8855 *Fax:* 0141-330 4920 *Telex:* 777070 UNIGLA

Yorkhill Research Ethics Committee
Room 1 Harley Street
Yorkhill NHS Trust
Glasgow
G3 8SJ

Tel number 0141 201 0728
Fax number 0141 201 6976

EM/

11 April 2000

C Slater
DCH
Yorkhill NHS Trust
GLASGOW

P46/99 Validation study of the mixed triglyceride breath test for assessing fat digestion

Thank you for your letter of the 3 March 2000 forwarding amendments as requested. The proposal P46/99 Validation study of the mixed triglyceride breath test for assessing fat digestion has the approval of the Yorkhill Research Ethics Committee.

With kind regards

Yours sincerely

Dr B Holland
Secretary Yorkhill Research Ethics Committee

Validation study of the mixed triglyceride breath test for assessing fat digestion

Information sheet for parents and volunteers

Children get most of their energy from fat and sugar in their diet. However, we know very little about how they digest these nutrients and what happens after they have been absorbed. One way of finding out is to label the fat and then measure how well it is digested and absorbed, by collecting samples of children's breath before and after a meal.

We are therefore inviting your child to take part in a research project which will give us information about children's digestion.

If your child decides to take part, we will ask you to bring your him or her to the hospital on two occasions, in the morning having missed breakfast. If you prefer we can do the test in your own home; whichever is the most convenient to you. We will put a heart rate monitor on your child. This consists of a strap, which is worn around the chest and a wrist watch which collects the data. We will ask your child to blow through a straw into a glass tube to give us a sample of their breath. Your child will then be asked to eat a biscuit made from oats, butter and honey and containing a small amount of fat labelled with carbon-13. This is a non-radioactive, naturally occuring element. The fat is a normal part of our everyday food. There are therefore no side effects associated with eating this biscuit.

The carbon-13 will gradually appear in your child's breath over the next few hours and we will collect breath samples by asking him or her to blow through a straw into a tube at intervals. After the first 3 hours, we will measure how much carbon dioxide your child is breathing out using a special hood connected to a 'calorimeter'. This takes about 15 minutes. Your child will then be able to have a meal made of his or her usual foods, but avoiding sweets, sugary drinks and foods containing corn. We will continue to collect breath samples for 6 hours on the first occasion and 10 hours on the second occasion. You will be free to go home after 6 hours, but we would ask you to collect breath samples in the tubes provided until bed time.

On the first occasion, we will measure the carbon dioxide produced in your child's breath when he or she is lying on a bed or sofa, when they are sitting up and while they are dancing to some music. This will not take longer than 30 minutes. We do this because heart rate is related to oxygen consumption and carbon dioxide production, and we hope that in the future we will be able to use the heart rate monitors alone to estimate carbon dioxide production.

It is up to you and your child to decide whether or not to take part. If your child decides to take part, you will both be asked to sign a consent form and will be given copies of the consent form and this sheet to keep. If your child decides to take part he or she is free to withdraw at any time and without giving a reason. This will not affect the standard of care your child receives. We have done hundreds of breath tests on children. Breath tests are used to diagnose a number of childhood diseases, and they are absolutely safe and painless. All information obtained during the study will be treated as confidential.

If you have any questions about the project please do not hesitate to contact Christine Slater on 0141-201-0502.

Thank you for reading this.

Christine Slater
Senior Research Assistant

Dr Tom Preston
Senior Lecturer

Prof Lawrence Weaver
Consultant Paediatrician

Validation study of the mixed triglyceride breath test for assessing fat digestion

Information sheet for children

We would like you to help us to find out more about how your food is digested after you have swallowed it. We need to know what happens in healthy children, so that we can help children who are ill.

You can help us by coming to the hospital for a day, or we can come to your house. We will ask you to eat a biscuit made of oats, butter and honey and then blow into a tube when we ask. Blowing into a tube is a way of collecting the air that you breath out.

We will also ask you to wear a heart-rate monitor. This is a belt that you wear round your chest, which can hear your heart beating. We would also like you to wear a watch which counts your heart-beats. This does not hurt in any way and you will be asked to keep it on all day.

You will not be allowed to run around, but you can watch TV, play computer games, read books or play board games. We will study 2 children each time, so you will have a friend to play with.

After a few hours we will ask you to lie on a bed and breath into a special machine. You have to lie still for about 10 minutes, if you can keep still for that long. It does not matter if you move about a little bit. We will also ask you to stand up and then jump up and down while we measure you breathing. I have some photographs of me lying on a bed and riding an exercise bike. If you want, we could take a photo for you to show your friends.

None of this hurts in any way, but if you are unhappy we can stop at any time.

Thank you for reading this.

Christine Slater Dr Preston Professor Weaver

UNIVERSITY
of
GLASGOW

Consent form

Validation study of the mixed triglyceride breath test for assessing fat digestion

I have read and understand the information sheet concerning the above study. I give permission for my child named below to take part in this study.

I understand that our participation is voluntary and that we are free to withdraw at any time, without giving any reason, without my child's medical care or legal rights being affected.

Name of Child .....

Date of Birth .....

Signature of Child ..... Date .....

Name of Parent/Guardian .....

Address .....

.....

Telephone number .....

Signature of Parent/Guardian ..... Date .....

Name of Researcher .....

Signature of Researcher.....Date .....

Name of Witness .....

Signature of Witness .....Date .....

DEPARTMENT OF CHILD HEALTH
Royal Hospital for Sick Children, Yorkhill, Glasgow G3 8SJ
Sanson Gemmell Chair of Child Health: Professor L T Weaver
Leonard Gao Lecturer: Dr T L Turner
Senior Lecturers: Dr M D C Donaldson, Dr K B Drummond, Dr J Y Paton, Dr D H Stone, Dr D M Tappin
Telephone: 0141-201 0000 (Hospital) *Fax:* 0141-201 0857

Appendix 2 HR calibration summary tables

Comparison of measured $\dot{V}CO_2$ normalised to body surface area ($mmol.min^{-1}.m^{-2}$) with $\dot{V}CO_2$ predicted from heart rate (HR) using the model stated. The first eight rows are individual calibrations for that subject. Generic relates to the effect of predicting $\dot{V}CO_2$ from HR by applying a generic calibration, which was obtained by combining data from all 24 subjects and fitting a sigmoid model. The Tables also show data normalised to $height^3$ ($mmol.min^{-1}.m^{-3}$) using individual and generic calibrations. The mean, standard error and 95% confidence interval for data normalised to $height^3$ cannot be directly compared with data normalised to body surface area as the units are different, but they can be compared between subjects.

N = number of data points in calibration curve

Mean = mean difference between measured and predicted $\dot{V}CO_2$ i.e. bias of the model

Best model has mean = 0

SEM = standard error on the mean

95 % CI = 95 % confidence interval for mean difference

P = probability that there is no difference between measured and predicted $\dot{V}CO_2$ using a 1-sample T-Test

BMI = Body mass index (weight (kg)/ height $(m)^2$)

BMI SDS = BMI Standard deviation score from British Growth Reference Charts (Child Growth Foundation 96)

$\dot{V}CO_2$ was predicted from $\dot{V}O_2$ assuming a RQ of 0.85. $\dot{V}O_2$ was normalised to body surface area and predicted from HR using a sigmoid model.

All generic predictions used a sigmoid model.

Surface area (m^2) = weight $(kg)^{0.5378}$ x height $(cm)^{0.3964}$ x 0.024265 (Haycock, 1978)

Subject: Adult 1, female, age 46 y, height 158.8 cm, weight 57.6 kg, BMI 22.8

Model	N	Mean	SEM	95 % CI	P
Linear-flex (sa)	75	0.00	0.22	-0.43, 0.44	0.99
Steady state (sa)	75	0.54	0.27	0.01, 1.07	0.05
3rd order polynomial, raw HR (sa)	75	-0.00	0.17	-0.34, 0.34	1.00
3rd order polynomial, sm HR* (sa)	75	0.00	0.17	-0.34, 0.34	1.00
Logistic, sm HR* (sa)	75	0.00	0.17	-0.34, 0.34	1.00
Sigmoid, raw HR (sa)	75	-0.00	0.17	-0.33, 0.33	1.00
Sigmoid, sm HR* (sa)	75	-0.00	0.17	-0.34, 0.34	1.00
$\dot{V}CO_2$ predicted from $\dot{V}O_2$ (sa)	75	0.82	0.19	0.44, 1.19	<0.001
Generic surface area	75	-0.05	0.22	-0.49, 0.40	0.83
Generic surface area and age	75	-1.53	0.31	-2.15, -0.92	<0.001
Sigmoid, sm HR* (height^3)	75	0.00	0.07	-0.13, 0.14	1.00
Generic height^3	75	0.03	0.08	-0.14, 0.19	0.76
Generic height^3 and age	75	-0.26	0.08	-0.43, -0.10	0.002

(sa) = $\dot{V}CO_2$ normalised to body surface area, predicted from height and weight
* sm HR = heart rate smoothed 2 points forward

Subject: Adult 2, male, age 47 y, height 182.9 cm, weight 74.2 kg, BMI 22.2

Model	N	Mean	SEM	95 % CI	P
Linear-flex (sa)	68	-1.31	0.53	-2.34, -0.25	0.02
Steady state (sa)	68	-0.66	0.68	-2.02, 0.71	0.34
3rd order polynomial, raw HR (sa)	68	-0.00	0.43	-0.85, 0.85	1.00
3rd order polynomial, sm HR* (sa)	68	-0.00	0.37	-0.74, 0.74	1.00
Logistic, sm HR* (sa)	68	-0.00	0.36	-0.72, 0.72	1.00
Sigmoid, raw HR (sa)	68	-0.00	0.42	-0.84, 0.84	1.00
Sigmoid, sm HR* (sa)	68	-0.00	0.36	-0.72, 0.72	1.00
$\dot{V}CO_2$ predicted from $\dot{V}O_2$ (sa)	68	1.01	0.46	0.10, 1.92	0.03
Generic surface area	68	2.86	0.64	1.56, 4.14	<0.001
Generic surface area and age	68	1.74	0.48	0.78, 2.71	<0.001
Sigmoid, sm HR* (height^3)	68	0.00	0.12	-0.23, 0.23	1.00
Generic height^3	68	0.41	0.17	0.06, 0.76	0.02
Generic height^3 and age	68	0.18	0.18	-1.18, 0.54	0.31

(sa) = $\dot{V}CO_2$ normalised to body surface area, predicted from height and weight
* sm HR = heart rate smoothed 2 points forward

Subject: Adult 3, male, age 21 y, height 187.0 cm, weight 81.7 kg, BMI 23.4

Model	N	Mean	SEM	95 % CI	P
Linear-flex (sa)	77	0.61	0.25	0.11, 1.15	0.02
Steady state (sa)	77	0.59	0.58	-0.56, 1.73	0.31
3rd order polynomial, raw HR (sa)	77	-0.00	0.24	-0.49, 0.49	1.00
3rd order polynomial, sm HR* (sa)	77	-0.00	0.26	-0.52, 0.52	1.00
Logistic, sm HR* (sa)	77	0.00	0.25	-0.50, 0,50	1.00
Sigmoid, raw HR (sa)	77	0.00	0.24	-0.48, 0.48	1.00
Sigmoid, sm HR* (sa)	77	-0.00	0.25	-0.50, 0.50	1.00
$\dot{V}CO_2$ predicted from $\dot{V}O_2$ (sa)	77	0.96	0.26	0.43, 1.48	<0.001
Generic surface area	77	0.13	0.31	-0.48, 0.74	0.67
Generic surface area and age	77	0.20	0.26	-0.32, 0.73	0.44
Sigmoid, sm HR* (height^3)	77	-0.00	0.08	-0.16, 0.16	1.00
Generic height^3	77	-0.59	0.08	-0.75, -0.42	<0.001
Generic height^3 and age	77	-0.48	0.08	-0.64, 0.31	<0.001

(sa) = $\dot{V}CO_2$ normalised to body surface area, predicted from height and weight
* sm HR = heart rate smoothed 2 points forward

Subject: Adult 4, female, age 22 y, height 162.9 cm, weight 67.0 kg, BMI 25.2

Model	N	Mean	SEM	95 % CI	P
Linear-flex (sa)	65	-0.30	0.24	-0.77, 0.17	0.21
Steady state (sa)	65	-0.49	0.25	-1.00, 0.02	0.06
3rd order polynomial, raw HR (sa)	65	-0.00	0.21	-0.42, 0.42	1.00
3rd order polynomial, sm HR* (sa)	65	-0.00	0.21	-0.42, 0.42	1.00
Logistic, sm HR* (sa)	65	0.00	0.20	-0.40, 0.40	1.00
Sigmoid, raw HR (sa)	65	0.00	0.21	-0.41, 0.41	1.00
Sigmoid, sm HR* (sa)	65	0.00	0.20	-0.40, 0.40	1.00
$\dot{V}CO_2$ predicted from $\dot{V}O_2$ (sa)	65	0.92	0.24	0.43, 1.41	<0.001
Generic surface area	65	-1.15	0.23	-1.62, -0.69	<0.001
Generic surface area and age	65	-1.42	0.23	-1.87, -0.97	<0.001
Sigmoid, sm HR* (height^3)	65	0.00	0.08	-0.16, 0.16	1.00
Generic height^3	65	-0.37	0.09	-0.56, -0.19	<0.001
Generic height^3 and age	65	-0.33	0.08	-0.49, -0.16	<0.001

(sa) = $\dot{V}CO_2$ normalised to body surface area, predicted from height and weight
* sm HR = heart rate smoothed 2 points forward

Subject: Adult 5, male, age 32 y, height 180.4 cm, weight 70.7 kg, BMI 21.7

Model	N	Mean	SEM	95 % CI	P
Linear-flex (sa)	74	-1.27	0.24	-1.75, -0.79	<0.001
Steady state (sa)	74	-1.85	0.26	-2.37, -1.34	<0.001
3rd order polynomial, raw HR (sa)	74	0.00	0.22	-0.44, 0.44	1.00
3rd order polynomial, sm HR* (sa)	74	-0.00	0.19	-0.38, 0.38	1.00
Logistic, sm HR* (sa)	74	-0.00	0.19	-0.38, 0.38	1.00
Sigmoid, raw HR (sa)	74	0.00	0.22	-0.44, 0.44	1.00
Sigmoid, sm HR* (sa)	74	-0.00	0.19	-0.38, 0.38	1.00
$\dot{V}CO_2$ predicted from $\dot{V}O_2$ (sa)	74	1.42	0.25	0.93, 1.91	<0.001
Generic surface area	74	0.75	0.30	0.15, 1.36	0.02
Generic surface area and age	74	0.21	0.23	-0.25, 0.67	0.37
Sigmoid, sm HR* (height^3)	74	-0.00	0.06	-0.12, 0.12	0.99
Generic height^3	74	-0.33	0.07	-0.47, -0.19	<0.001
Generic height^3 and age	74	-0.37	0.07	-0.51, -0.23	<0.001

(sa) = $\dot{V}CO_2$ normalised to body surface area, predicted from height and weight
* sm HR = heart rate smoothed 2 points forward

Subject: Adult 6, male, age 26 y, height 182.2 cm, weight 68.7 kg, BMI 20.7

Model	N	Mean	SEM	95 % CI	P
Linear-flex (sa)	60	0.31	0.39	-0.47, 1.10	0.43
Steady state (sa)	60	-0.31	0.49	-1.28, 0.66	0.53
3rd order polynomial, raw HR (sa)	60	-0.00	0.38	-0.77, 0.77	1.00
3rd order polynomial, sm HR* (sa)	60	-0.00	0.29	-0.58, 0.58	1.00
Logistic, sm HR* (sa)	60	0.00	0.29	-0.58, 0.58	1.00
Sigmoid, raw HR (sa)	60	0.00	0.38	-0.77, 0.77	1.00
Sigmoid, sm HR* (sa)	60	0.00	0.29	-0.58, 0.58	1.00
$\dot{V}CO_2$ predicted from $\dot{V}O_2$ (sa)	60	0.57	0.39	-0.21, 1.35	0.15
Generic surface area	60	0.17	0.34	-0.51, 0.85	0.61
Generic surface area and age	60	-0.04	0.30	-0.63, 0.55	0.90
Sigmoid, sm HR* (height^3)	60	-0.00	0.09	-0.18, 0.18	1.00
Generic height^3	60	-0.51	0.09	-0.69, -0.33	<0.001
Generic height^3 and age	60	-0.54	0.10	-0.74, -0.35	<0.001

(sa) = $\dot{V}CO_2$ normalised to body surface area, predicted from height and weight
sm HR = heart rate smoothed 2 points forward

Subject: Adult 7, male, age 26 y, height 177.6 cm, weight 108.2 kg, BMI 34.3

Model	N	Mean	SEM	95 % CI	P
Linear-flex (sa)	74	-0.81	0.30	-0.78, 0.41	0.55
Steady state (sa)	74	-0.98	0.27	-0.51, -0.44	<0.001
3rd order polynomial, raw HR (sa)	74	-0.00	0.24	-0.48, 0.48	1.00
3rd order polynomial, sm HR* (sa)	74	-0.00	0.23	-0.46, 0.46	1.00
Logistic, sm HR* (sa)	74	0.00	0.22	-0.44, 0.44	1.00
Sigmoid, raw HR (sa)	74	0.00	0.23	-0.47, 0.47	1.00
Sigmoid, sm HR* (sa)	74	-0.00	0.22	-0.44, 0.44	1.00
$\dot{V}CO_2$ predicted from $\dot{V}O_2$ (sa)	74	0.45	0.23	-0.02, 0.91	0.06
Generic surface area	74	-0.41	0.26	-0.93, 0.12	0.13
Generic surface area and age	74	-0.86	0.25	-1.36, -0.37	<0.001
Sigmoid, sm HR* (height^3)	74	-0.00	0.10	-0.19, 0.19	1.00
Generic height^3	74	0.02	0.10	-0.19, 0.24	0.83
Generic height^3 and age	74	0.04	0.10	-0.15, 0.24	0.66

(sa) = $\dot{V}CO_2$ normalised to body surface area, predicted from height and weight
* sm HR = heart rate smoothed 2 points forward

Subject: Adult 8, male, age 21 y, height 171.0 cm, weight 68.4 kg, BMI 23.4

Model	N	Mean	SEM	95 % CI	P
Linear-flex (sa)	66	-0.75	0.49	-1.73, 0.22	0.13
Steady state (sa)	66	1.32	0.82	-0.33, 2.96	0.11
3rd order polynomial, raw HR (sa)	66	-0.00	0.42	-0.84, 0.84	1.00
3rd order polynomial, sm HR* (sa)	66	-0.00	0.37	-0.73, 0.73	1.00
Logistic, sm HR* (sa)	66	0.00	0.36	-0.72, 0.72	1.00
Sigmoid, raw HR (sa)	66	-0.00	0.42	-0.83, 0.83	1.00
Sigmoid, sm HR* (sa)	66	-0.00	0.36	-0.72, 0.72	1.00
$\dot{V}CO_2$ predicted from $\dot{V}O_2$ (sa)	66	0.34	0.43	-0.53, 1.20	0.44
Generic surface area	66	2.75	0.64	1.47, 4.04	<0.001
Generic surface area and age	66	3.05	0.64	1.79, 4.43	<0.001
Sigmoid, sm HR* (height^3)	66	-0.00	0.13	-0.26, 0.26	1.00
Generic height^3	66	0.87	0.22	0.43, 1.31	<0.001
Generic height^3 and age	66	0.94	0.23	0.48, 1.40	<0.001

(sa) = $\dot{V}CO_2$ normalised to body surface area, predicted from height and weight
* sm HR = heart rate smoothed 2 points forward

Subject: Child 1, male, age 13.6 y, height 145.5 cm, weight 57.2 kg, BMI SDS 2.28

Model	N	Mean	SEM	95 % CI	P
Linear-flex (sa)	30	0.48	0.62	-0.79, 1.749	0.45
Steady state (sa)	30	-0.50	0.78	-2.10, 1.09	0.52
3rd order polynomial, raw HR (sa)	30	-0.00	0.46	-0.94, 0.94	1.00
3rd order polynomial, sm HR* (sa)	30	0.00	0.39	-0.80, 0.80	1.00
Sigmoid, raw HR (sa)	30	0.00	0.49	-1.00, 1.00	1.00
Sigmoid, sm HR* (sa)	30	0.00	0.34	-0.69, 0.69	1.00
$\dot{V}CO_2$ predicted from $\dot{V}O_2$ (sa)	30	0.34	0.75	-1.20, 1.88	0.65
Generic surface area	30	0.53	0.46	-0.41, 1.47	0.26
Generic surface area and age	30	1.06	0.46	0.11, 2.01	0.03
Sigmoid, sm HR* (height^3)	30	0.00	0.17	-0.34, 0.34	1.00
Generic height^3	30	1.04	0.20	0.63, 1.46	<0.001
Generic height^3 and age	30	1.26	0.21	0.84, 1.69	<0.001

(sa) = $\dot{V}CO_2$ normalised to body surface area, predicted from height and weight
* sm HR = heart rate smoothed 2 points forward

Subject: Child 2, female, age 11.1 y, height 137.3 cm, weight 43.6 kg, BMI SDS 1.81

Model	N	Mean	SEM	95 % CI	P
Linear-flex (sa)	27	-0.56	0.71	-2.03, 0.90	0.44
Steady state (sa)	27	-0.40	0.43	-1.29, 0.49	0.36
3rd order polynomial, raw HR (sa)	27	0.00	0.29	-0.60, 0.60	1.00
3rd order polynomial, sm HR* (sa)	27	-0.00	0.24	-0.48, 0.48	1.00
Sigmoid, raw HR (sa)	27	-0.00	0.32	-0.65, 0.65	1.00
Sigmoid, sm HR* (sa)	27	0.00	0.24	-0.49, 0.49	1.00
$\dot{V}CO_2$ predicted from $\dot{V}O_2$ (sa)	27	0.28	0.32	-0,38, 0.94	0.39
Generic surface area	27	-1.10	0.27	-1.65, -0.55	<0.001
Generic surface area and age	27	-0.52	0.33	-1.20, 0.16	0.13
Sigmoid, sm HR* (height^3)	27	0.00	0.08	-0.16, 0.16	1.00
Generic height^3	27	0.22	0.13	-0.05, 0.48	0.11
Generic height^3 and age	27	0.42	0.14	0.12, 0.72	0.007

(sa) = $\dot{V}CO_2$ normalised to body surface area, predicted from height and weight
* sm HR = heart rate smoothed 2 points forward

Subject: Child 3, male, age 9.0 y, height 123.4 cm, weight 35.1 kg, BMI SDS 2.54

Model	N	Mean	SEM	95 % CI	P
Linear-flex (sa)	29	-0.56	0.40	-1.39, 0.26	0.17
Steady state (sa)	29	-0.80	0.44	-1.69, 0.10	0.08
3rd order polynomial, raw HR (sa)	29	-0.00	0.37	-0.75, 0.75	1.00
3rd order polynomial, sm HR* (sa)	29	-0.00	0.23	-0.47, 0.47	1.00
Sigmoid, raw HR (sa)	29	-0.00	0.37	-0.75, 0.75	1.00
Sigmoid, sm HR* (sa)	29	-0.00	0.23	-0.47, 0.47	1.00
$\dot{V}CO_2$ predicted from $\dot{V}O_2$ (sa)	29	0.35	0.42	-0.51, 1.21	0.41
Generic surface area	29	-3.21	0.23	-3.68, -2.74	<0.001
Generic surface area and age	29	-2.57	0.27	-3.12, -2.02	<0.001
Sigmoid, sm HR* (height^3)	29	0.00	0.12	-0.26, 0.26	1.00
Generic height^3	29	0.16	0.16	-0.17, 0.49	0.31
Generic height^3 and age	29	0.58	0.14	0.29, 0.87	<0.001

(sa) = $\dot{V}CO_2$ normalised to body surface area, predicted from height and weight
* sm HR = heart rate smoothed 2 points forward

Subject: Child 4, female, age 14.3 y, height 152.9 cm, weight 40.8 kg, BMI SDS –0.96

Model	N	Mean	SEM	95 % CI	P
Linear-flex (sa)	33	-2.44	1.33	-5.15, 0.27	0.08
Steady state (sa)	33	-1.32	1.09	-3.54, 0.90	0.24
3rd order polynomial, raw HR (sa)	33	0.00	0.73	-1.48, 1.48	1.00
3rd order polynomial, sm HR* (sa)	33	0.00	0.59	-1.21, 1.21	1.00
Sigmoid, raw HR (sa)	33	0.00	0.73	-1.49, 1.49	1.00
Sigmoid, sm HR* (sa)	33	0.00	0.61	-1.24, 1.24	1.00
$\dot{V}CO_2$ predicted from $\dot{V}O_2$ (sa)	33	2.48	0.82	0.81, 4.14	0.005
Generic surface area	33	4.47	0.80	2.85, 6.09	<0.001
Generic surface area and age	33	4.84	0.74	3.34, 6.36	<0.001
Sigmoid, sm HR* (height^3)	33	0.00	0.22	-0.45, 0.45	1.00
Generic height^3	33	1.43	0.27	0.89, 1.98	<0.001
Generic height^3 and age	33	1.59	0.27	1.04, 2.13	<0.001

(sa) = $\dot{V}CO_2$ normalised to body surface area, predicted from height and weight
* sm HR = heart rate smoothed 2 points forward

Subject: Child 5, male, age 9.5 y, height 130.4 cm, weight 31.5 kg, BMI SDS 1.11

Model	N	Mean	SEM	95 % CI	P
Linear-flex (sa)	23	0.09	0.26	-0.44, 0.62	0.73
Steady state (sa)	23	-0.78	0.28	-1.36, -0.191	0.01
3rd order polynomial, raw HR (sa)	23	0.00	0.24	-0.49, 0.49	1.00
3rd order polynomial, sm HR* (sa)	23	0.00	0.26	-0.54, 0.54	1.00
Sigmoid, raw HR (sa)	23	0.00	0.24	-0.49, 0.49	1.00
Sigmoid, sm HR* (sa)	23	0.00	0.26	-0.54, 0.54	1.00
$\dot{V}CO_2$ predicted from $\dot{V}O_2$ (sa)	23	0.93	0.24	0.43, 1.42	<0.001
Generic surface area	23	-0.28	0.27	-0.84, 0.27	0.31
Generic surface area and age	23	0.51	0.28	-0.07, 1.10	0.08
Sigmoid, sm HR* (height^3)	23	0.00	0.12	-0.26, 0.26	1.00
Generic height^3	23	0.62	0.13	0.29, 0.83	<0.001
Generic height^3 and age	23	0.60	0.13	0.65, 1.17	<0.001

(sa) = $\dot{V}CO_2$ normalised to body surface area, predicted from height and weight
* sm HR = heart rate smoothed 2 points forward

Subject: Child 6, female, age 8.5 y, height 120.6 cm, weight 25.9 kg, BMI SDS 0.76

Model	N	Mean	SEM	95 % CI	P
Linear-flex (sa)	22	0.77	0.46	-0.19, 1.73	0.11
Steady state (sa)	22	-0.34	0.36	-1.09, 0.42	0.36
3rd order polynomial, raw HR (sa)	22	-0.00	0.33	-0.68, 0.68	1.00
3rd order polynomial, sm HR* (sa)	22	0.00	0.30	-0.61, 0.62	1.00
Sigmoid, raw HR (sa)	22	-0.00	0.33	-0.68, 0.68	1.00
Sigmoid, sm HR* (sa)	22	0.00	0.30	-0.62, 0.62	1.00
$\dot{V}CO_2$ predicted from $\dot{V}O_2$ (sa)	22	0.59	1.01	-1.51, 2.69	0.56
Generic surface area	22	1.02	0.38	0.24, 1.80	0.01
Generic surface area and age	22	1.59	0.35	0.87, 2.31	<0.001
Sigmoid, sm HR* (height^3)	22	0.00	0.16	-0.33, 0.33	1.00
Generic height^3	22	1.75	0.26	1.21, 2.87	<0.001
Generic height^3 and age	22	2.04	0.26	1.51, 2.58	<0.001

(sa) = $\dot{V}CO_2$ normalised to body surface area, predicted from height and weight
* sm HR = heart rate smoothed 2 points forward

Subject: Child 7, female, age 5.5 y, height 108.4 cm, weight 20.2 kg, BMI SDS 1.03

Model	N	Mean	SEM	95 % CI	P
Linear-flex (sa)	29	0.59	0.31	-0.04, 1.22	0.07
Steady state (sa)	29	-0.47	0.37	-1.22, 0.28	0.21
3rd order polynomial, raw HR (sa)	29	0.00	0.23	-0.48, 0.48	1.00
3rd order polynomial, sm HR* (sa)	29	-0.00	0.16	-0.32, 0.32	1.00
Sigmoid, raw HR (sa)	29	-0.00	0.24	-0.50, 0.50	1.00
Sigmoid, sm HR* (sa)	29	0.00	0.16	-0.32, 0.32	1.00
$\dot{V}CO_2$ predicted from $\dot{V}O_2$ (sa)	29	1.02	0.17	0.68, 1.37	<0.001
Generic surface area	29	-6.55	0.28	-7.13, -5.97	<0.001
Generic surface area and age	29	-5.30	0.26	-5.82, -4.77	<0.001
Sigmoid, sm HR* (height^3)	29	0.00	0.09	-0.20, 0.19	0.99
Generic height^3	29	-1.27	0.10	-1.48, -1.07	<0.001
Generic height^3 and age	29	-0.69	0.13	-0.96, -0.42	<0.001

(sa) = $\dot{V}CO_2$ normalised to body surface area, predicted from height and weight
* sm HR = heart rate smoothed 2 points forward

Subject: Child 8, male, age 14.7 y, height 178.2 cm, weight 62.3 kg, BMI SDS 0.21

Model	N	Mean	SEM	95 % CI	P
Linear-flex (sa)	56	0.28	0.30	-0.32, 0.88	0.35
Steady state (sa)	56	0.32	0.31	-0.30, 0.93	0.30
3rd order polynomial, raw HR (sa)	56	0.01	0.29	-0.57, 0.59	0.97
3rd order polynomial, sm HR* (sa)	56	0.00	0.28	-0.57, 0.57	1.00
Sigmoid, raw HR (sa)	56	0.01	0.29	-0.57, 0.57	1.00
Sigmoid, sm HR* (sa)	56	0.00	0.28	-0.56, 0.56	1.00
$\dot{V}CO_2$ predicted from $\dot{V}O_2$ (sa)	56	0.73	0.29	0.14, 1.32	0.02
Generic surface area	56	-3.48	0.38	-4.24, -2.72	<0.001
Generic surface area and age	56	-3.29	0.48	-4.25, -2.33	<0.001
Sigmoid, sm HR* (height^3)	56	0.00	0.09	-0.17, 0.17	1.00
Generic height^3	56	-2.14	0.17	-2.47, -1.81	<0.001
Generic height^3 and age	56	-1.89	0.18	-2.26, -1.52	<0.001

(sa) = $\dot{V}CO_2$ normalised to body surface area, predicted from height and weight
* sm HR = heart rate smoothed 2 points forward

Subject: Child 9, male, age 8.8 y, height 132.0 cm, weight 25.8 kg, BMI SDS -0.79

Model	N	Mean	SEM	95 % CI	P
Linear-flex (sa)	42	-0.22	0.42	-1.07, 0.63	0.61
Steady state (sa)	42	-1.84	0.72	-3.30, -0.38	0.02
3rd order polynomial, raw HR (sa)	42	0.01	0.48	-0.97, 0.98	0.99
3rd order polynomial, sm HR* (sa)	42	-0.00	0.34	-0.69, 0.69	1.00
Sigmoid, raw HR (sa)	42	-0.00	0.48	-0.97, 0.97	1.00
Sigmoid, sm HR* (sa)	42	-0.00	0.35	-0.71, 0.71	1.00
$\dot{V}CO_2$ predicted from $\dot{V}O_2$ (sa)	42	0.83	0.57	-0.32, 1.99	0.15
Generic surface area	42	0.48	0.40	-0.33, 1.28	0.24
Generic surface area and age	42	1.46	0.37	0.72, 2.21	<0.001
Sigmoid, sm HR* (height^3)	42	0.04	0.14	-0.25, 0.34	0.76
Generic height^3	42	0.36	0.16	0.03, 0.69	0.03
Generic height^3 and age	42	0.76	0.16	0.45, 1.08	<0.001

(sa) = $\dot{V}CO_2$ normalised to body surface area, predicted from height and weight
* sm HR = heart rate smoothed 2 points forward

Subject: Child 10, female, age 15.2 y, height 151.8 cm, weight 49.3 kg, BMI SDS 0.48

Model	N	Mean	SEM	95 % CI	P
Linear-flex (sa)	40	-0.34	0.27	-0.88, 0.19	0.20
Steady state (sa)	40	-0.91	0.30	-1.51, -0.32	0.004
3rd order polynomial, raw HR (sa)	40	-0.17	0.34	-0.87, 0.53	0.62
3rd order polynomial, sm HR* (sa)	40	0.00	0.37	-0.74, 0.74	1.00
Sigmoid, raw HR (sa)	40	0.05	0.28	-0.52, 0.62	0.87
Sigmoid, sm HR* (sa)	40	0.00	0.37	-0.75, 0.75	1.00
$\dot{V}CO_2$ predicted from $\dot{V}O_2$ (sa)	40	1.08	0.42	0.23, 1.92	0.01
Generic surface area	40	0.05	0.44	-0.85, 0.95	0.91
Generic surface area and age	40	0.55	0.44	-0.33, 1.44	0.22
Sigmoid, sm HR* (height^3)	40	-0.00	0.15	-0.31, 0.31	1.00
Generic height^3	40	0.14	0.19	-0.23, 0.52	0.45
Generic height^3 and age	40	0.31	0.18	-0.06, 0.68	0.10

(sa) = $\dot{V}CO_2$ normalised to body surface area, predicted from height and weight
* sm HR = heart rate smoothed 2 points forward

Subject: CF1, male, age 13.8 y, height 146.3 cm, weight 37.1 kg, BMI SDS –0.61

Model	N	Mean	SEM	95 % CI	P
Linear-flex (sa)	39	0.16	0.33	-0.52, 0.84	0.64
Steady state (sa)	39	-2.11	0.37	-2.86, -1.36	<0.001
3rd order polynomial, raw HR (sa)	39	0.00	0.32	-0.64, 0.64	1.00
3rd order polynomial, sm HR* (sa)	39	-0.00	0.28	-0.56, 0.56	1.00
Sigmoid, raw HR (sa)	39	0.00	0.32	-0.64, 0.64	1.00
Sigmoid, sm HR* (sa)	39	0.00	0.29	-0.58, 0.58	1.00
$\dot{V}CO_2$ predicted from $\dot{V}O_2$ (sa)	39	-1.30	0.67	-2.66, 0.05	0.06
Generic surface area	39	-0.39	0.30	-1.00, 0.22	0.21
Generic surface area and age	39	0.29	0.32	-0.36, 0.94	0.38
Sigmoid, sm HR* (height^3)	39	-0.00	0.11	-0.22, 0.22	1.00
Generic height^3	39	-0.24	0.12	-0.49, 0.01	0.06
Generic height^3 and age	39	0.10	0.12	-0.14, 0.35	0.40

(sa) = $\dot{V}CO_2$ normalised to body surface area, predicted from height and weight
* sm HR = heart rate smoothed 2 points forward

Subject: CF3, male, age 14.4 y, height 176.2 cm, weight 57.8 kg, BMI SDS –0.42

Model	N	Mean	SEM	95 % CI	P
Linear-flex (sa)	35	-1.20	0.73	-2.69, 0.28	0.11
Steady state (sa)	35	-1.79	0.69	-3.19, -0.38	0.01
3rd order polynomial, raw HR (sa)	35	-0.00	0.52	-1.06, 1.06	1.00
3rd order polynomial, sm HR* (sa)	35	-0.00	0.51	-1.03, 1.03	1.00
Sigmoid, raw HR (sa)	35	-0.09	0.63	-1.37, 1.19	0.89
Sigmoid, sm HR* (sa)	35	-0.00	0.51	-1.03, 1.03	1.00
$\dot{V}CO_2$ predicted from $\dot{V}O_2$ (sa)	35	0.32	0.50	-0.70, 1.35	0.53
Generic surface area	35	1.83	0.52	0.78, 2.88	0.001
Generic surface area and age	35	2.28	0.52	1.22, 3.33	0.001
Sigmoid, sm HR* (height^3)	35	-0.00	0.15	-0.32, 0.32	1.00
Generic height^3	35	-0.09	0.16	-0.42, 0.24	0.60
Generic height^3 and age	35	-0.09	0.16	-0.42, 0.24	0.60

(sa) = $\dot{V}CO_2$ normalised to body surface area, predicted from height and weight
* sm HR = heart rate smoothed 2 points forward

Subject: CF5, female, age 14.9 y, height 158.3 cm, weight 44.9 kg, BMI SDS –0.87

Model	N	Mean	SEM	95 % CI	P
Linear-flex (sa)	44	-0.16	0.36	-0.88, 0.55	0.65
Steady state (sa)	44	-1.62	0.45	-2.53, -0.71	<0.001
3rd order polynomial, raw HR (sa)	44	0.05	0.35	-0.66, 0.76	0.88
3rd order polynomial, sm HR* (sa)	44	0.30	0.31	-0.34, 0.93	0.35
Sigmoid, raw HR (sa)	44	0.00	0.34	-0.69, 0.69	1.00
Sigmoid, sm HR* (sa)	44	0.00	0.24	-0.49, 0.49	1.00
$\dot{V}CO_2$ predicted from $\dot{V}O_2$ (sa)	44	1.27	0.33	0.61, 1.94	<0.001
Generic surface area	44	0.21	0.49	-0.79, 1.19	0.68
Generic surface area and age	44	0.57	0.49	-0.42, 1.56	0.25
Sigmoid, sm HR* (height^3)	44	-0.00	0.09	-0.17, 0.17	1.00
Generic height^3	44	-0.30	0.18	-0.66, 0.06	0.10
Generic height^3 and age	44	-0.11	0.18	-0.47, 0.25	0.55

(sa) = $\dot{V}CO_2$ normalised to body surface area, predicted from height and weight
* sm HR = heart rate smoothed 2 points forward

Subject: CF6, female, age 12.5 y, height 156.1 cm, weight 40.8 kg, BMI SDS –0.52

Model	N	Mean	SEM	95 % CI	P
Linear-flex (sa)	51	-0.07	0.26	-0.61, 0.46	0.78
Steady state (sa)	51	-1.05	0.28	-1.62, -0.49	<0.001
3rd order polynomial, raw HR (sa)	51	-0.00	0.24	-0.48, 0.48	1.00
3rd order polynomial, sm HR* (sa)	51	-0.00	0.18	-0.36, 0.36	1.00
Sigmoid, raw HR (sa)	51	0.00	0.21	-0.42, 0.42	1.00
Sigmoid, sm HR* (sa)	51	-0.00	0.17	-0.33, 0.33	1.00
$\dot{V}CO_2$ predicted from $\dot{V}O_2$ (sa)	51	0.68	0.28	0.11, 1.25	0.02
Generic surface area	51	-1.99	0.23	-2.46, -1.52	<0.001
Generic surface area and age	51	-1.48	0.23	-1.94, -1.03	<0.001
Sigmoid, sm HR* (height^3)	51	0.00	0.06	-0.11, 0.11	1.00
Generic height^3	51	-1.24	0.08	-0.41, -1.07	<0.001
Generic height^3 and age	51	-0.91	0.08	-1.08, -0.74	<0.001

(sa) = $\dot{V}CO_2$ normalised to body surface area, predicted from height and weight
* sm HR = heart rate smoothed 2 points forward

Subject: CF8, female, age 8.9 y, height 130.8 cm, weight 26.0 kg, BMI SDS –0.54

Model	N	Mean	SEM	95 % CI	P
Linear-flex (sa)	38	0.07	0.15	-0.24, 0.38	0.65
Steady state (sa)	38	-0.61	0.15	-0.91, -0.31	<0.001
3rd order polynomial, raw HR (sa)	38	0.00	0.14	-0.29, 0.29	1.00
3rd order polynomial, sm HR* (sa)	38	-0.00	0.15	-0.31, 0.31	1.00
Sigmoid, raw HR (sa)	38	0.00	0.13	-0.26, 0.26	1.00
Sigmoid, sm HR* (sa)	38	-0.00	0.15	-0.31, 0.31	1.00
$\dot{V}CO_2$ predicted from $\dot{V}O_2$ (sa)	38	0.06	0.32	-0.58, 0.71	0.84
Generic surface area	38	-6.58	0.34	-7.28, -5.89	<0.001
Generic surface area and age	38	-6.34	0.43	-7.22, -5.46	<0.001
Sigmoid, sm HR* (height^3)	38	-0.00	0.06	-0.13, 0.13	1.00
Generic height^3	38	-2.60	0.13	-2.87, -2.32	<0.001
Generic height^3 and age	38	-2.29	0.15	-2.60, -1.98	<0.001

(sa) = $\dot{V}CO_2$ normalised to body surface area, predicted from height and weight
* sm HR = heart rate smoothed 2 points forward

Subject: CF9, female, age 8.4 y, height 124.3 cm, weight 25.0 kg, BMI SDS 0.02

Model	N	Mean	SEM	95 % CI	P
Linear-flex (sa)	41	0.60	0.26	0.07, 1.14	0.03
Steady state (sa)	41	-0.20	0.28	-0.78, 0.38	0.49
3rd order polynomial, raw HR (sa)	41	-0.00	0.27	-0.54, 0.54	0.99
3rd order polynomial, sm HR* (sa)	41	-0.00	0.16	-0.34, 0.33	0.97
Sigmoid, raw HR (sa)	41	0.00	0.24	-0.49, 0.49	1.00
Sigmoid, sm HR* (sa)	41	0.00	0.16	-0.33, 0.33	1.00
$\dot{V}CO_2$ predicted from $\dot{V}O_2$ (sa)	41	0.13	0.27	-0.42, 0.69	0.63
Generic surface area	41	-4.22	0.32	-4.86, -3.58	<0.001
Generic surface area and age	41	-3.51	0.35	-4.21, -2.81	<0.001
Sigmoid, sm HR* (height^3)	41	-0.00	0.08	-0.16, 0.16	1.00
Generic height^3	41	-1.14	0.19	-1.53, -0.74	<0.001
Generic height^3 and age	41	-0.69	0.20	-1.10, -0.28	0.001

(sa) = $\dot{V}CO_2$ normalised to body surface area, predicted from height and weight
* sm HR = heart rate smoothed 2 points forward

Appendix 3 Individual results from ^{13}C-breath tests

Table A3.1 Effect of position on measured resting $\dot{V}CO_2$

	Measured $\dot{V}CO_2$ (mmol.min^{-1}.m^{-2})		
Subject	Lying	Sitting	Difference
Adult 1	4.81	5.56	-0.76
Adult 2	4.71	4.39	0.32
Adult 3	4.46	4.22	0.24
Adult 4	4.55	4.51	0.04
Adult 5	6.78	6.68	0.10
Adult 6	4.34	3.59	0.75
Adult 7	4.76	5.49	-0.73
Adult 8	4.61	4.90	-0.29
Child 1	5.13	5.13	0.00
Child 2	4.48	4.09	0.38
Child 3	5.10	5.36	-0.26
Child 4	6.52	6.92	-0.40
Child 5	5.80	6.32	-0.52
Child 6	4.73	6.98	-2.25
Child 7	5.72	5.85	-0.13
Child 8	5.53	5.19	0.34
Child 9	6.58	6.26	0.32
Child 10	4.58	3.94	0.64
CF1	6.82	6.56	0.26
CF3	6.35	5.88	0.46
CF5	5.48	5.36	0.12
CF6	5.80	4.54	1.26
CF8	6.15	4.62	1.53
CF9	6.03	5.46	0.57

Table A3.2 Cumulative PDR at 6 h during the [^{13}C]MTG breath test

	Cumulative PDR (6 h)				
Subject	Shreeve	Schofield	Measured resting	HR predicted	PAL*
Adult 1	43.1	38.4	31.1	38.6	1.2
Adult 2	29.2	28.2	25.5	25.8	1.0
Adult 3	32.7	33.2	30.6	35.0	1.1
Adult 4	33.6	30.8.	25.8	39.7	1.5
Adult 5	37.3	37.7	30.7	38.6	1.3
Adult 6	35.2	37.9	30.4	42.2	1.4
Adult 7	33.5	32.9	33.3	44.1	1.3
Adult 8	31.7	32.9	26.8	41.9	1.6
Child 1	17.2	20.0	17.9	36.3	2.1
Child 2	27.3	27.7	21.0	44.3	2.1
Child 3	32.3	40.2	33.6	46.8	1.4
Child 4	21.4	22.4	28.2	51.8	1.7
Child 5	19.2	23.6	22.9	34.9	1.5
Child 6	28.6	33.9	27.8	61.6	2.2
Child 7	25.4	31.5	19.4	32.7	1.7
Child 8	29.0	32.1	31.3	31.9	1.0
Child 9	33.5	41.3	43.2	57.6	1.4
Child 10	39.8	39.6	32.7	40.2	1.3
CF1	4.1	4.9	5.1	6.1	1.2
CF3	10.3	11.4	11.3	14.7	1.3[$]
CF4	10.7	12.8	11.4	-	-
CF5	20.2	20.7	19.9	16.8	1.2
CF6	28.8	30.2	32.0	41.0	1.3
CF8	12.0	13.9	11.0	16.8	1.5
CF9	9.3	10.9	11.0	13.8	1.3

*PAL = cPDR calculated using $\dot{V}CO_2$ estimated from heart rate/measured resting $\dot{V}CO_2$
= non-resting $\dot{V}CO_2$/resting $\dot{V}CO_2$ or TEE/REE

[$] assumed PAL due to problem recording heart rate during the test

Please refer to the note following Table A3.3.

Table A3.3 Cumulative PDR at 6 h during the [1-^{13}C]acetate breath test

	Cumulative PDR (6 h)				
Subject	Shreeve	Schofield	Measured resting	HR predicted	PAL*
Adult 1	44.6	39.9	38.3	41.5	1.1
Adult 2	29.8	28.8	27.5	26.1	1.0
Adult 3	22.4	22.8	21.0	26.9	1.3
Adult 4	38.7	35.4	29.6	35.0	1.2
Adult 5	37.4	37.8	30.7	37.4	1.2
Adult 6	33.4	35.9	28.8	39.5	1.4
Adult 7	30.9	30.3	30.6	40.0	1.3
Adult 8	25.8	26.8	21.8	31.6	1.4
Child 1	18.7	21.8	19.5	33.6	1.7
Child 2	36.1	36.6	27.8	63.7	2.3
Child 3	29.2	36.4	30.4	35.0	1.1
Child 4	25.0	26.2	32.9	54.2	1.6
Child 5	27.0	33.2	32.3	46.6	1.4
Child 6	25.5	30.2	24.8	63.1	2.5
Child 7	31.8	39.4	24.3	40.3	1.7
Child 8	31.1	34.5	33.6	33.0	1.0
Child 9	19.7	24.3	25.4	44.6	1.8
CF1	26.1	30.7	32.1	40.9	1.3
CF4	20.4	24.4	21.8	-	-
CF8	26.7	30.9	24.6	37.2	1.5

*PAL = cPDR calculated using VCO_2 estimated from heart rate/measured resting VCO_2 = non-resting VCO_2/resting VCO_2 or TEE/REE

Please refer to the note on the following page.

Notes for Tables A3.2 and A3.3:

1. Control child 6 had a poor heart rate calibration due to insufficient measurements at near resting conditions and therefore may have overestimated $\dot{V}CO_2$ at low levels of energy expenditure, resulting in high PDR and high PAL. This subject performed the test at the same time as subjects 4, 5 and 7 and had a similar pattern of activity during the test. Her PAL should have been between 1.5 and 1.7. The high PAL in control children 1 and 2 is consistent with the observed behaviour of these children, although a detailed activity diary was not kept during the test.

2. Healthy control children 1-8 and CF9 performed the tests in the familiar surroundings of their own home, where there was a greater choice of activities than at the ambulatory day care unit, Royal Hospital for Sick Children, Glasgow. Control children 9 and 10 and the remainder of children with cystic fibrosis performed the test at the Royal Hospital for Sick Children.

3. Subject CF1 was normally on high dose pancreatic enzyme replacement therapy (PERT). Subject CF6 did not normally take PERT. Subject CF 4 could not be fitted with a heart rate monitor. This problem was not identified until the day of the test.

Subject	$\dot{V}CO_2$ estimate						
	Shreeve	Measured resting	HR individual calibration	HR generic surface area (sa)	HR generic sa & age	HR generic height^3	HR generic height^3 & age
1	43.1	31.1	38.6	43.2	42.2	40.1	41.2
2	29.2	25.5	25.8	29.3	28.9	33.2	34.3
3	32.7	30.6	35.0	39.6	33.3	48.2	42.7
4	33.6	25.8	39.7	52.6	49.5	52.1	47.4
5	37.3	30.7	38.6	41.9	38.3	51.8	49.2
6	35.2	30.4	42.2	49.6	45.5	46.3	42.0
7	33.5	33.3	44.1	43.4	41.2	54.1	51.2
8	31.7	26.8	41.9	35.7	32.0	37.4	35.1

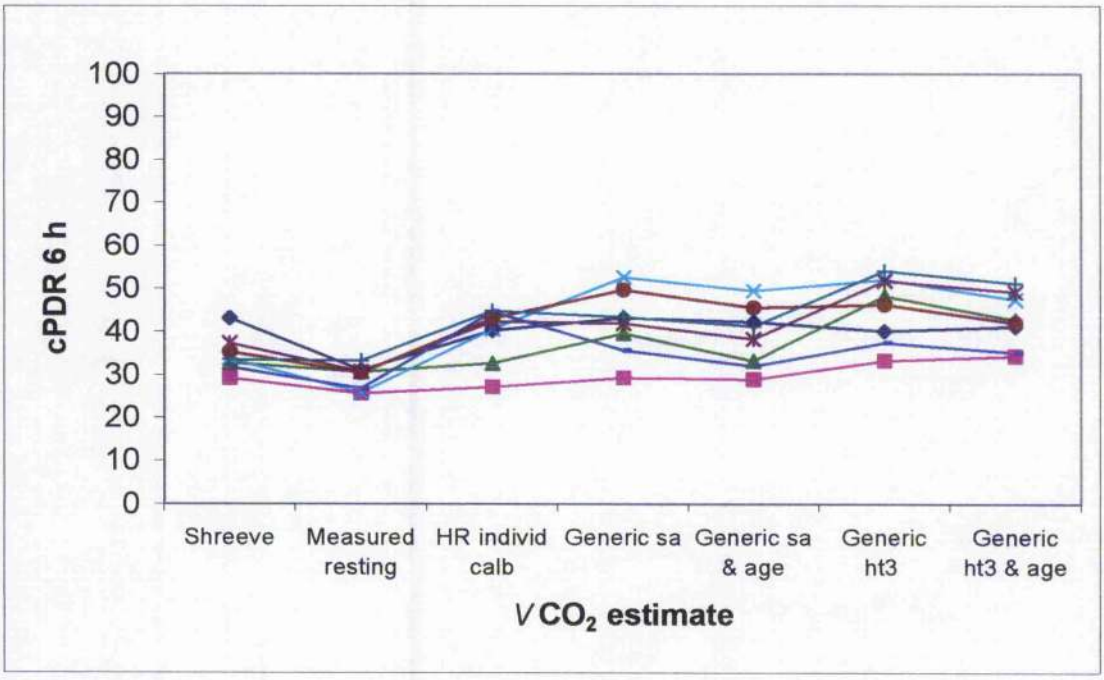

Measured resting = resting $\dot{V}CO_2$ measured using a ventilated hood indirect calorimeter

Figure A3.1 Cumulative excretion (6 h) of ^{13}C in breath CO_2 following ingestion of [^{13}C]MTG in eight healthy adults

	$V\dot{C}O_2$ estimate						
Subject	Shreeve	Measured resting	HR individual calibration	HR generic surface area (sa)	HR generic sa & age	HR generic height^3	HR generic height^3 & age
1	17.2	17.9	36.3	31.1	29.8	26.1	24.1
2	27.3	21.0	44.3	49.3	44.8	39.1	34.7
3	32.3	33.6	46.8	67.7	63.6	46.8	42.3
4	21.4	28.2	51.8	30.5	27.6	32.7	29.7
5	19.2	22.9	34.9	37.1	33.8	31.1	27.7
6	28.6	27.8	61.6	53.1	47.4	39.7	34.8
7	25.4	19.4	32.7	64.8	60.9	44.6	40.7
8	29.0	31.3	31.9	40.0	35.9	50.6	45.8
9	33.5	43.2	57.6	57.0	49.5	54.4	46.8
10	39.8	32.7	40.2	45.2	41.2	41.7	39.6

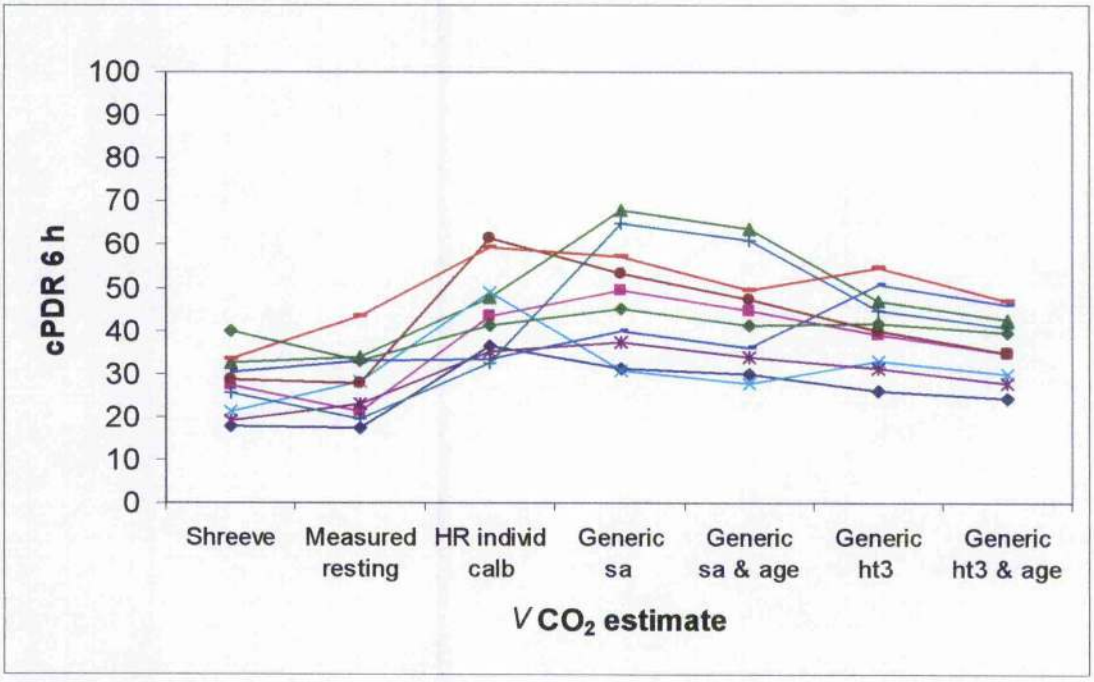

Measured resting = resting $V\dot{C}O_2$ measured using a ventilated hood indirect calorimeter

Figure A3.2 Cumulative excretion (6 h) of ^{13}C in breath CO_2 following ingestion of [^{13}C]MTG in ten healthy children

	VCO_2 estimate						
Subject	Shreeve	Measured resting	HR individual calibration	HR generic surface area (sa)	HR generic sa & age	HR generic height^3	HR generic height^3 & age
CF1	4.1	5.1	6.1	6.5	5.9	6.6	5.9
CF5	20.2	19.9	16.8	29.0	25.1	32.3	28.5
CF6	28.8	32.0	41.0	53.6	50.1	62.5	56.4
CF8	12.0	11.0	16.8	33.8	33.9	32.4	30.4
CF9	9.3	11.0	13.8	21.7	18.2	18.5	15.7

CF6 was not normally taking pancreatic enzyme replacement therapy

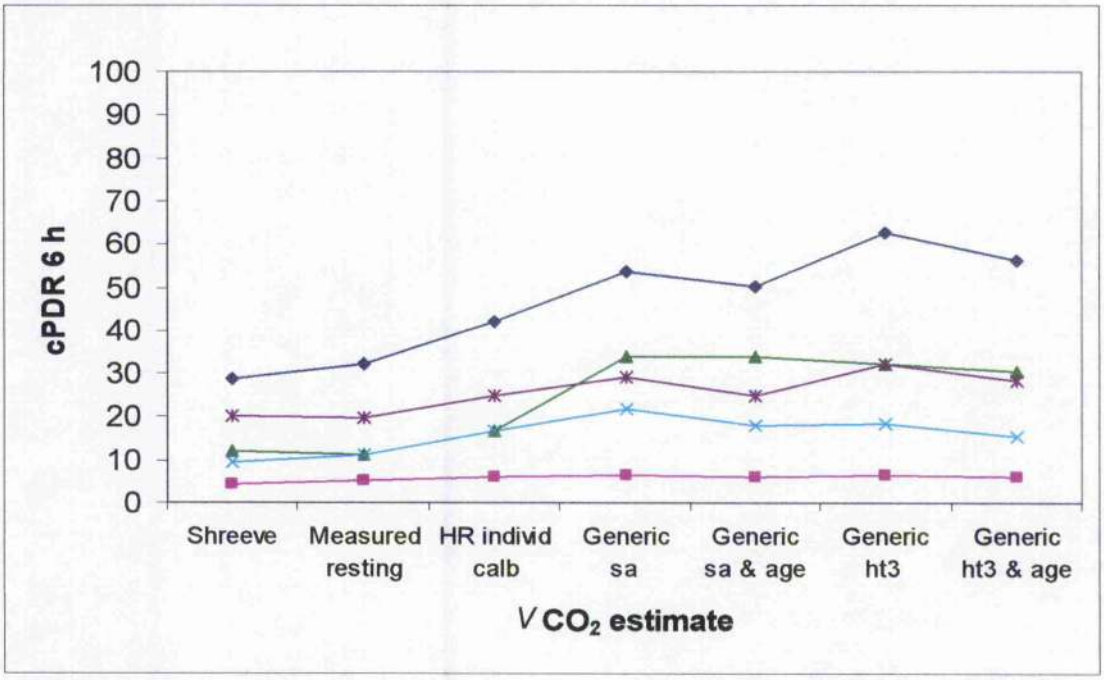

Measured resting = resting VCO_2 measured using a ventilated hood indirect calorimeter

Figure A3.3 Cumulative excretion (6 h) of ^{13}C in breath CO_2 following ingestion of [^{13}C]MTG in five children with cystic fibrosis

	$V\text{CO}_2$ estimate						
Subject	Shreeve	Measured resting	HR individual calibration	HR generic surface area (sa)	HR generic sa & age	HR generic height^3	HR generic height^3 & age
1	44.6	38.3	41.5	47.9	46.5	45.3	45.4
2	29.8	27.5	26.1	29.6	29.4	34.0	35.2
3	22.4	21.0	26.9	27.4	25.5	32.5	36.7
4	38.7	29.6	35.0	42.4	40.0	37.3	36.5
5	37.4	30.7	37.4	40.7	37.6	50.0	48.3
6	33.4	28.8	39.5	46.5	42.5	42.7	38.7
7	30.9	30.6	40.0	39.2	37.3	48.1	45.7
8	25.8	21.8	31.6	27.7	25.3	28.9	27.9

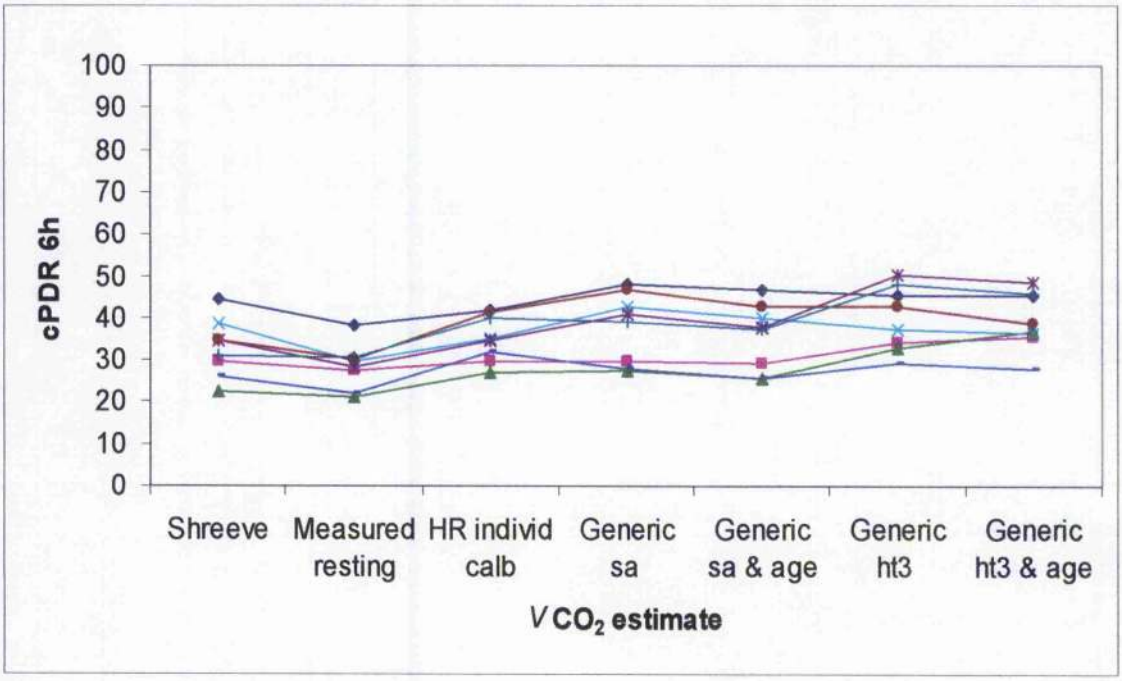

Measured resting = resting $V\text{CO}_2$ measured using a ventilated hood indirect calorimeter

Figure A3.4 Cumulative excretion (6 h) of ^{13}C in breath CO_2 following ingestion of [1-^{13}C]acetate in eight healthy adults

	VCO_2 estimate						
Subject	Shreeve	Measured resting	HR individual calibration	HR generic surface area (sa)	HR generic sa & age	HR generic height^3	HR generic height^3 & age
1	18.7	19.5	33.6	81.0	76.4	52.1	40.7
2	36.1	27.8	63.7	54.3	50.7	41.0	37.1
3	29.2	30.4	35.0	53.2	47.0	36.2	31.4
4	25.0	32.9	54.2	49.1	44.5	36.6	32.3
5	27.0	32.3	46.6	72.8	69.1	58.4	53.2
6	25.5	24.8	63.1	30.0	27.1	25.2	22.4
7	31.8	24.3	40.3	34.1	30.5	36.9	30.0
8	31.1	33.6	33.0	39.5	34.6	49.3	44.5
9	19.7	25.4	44.6	40.9	38.1	40.0	36.1
CF1	26.1	32.1	40.9	43.9	40.0	45.0	40.1
CF8	26.7	24.6	37.2	68.8	68.7	65.6	62.7

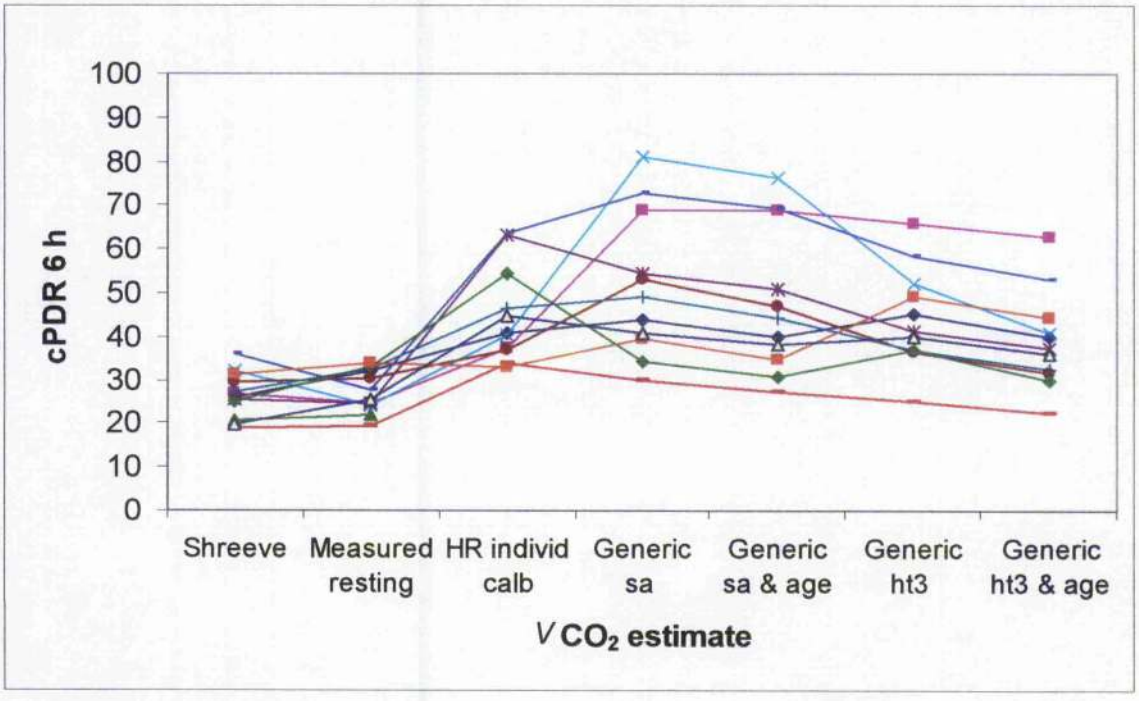

Measured resting = resting VCO_2 measured using a ventilated hood indirect calorimeter

Figure A3.5 Cumulative excretion (6 h) of ^{13}C in breath CO_2 following ingestion of [1-^{13}C]acetate in nine healthy children and two children with cystic fibrosis

Table A3.4 Cumulative PDR 6 h (Shreeve VCO_2) with acetate recovery

	Cumulative PDR (6 h)		
Subject	MTG	Acetate	MTG with acetate recovery
Adult 1	43.1	44.6	96.8
Adult 2	29.2	29.8	98.0
Adult 3	32.7	22.4	145.9*
Adult 4	33.6	38.7	86.9*
Adult 5	37.3	37.4	108.1
Adult 6	35.2	33.4	101.7
Adult 7	33.5	30.9	108.5
Adult 8	31.7	25.8	122.9*
Child 1	17.2	18.7	91.7*
Child 2	27.3	36.1	75.7*
Child 3	32.3	29.2	110.4*
Child 4	21.4	25.0	85.6
Child 5	19.2	27.0	71.0
Child 6	28.6	25.5	112.1*
Child 7	25.4	31.8	79.9
Child 8	29.0	31.1	93.2
Child 9	33.5	19.7	170.2*
CF1	4.2	26.1	16.0
CF4	10.7	20.4	52.3
CF8	12.0	26.7	44.8

*PAL more than 0.1 units different between tests (Tables A3.2 & A3.3)

Table A3.5 Cumulative PDR 6 h ($\dot{V}CO_2$ estimated from HR) with acetate recovery

	Cumulative PDR (6 h)		
Subject	MTG	Acetate	MTG with acetate recovery
Adult 1	38.6	41.5	92.9
Adult 2	25.8	26.1	98.1
Adult 3	35.0	26.9	130.5
Adult 4	39.7	35.0	113.4
Adult 5	38.6	37.4	111.4
Adult 6	42.2	39.5	106.9
Adult 7	44.1	40.0	110.2
Adult 8	41.9	31.6	132.5
Child 1	36.3	33.6	103.9
Child 2	44.3	63.7	71.2
Child 3	46.8	35.0	133.7
Child 4	51.8	54.2	95.6
Child 5	34.9	46.6	75.0
Child 6	61.6	63.1	97.5
Child 7	32.7	40.3	81.0
Child 8	31.9	33.0	96.6
Child 9	57.6	44.6	129.1
CF1	6.1	40.9	15.1
CF4	16.0*	30.6	52.3
CF8	16.8	37.2	44.8

*Assuming PAL 1.5 same as subject CF8, who did test at same time